Assessing Ozone Impacts on Arable Crops in South Asia: Identification of Suitable Risk Assessment Methods to Improve Crop Biotechnology

Chubamenla Jamir

Submitted for the

Degree of

PhD

University of York

Environment

October 2011

Abstract

This study has applied a number of different O_3 risk assessment methods in South Asia to assess the extent and magnitude of O_3 risk to crops and investigate how appropriate different methods are in identifying local environmental conditions and crop physiological traits that might alter crop sensitivity to O_3.

Concentration based methods are used in combination with tools and datasets tailored for South Asian conditions to investigate O_3 impacts on wheat, rice, soybean and potato. Relative yield losses are substantially smaller (0.1 to 11.5 %) than those found in previously conducted global modelling studies (3 to 30 %) which is attributed to the improved resolution of the O_3 photochemical model and crop distribution datasets used in this South Asian analysis.

For the first time O_3 flux based risk assessment methods are also applied for wheat in India. The stomatal conductance component of this flux method has been parameterised for Indian wheat based on available crop physiology data. Comparisons show that flux based methods tend to estimate larger relative yield losses than concentration based methods (16 % compared to 0.6 to 11.5 % for India). There are also differences in the spatial pattern of estimated risk though both methods clearly identify the Indo-Gangetic Plains as a high O_3 risk region. The co-variation in O_3 concentrations, crop distribution (both growth periods and geographical location), local meteorology (especially temperature and VPD) and crop physiology are all important in determining flux estimated O_3 sensitivity.

Finally, the flux based method is used to assess phenological traits (sowing times and maturing periods) introduced in new Indian wheat cultivars. This highlights the importance of crop phenology in determining O_3 sensitivity as a function of both O_3 concentration and environmental conditions and emphasises the potential application of flux based approaches as a tool capable of informing future crop biotechnology efforts.

Table of Contents

Abstract 3
List of Tables 10
List of Figures 12
Acknowledgements 17
Author's declaration 19

Chapter 1 Introduction 21
1.1 Agriculture and food security in South Asia (SA) 21
1.1.1 Current status of agriculture in India 24
1.2 Ground Level O_3 in SA 30
1.2.1 Ozone formation 30
1.2.2 Emissions of O_3 precursors in India 34
1.2.3 O_3 climate across SA 38
1.3 O_3 impacts on agriculture 39
1.3.1 O_3 mode of action 39
1.3.1.1 Biochemical effect 39
1.3.1.2 Physiological effect 40
1.3.1.3 Effects on carbon allocation 41
1.3.1.4 Yield losses 41
1.3.2 Experimental evidence of O_3 impacts on crops collected in India 42
1.4 Future threats to agriculture in SA 47
1.5 Research aims and questions 49

Chapter 2 Concentration based O_3 risk assessment 53
2.1 Introduction 53
2.2 Methodology 56
2.2.1 O_3 data 57
2.2.1.1 MATCH model and O_3 concentration field 57
2.2.2 Crop data 60
2.2.2 .1 Selection criteria of the crops and crop distribution 60
2.2.2.2 Crop data collection 62
2.2.3 Spatial resolution of the data 66
2.2.4 O_3 exposure indices 69
2.2.4.1 Seasonal average O_3 concentrations 70
2.2.4.2 Cumulative O_3 concentrations 72

2.2.5 Exposure-Response (ER) functions 73
2.2.6 Crop loss evaluation 79
2.2.7 Economic loss (EL) 80
2.3 Results 81
2.3.1 Relative Yield Loss (RYL) 82
2.3.2 Crop production loss (CPL) and Economic loss (EL) estimates 91
2.3.3 Potential effect of O_3 induced EL on the gross domestic product (GDP) of the region 97
2.4 Discussion 99
2.4.1 Comparison of O_3 induced yield and production losses with other experimental and modelling studies 99
2.4.2 O_3 concentration data 105
2.4.2.1 Description of MATCH, MOZART-2 and TM5 106
2.4.2.2 Comparison of modelled estimates with monitored O_3 data 112
2.4.3 Crop phenology data 116
2.4.4 Crop distribution and production data 116
2.4.5 Crop RYLs and ER functions 117
2.5 Conclusions 122

Chapter 3 Stomatal O_3 flux based risk assessment in India 125
3.1 Introduction 125
3.2 Factors determining O_3 deposition to vegetation 127
3.2.1 Non-stomatal O_3 uptake 128
3.2.2 Stomatal O_3 uptake 129
3.2.2.1 Temperature 130
3.2.2.2 Vapour Pressure Deficit (VPD) 130
3.2.2.3 Soil water content 131
3.2.2.4 Irradiance 132
3.2.2.5 Phenology 132
3.2.2.6 Carbon dioxide (CO_2) 133
3.2.2.7 Salinity 133
3.3 The benefit of a flux-based O_3 risk assessment. 133
3.3.1 Methods for estimating O_3 flux 134
3.3.2 The DO_3SE model 135
3.4 Application of the DO_3SE stomatal O_3 flux (F_{st}) model for wheat in India 136
3.4.1 Data required for the application of the DO_3SE F_{st} model in India. 137
3.4.2 Description of the DO_3SE F_{st} model 144
3.4.3 The DO_3SE multiplicative g_{sto} algorithm 145
3.4.3.1 g_{max} and f_{min} 146

3.4.3.2 Seasonal parameters 147
3.4.3.3 Diurnal parameters 149
3.4.4 Estimating yield, production and economic loss from DO_3SE F_{st} 153
3.4.5 Estimating relative exceedance of critical levels (R_{CL}) 155
3.5 Methods to parameterize the DO_3SE F_{st} model. 156

Chapter 4 Parameterization and application of the O_3 flux model for wheat in India 161
4.1 Introduction 161
4.2 Stomatal ozone flux (F_{st}) accumulation period for wheat crops grown in India . 165
4.2.1 Phenological data collection 165
4.2.2 Wheat sowing date 168
4.2.3 Defining the phenological stages in the F_{st} accumulation period 170
4.2.3.1 Fixed day (DAS) accumulation period 170
4.2.3.2 Thermal time (GDD) accumulation period 171
4.2.3.3 Comparison of DAS and GDD for defining F_{st} accumulation period 171
4.3 Parameterization of the g_{sto} model for Indian wheat 174
4.3.1 g_{max} and f_{min} of wheat crops grown in India 182
4.3.1.1 g_{max} 182
4.3.1.2 f_{min} 184
4.3.2 Seasonal g_{sto} parameters 185
4.3.2.1 g_{sto} as a function of wheat phenology (f_{phen}) 185
4.3.3 Diurnal parameters 188
4.3.3.1 g_{sto} as a function of irradiance (f_{light}) 188
4.3.3.2 g_{sto} as a function of temperature (f_{temp}) 190
4.3.3.3 g_{sto} as a function of VPD (f_{VPD}) 197
4.3.3.4 g_{sto} as a function of soil water 198
4.4 Summary of the parameterization of the g_{sto} model for India 199

Chapter 5 Results of the O_3 flux based risk assessment 201
5.1 Introduction 201
5.2 Comparison of F_{st} and AOT40 risk assessment methods for India. 205
5.2.1 Spatial variation in F_{st} and AOT40 across India 206
5.2.2 Variation in relative critical level exceedance, yield and production losses based on F_{st} and *AOT40* across India 209
5.2.2.1 Relative critical level exceedance (R_{CL}) 209
5.2.2.2 Relative yield loss (RYL) and crop production loss (CPL) 212
5.2.3 Temporal variation in F_{st} and AOT40 within the important wheat growing AGZs 216
5.2.3.1 Seasonal variation in F_{st} and $AOT40_A$ for the three AGZ grids 218

5.2.3.2 Diurnal variation in F_{st} and $AOT40_A$ for the three AGZ grids 221
5.3.2 Factors limiting F_{st} 224
5.3.2.1 g_{max} 224
5.3.2.2 Seasonal factors limiting F_{st} 225
5.3.2.3 Diurnal factors limiting F_{st} 228
5.3.2.4 Factors limiting uptake of O_3 above 60 ppb 230
5.3.3 Comparison of different DO_3SE model parameterizations 233
5.3.3.1 Spatial variation in F_{st} values estimated using the IN_{450} and EU model parameterization across India 234
5.3.3.2 Temporal variation in fluxes within the important AGZs 237
5.4 Sensitivity analysis of the stomatal flux model 248
5.5 Discussion 254
5.6 Conclusion 266

Chapter 6 Biotechnological advancements and wheat sensitivity to O_3 in India .. 269
6.1 Introduction 269
6.1.1 Literature and database review of biotechnology interventions for wheat in India 274
6.2 New wheat varietal traits 277
6.2.1 Heat tolerance and early maturity 279
6.2.2 Rust resistance 280
6.2.3. Drought resistance 281
6.3 Assessment of key varietal traits and their influence on F_{st} 283
6.3.1 Methodology 284
6.3.1.1 Data collection 284
6.3.1.2 Defining the phenological characteristics of the new Indian wheat cultivars 286
6.3.1.3 Model Runs 291
6.3.2 Results 291
6.3.2.1 GDD estimated growth and O_3 accumulation periods by AGZ 292
6.3.2.2 Temperature and O_3 climate of GDD estimated growth periods 293
6.3.2.3 Stomatal O_3 flux in wheat under different scenarios 296
6.4 Discussions and conclusions 298
6.5 Limitations 305

Chapter 7 Discussions and conclusions 307
7.1 Summary of key findings of the research 307
7.2 Limitations of the current study 312
7.2.1 O_3 concentrations 312
7.2.2 Experimental data describing O_3 induced yield losses 313

7.2.3 Multiple stresses 314
7.2.4 Food security 316
7.3 Policy response to O_3 in SA 318

Definitions 321
Glossary 323
References 325

List of Tables

Table 1-1: Summary of collated South Asian data describing the yield response of crops to ambient O_3. 46

Table 2-1: Comparison of the spatial resolution of atmospheric chemistry models that have been used for simulating O_3 concentrations in SA.. 60

Table 2-2: List of national and international databases from which the relevant crop data were obtained. 62

Table 2-3: The main crop growing season along with its percentage share in crop production as compared to the total production in SA. 63

Table 2-4: The harvest date of rice, potato and soybean crops grown in SA 65

Table 2-5: Crop production (CP) and crop area under cultivation of wheat, rice, potato and soybean in the 6 different countries of SA 66

Table 2-6: Details of the Exposure-Response relationships used in this assessment. 75

Table 2-7: O_3 induced economic loss for the four crops and its effect on annual GDP growth and agricultural GDP in SA.. 98

Table 2-8: Comparison of RYL estimates derived in this study with yield losses observed under ambient O_3 as reported from experimental studies. 101

Table 2-9: Comparison of RYL estimates derived in this study with others based on the application of similar regional O_3 risk assessments.. 104

Table 2-10: overview of the atmospheric chemistry models used in this study and in other studies that have estimated O_3 risk to crops in SA. 108

Table 3-1: Details of the meteorological data provided by the ECWMF model and the corresponding meteorological data required by the DO_3SE F_{st} model. 139

Table 3-2: Summary of the parameterization of the different DO_3SE F_{st} model parametersations of the g_{sto} algorithm for wheat flag leaves grown in Europe. 158

Table 4-1: Wheat agro-climatic zones (AGZs) in India as outlined by the Directorate of Wheat Development (DWD, Government of India), along with wheat area cultivated, production and yield during the cropping season 1999-2000. 163

Table 4-2: Literature used to extract wheat phenology data. Listed are the publication-specific range of values of both DAS and GDD for wheat phenological stages.. 167

Table 4-3: Days after sowing (DAS) for different phenological stages of wheat grown in India. 170

Table 4-4: Cumulative growing degree days (GDD, °C days) for different phenological stages of wheat grown in India. 171

Table 4-5: Details of the conditions under which the g_{sto} data used for deriving maximum stomatal conductance (g_{max}) in wheat were collected. 176

Table 4-6: Data collected from Indian studies used to define the ratio between adaxial and abaxial g_{sto} and stomatal frequency of wheat. 182

Table 4-7: List of literature for deriving f_{phen} values for Indian wheat. 186

Table 4-8: List of literature for deriving f_{light} values for Indian wheat. 188

Table 4-9: Details of data available on the influence of temperature on g_{sto} of wheat crops grown in India. 190

Table 4-10: T_{opt}, T_{min} and T_{max} values for the three AGZs: NEPZ, NWPZ and CZ.. 194

Table 4-11: The calculated T_{max} and T_{min}, and the F_{st} accumulation period average minimum and maximum temperature in Varanasi and Ahmadnagar. 195

Table 4-12: Summary of the parameterization of the different parameters of the DO_3SE F_{st} model for wheat flag leaves grown in India. 199

Table 5-1: Details of the location, grid fraction area, production and yield of wheat for the cropping year 1999-2000 for the three grid cells selected for further analysis in each of the AGZs. 203

Table 5-2: POD_6 and $AOT40_A$ estimates for the three AGZs. 216

Table 5-3: Summary of the sensitivity tests on model parameters. 249

Table 5-4: Comparison of the Indian wheat parameterization (IN) with the European wheat parameterization (EU). 259

Table 6-1: The new wheat cultivars (released between 1995 to 2008) used to define the phenological characteristics in relation to sowing date and days to maturity. 286

Table 6-2: Parameterization for A_{start}, mid-anthesis, A_{end}, f_{phen_e} and f_{phen_f} for each of the phenology types in GDD. 290

Table 7-1: Summary of the relative yield losses (in %) for wheat grown in India estimated using different O_3 exposure metrics and comparison with estimates from other global study. 308

Table 7-2: RYLs for the year 2030 under different scenarios estimated by global risk assessment studies using AOT40 and M7 metrics for wheat in India. 311

Table 7-3: List of O_3 air quality standards in different parts of the world. 319

List of Figures

Figure 1-1: Production of major foodgrains and horticultural products in SA.. 21

Figure 1-2: Production, area and yield of rice and wheat grains in India and South Asia. 22

Figure 1-3: Production, area and yield of pulses and coarse grains in South Asia. 23

Figure 1-4: Production of major foodgrains and horticultural products in SA.. 24

Figure 1-5: Area and number of farm holdings in India for different categories of holding size..... 25

Figure 1-6: Agro-ecological analysis of rice-wheat area and productivity in the Indo-Gangetic plains of SA. 27

Figure 1-7: Agriculture value added GDP as percentage of total GDP. 28

Figure 1-8: Area, yield and production statistics for wheat growing in India between 1965 to 2009. 29

Figure 1-9: Schematic of sources and sinks of O_3 in the atmosphere 34

Figure 1-10: Annual emission of NO_X, CO and CH_4 in India. 35

Figure 1-11: Main sources of O_3 precursor gasses in India, (a) Methane (CH_4), (b) NO_X, CO. 37

Figure 1-12: Average growing season of wheat, rice, potato and soybean and the annual O_3 trend in South Asia. 38

Figure 1-13: Summary of collated Indian data describing the different O_3 experiments that have been performed on crops in India. 43

Figure 1-14: Map showing the locations where experimental studies of O_3 effects on crops have been carried out. 45

Figure 2-1: Schematic of the steps involved in the concentration-based risk assessment of O_3 impacts on staple crops in SA. 57

Figure 2-2: Map of SA showing the spatial resolution of the MATCH model grids used for O_3 concentration simulations. 59

Figure 2-3: SA's percentage share in the World production and area harvest of potato, rice, soybean and wheat..... 61

Figure 2-4: Harvest dates obtained from data sources listed in Table 2-2 plotted as a function of latitude for wheat growing across the region. 64

Figure 2-5: Map of SA showing the spatial resolution at which the crop statistics data was obtained.. 68

Figure 2-6: An example of aggregations of MATCH grids into the district map of SA.. 69

Figure 2-7: Definition of the daylight hour period over which the M7 and M12 indices are calculated based on data from SA 71

Figure 2-8: Producer price in US$/tonnes for the four crops in the six countries of SA for the year 2000..... 81

Figure 2-9: O_3 induced RYL (%) for wheat, rice, potato and soybean in different

countries of SA based on AOT40, M7/M12, W126 and SUM06 exposure indices. 83

Figure 2-10: Estimates of RYL for wheat based on MATCH O_3 concentration data expressed as different exposure indices (AOT40, M7, W126 and SUM06) and associated ER functions across SA for the cropping year 1999-2000.....84

Figure 2-11: Estimates of RYL for rice based on MATCH O_3 concentration data expressed as different exposure indices (AOT40 and M7) and associated ER functions across SA for the cropping year 2000.. 86

Figure 2-12: Estimates of RYL for potato based on MATCH O_3 concentration data expressed as different exposure indices (AOT40, W126 and SUM06) and associated ER functions across SA for the cropping year 1999-2000. The circles indicate potato yield (in tonnes/ha) in each grid. 88

Figure 2-13: Estimates of RYL for soybean based on MATCH O_3 concentration data expressed as different exposure indices (AOT40, M7, W126 and SUM06) and associated ER functions across SA for the cropping year 2000. 90

Figure 2-14: O_3 induced crop production loss (CPL) given as million tonnes for countries in SA estimated for wheat and potato during the 1999-2000 cropping year and for rice and soybean during the 2000 cropping year for each of the four O_3 indices; AOT40, M7/M12, W126 and SUM06. 92

Figure 2-15: O_3 induced economic loss (EL) given as millions of US$ for countries in SA estimated for wheat and potato during the 1999-2000 cropping year and for rice and soybean during the 2000 cropping year for each of the four O_3 indices; AOT40, M7/M12, W126 and SUM06.....93

Figure 2-16: Estimates of O_3 induced CPL for wheat, rice, soybean and potato crops grown across SA based on the AOT40 index and associated ER function for the cropping year 1999-2000 for wheat and potato and for the cropping year 2000 for rice and soybean. 95

Figure 2-17: Estimates of O_3 induced CPL for wheat, rice and soybean grown across SA based on the M7 (M12 for soybean) index and associated ER function for the cropping year 1999-2000 for wheat and 2000 for rice and soybean. 96

Figure 2-18: Estimates of O_3 induced maximum and minimum economic loss (EL) given in millions of US$ for the four crops in SA for the year 1999/2000 based on AOT40, M7 (M12 for soybean), W126 and SUM06 indices. 97

Figure 2-19: Total O_3 precursors emissions in the year 2000 that were used in this SA study (TRACE-P), Van Dingenen *et al.* (2009) (EDGAR 3.2) and Avnery *et al.* (2011) (EDGAR 2.0). 110

Figure 2-20: Comparisons of annual monthly mean, surface O_3 concentrations for North India and South India. 113

Figure 2-21: Comparisons of annual monthly mean, surface O_3 concentrations for three different rural locations in SA.. 115

Figure 2-2-22: RYLs estimated for wheat, rice and soybean using M7 (M12 for soybean), W126 and SUM06 indices (as available) plotted against estimates made using AOT40 for each MATCH grid. 119

Figure 2-2-23: O_3 exposure response indices for wheat, rice, potato and soybean. 121

Figure 3-1: Diagrammatic representation of stomatal and non-stomatal uptake of O_3. 128

Figure 3-2: The resistances to O_3 transfer from atmosphere to crop canopy include in the

DO_3SE O_3 dry deposition model. 136

Figure 3-3: Grids with wheat cultivation.. 141

Figure 3-4: Broad outline of the steps that are involved in applying the flux based O_3 risk assessment for wheat in India. 143

Figure 3-5: The f_{phen} profile in relation to the different f_{phen} components 148

Figure 3-6: O_3 Exposure response relationship using AOT40 and flux response relationship using POD_6 for European wheat (LRTAP Convention, 2004) 154

Figure 4-1: Wheat growing agro-climatic zones (AGZs) in India as defined by the Directorate of Wheat Development (DWD, Government of India).. 164

Figure 4-2: Effect of different sowing dates on wheat yield under different meteorological subdivisions in NWPZ, NEPZ and CZ agroclimatic zones in India 169

Figure 4-3: Wheat accumulation period. (a) based on DAS. 172

Figure 4-4: Parameterisation of g_{max} for wheat stomatal conductance model. 184

Figure 4-5: Parameterisation of f_{phen} for the wheat g_{sto} model. 187

Figure 4-6: Parameterization of f_{light} for wheat.. 189

Figure 4-7: Available g_{sto} data for parameterisation of f_{temp}, based on Equations [3-11] and [3-12].. 191

Figure 4-8: Parameterisation of f_{temp} for the wheat g_{sto} model. f_{temp_IN} and the f_{temp_EU} plotted along with, (a) observed relative g_{sto}. 197

Figure 4-9: Parameterisation of f_{VPD} for the European wheat g_{sto} model, represented by black line and the VPDmax. And VPDmin represented by the dotted line. 198

Figure 5-1: MATCH model grids under wheat cultivation, defined as fraction of wheat area per grid. 202

Figure 5-2: Hourly daytime average meteorological conditions and average O_3 concentrations during the O_3 accumulation period calculated using the Indian wheat phenology (IN) with the MATCH data for the cropping year 1999-2000 for the three AGZs in India. 204

Figure 5-3: The 3 different stages of the O_3 accumulation period that have been used for further analysis of F_{st} characteristics; these periods are defined by GDD. 205

Figure 5-4: Flux- and concentration-based O_3 risk to wheat in India 208

Figure 5-5: Relationship between R_{CL_POD6} and R_{CL_AOT40}. 210

Figure 5-6: The relative exceedances of the respective critical levels for POD_6 and AOT40 for wheat across India during the cropping year 1999-2000. 211

Figure 5-7: Relationship between RYL_{POD6} and RYL_{AOT40} 212

Figure 5-8: Estimates of RYL for wheat for the cropping year 1999-2000 based on POD_6 calculated using the EU parameterization and associated European wheat O_3 flux-response functions.. 213

Figure 5-9: Relationship between RYL_{POD6} and RYL_{AOT40}. The data points represent all the grids where wheat is grown. 214

Figure 5-10: Estimates of CPL for wheat for the cropping year 1999-2000 based on (a) POD_6 (CPL_{POD6}) calculated using the EU parameterization and associated European

wheat O_3 flux-response function and (b) AOT40 (CPL_{AOT40}) accumulated over the 3 month growth period defined in Chapter 2. 215

Figure 5-11: Figure 5-9: Relationship between hourly O_3 concentrations and Fst values for the three AGZ grids during the O_3 flux accumulation period..... 218

Figure 5-12: Accumulation of POD_6 and $AOT40_A$ during the O_3 accumulation period for the three selected grids of each AGZ (NEPZ, NWPZ and CZ).. 219

Figure 5-13: Daily maximum stomatal O_3 flux (F_{st}) calculated using IN parameterization, and the corresponding daily average O_3 concentration for grids of the three AGZs.. 220

Figure 5-14: Hourly diurnal O_3 concentration g_{sto} and F_{st} values averaged for the O_3 accumulation period for the NEPZ, NWPZ and CZ grids. 222

Figure 5-15: Hourly diurnal F_{st} (nmol O_3 m^{-2} PLA s^{-1}) values averaged for each of the three stages (I to III) of the O_3 accumulation period for the NEPZ, NWPZ and CZ grids. 223

Figure 5-16: Daily maximum VPD (10*kPa) and daily maximum temperature (°C) during the O_3 accumulation period plotted in relation to f_{phen} for the three grids of each AGZs.. 227

Figure 5-17: Diurnal profiles of F_{st}, f_{temp}, f_{VPD} and f_{light} during the three stages of the O_3 accumulation period 229

Figure 5-18: Average values for f_{light}, f_{temp} and f_{VPD} for a combination of conditions categorized as O_3 concentrations. 231

Figure 5-19: Average values for f_{light}, f_{temp} and f_{VPD} for a combination of conditions categorized as O_3 concentrations. 232

Figure 5-20: Average values for f_{light}, f_{temp} and f_{VPD} for a combination of conditions categorized as O_3 concentrations. 233

Figure 5-21: Relationship between $POD6_{IN}$ and $POD6_{EU}$. 235

Figure 5-22: POD_6 values for wheat in India estimated during the O_3 accumulation period 236

Figure 5-24: Hourly average meteorological conditions and average O_3 concentrations during the O_3 accumulation period 238

Figure 5-25: Evolution of POD_6 calculated using IN_{450} and EU parameterizations over the course of the O_3 accumulation period for the three AGZ grids. 239

Figure 5-26: GDD calculated from SGS until A_{end} using a base temperatures of 0°C (EU) and 5°C (IN_{450}) for the NEPZ grid. 240

Figure 5-27: Daily maximum F_{st} values calculated using the IN_{450} and EU parameterizations..... 241

Figure 5-28: Daily maximum VPD (10*kPa) and daily maximum temperature (°C) during the O_3 accumulation period..... 243

Figure 5-29: Diurnal profile of F_{st}, f_{temp}, f_{VPD} and f_{light} during the three stages of O_3 accumulation period. 245

Figure 5-30: Diurnal profile of F_{st}, f_{temp}, f_{VPD} and f_{light} during the three stages of O_3 accumulation period 246

Figure 5-31: Diurnal profile of F_{st}, f_{temp}, f_{VPD} and f_{light} during the three stages of O_3 accumulation period 247

Figure 5-32: Results of sensitivity analysis for stomatal flux model parameters when the values of each parameter are changed by 20%.....252

Figure 5-33: Results of sensitivity analysis for stomatal flux model parameters when the values of each parameter are changed by 20%.....253

Figure 5-34: Comparison of the difference in spatial pattern between flux and AOT40 in (a) the current study and (b) Simpson *et al.* (2007).....256

Figure 5-35: Comparison of the difference in spatial pattern between flux and AOT40 (Mills *et al.*, 2010).....257

Figure 5-36: Stomatal conductance of wheat grown in India grouped by (a) type of leaf and stands characteristics, (b) measuring instrument, (c) region and (d) research group.....262

Figure 6-1: Area, yield and production statistics for wheat growing in India between 1965 to 2009.....270

Figure 6-2: Decadal (5 yearly) growth in wheat area, yield and production in India.....271

Figure 6-3: Change in area under irrigation for both rain-fed and irrigated wheat between 1955 to 2005.....271

Figure 6-4: The number of new wheat cultivars released in India since 1965 276

Figure 6-5: The number of wheat cultivars bred for a number of different traits that have been released between 1995 to 2008 in India.....277

Figure 6-6: Recommended growing conditions for new wheat cultivars released from 1995 onwards in India. 278

Figure 6-7: Comparison of the 6 different phenological types, including the two scenarios defined to represent new Indian wheat cultivars based on time of sowing and time to maturity. 289

Figure 6-8: The wheat growing period in growing degree days (GDD) for the different wheat phenology types in the three main wheat AGZs in India 293

Figure 6-9: Growing period of late and timely sown cultivars plotted with moving monthly averages of maximum temperature and maximum O_3 for each AGZ.....294

Figure 6-10: Days required to attain vegetative and accumulation (reproductive) period of old and new wheat cultivars in the three AGZ.....295

Figure 6-11: POD_6 and AOT40 values of different wheat categories for the three AGZs. "Base" represents the default phenology.....296

Figure 6-12: The different phenological categories of wheat cultivars in India under scenario I and II and the associated POD_6 and AOT40 values. 298

Figure 7-1: Mean surface O_3 changes over North America, Europe, South Asia and East Asia based on different RCP scenarios constructed for IPCC-AR5. 312

Figure 7-2: Wheat production and consumption statistics for five major wheat producing states and rest of India for the year 2000. 317

Acknowledgements

I would like to thank the following organisations and individuals for their contribution to the writing and completion of this academic thesis:

- The Ministry of Tribal Affairs, Government of India for providing funding for this PhD;
- Dr. Lisa Emberson, PhD supervisor, for her support throughout the research and for the diligent manner in which she reviewed and edited this thesis, particularly during the final few months;
- Prof. Mike Ashmore, Chair of the Thesis Advisory Committee (TAC) for reviewing this thesis and also the TAC members, Dr. Jennie Barron and Dr. Jim Smart for their support and guidance;
- A special word of thanks goes to Dr. Patrick Büker for his help throughout the course of this PhD and reviewing of this thesis;
- Dr. Magnus Engardt for providing O_3 concentration data, Steve Cinderby for producing the GIS maps contained in this thesis and Erik Willis for assisting with the data figures;
- The Stockholm Environment Institute at York for providing a space to work and a truly remarkable working environment;
- Eline and Gonzalo, my housemates, for their help and encouragement during the past three years;
- Ellie Dawkins for providing housing during the final stages of this PhD and for support and encouragement;
- Carine, Kerstin, Annemarieke, Dipu, Gurmeet and all my friends for their support and encouragement;
- Prof. A.K. Attri who encouraged me to undertake this PhD and for his support and advice;
- my family for their love, support and continued source of inspiration throughout the past four years;
- and above all, the Lord Almighty for His faithfulness and hand of grace.

Author's declaration

The work in this thesis is the result of my own investigations conducted under the supervision of Dr. Lisa D. Emberson. I declare that all the work contained within this thesis, apart from work whose authors are clearly acknowledged, is the result of my very own and original work.

No part of this thesis has been submitted for a degree at any other university.

Some of this work has been written up in a peer-review journal.

Chapter 2:

Emberson, L.D., Büker, P., Ashmore, M.R., Mills, G., Jackson, L.S., Agrawal, M., Atikuzzaman, M.D., Cinderby, S., Engardt, M., **Jamir, C.,** Kobayashi, K., Oanh, N.T.K., Quadir, Q.F., Wahid, A., 2009. A comparison of North American and Asian exposure–response data for ozone effects on crop yields, Atmospheric Environment 43 (12), 1945-1953.

Contribution to the paper: Provided the latitude function for wheat growing period (Chapter 2, Figure 2-4) for calculating O_3 exposure to crops in South Asia.

Chapter 1 Introduction

1.1 Agriculture and food security in South Asia (SA)

South Asia (SA) comprises Bangladesh, Bhutan, India, Maldives, Nepal, Pakistan and Sri Lanka and is home to more than 20% of the world's population (UNPP, 2009). Agriculture has always been the backbone of sustenance for the people living in SA. Agriculture occupies 40% of SA's total land area and it provides livelihood for more than 50% of the population and contributes to more than 20% of the region's GDP (IFPRI, 2001).

SA has seen a tremendous increase in agricultural food production in the past five decades; foodgrain (cereals and pulses) production has increased from 80 million tonnes to over 200 million tonnes (Agricultural statistics at a glance, GOI, 2007). This increase was mainly driven by massive increases in production of rice and wheat which rose from about 70 million tonnes to 194 million tonnes in the same period. SA's food supply is dominated by rice and wheat, which accounts for ~ 90% of the region's total cereal production (Figure 1-1). About 70% of the rice and wheat produced in SA comes from India, 16% from Bangladesh and the remaining 14% from Nepal, Bhutan and Pakistan.

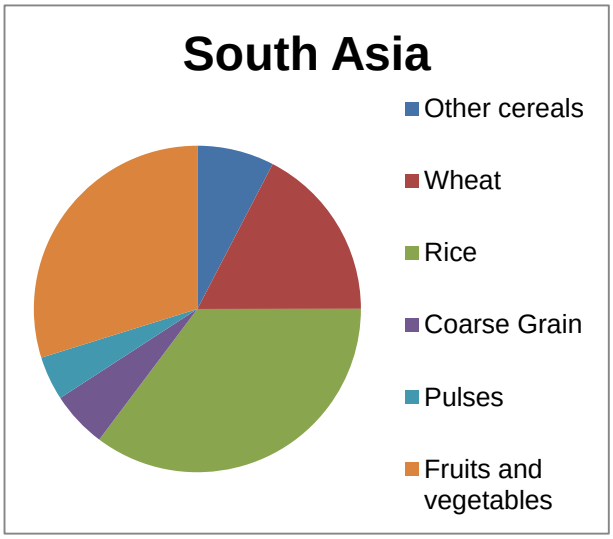

Figure 1-1: Production of major foodgrains and horticultural products in SA. The values are average of 5 years data, 2005 to 2009. Data Source: FAOSTAT (2011)

A key factor for this change was the tremendous increase in India's rice and wheat production (Aggarwal *et al.*, 2008) due in part to associated increases in yield (Figure 1-2; FAOSTAT, 2011). The rice and wheat production increased by a multiple of four and five respectively between 1961 to 2009 (Figure 1-2). Pre-1960, India was food deficient, characterized by low food production and frequent famines and most of its demand was met through imports (Swaminathan, 2010). The Green Revolution in the 1960s played a major role in turning India from a food grain deficient state (prior to the 1960s) to the primarily food grain self-sufficient state that it is at present and has been since the late 1990s (Larson *et al.*, 2004; Singh, 2000).

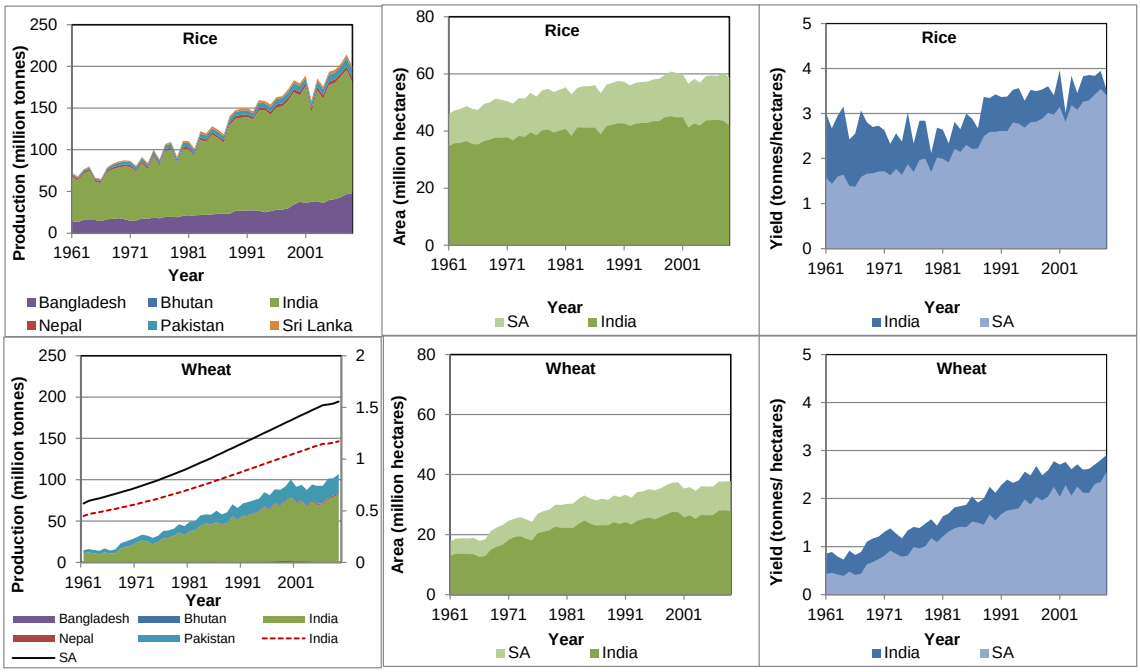

Figure 1-2: Production, area and yield of rice and wheat grains in India and South Asia. Data source: FAOSTAT (2011).

The main factors that contributed to the increase in crop yield and production were

(i) increase in crop cultivation area (Figure 1-2).

(ii) Improved technology and management practices. These included a substantial increase in inputs e.g., use of fertilizers, pesticides and irrigation, use of better

machinery, crop diversification and introduction of high yielding, biotic or abiotic stress resistant cultivars, especially over recent decades (Sankaran *et al.*, 2000; Chatranth *et al.*, 2006; Rane *et al.*, 2007; Swaminathan, 2010). For example, more than 85% of the total wheat area is irrigated (Aggarwal et al., 2008; FAOSTAT, 2011).

(iii) Improved services which includes setting up of various Government agencies (e.g., the National Seed Corporation), specialised institutes (e.g., Indian Agricultural Research institute), research programs (e.g., All India Coordinated Wheat Improvement Project), improvement in rural electrification and communication and introduction of food support policies (e.g., input price subsidies, minimum support price) (Swaminathan *et al.*, 2007; Singh, 2009).

The main impact of the Green Revolution was on the production of rice and wheat, though other agricultural commodities also benefited (Singh, 2009). For example, the production of coarse grains has increased due to increases in the yield but the actual area under production has decreased (Figure 1-3). In contrast, the production of pulses has remained constant between the years 1961 to 2009. These changes reflect the significant growth in income of many people in SA and shift in diets from coarse grains to rice and wheat and away from the consumption of pulses. More recently there has been a decline in per capita cereal consumption as diets are becoming more W esternised and the consumption of meat products is increasing (Mittal, 2008).

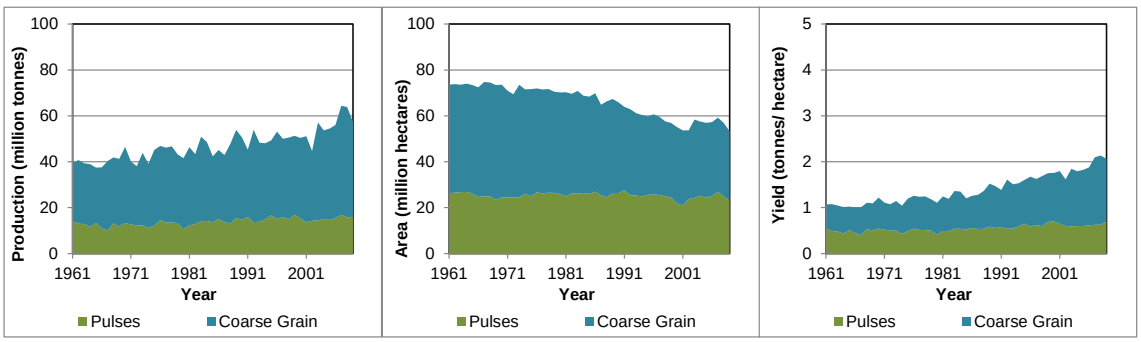

Figure 1-3: Production, area and yield of pulses and coarse grains in South Asia. Data source: FAOSTAT, (2011).

1.1.1 Current status of agriculture in India

Currently, 15% of the total world's cropland lies in SA and it is a major producer of many of the important food crops in the world. SA produces 30%, 18% and 11% of the world's rice, wheat and potato (FAOSTAT, 2011; average of 10 years data, 1995 to 2005). India plays an important role in SA's agriculture; India's share in cereal production is about 75% of SA's total production while in other important crops it is >80% (Figure 1-4). Wheat and rice, serve as the staple food crops for the more than 1 billion people living in India (Joshi *et al.*, 2007b; UNPP, 2009).

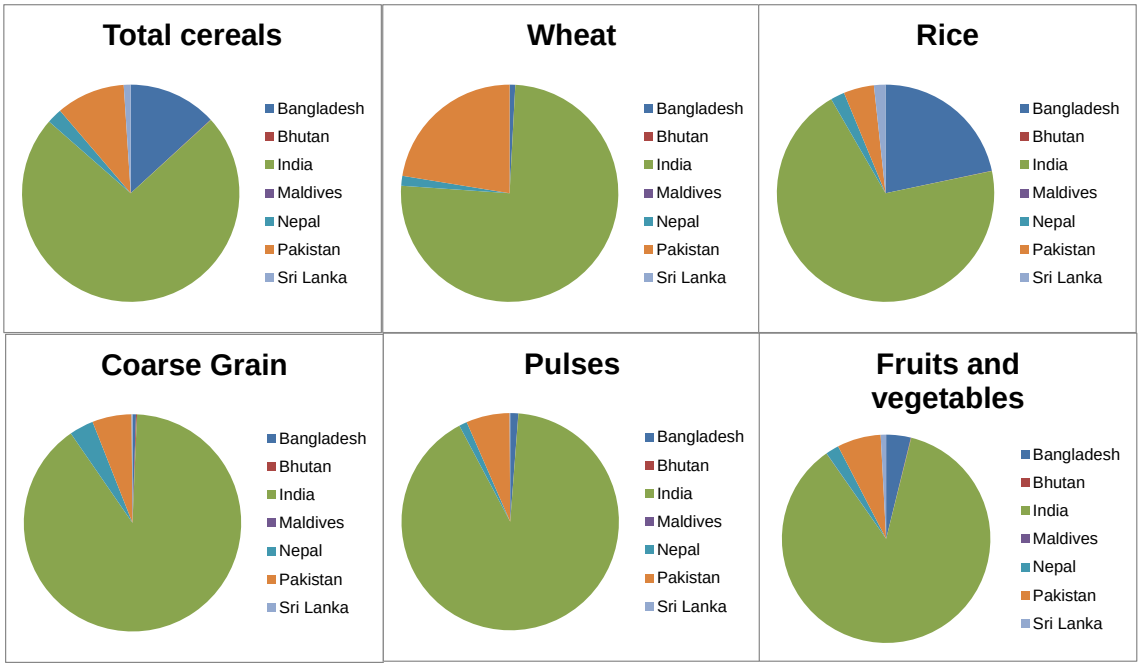

Figure 1-4: Production of major foodgrains and horticultural products in SA. The values are average of 5 years data, 2005 to 2009. Data Source: FAOSTAT (2011).

The most important and agriculturally intensive region in SA are the Indo–Gangetic Plains (IGP). Initially, rice was predominantly grown in the eastern part of the IGP while wheat was grown in the west but now both crops are grown in most parts. Due to the diversification of crops, in most parts of SA, especially the IGP, multiple crops are grown and currently there are more than 20 cropping systems existing within the region (Yadav *et al.*, 1998). The rice-wheat cropping system is the most prominent one with

rice and wheat crops grown in rotation on 13.5 million hectares of land in the IGP spread over Bangladesh, India, Nepal and Pakistan, these systems feed more than 400 million people (Ladha *et al.*, 2000). Diversification of food crops in the region has improved the production of food and feed. However, the production of crops is not always driven by the fact that favourable conditions for crop production exist; for example, despite high potentials for good sorghum yield, production and consumption of sorghum and its products have dropped by over 40% between 1992-93 to 2004-2005 (NSS, 2007; Singh, 2009).

Unlike the developed countries where there have been increases in farm size since 1970, there has been a decline in the size of farms in India (Aggarwal *et al.*, 2004; Chand *et al.*, 2011). In India, 65% of the total number of farmholdings belong to marginal farmholders (<1 hectares) but they own only 20% of the total cropping area (Figure 1-5). Small landholders comprise 19% of the landholders and own 21% of the total cropping area while the remaining 59% of the cropping area is owned by 17% of landholders who own > 2 hectares of land area (Figure 1-5).

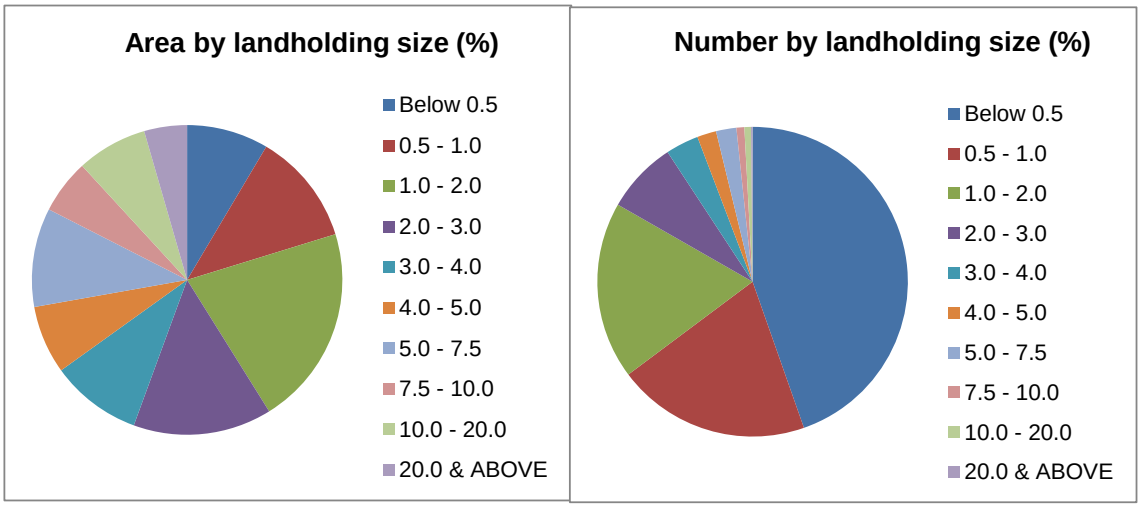

Figure 1-5: Area and number of farm holdings in India for different categories of holding size. Data Source: Agriculture Census Database, National Informatics Center, Government of India (http://agcensus.dacnet.nic.in/nationalsizedisplay.aspx).

This has implications for the use of technology and the level of management which vary widely across the region; this in turn leads to differences in yields between regions (Agrawal *et al.,* 2004). Even within the IGP, the western IGP is characterised by high investment in infrastructure and institutions and effective policy support. This leads to intensive agriculture (using higher inputs of agrochemicals and ground-water for irrigation), surplus food production which has been responsible for regional food security, and seasonal in-migration of male labour. In contrast, the eastern region has relatively low productivity, compounded by poor infrastructure and limited capacity for private investment, and is prone to flooding and drought. It is a food deficient region with widespread poverty, hunger and malnutrition, and has out-migration of male labour to other regions (Abrol, 1999; Agrawal *et al.,* 2004; Erenstein, 2011). An example of the differences between the western and eastern IGP is the use of fertilizer; many small-scale subsistence farmers in eastern IGP (e.g., Bangladesh and Nepal) still rely on farm yard manure (FYM) combined with small amounts of inorganic fertilizers (Morris *et al.,* 1997; Adhikari *et al.,* 1999) while in the western IGP, large amounts of fertilizer are fed into the system (e.g., in Punjab, > 200 kg N/ ha/year; Yadav *et al.,* 1998b).

The irrigation facilities in the SA region have increased significantly between 1960 to 2009 but the improvement has been restricted to a few crops and particular regions. Across India, only 40% of the gross cropping area is irrigated while 60% is still under rain-fed conditions (Mall *et al.,* 2006). Wheat is predominantly grown in the dry season between November to April and more than 85% is irrigated (Figure 1-6) while rice is predominantly grown in the monsoon period (between July to November) and is a rain-fed crop with only ~ 50 % irrigated (DRR, 2011). Figure 1-6 shows that most of the western IGP is irrigated and is predominantly under wheat cultivation.

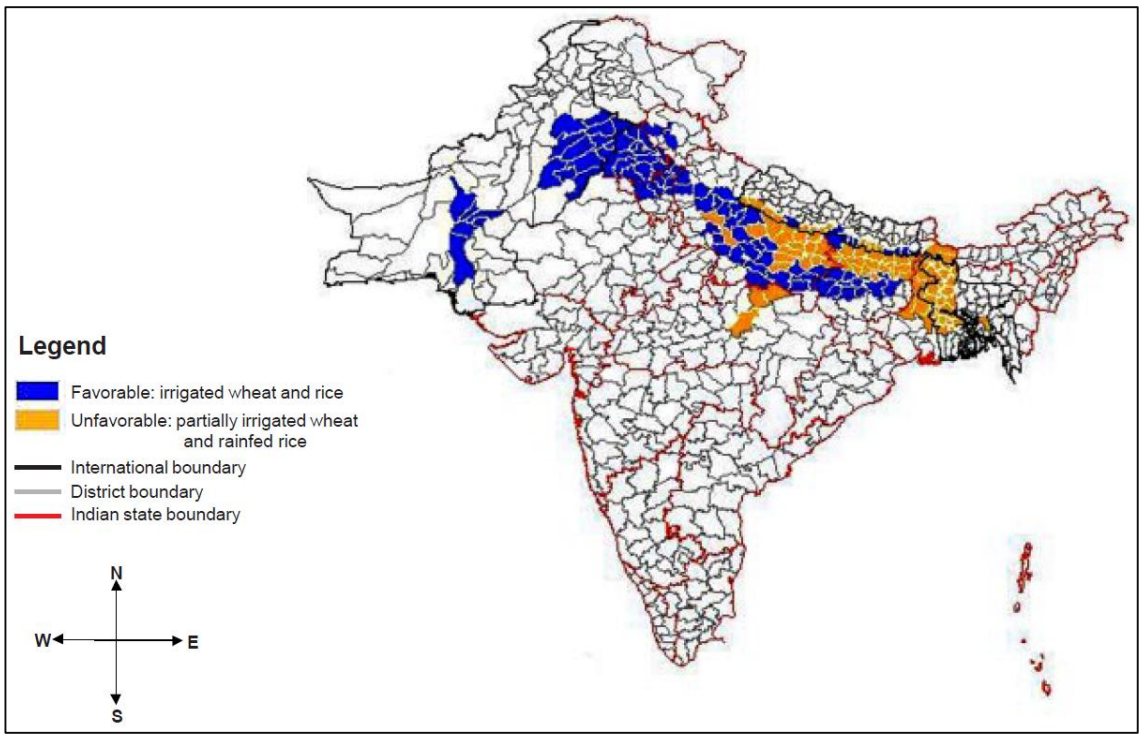

Figure 1-6: Agro-ecological analysis of rice-wheat area and productivity in the Indo-Gangetic plains of SA (Ladha *et al.*, 2000).

At the national level, India's food production has managed to keep pace with the increasing demand in food. The growth in food demand is mainly from the ever growing population and changes in consumption pattern of the population due to increases in income. However, the growth in production of major foods like wheat and rice have been stagnant since the late 1990s while the population continues to grow along with the economy in the region. The stagnation or declining production of pulses and oilseeds has already distorted the balance of supply and demand and India is currently meeting the domestic consumption through imports (Mittal, 2008).

Long term experiments (LTE) performed throughout Asia have shown that the growth in the yield of major crops such as rice and wheat have become stagnant (Bhandari *et al.*, 2002; Dawe *et al.*, 2000; Duxbury *et al.*, 2000; Ladha *et al.*, 2002; Regmi *et al.*, 2002; Yadav *et al.*, 2000). These studies concluded that the possible cause of yield decline are depletion of soil nutrient supplying capacity, delay in planting, increase in pest incidence, and change in climatic variable's like decrease in solar radiation and increase in temperature (Pathak *et al.*, 2003).

In spite of this the increase in rice and wheat production has remained the major source of markets surplus for food grains for feeding the growing urban population (Pathak *et al.,* 2003b). The share of agriculture in the total GPD of the region has decreased from 1981-1985 to 2005-2009 but it still remains an important part of the region's economy with a share of ~20% of GDP in all the countries in SA with the exception of Sri Lanka (Figure 1-7). During this period, the share of agriculture in total employment in India dropped from 63% to 57%) which was mainly due to an increase of employment in industrial, services and other sectors in the region associated with the region's economic development (Mall *et al.,* 2006; World bank, 2011).

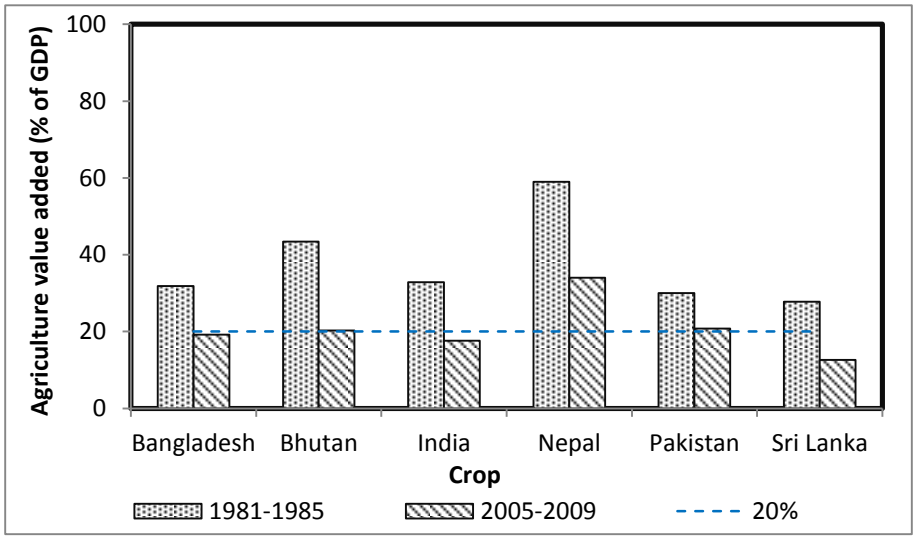

Figure 1-7: Agriculture value added GDP as percentage of total GDP. Data source: UNCTS, (2011) and World Bank, (2011).

Again focussing on India, at national level India may have attained a food secure state; however, at the individual level it is far from being food secure. Approximately 25% of the world's undernourished live in India (FAO, 2006a). The percentage of undernourished people in India has decreased in the past two decades but in absolute terms, the numbers of people undernourished have increased.

The gradual increase in environmental degradation through intensive cropping systems is further compounding problems of food security. There is now a great concern about

the decline in soil fertility, changes in water table depth, rising salinity, resistance of harmful organisms to many pesticides and degradation of the quality of irrigation water, especially in north-western India (Sinha *et al.*, 1998). The western IGP is heavily irrigated and the current yields in this region are getting very close to potential yields, however there are still large yield gaps in the eastern IGP (Ladha *et al.*, 2000). The rain-fed areas are considered to have vast untapped potential for increasing production in the future by upgrading rain-fed agriculture through the introduction of additional inputs (Aggarwal *et al.*, 2008).

Agricultural intensification and diversification in the region, especially in the IGP, in the past few decades has no doubt increased the production of food. However this has also led to degradation of the arable land in the region (Singh *et al.*, 1998). This problem is compounded by the increase in occurrences of crop diseases and pests, increases in temperature and more recently, air pollution. In the IGP aerosol pollution has been identified as an increasing problem causing a reduction in the incoming solar radiation (Verma *et al.*, 2011) which is thought to reduce crop photosynthesis. Aerosol pollution is more prevalent during the winter season in IGP where important crops like wheat, potato, etc., are grown. In addition to aerosol pollution, pollution by ground level ozone (O_3) has also been identified as a potential threat to food security across the region (Royal Society, 2008; Emberson *et al.*, 2009).

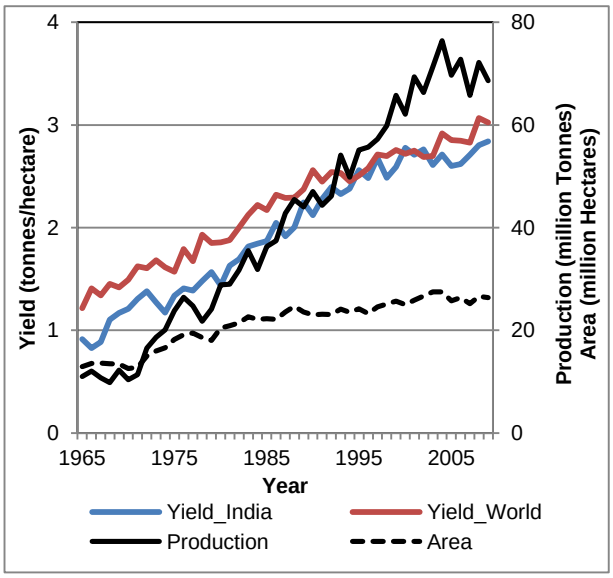

Figure 1-8: Area, yield and production statistics for wheat growing in India between 1965 to 2009. Also shown for comparison is trends in global average wheat yields for the same time period (FAOSTAT, 2011).

1.2 Ground Level O_3 in SA

Ozone (O_3) is a naturally occurring chemical present both in the stratosphere as well as the troposphere (Royal Society, 2008). In the stratosphere, O_3 acts as a protective layer filtering out the harmful UV radiation from the sun (IPCC, 2007), while in the troposphere (at ground level), it is harmful for humans causing health problems such as inflammation of the lungs and bronchia (Anennberg *et al.,* 2010). Ground level O_3 also affects the environment, causing severe damage to ecosystems, forests and agricultural crops (Fuhrer, 2009; Paoletti and Manning, 2007). O_3 is the most abundant tropospheric oxidant and is considered the third most important greenhouse gas (Kley *et al.,* 1999; IPCC, 2007).

1.2.1 Ozone formation

The residence time of O_3 in the atmosphere is ranges between 1-2 days to 3-15 weeks (Royal Society, 2008). About 10 % of O_3 in the troposphere is from stratospheric influx while the remaining ~90 % is produced in the atmosphere. In the troposphere, O_3 is a secondary pollutant and is produced mainly by photochemical reactions of precursors from industrial and other anthropogenic emissions of carbon monoxide (CO), volatile organic compounds (VOC) and nitrogen oxides (NO_X), from burning of the fossil fuels and biomass as well as from natural emission sources including lightning, wildfires, soils, and vegetation (Mittal *et al.,* 2007). These photochemical reactions are driven by meteorological conditions such as high levels of solar radiation, low wind speeds, high temperatures and pressure.

Ultraviolet light (UV) drives the photolysis of either oxygen (O_2) or O_3 which leads to the formation of excited oxygen (O) atoms which then combine with O_2 producing O_3 as described in equations [1-1] to [1-4]

$$O_2 + h\nu \rightarrow O + O \qquad [1\text{-}1]$$

$$O_3 + h\nu \rightarrow O + O_2 \qquad [1\text{-}2]$$

$$O + O_2 \rightarrow O_3\ (+M) \qquad [1\text{-}3]$$

where *hν* =280-290 nm and M is any molecule (e.g., N_2 or O_2)

The excited O atoms also react with water vapour (H_2O) forming hydroxyl (OH) radicals as described in equation [1-4]

$$O + H_2O \rightarrow OH + OH \qquad [1\text{-}4]$$

The production of OH depends on the amount of H_2O in the air which is in turn dependent on temperature and relative humidity (Royal Society, 2008).

The atmospheric concentration of NO_X is an important factor that determines the amount of O_3 production or removal (Royal Society, 2008). In a typical unpolluted atmosphere, the concentration of O_3 is governed by the reactions of NO, O_3 and NO_2 (NEGTAP, 2001). These reactions are given in equations [1-5] and [1-6].

$$NO + O_3 \rightarrow NO_2 + O_2 \qquad [1\text{-}5]$$

$$NO_2 + h\nu \rightarrow NO + O \qquad \text{where } h\nu = 280\text{-}290 \text{ nm} \qquad [1\text{-}6]$$

The O molecule then combines with O_2 to form O_3 as given in equation [1-3].

These reactions mainly occur under typical daytime conditions when the atmosphere is well mixed; under such conditions O_3 concentrations remain fairly low. Additional O_3 can also be produced in very complex processes which involve several hundreds of NMVOCs, radicals, NO_X and VOCs (NEGTAP, 2001). OH radicals play an important role in the tropospheric O_3 chemistry as it combines with methane (CH_4) and CO to initiate the O_3 production and removal reaction cycles. The OH radical can combine with CH_4 and CO to form peroxy radicals (CH_3O_2 and HO_2).

In clean environments with low NO_X level of less than 20 parts per trillion (ppt) CH_3O_2 and HO_2 are removed by mutual reactions to form methylhyperoxide and H_2O_2 (Royal Society, 2008) as given in equation [1-7] and [1-8];

$$CH_3O_2 + HO_2 \rightarrow CH_3OOH + O_2 \qquad [1\text{-}7]$$

$$HO_2 + HO_2 \rightarrow H_2O_2 + O_2 \qquad [1\text{-}8]$$

These reactions lead to a removal of O_3 since the reaction sequence is initiated by O_3 photolysis as given in equation [1-1].

In polluted environments where NO_X concentrations are above 20 ppt, CH_3O_2 and HO_2 combine with NO to form an alkoxy radical (CH_3O) or OH radical and NO_2 as given in equation [1-9] and [1-10].

$$CH_3O_2 + NO \rightarrow CH_3O + NO_2 \quad [1\text{-}9]$$

$$HO_2 + NO \rightarrow OH + NO_2 \quad [1\text{-}10]$$

NO_2 is then photolysed forming O_3 in reaction [1-6] followed by reaction [1-3]. Under lower NO_X concentrations (but above 20 ppt) equations [1-7] and [1-8] dominate the O_3 photochemistry. However, as the NO_X concentration increases the O_3 formation rate increases as a consequence of competition between equations [1-7] and [1-9] for CH_3O_2 and equations [1-8] and [1-10] for HO_2.

Equations [1-9] and [1-10] dominate when the NO_X concentration is very high and reaches a point where OH reacts with NO_2 to form HNO_3 as given in equation [1-11].

$$OH + NO_2 + M \rightarrow HNO_3 + M \quad [1\text{-}11]$$

Under these conditions, if only the NO_X concentration increases, this will decrease the amount of free-radical propagated O_3 forming cycles through reduction in free radicals. However, increasing emissions of CH_4, CO and NMVOCs will allow the free radical propagated O_3 forming cycles to compete more effectively for OH in equation [1-11] and increase O_3 production.

The O_3 concentrations vary seasonally as well as diurnally and are governed by changes in the planetary boundary layer (PBL) and free troposphere. During the day time, turbulent mixing in the PBL due to wind and thermal convection leads to transport of O_3 from the free troposphere (Stull, 1989). High emissions of VOCs and NO_X during the day time, especially in the afternoon hours, coupled with high solar radiation, enhance O_3 formation leading to an O_3 peak during the afternoon hours (Mittal *et al.*, 2007). The major O_3 forming reactions occur during the day as sunlight is required for most of the key reactions leading to O_3 formation but there are potentially significant processes at

night which lead to O_3 removal (PORG, 1998). At night in urban environments, emission of NO_X reduces the concentrations of O_3 through reactions given in equation [1-5] but this does not happen in the rural environment as there are no NO_X emission. This causes high diurnal variability in urban O_3 concentrations while in rural areas there is less variability due to the absence of NO_X emissions (Mittal *et al.,* 2007). In urban areas, night time depletion of O_3 by NO_X in the absence of sunlight plays an important role in O_3 removal form the atmosphere while in rural areas, dry deposition dominates the process of O_3 removal (Mittal *et al.,* 2007; Royal Society, 2008).

In addition, increased amounts of biogenic VOCs are emitted from vegetation which reacts with NO to form the O_3 producing NO_2, this increases the concentration of O_3 by (i) decreasing the amount of O_3 destruction by NO, and (ii) increasing the O_3 producing NO_2. Due to this, higher concentrations and longer episodes of O_3 have been observed in rural areas downwind of the pollutant sources (Mittal *et al.,* 2007). These rural areas are generally agriculturally important areas.

Figure 1-9 shows the O_3 budget within the stratosphere and troposphere and the key tropospheric photochemical mechanisms leading to O_3 formation and destruction. The fact that O_3 is a secondary pollutant and that O_3 formation process take some time to complete is indicated in the figure by O_3 formation and deposition occurring some distance downwind of O_3 precursor emission sources. O_3 precursors are highly mobile and can be transported long distances from their source of origin, as a result of this O_3 can be formed in relatively rural and remote regions which might be free from industrial or vehicular activity (Miller, 1983, in: Miller *et al.,* 1994; Syri *et al.,* 2001; Saitanis, 2003). In addition to this, the life time of O_3 ranges from 1-2 days to 3-15 weeks which means that O_3 can be found at relatively high concentrations some distance away from the from the site of formation (Jonson *et al.,* 2001); it is through O_3 deposition that this pollutant will cause damage to vegetation.

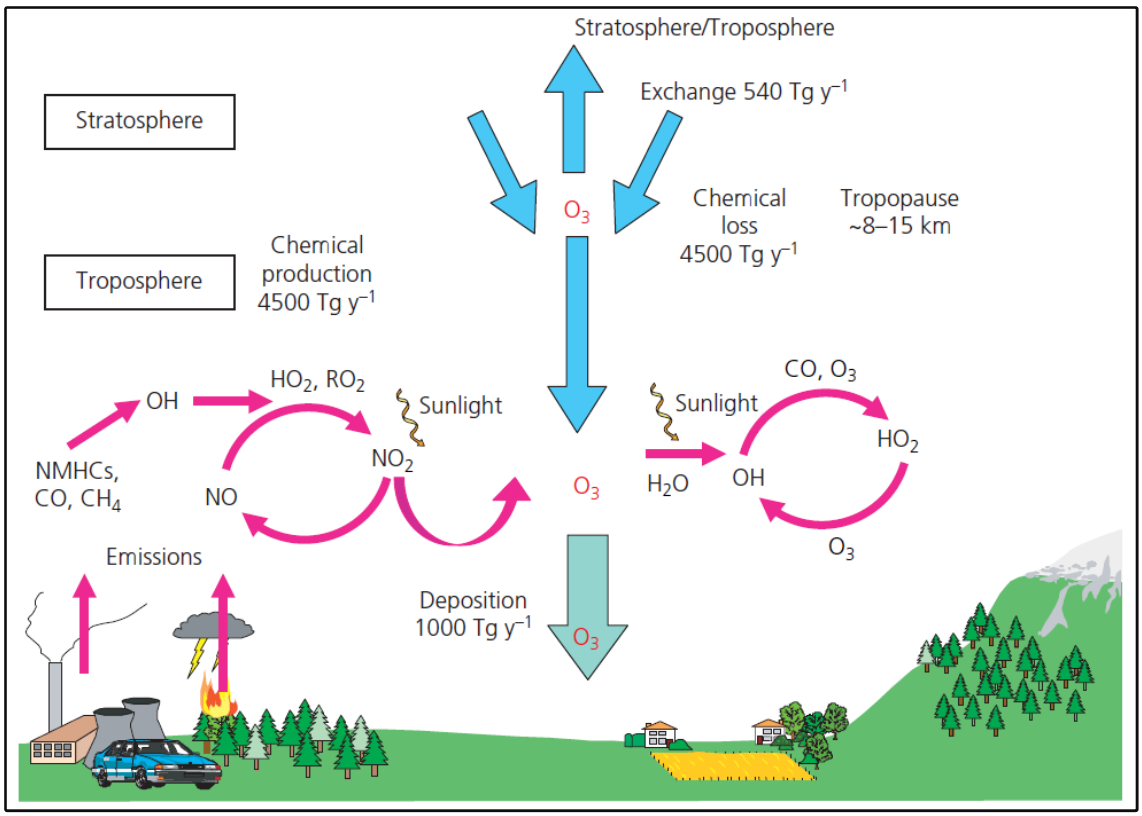

Figure 1-9: Schematic of sources and sinks of O_3 in the atmosphere (Royal Society, 2008).

1.2.2 Emissions of O_3 precursors in India

Modelling studies have shown that there are high concentrations of ground level O_3 across India especially in the IGP. This is mainly due to increases in the occurrence of high emission loads of O_3 precursor gases such as CH_4, NO_X, CO and VOCs. There has been a steady increase in the emission of these gases in India over recent decades (Figure 1-10). Unlike in Europe and North America, where the anthropogenic emissions are mostly from fossil fuel combustion, in Asia, these pollutants arise from fossil fuel combustion but also from biofuels and biomass burning (Phadnis *et al.*, 2002). NO_X and CO emissions in India show a strong seasonality with an early spring peak (monthly mean NO_X = 0.2 TgN; CO = ~ 10Tg) and a late fall minimum (NO_X = ~ 0.12 TgN; CO = ~ 5Tg), (Phadnis *et al.*, 2002). In the spring during the biomass burning season only about half of the NO_X and CO emissions come from fossil fuel combustion but the fossil fuel combustion dominates emissions during the summer and fall (Phadnis *et al.*, 2002). The main anthropogenic sources of these precursor gases are described briefly

below.

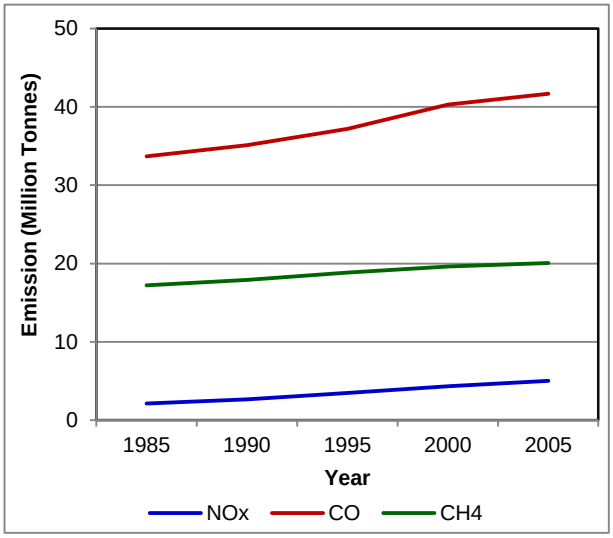

Figure 1-10: Annual emission of NO_X (expressed as Tg-NOx), CO (expressed as Tg-CO) and CH_4 (expressed as Tg- CH_4) in India (based on Garg *et al.*, 2006).

Figure 1-11 gives the main sources of O_3 precursor gases in India. India's NO_X emissions are dominated by emissions from transport and coal generated power plants. It is estimated that NO_X in India has been growing at a rate of 4.4 % annually between 1985 to 2005 and the total estimated NO_X emissions were 5.02 million tonnes (Mt) out of which 34% was from road transport and 30 % from power plants (Garg *et al.*, 2006). Emissions from transport and power plants have increased since 1985 while the percentage of NO_X emissions from biomass burning has decreased but increased in terms of absolute values. The decrease in NO_X emission growth rate is due to improved technologies in the power sector and the introduction of Euro II norms in automobiles (Garg *et al.*, 2011). Ohara *et al.*, 2007 reported that India contributes to 17% of Asia's total emission of NO_X.

India has the highest CH_4 emissions in SA (Yamaji *et al.*, 2003). In India it is estimated that the CH_4 emissions have grown from 18.85 Tg in 1985 to 20.56 Tg in 2008 (Garg *et al.*, 2011). About 61% of this is contributed by the agricultural sector which includes 40% from livestock related activities, 17% from rice cultivation and 21% from biomass

burning (Garg *et al.,* 2011). The other sectors contributing to CH_4 emissions include solid waste disposal (7%), coal mining (5%), fugitive emissions from oil and natural gas production and handling (4%) and waste water disposal (1%).

CO emissions are predominantly due to inefficient and incomplete burning. Biomass burning, especially for cooking in rural households, is the main source of CO in India followed by the transport sector (Garg *et al.,* 2006). The CO emission rate has been increasing by 1.1% annually between 1985 to 2005 and in the year 2005 the annul emission of CO was 41.7 TG (Garg *et al.,* 2006). There is a gradual decrease in the CO emission rate and this is due to the introduction of cleaner technology and fuels. India contributes 26% of Asia's total CO emission (Ohara *et al.*, 2007).

The main source of anthoropogenic NMVOCs in India are fuel consumption for power generation and domestic use (Varshney and Padhy, 1999).

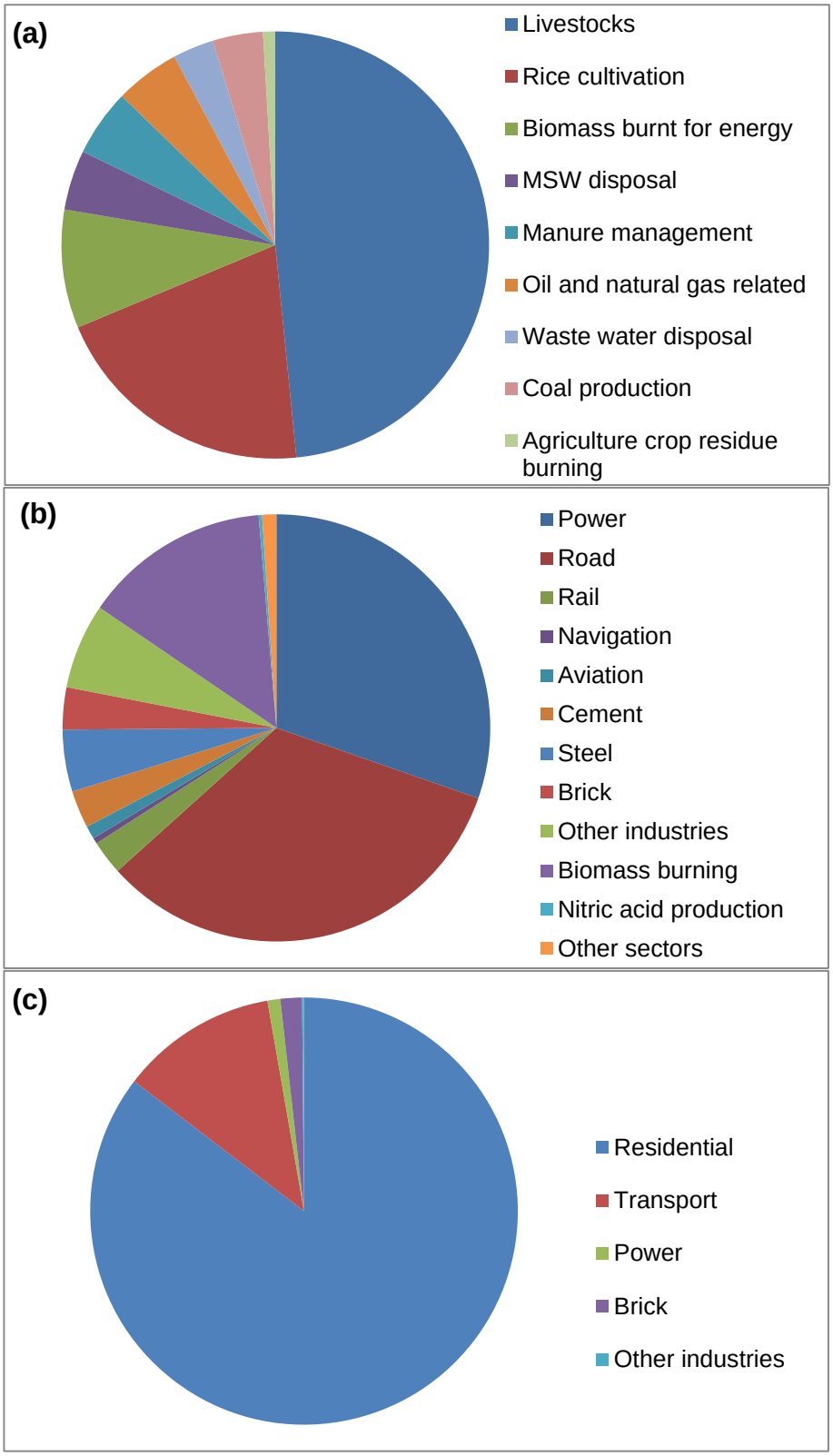

Figure 1-11: Main sources of O_3 precursor gasses in India, (a) Methane (CH_4), (b) NO_X, (c) CO (based on data from Garg *et al.*, 2006).

1.2.3 O_3 climate across SA

O_3 monitoring has been conducted mostly in urban areas (Satsangi *et al.*, 2004; Lal *et al.*, 2000; Pulekisi *et al.*, 2006; Debaje and Kakade, 2006; Khemani et al.., 1995; Nair *et al.*, 2002) with only a few studies having been made at rural locations (Chand and Lal, 2004; Naja and Lal, 2002; Debaje and Kakade, 2006; Ahammed *et al.*, 2006) and semi urban sites (Debaje and Kakade, 2009; Beig *et al.*, 2007; Agrawal *et al.*, 2003, 2005; Rai *et al.*, 2007). These studies show that the O_3 concentration is variable spatially and temporally. The higher O_3 concentrations are observed during the winter to spring months when important crops like wheat and potato are grown (Figure 1-12). This also coincides with spring time when the O_3 precursors like NO_X and CO tend to be high (Garg *et al.*, 2006). During the summer O_3 concentrations are relatively low; this is predominantly due both to the occurrence of the monsoon season as well as O_3 precursor concentrations being lower. Regional chemical transport models also show that the O_3 concentration in the region are high especially during the winter and spring seasons (Mittal *et al.*, 2007; Engardt *et al.*, 2008).

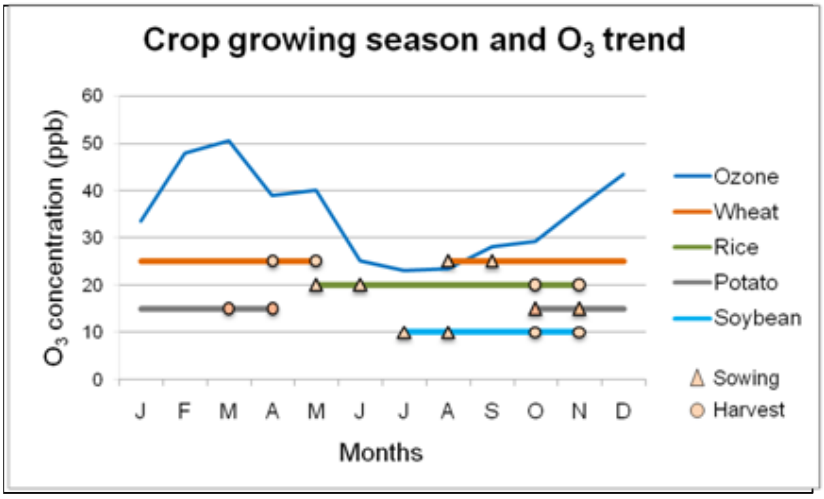

Figure 1-12: Average growing season of wheat, rice, potato and soybean and the annual O_3 trend in South Asia. The crop growing season data is listed in Chapter 2, Table 2-2. Monthly O_3 data are taken from Debaje and Kakade, 2009; Beig *et al.*, 2007; Ahammed *et al.*, 2006.

1.3 O_3 impacts on agriculture

There is now strong evidence from across the globe that current levels of O_3 are sufficiently high to reduce yields of major staple crops like rice (Ainsworth, 2008), wheat (McKee and Long, 2001), potato (Hassan, 2006) and maize (Leitao *et al.*, 2007). Some of these effects include reduction in grain yield (Fuhrer and Booker, 2003), nutritional value (Pleijel *et al.*, 2007) and visible injury to leafy vegetables (Velisariou 1999). These results are based on well-co-ordinated regional O_3 risk assessment studies like the National Crop loss Assessment network (NCLAN) in North America, the European Open-top Chamber experiments (EOTC) in Europe and a number of individual studies in Asia (Wahid, 2006; Feng and Kobayashi, 2009; Singh and Agrawal, 2010) using chambers, EDU (an O_3 specific chemical protectant) and transect studies. Several studies in Asia have shown that current levels of O_3 affects yield of important crops like rice (Feng *et al.*, 2003; Pang *et al.*, 2009), wheat (Ambhast and Agrawal, 2003; Sarkar and Agrawal, 2010), pulses (Agrawal *et al.*, 2005). Many studies have demonstrated inter- as well as intra-specific variability in the sensitivity of the corps to O_3. Crops like wheat, soybean and pulses are considered sensitive to O_3 while potato and rice are considered moderately sensitive (Mills *et al.*, 2007). However, a recent meta-analysis has shown that Asian rice cultivars may be more sensitive to O_3 (Emberson *et al.*, 2009).

1.3.1 O_3 mode of action

The main entry route of O_3 into the plant is through the stomates and the main site of damage by O_3 occurs inside the plant. Once it enters the plant, it affects the plant's biochemistry and physiology ultimately leading to impacts such as reduced growth and yield.

1.3.1.1 **Biochemical effect**

O_3 is a highly oxidizing gas. Once it enters the leaf, it either causes impacts directly by reacting with the cell components in the apoplastic region or indirectly through reaction with the water available in the leaf apoplastic region to form 'Reactive O_3 Species' (ROS) like hydrogen peroxide and hydroxyl radicals (Fuhrer, 2009). Usually the plants'

oxidative stress defence mechanism which consists of radical scavengers such as superoxide dismutase, ascorbate and glutathione peroxidases scavenge some of the O_3 and ROS in the extra cellular and intra cellular spaces (Heath *et al.,* 2008; Matyssek *et al.,* 2008). Unscavanged O_3 and ROS can oxidize various cellular components such as carbohydrates, membrane lipids, amino acids, proteins and unsaturated fatty acids (Mudd, 1996; Gimeno *et al.,* 1999). Such oxidation will damage cell membranes and ultimately lead to the death of cells; this process is that which causes visible leaf damage such as 'fleckings' (Krupa *et al.,* 1998; Velisariou, 1999) or 'leaf bronzing' (Rao and Davis, 2001; Baier *et al.,* 2005; Fiscus *et al.,* 2005). ROS also impairs RUBISCO activity in the cell which can affect photosynthetic CO_2 fixation (Long *et al.,* 2005) and accelerate leaf senescensce (Morgan *et al.,* 2004).

The sensitivity of leaves to O_3 varies with age and position within the canopy, leaves that are still expanding or which have just achieved full maturity are most susceptible to O_3 (Lacasse and Treshow, 1976; Pääkkönen *et al.,* 1995). The O_3 effect at the tissue level can be either acute or chronic. Acute O_3 exposure is the result of oxidative damage to the plant while chronic O_3 exposure is caused by biochemical and physiological damage to the plant (Fares *et al.,* 2010). At acute O_3 doses (i.e. hourly O_3 concentrations greater than 60 ppb v) there is rapid reduction in stomatal aperture and conductance (Aben *et al.,* 1990), reduction in photosynthesis (up to 40% reduction; Paoletti *et al.,* 2007) or unregulated cell death at > 150 ppb v O_3. Under chronic exposures (e.g., 70 ppb v, over 8 hours per day, for 1 month in crops; Paoletti and Grulke, 2010), the stomatal response becomes sluggish (McAinsh *et al.,* 2001; Paoletti and Grulke, 2010), lesions can develop over days or weeks and leaf senescence can be accelerated.

1.3.1.2 **Physiological effect**

The uptake of O_3 into the leaf mesophyll occurs mainly through the stomates during photosynthetic gas exchange (Fiscus *et al.,* 2005). O_3 affects both the stomatal functioning as well as the photosynthetic system in plants.

O_3 induces stomatal closure mainly through effects on the guard cells (McAinsh *et al.,* 2002; Goumenaki *et al.,* 2010) and this decreases the CO_2 uptake and thereby decreases photosynthesis. O_3 reduces the photosynthetic efficiency of the plants as a result of

reduction in the RUBISCO activity and content (Dann and Pell, 1989; Mckee *et al.,* 2000; Guidi, 2002) and sunsequent loss of carboxylation efficiency (Farage *et al.,* 1991; Morgan *et al.,* 2003, 2004; Fiscus *et al.,* 2005; Frie *et al.,* 2008). O_3 induced accelerated leaf senescence may also reduce irradiance interception thereby reducing photosynthetic carbon assimilation and food production (Long and Naidu, 2002; Morgan *et al.,* 2003; 2006; Dermody *et al.,* 2008).

1.3.1.3 Effects on carbon allocation

Exposure of crops to O_3 reduces root to shoot ratio, reduces harvest index and alters leaf chemistry. O_3 affects the root to shoot biomass ratio in crops by altering assimilate partitioning (Cooley and Manning, 1987; Grantz and Yang, 2000; Morgan *et al.,* 2003). Chronic exposure of O_3 to crops diverts the allocation of assimilates from root to aerial biomass (Miller *et al.,* 2008; Cooley and Manning). However, some studies have shown that O_3 affects both roots and shoots equally (Morgan *et al.,* 2003).

Reduced assimilate allocation to roots may lower the soil moisture availability (Grantz *et al.,* 1999) and affect the mycorrhizal development and rhizobial nodulation which may reduce the plant nutrient availability (Runeckles and Chevone, 1992; Fuhrer and Brooker, 2003) and pathogen susceptibility of roots (Cooley and Manning, 1987). Decreased allocation to roots also reduces carbon flux to leaves (Andersen, 2003) and long-term carbon balance (Felzer *et al.,* 2005). O_3 effects phloem loading and assimilate partitioning to grain is reduced while carbohydrates are retained in the leaves (Fuhrer and Broker).

1.3.1.4 Yield losses

O_3 causes reduction in grain size, grain weight, grain number, and ultimately reduces the yield of crops (Fiscus *et al.,* 2005; Black *et al.,* 2000; Bender and Weigel, 2011; Feng *et al.,* 2003). These changes are either due to O_3 effects on photosynthetic efficiency or shifts in carbon allocation. Studies have shown that O_3 induces a reduction in photosynthetic capacity of the crop after the flowering stage which can affect seed/

grain development (Morgan *et al.,* 2006). Although most studies show reductions in yield, some studies report an increase in biomass and yield of crops when exposed to low O_3 concentrations (Finnan *et al.,* 1996) and in some studies no significant changes have also been observed (Mulholland *et al.,* 1997).

O_3 can also affect the economic value of crops by reducing the quality of grains (eg., protein content; Feng *et al.,* 2008), tubers (Vorne *et al.,* 2002) or leafy vegetables (Velissariou, 1999). However some studies have reported that while O_3 reduces the grain yield it increases the grain quality by increasing its protein content (Pleijel *et al.,* 1999; Pikki *et al.,* 2008).

1.3.2 Experimental evidence of O_3 impacts on crops collected in India

All available data related to O_3 effects on crops grown in SA were collected from peer reviewed literatures to get an overview of the level of information on O_3 impacts to crops in SA (Figure 1-13; only studies from India are provided in the figure). The experimental methods consisted of four types (transect, open top chamber (OTC), closed top chamber (CTC) and chemical protectant studies (EDU)). However, out of this only OTC (only filtration), transect and EDU studies were used to study the impact of ambient O_3 on crops in India (Table 1-1). In transect studies, simultaneous experiments are done in different field sites with varying O_3 concentrations; in OTC experiments the ambient air is either filtered to remove O_3 (filtration) or additional O_3 is added to ambient air (fumigation); in EDU studies, certain amount of EDU is applied to the plants to protect from O_3. The control treatment was charcoal filtered air (CF) for fumigation studies, field site with O_3 concentration <10 ppb v in transect studies and non-EDU treated crops in EDU studies. Field studies are important to be able to study O_3 impacts but it is not always easy to interpret the O_3 impacts as there are other pollutants and crop growing factors that affect the crop in the field.

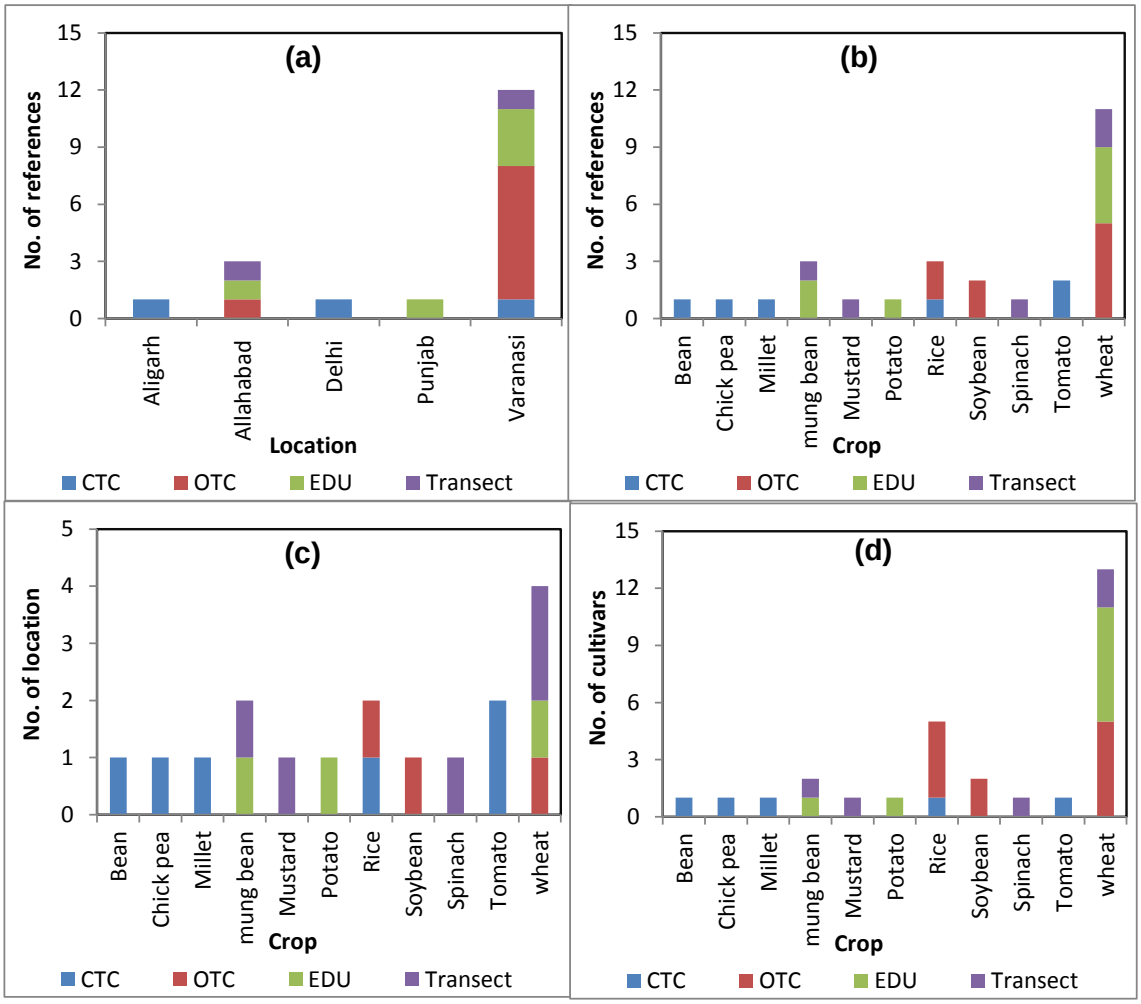

Figure 1-13: Summary of collated Indian data describing the different O_3 experiments that have been performed on crops in India (a) the number of references describing O_3 experiments by different locations, (b) the no. of references describing O_3 experiments by crop type, (c) the no. of locations where O_3 experimental studies on different crops have been performed and, (d) the no. of cultivars studied for different crops. For all combinations of data the experimental method used (closed top chamber (CTC); open top chamber (OTC), chemical protectant study (EDU), Transect study (transect) is also indicated.

Although there have not been many O_3 crops loss studies carried out in SA, those that have been performed show that current levels of O_3 in the region during the crop growing season can have an effect on crop yield (Agrawal *et al.*, 2005; Singh and Agrawal, 2010; Wahid *et al.*, 2011). All the experimental studies have to date been carried out in the IGP region at three locations in the western IGP and two locations in

the eastern IGP (Figure 1-13 and Figure 1-14). However out of 18 studies conducted in India, 12 studies were conducted in Varanasi with most of the studies using open top chambers (OTC) and either O_3 filtration or fumigation techniques (Figure 1-13). Wheat was the most studied (12 studies) crop.

The studies show that average O_3 concentrations during the crop growing period frequently exceed 40 ppb and the yield losses under ambient O_3 concentrations range between 0.5 to 25% for wheat (Agrawal *et al.,* 2003; Ambhast and Agrawal, 2003; Rai *et al.,* 2007; Sarkar and Agrawal. 2010; Singh and Agrawal, 2009, 2010; Tiwari *et al.,* 2005), 32 to 73% for mungbean (Agrawal *et al.,* 2003; Agrawal *et al.,* 2005), 5 to 4% for spinach (Agrawal *et al.,* 2003) and 6 to 20 % for mustard (Agrawal *et al.,* 2003). A summary of the experimental conditions from which these yield loss data have been derived is given in Table 1-1. Experimental studies have also been carried out on rice (Agrawal, 1982 cf. Agrawal 2003; Rai *et al.,* 2010) and soybean (Singh *et al.,* 2010; Singh, 1998) and these show that exposure to O_3 causes reduction in photosynthesis, chlorophyll and ascorbic acid content and biomass.

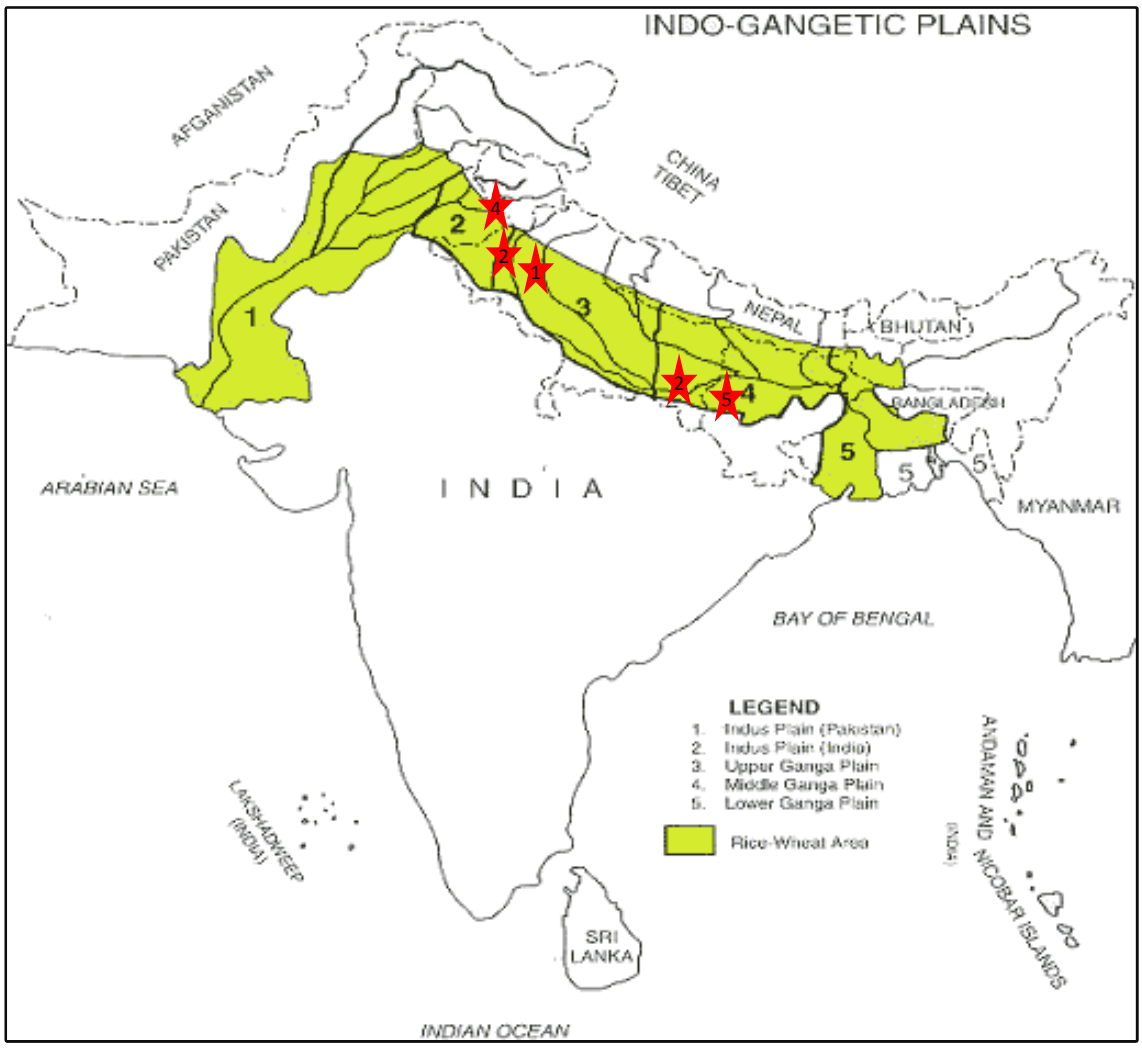

Figure 1-14: Map showing the locations where experimental studies of O_3 effects on crops have been carried out. The stars indicate the locations; 1=Aligarh; 2= Allahabad; 3=Delhi; 4= Punjab; 5= Varanasi. Also shown for reference is the rice wheat cropping area in SA. Map source: CYMMIT, http://www.cimmyt.org/

Table 1-1: Summary of collated South Asian data describing the yield response of crops to ambient O_3.

Crop	**Location**	**Experiment type**	**O_3 concentration, ppb v; averaging period in hours (h)**	**Yield loss (%)**	**References**
Mungbean	Allahabad	EDU	13-67; 8h	32	Agrawal *et al.*, 2005
	Varanasi	Transect	25-59; 6h daily average for 45 days	50 to 73	Agrawal *et al.*, 2003
Mustard	Varanasi	Transect	11-15; 6h daily average for 45 days	6 to 20	Agrawal *et al.*, 2003
Spinach	Varanasi	Transect	25-59; 6h daily average for 45 days	5 to 40	Agrawal *et al.*, 2003
Rice	Faisalabad	OTC, potted	75; 8 h daily mean	29 to 37	Wahid *et al.*, 2011
Wheat	Varanasi	OTC	45-47; daytime growing season mean	11 to 20	Sarkar and Agrawal. 2010
	Varanasi	EDU	35-54: 8h	8 to 20	Singh and Agrawal, 2009
	Varanasi	EDU	45; 8h	5 to 10	Singh and Agrawal, 2010
	Varanasi	OTC	42; 8h	21	Rai *et al.*, 2007
	Varanasi	EDU	34-54; 8h	2 to 21	Singh *et al.*, 2009
	Varanasi	Transect	70; 4h	9	Ambhast and Agrawal, (2003)
	Varanasi	Transect	11-15; 6h daily mean for 45 days	0.5 to 25	Agrawal *et al.*, 2003
	Varanasi	EDU	41; 8h	13 to 19	Tiwari *et al.*, 2005
	Lahore	OTC, potted	72; 8 h	18 to 43	Wahid, 2006

It is evident from these studies that current O_3 levels are affecting the crops grown in the region, however standardised experimental studies are required to improve understanding of the response of crops grown in India to O_3 levels experienced across the crop growing regions.

To be able to extrapolate site-specific experimental studies to wider agricultural regions such that the extent and magnitude of potential O_3 induced yield losses might be assessed has traditionally been performed through the derivation of dose-response relationships. Although currently no dose-response relationships for SA exist, those developed for certain crops in North America and Europe have been applied under SA conditions. The results from the experimental studies summarised above are generally in agreement with modelling studies that have used these dose-response relationships and show that current levels of O_3 in SA may be already having detrimental impacts on production of important crops in the region like wheat and rice (Van Dingenen *et al.,* 2009; Roy *et al.,* 2009; Debajee *et al.,* 2010; Avnery *et al.,* 2011a). However due to the localised data availability and also inconsistencies in the methods used, the results from the experimental studies are not sufficient to fully validate these model results. Nevertheless, the modelled results show that the risk of O_3 on crops is more in the IGP region and wheat crops are at higher risk from O_3 impacts because of the high O_3 concentrations that are prevalent in the region.

1.4 Future threats to agriculture in SA

The population of SA and India is projected to increase by 47% and 50% between 2000 (1.4 and 1.0 billion) and 2030 (2.0 and 1.5 billion) respectively (UNPP, 2008). This means that there will be a high increase in food demand which will primarily have to be met by increases in production of food crops like cereals. In the past, the ever growing increase in food demand has been largely met by the increases in crops, primarily rice and wheat. However, currently the growth in production of staple crops like rice and wheat have been stagnant and production of crops like sorghum has decreased. Studies show that there are yield gaps in many crop growing regions across India particularly in the rain-fed cropping areas of eastern IGP (Aggarwal *et al.,* 2008).

These are mainly due to a number of stresses that are prevalent in the region, such as

heat stress due to rising temperatures (Joshi *et al*., 2007c), changes in weather patterns including the frequent delays in monsoon (Phadnis *et al*., 2002) which are critical for > 50% of the rain-fed cropping areas in India, rising salinity, especially in the irrigated regions (Ladha *et al.,* 2003; Rodell *et al.,* 2009), decreasing the water table depths (Singh, 2000), drought and biological stresses (Sankaran *et al.,* 2000; Chatranth *et al.,* 2006). The most feasible way to increase the production is to bridge the existing yield gaps through improvement in crop management practices and the development of better higher yielding cultivars. Efforts are underway to develop higher yielding cultivars for 'recognised' stresses in India (Mishra *et al.,* 2007). However, these efforts may be compounded by additional stresses like O_3.

A number of special reports in the past decade have highlighted the SA region, and especially the IGP region, to be at risk from climate change factors which include increases in temperature and air pollutants, especially O_3 (IPCC, 2007; Royal Society, 2008; Ramanathan *et al.,* 2008). It is predicted that crop yields in SA could potentially decrease by up to 30% due to climate change even if the direct positive effect of increased CO_2 on crops is taken into account (IPCC, 2007). Modelled studies show that the O_3 risk will increase even further in the future (Van Dingenen *et al.,* 2009; Avnery *et al.,* 2011b) and aggravate the problem of food security in the future due to its adverse impact on production of major staple crops. It is projected that there will be an increase of 23 % in global surface O_3 concentration by 2050 (Prather *et al.,* 2001). Krupa (2003) estimated that by 2025, 30-75% of the world's cereals might be grown in regions with detrimental levels of O_3.

The high projected increases in O_3 in the SA region will further increase the already existing risk of crops to O_3. It is important therefore to understand the threat posed by O_3 across SA and particularly in India. The experimental studies are localised and limited and therefore do not give a very good representation of O_3 risk in the region. Therefore, to gain a better understanding of the potential threat from O_3 across the region it is useful to model O_3 risk and to identify the regions that are most at risk from O_3 pollution and identify the factors that might be important in determining the sensitivity of crops to O_3 across the region. It is also important to investigate whether new crop traits that breeders in the region are introducing might affect O_3 sensitivity.

1.5 Research aims and questions

Agriculture, especially production of staple crops like rice and wheat, is vital for the sustenance of the society. The projected increases in food demand through increases in population and the increases in biological (e.g., diseases) and physical stresses (e.g., climate change factors like increase in temperature) and air pollution (e.g., O_3) may pose an additional threat to food security in the near future. Efforts are under way to improve yields by developing high yielding crop cultivars that are tolerant to the existing stresses prevalent in SA. O_3 pollution in SA may worsen in the near future (Royal Society, 2008) and hence pose an even greater threat to future crop yields. Therefore it is important to consider O_3 tolerance when developing new crop cultivars. As such, it is important to identify the regions and crops that might be most at risk from O_3 in order to aid future research.

With this in view, the research questions for this study are:

1. Does ground level O_3 pose a threat to staple crops grown in SA?

2. Do differences in geographical location and cropping patterns influence O_3 sensitivity?

3. Are there differences in O_3 risk estimated using concentration- and flux-based O_3 indices?

4. What are the main factors influencing flux based assessments of crop sensitivity to O_3 on crops grown in India?

5. Can the flux based method be used as a tool to identify crop physiological traits that might influence O_3 sensitivity, and hence inform future efforts in crop biotechnology?

6. How are the traits being introduced in new wheat cultivars likely to affect O_3 sensitivity?

In answering these research questions the thesis is structured such that each Chapter deals with a particular aspect of the research, a short summary of each Chapter is given below.

Chapter 2: A regional O_3 risk assessment was performed to assess the potential extent of O_3 impacts on staple crop yields across the region. The O_3 induced yield losses were calculated based on existing concentration based European and North American O_3 exposure indices and modelled O_3 concentrations. Crop production and related economic losses were estimated to assess the magnitude of the O_3 threat. The economic loss is compared with the gross domestic product (GDP) of SA to place the potential O_3 threat in the context of the region's economy.

Chapter 3: This Chapter investigates the appropriateness and feasibility of using more biological meaningful approaches, which allow for crop specific and environmental conditions to modify sensitivity to ozone, to conduct O_3 risk assessments for crops in the region. Focus is made on wheat crops grown in India as wheat is the most studied crop in terms of O_3 and due to the crop's importance in the region.

Chapter 4: This Chapter discusses the methods used to parameterize the more biologically robust O_3 flux based risk assessment model for wheat crops grown in India. Data on O_3 flux influencing parameters for Indian wheat cultivars were collected from relevant peer reviewed literature and national databases.

Chapter 5: This Chapter describes the results of the application of the O_3 flux based model. The results are compared with those of the concentration based risk assessment methods and analysis is performed to understand which crop physiology, phenology and environmental factors are most influential in determining O_3 risk. The importance of the parameterization of the model is also assessed to understand the robustness of the Indian

parameterization. A sensitivity analysis is performed to identify those model parameters that most important in determining model output and results.

Chapter 6: This Chapter explores the potential application of flux based approaches as a tool capable of informing future efforts in crop biotechnology. A comprehensive literature and data base review was performed to identify the main traits/ characteristics that are being bred for in the new wheat cultivars and which of these may influence O_3 sensitivity. Flux based risk assessments were performed for these traits to study whether new wheat cultivars may be more sensitive to O_3 pollution.

Chapter 7: This final chapter gives an overall discussion of the results from Chapter 2 to 6 and identifies areas of potential future research.

Some of this work has been written up in a peer-reviewed paper;

Emberson, L.D., Büker, P., Ashmore, M.R., Mills, G., Jackson, L.S., Agrawal, M., Atikuzzaman, M.D., Cinderby, S., Engardt, M., **Jamir, C.,** Kobayashi, K., Oanh, N.T.K., Quadir, Q.F., Wahid, A., 2009. A comparison of North American and Asian exposure–response data for ozone effects on crop yields, Atmospheric Environment 43 (12), 1945-1953.

Chapter 2 Concentration based O_3 risk assessment

2.1 Introduction

The literature review in Chapter 1 summarizes the experimental evidence describing ground level ozone (O_3) effects on arable crops in SA; these data clearly suggest that O_3 might be a threat to important crops growing across the region, though it is recognised that the experimental evidence is limited in terms of geographical area covered with most data being collected at only a few sites in the IGP region. Agriculture is vital to the wellbeing of the population of the region (FAO, 2006). The relatively high O_3 concentrations that photochemical models estimate to occur across the region under the current day, with monthly means in the northern India ranging from 30–45 ppb (Engardt, 2008) and the projected increases in these O_3 concentrations over the next few decades under current legislation (CLE) emission scenarios (Dentener *et al.*, 2006; Royal Society, 2008) suggest O_3 to be an issue of increasing concern for SA. This concern is heightened given the likely effects high O_3 concentrations might have on crop yield and given the fact that there is likely to be a substantial increase in food demand in SA (Chatranth *et al.*, 2006). As such, O_3 may pose a significant threat to food security in the region. Therefore, it is important to investigate the potential O_3 risk to crop production in SA to assess both the magnitude and spatial extent of the problem.

Risk assessment studies to assess the potential impact of O_3 on crop productivity have been performed at the regional level, in the US (Adams *et al.*, 1989), Europe (Holland *et al.*, 2002; Holland *et al.*, 2006) and more recently in East Asia (Wang and Mauzerall, 2004; Aunan *et al.*, 2000; Roy *et al.*, 2009) as well as on a global scale (Van Dingenen *et al.*, 2009; Avnery *et al.*, 2011a). The global study conducted by Van Dingenen *et al.* (2009) highlighted the SA region as a high risk area, both in terms of scale of the crop yield losses predicted (which ranged between 13 to 28% for wheat grown across India), and the subsequent effects on crop production, with estimates of 11.6 to 29.1 tonnes/ha production losses. The economic losses in wheat crops were also substantial with estimates of between 1.7 to 4.3 billion $US for the year 2000, with losses rising to 10.7 % by 2030 under a CLE emission scenario.

O_3 exposure-response (ER) relationships are necessary to perform these risk assessments as they allow quantification of the plant response to O_3 exposure in terms

of yield loss (Emberson *et al.*, 2009). ERs provide the relationship between the exposure of the plant to O_3 and its effect on the plant (e.g. reduction in grain yield for crops) and hence quantify effects based on O_3 exposure. ER functions are obtained by an empirical fit of experimental data which identifies the function that provides the best statistical correlation between exposure (based on an exposure index) and response (e.g. yield, biomass loss etc...). To date ER functions have largely been based on Weibull (Adams *et al.*, 1989; Wang and Mauzerall, 2004) or linear functions (Mills *et al.*, 2007). The data represent the average response of the commonly grown cultivars in the region and therefore should be representative of the crop responses to O_3 at regional and national levels (Van Dingenen *et al.*, 2009).

To derive these ER functions, an extensive amount of data describing crop response (e.g. yield loss) for a range of pollutant concentrations needs to be collected from well-coordinated experimental studies; co-ordination of studies is important since this enables data to be collected from across a geographical region so that ERs are representative of environmental and pollution conditions (Unsworth and Geissler, 1992; Emberson *et al.*, 2009). There have been a number of extensive field studies in the US (National Crop Loss Assessment Network-NCLAN; Heagle 1989) and Europe (European Open Top Chamber Program-EOTCP; Jager *et al.*, 1992 and Changing Climate and Potential Impact on Potato Yield and Quality-CHIP; Temmerman *et al.*, 2002) to study and understand crop response to O_3 exposure. The data collected from these studies have been used to establish crop-specific O_3 ER relationships using different O_3 exposure indices (Wang and Mauzerall, 2004; Mills *et al.*, 2007; Lesser *et al.*, 1990; U.S.-EPA, 1996 and 2006). Such extensive studies for deriving ER functions have not been conducted in SA. Due to the absence of Asian ER functions, risk assessment studies conducted in the Asian region (Wang and Mauzerall, 2004; Van Dingenen *et al.*, 2009) have had to rely on the ERs that have been developed using data predominantly collected from the US and Europe.

The most commonly used O_3 exposure indices for studying O_3 impact on crops in Europe and the US are seasonal 7 hour or 12 hour mean O_3 concentrations during daylight hours (M7 and M12 respectively; Adams *et al.*, 1989; Lesser *et al.*, 1990) and seasonal cumulative O_3 over a threshold of 40 ppb and 60 ppb (AOT40 and SUM06 respectively; Mills *et al.*, 2007; U.S.-EPA, 1996). .

Many studies have reported that the O_3 impacts on crops are more closely related to cumulative exposure above a threshold concentration when summed over the crop growth period. This is because cumulative O_3 exposure indices gives more weight to the higher O_3 concentrations which are considered to be important in influencing the *O_3* effect on crops (Lee *et al.*, 1988; Lefohn *et al.*, 1988) as compared to the seasonal means which give equal weighting to all concentrations.

The threshold concentration is a cut-off concentration above which cumulative O_3 concentrations show a statistical relationship with plant response (Musselman and Lefohn, 2007). The cut-off concentration selected to assess O_3 effects for crops grown in Europe is 40 ppb with hourly O_3 concentrations above 40 pbb v adding to the index termed the Accumulated over a Threshold concentration of 40 ppb (AOT40). In the US a similar index, the SUM06, uses a higher threshold level of 60 ppb and sums all of the hourly O_3 concentration between zero and 60 ppb. W126 is a biologically based cumulative O_3 exposure index that gives higher weight to higher O_3 concentrations but also takes the lower O_3 concentrations into account. It uses a sigmoidal function to weight O_3 concentrations (Lefohn and Runeckles, 1987; Lehfohn *et al.*, 1988; U.S.-EPA, 1996, 2006).

ER functions therefore help relate O_3 concentrations to crop damage, usually described as crop yield loss. Therefore to perform regional level O_3 risk assessments these ER functions need to be used in conjunction with regional estimates of O_3 concentration, usually derived from photochemical O_3 models (capable of estimating O_3 concentration fields predominantly as a function of O_3 precursor emissions and meteorology). The crop yield loss that is quantified from these O_3 regional risk assessments can be translated into production and economic crop loss estimates through combination with agricultural production statistics (Adams *et al.*, 1989; Wang and Mauzerall, 2004).

This method is applied in this Chapter with the objectives to:

(1) To estimate the potential risk, both in terms of crop yield loss and subsequent crop production loss, of O_3 to key agricultural crops grown in SA;
(2) To assess which crops might be most at risk from O_3 in SA;
(3) To examine the spatial variation of the O_3 risk to crops across SA and;
(4) To assess the suitability of the existing O_3 exposure indices and associated ERs in assessing O_3 risk for crops grown in SA.

2.2 Methodology

In this chapter O_3 concentration ER functions are used in conjunction with modelled O_3 concentrations and crop distribution and production statistics to estimate the impact of O_3 on crops grown across SA. The crop impacts are presented in terms of yield losses which are translated into crop production and economic loss estimates. Figure 2-1 describes the combination of datasets used in this modelling approach. The crop related data describing the location, growth period and production of staple crops were obtained at the district level for India and Pakistan and at the country level for the rest of SA. The O_3 data were obtained from the Multi-scale Atmospheric Transport and Chemistry (MATCH) photochemical model for the year 2000 (Engardt, 2008) in the form of gridded hourly O_3 values (0.5° x 0.5°). A Geographical Information System (GIS) was used to integrate these two sets of data using crop specific ER functions such that the O_3 effect on crops in terms of yield, production and economic loss across SA could be defined. An overview of the integration of these different datasets describing crop information and O_3 data with O_3 ER functions to estimate the O_3 induced yield losses and subsequent crop production and economic losses is given in Figure 2-1. Further details of the data and methods used in this concentration based risk assessment of O_3 impacts on staple crops grown in SA is given in the following section.

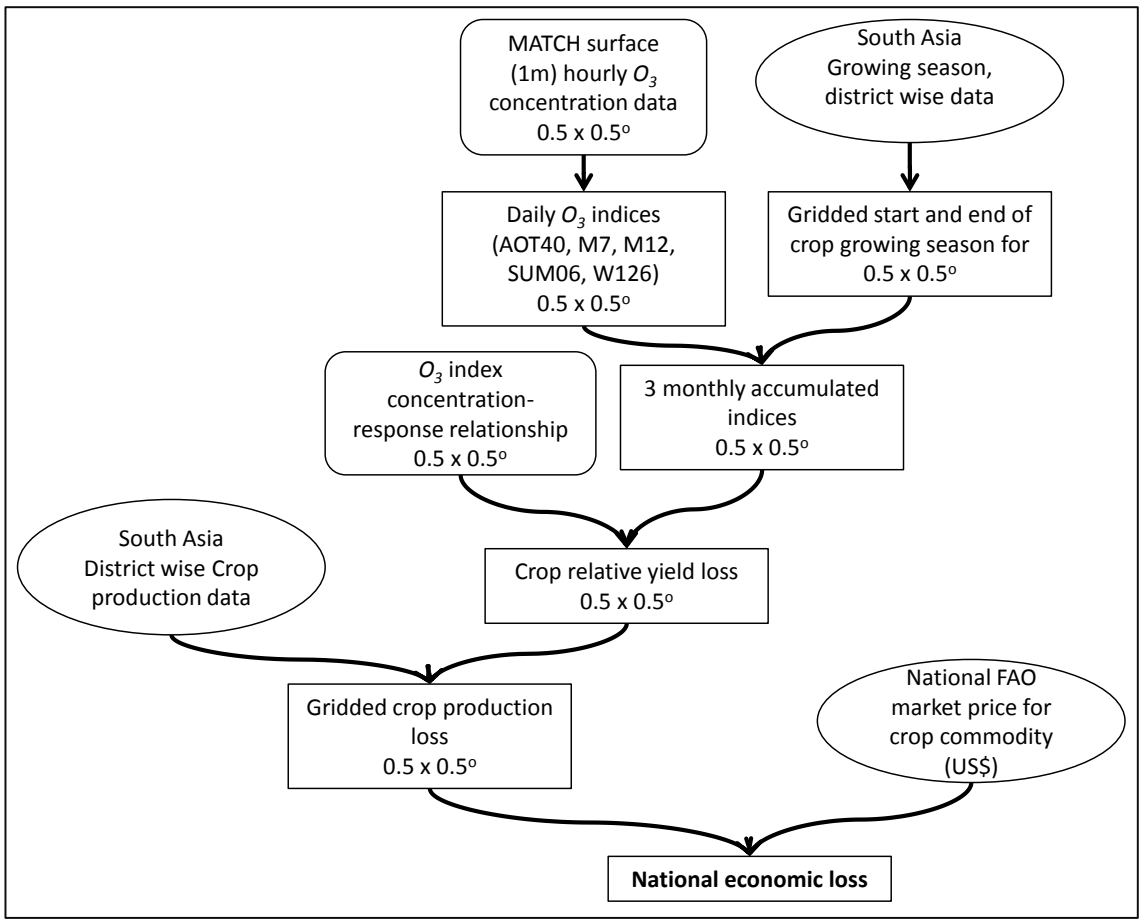

Figure 2-1: Schematic of the steps involved in the concentration-based risk assessment of O_3 impacts on staple crops in SA.

2.2.1 O_3 data

2.2.1.1 MATCH model and O_3 concentration field

Modelled hourly O_3 concentrations for the entire SA region were provided by Magnus Engardt, SMHI (Swedish Meteorological and Hydrological Institute), Sweden. The O_3 concentrations were modelled using the MATCH model, a regional Eulerian offline chemistry transport model that is used to estimate hourly, three dimensional fields of O_3 (Engardt *et al.*, 2008). Concentrations were provided that simulated O_3 levels at an assumed crop canopy height of 1 meter. The MATCH model (Engardt, 2008) estimates O_3 concentration fields across SA based on emission data using anthropogenic Transport and Chemical Evolution over the Pacific (TRACE-P) emission (Streets *et al.*, 2003; Carmichael *et al.*, 2007) and biogenic emissions from Global Emission Inventory

Activity (GEIA) (http://www.geiacenter.org/; Guenther *et al.,* 1995) along with meteorological data provided by the European Centre for Medium-Range Weather Forecasts (ECMWF, http://www.ecmwf.int/products/data/; Uppala *et al.,* 2005).

MATCH was developed at SMHI and originally intended for modelling O_3 concentrations in Europe (Robertson *et al.,* 1999). It has been validated in a number of studies related to modelling O_3 in Europe (Tilmes *et al.,* 2002; Roemer *et al.,* 2003; Laurila *et al.,* 2004; Solberg *et al,.* 2005; Tarrasón *et al.,* 2005). It has also been parameterized to simulate O_3 concentrations for SA; an initial evaluation of the model against O_3 monitoring data for this region has been performed (Engardt, 2008). The horizontal spatial resolution of the model is 0.5° latitude x 0.5° longitude and it has 30 vertical layers with 10 layers in the lowest 1 km (Engardt, 2008). Figure 2-2 shows a map of SA with the spatial resolution of the gridded MATCH modelled O_3 data. A comparison of the MATCH spatial resolution with other models that have been used to simulate O_3 concentrations across SA is given in Table 2-1. This comparison would suggest that the MATCH model has a finer spatial resolution than most of the photochemical models developed for SA application.

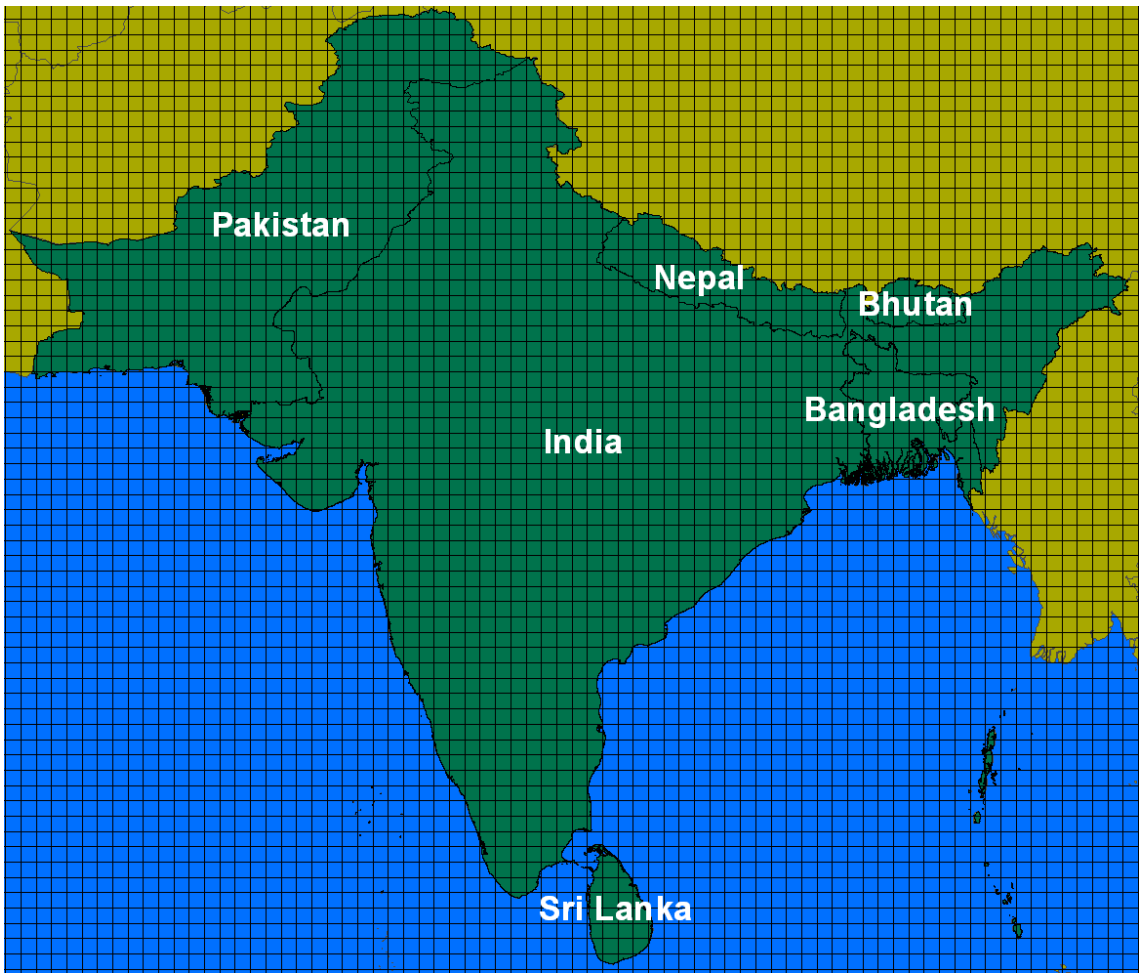

Figure 2-2: Map of SA showing the spatial resolution of the MATCH model grids (0.5° x 0.5°) used for O_3 concentration simulations (Engardt, Pers. Comm.)

Table 2-1: Comparison of the spatial resolution of atmospheric chemistry models that have been used for simulating O_3 concentrations in SA. All the models have used meteorological data from ECMWF.

Model	Horizontal resolution	Vertical resolution	References
HANK	60 km x 60 km	38 vertical layers; lowest layer, 10mbar thick	Mittal *et al.*, 2007
MATCH	50 km x 50 km (0.5° x 0.5°)	30 vertical layers;10 layers in the lowest 1km	Engardt, 2008
MOZART-2	2.8° x 2.8°	34 vertical levels extending up to approximately 40 km	Avnery *et al.*, 2011a and b
REMO-CTM	0.5° × 0.5°	20 vertical layers; lowest layer, 10hPa pressure level	Roy *et al.*, 2009
TM5 (JRC)	GAINS Asia: 1° x 1°	25 vertical layers; Lowest layer, 50m	Dentener and Dingenen, 2007; Dingenen *et al.*, 2009

2.2.2 Crop data

2.2.2 .1 Selection criteria of the crops and crop distribution

Four major arable crops grown in SA (rice, wheat, potato and soybean) were investigated in this assessment; these crops were selected for investigation for the following reasons: (i) the wide geographical distribution of the crops across the region; (ii) the economic importance of the crops in the region and; (iii) the availability of ER functions for the crops. The two main staple crops in the region are rice and wheat which contribute ~ 90% of the total cereal production of the region (FAOSTAT, 2011: average of 10 years data, 1995- 2005). Potato and soybean, which are also part of the main diet of the people in the region, contribute ~ 80% of total production of roots and tubers and 30% of pulses respectively (FAOSTAT, 2011: average of 10 years data, 1995- 2005). SA has a major share in the world's production of rice, wheat, potato and

soybean (Figure 2-3: SA's percentage share in the World production and area harvested of potatoes, rice, soybean and wheat (FAOSTAT, 2011). The values on the y-axis indicate the percentage share for each of the crops). These crops also give a good coverage of the cropping season over the whole year; wheat and potato are grown during the winter (from November to May) and rice and soybean are grown during the summer/ monsoon period (from May to November) (Figure 1-2).

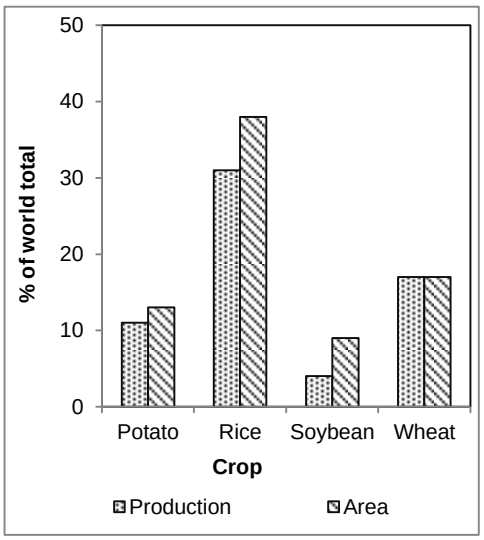

Figure 2-3: SA's percentage share in the World production and area harvest of potato, rice, soybean and wheat (FAOSTAT, 2011). The values on the *y*-axis indicate the percentage share for each of the crops and *x*-axis indicate the crops.

The SA countries studied in this assessment are: Bangladesh, Bhutan, India, Nepal, Pakistan and Sri Lanka. These are the countries that are included in the UNEP Malé Declaration on Control and Prevention of Air Pollution (http://www.rrcap.unep.org/male/). The Maldives, which is also a Malé Declaration country, is not included in the present study as very little agricultural production takes place on the islands that make up this country (FAOSTAT, 2011). There is no wheat production in Sri Lanka; the country's entire wheat needs are met through imports (FAS-USDA, 2005). Similarly, in Bangladesh there is no production of soybean (Table 2-5).

2.2.2.2 Crop data collection

Crop data sources

The crop phenology (sowing and harvest dates) and crop production statistics (production, area and yield) of rice, wheat, potato and soybean were obtained from national and international databases that are listed in Table 2-2. SeedNet, DWD and NFSM are national databases provided by the Ministry of Agriculture, India. These databases offer the most comprehensive and standardized data.

Table 2-2: List of national and international databases from which the relevant crop data were obtained. The references that correspond to the numbers in the table are given below.

Parameter	**Data Source**					
	Bangladesh	**Bhutan**	**India**	**Nepal**	**Pakistan**	**Sri Lanka**
Sowing and harvest dates	*	*	2, 3,4,5, 7	*	*	*
Production, area and yield	1	1	1, 2, 3,4,5	1	1, 6	1

1 – FAOSTAT - http://faostat.fao.org/site/567/default.aspx#ancor

2 - Directorate of Wheat Development (DWD), Ministry of Agriculture India (http://dacnet.nic.in/dwd/)

3 - National Food Security Mission, Ministry of Agriculture, India (http://nfsm.gov.in/)

4 – Madhya Pradesh state agricultural board (for soybean), http://www.mpmandiboard.com/comp2003/comp1.htm

5 - International Potato Center, CGIAR, http://research.cip.cgiar.org/confluence/display/wpa/India

6- Ministry of Food, Agriculture & Livestock, Pakistan

7- Directorate of Rice Development (DRD), Ministry of Agriculture, India (http://drd.dacnet.nic.in/)

8- Central Potato Research Institute (CPRI), http://cpri.ernet.in/, Shimla, India

* The sowing and harvest dates of India were used for all the other countries.

9 – SeedNet, National initiative for information on quality seeds, Government of India, http://seednet.gov.in/

Crop phenology

There are different types of climatic regions across SA (Aggarwal and Mall, 2002). There is also a spatial (regional) variation in the crop cultivars used as well as the cropping pattern for specific crops. For example, the growing period of wheat is shorter at lower latitudes (Mitra and Bhatia, 2008). In many parts of SA most crops can be grown successfully over a range of growth periods (i.e. have multiple cropping seasons) but there is usually one dominant or main cropping season for each crop; only a very small percentage of the crop will be grown outside of this main growth period. In this study, the main cropping season defined in Table 2-3 for each of the four crops investigated is used.

Table 2-3: The main crop growing season along with its percentage share in crop production as compared to the total production in SA. The sowing and harvest dates are defined from the data sources listed in Table 2-2.

Crop	**Main growing season**	**Sowing**	**Harvest**	**Share of total production in SA**	**References**
Wheat	Winter (Kharif)	Irrigated Timely sown-10-25 November; Irrigated Late sown: 25 Nov.-25 Dec.; Rain-fed timely sown: 25 Oct.-10 Nov.	NEPZ: 15 March-15 April NWPZ: 15-30 April CZ: 20Feb-30Mar PZ: 15Feb-15Mar HZ: May-June	~ 80 %	DWD
Rice	Monsoon	May - July	September – November	~75%	FAO, 2005
Soybean	Monsoon	Mid June – Mid July	September	99%	FAS-USDA, 2005
Potato	Winter (Kharif)	November	March	~ 80%	CGIAR

The harvest time of wheat across the region varies with latitude, with regions in the lower latitudes harvesting earlier than those in the higher latitudes (DWD; Rane *et al.*, 2007; Mitra and Bhatia, 2008). To assess whether it is possible to establish a robust relationship between the wheat harvest date and latitude, wheat harvest dates for 20 wheat growing states in India were collected (DWD) and plotted against their respective latitudes (Figure 2-4). Based on these data, a latitude function (Lat_{fn}) was derived. There was a significant linear relationship between harvest date and latitude (r^2= 0.73) represented by equation [2-1].

The Lat_{fn} is given by,

$$H_W = 3.5077x + 1.7419 \qquad [2\text{-}1]$$

Where, H_W is the harvest date of wheat and x is the latitude location in degree radians.

This latitude function, Lat_{fn} was used to calculate the harvest date and subsequently the three month O_3 accumulation period of wheat (Section 2.2.4.2). The values calculated using Lat_{fn} for wheat are comparable to the observed dates recorded in other studies (Rane *et al.*, 2007; Mitra and Bhatia, 2008).

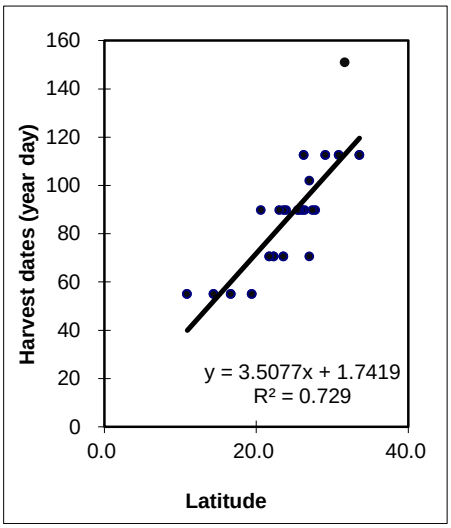

Figure 2-4: Harvest dates obtained from data sources listed in Table 2-2 plotted as a function of latitude for wheat growing across the region.

A similar method was used to establish whether the harvest date of the other crops, rice, potato and soybean, could also be established. No strong relationships between latitude and harvest were found for these crops and therefore fixed dates, calculated from the plant phenological data obtained described in Table 2-2 and Table 2-3, were used to define the harvest period. Median values of these data used to define the harvest dates as described in Table 2-4.

Table 2-4: The harvest date of rice, potato and soybean crops grown in SA based on data from the literature listed in Table 2-2 and Table 2-3.

Crop	**Harvest date (year day)**	
	(Median)	**(Mean)**
Rice	305	300±24
Potato	75	55±13
Soybean	299	297±6

(b) Crop statistics

India is divided into states and Pakistan into provinces. These states and provinces are further sub-divided into districts. District level crop production, area and yield data for India and Pakistan (554 districts + 70 districts respectively) were collected from the sources listed earlier in Table 2-3. The crop statistics for the remaining SA countries were obtained from FAOSTAT (2011), this information is defined at the country level (Table 2-5). The rice and soybean crop statistics were for the cropping year 2000 while for potato and wheat data represent the cropping year 1999-2000. This is because potato and wheat are sown in between Nov-Dec and harvested the following year. To have consistency in the data used across the entire SA region, the district level crop production data of the year 2000 for India and Pakistan was normalized to the FAO 2000 crop data.

Year 2000 was selected as the base year to allow for comparison with the global risk

assessment conducted by Van Dingenen *et al.* (2009), which also used data from 2000. Analysis of meteorological data obtained from (NOAA, 2009) also showed that the year 2000 was a moderate year with regards to temperature suggesting that this year would also be moderate in terms of O_3 concentrations.

Table 2-5: Crop production (CP) and crop area under cultivation of wheat, rice, potato and soybean in the 6 different countries of SA investigated in this study; data are provided for the cropping year 1999-2000. District and state level data obtained for India and Pakistan (see text) are standardized to national data level data (FAOSTAT, 2011).

Country	**Wheat**		**Rice**		**Potato**		**Soybean**	
	CP	**Area**	**CP**	**Area**	**CP**	**Area**	**CP**	**Area**
Bangladesh	1840	832	37628	10801	2933	243		
Bhutan	4	4.6	44	26	22	3	1	1
India	80058	27486	127400	44712	24713	1340	5276	6420
Nepal	1184	660	4216	1560	1183	122.6	17	19.8
Pakistan	20707	8463	7114	2377	1848	111	1	1
Sri Lanka			2860	832	48	4	1	1
SA	103793	37500	179262	60310	30747	1820	5295	6440

Note: Crop production (CP) is provided in units of 1000 tonnes and crop area in units of 1000 hectares.

2.2.3 Spatial resolution of the data

The O_3 and crop production data required to perform this risk assessment are available on different spatial resolutions. The MATCH O_3 concentration data were provided on a gridded resolution of 0.5° x 0.5° (Figure 2-2) and the crop production data on a district, province or country level spatial resolution. In order to combine these data to perform the risk assessment required aggregation to a common spatial resolution; the MATCH

grid was used to define this spatial distribution. A district map for the crop data was obtained from GADM (Global Administrative Area Database), http://www.gadm.org/ (Figure 2-5). The GADM is a spatial database which gives spatial details of the world's administrative areas (or administrative boundaries) specifically designed for use in GIS and other related mapping software. This database was used to obtain the location and area of the countries in SA as well as the districts in India and the provinces in Pakistan and was used in conjunction with the GIS software to convert the country and district level crop statistics into gridded data.

The areas (districts, provinces and countries) by which crop production statistics were provided were divided according to the MATCH grid producing smaller area units termed district polygons (DP; Figure 2-6). The percentage share in area (PA_{DP}) of each DP to the total area of each district was calculated as

$$PA_{DP} = \frac{Area_{DP}}{Area_{D}} \times 100 \qquad [2\text{-}2]$$

where $Area_{DP}$ is the area of the DP and $Area_{D}$ is the area of the district, province or country.

The crop production statistics for each DP were then calculated as area weighted averages according to

$$P_{DP} = P_{D} \times \frac{PA_{DP}}{100} \qquad [2\text{-}3]$$

where P_D is the crop production of each district.

This resulted in the SA region being divided into 6453 DPs each with its own crop production statistics and O_3 concentration data.

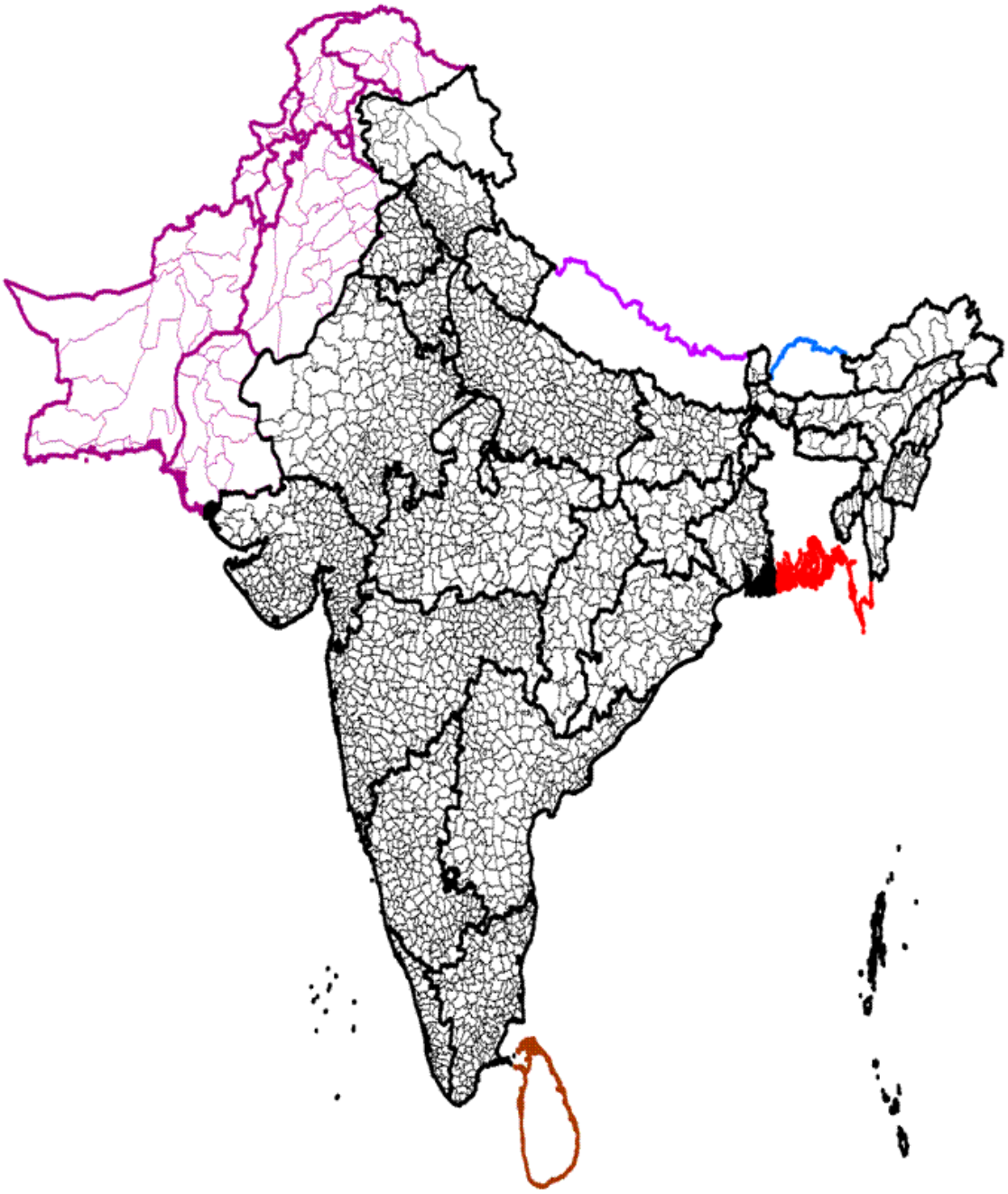

Figure 2-5: Map of SA showing the spatial resolution at which the crop statistics data was obtained. Map source - GADM (2008).

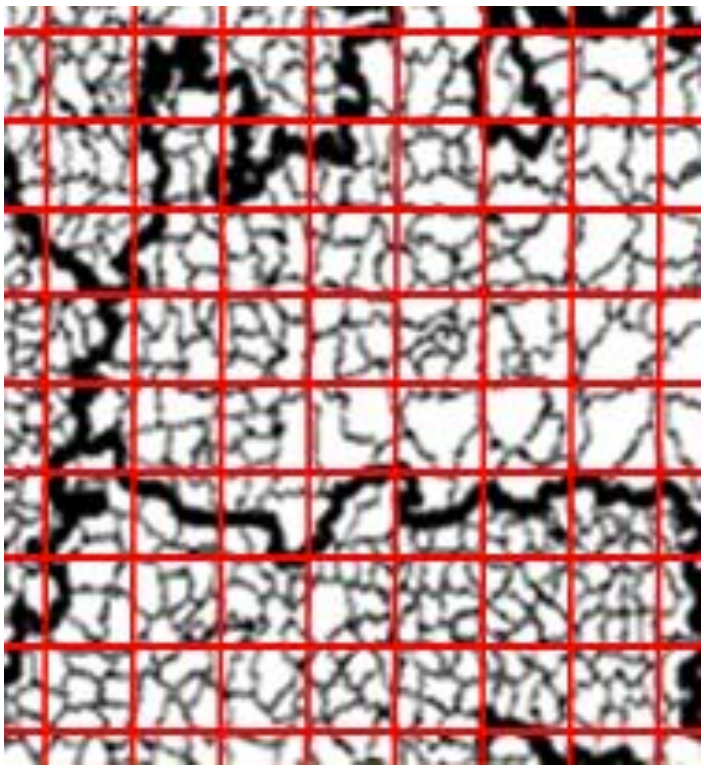

Figure 2-6: An example of aggregations of MATCH grids into the district map of SA. The districts are divided into smaller units, district polygons (DPs), according to the MATCH grids. The red grids indicate MATCH grids (0.5° x 0.5°).

2.2.4 O_3 exposure indices

Four concentration based O_3 exposure indices, AOT40, M7 (M12 for soybean), W126 and SUM06 were used to characterise the impact of O_3 on crops grown in SA (Fuhrer, 1997; LRTAP Convention, 2004; Heagle *et al.*, 1987; Adams *et al.*, 1989; Lesser *et al.*, 1990; U.S.-EPA, 1996, 2006). These indices were selected for the following reasons: (i) they are most widely used O_3 exposure response indices for regional O_3 risk assessment having been applied in Europe (Mills *et al.*, 2010), North America (U.S.-EPA, 1996, 2006), Asia (Wang and Mauzerall, 2004) as well as globally (Van Dingenen *et al.*, 2009; Avnery *et al.*, 2011a and b); (ii) they represent two broad categories of O_3 exposure indices, i.e., they characterize O_3 concentrations either as mean or cumulative values over a crop growth period and; (iii) the ER functions for these indices are available from the literature for the four crops, wheat, rice, soybean and potato, that are being assessed in the present study. Table 2-6 shows which indices were used for each of the 4 crops

based on availability of the ER functions. The methods developed to apply these exposure indices under SA conditions are presented below; essentially application requires that the daylight hours and the crop growing season, both length and timing, over which the indices are calculated need to be defined for SA conditions. To ensure consistency in the application of these different indices, the length and the timing of each crops growing season is defined and kept constant for all O_3 index calculations. The definition of daylight hours varies by index and the methods used to define these are described in turn for each index.

For consistency, the application of the index in terms of growth period needs to mirror the experimental studies that were used to derive the exposure response relationships for which the indices have been used to derive yield losses. AOT40, W126 and SUM06 are calculated over a three month accumulation period. The time period for calculating M7/ M12 seasonal mean O_3 concentrations is not uniform since the exposure period used to derive ER functions for M7 and M12 varied. However, since this variation included periods of up to 3 months (55 to 92 days for wheat and 80 and 90 days for soybean), it was considered appropriate to use a 3 month averaging period since this allowed consistency with the other indices. Further, since this is a growing season average, the use of an extended averaging period will, if anything underestimates yield losses and therefore errs on the side of caution.

The O_3 exposure indices are calculated for the three month before the date of harvest. Thus the end of the averaging or accumulation period is taken as the harvest data and the start of the averaging or accumulation period is taken as 90 days before the harvest date. The identification of the harvest dates for the 4 crops used in this study has been described previously and listed in Table 2-4 and, for wheat, described in equation [2-1].

2.2.4.1 Seasonal average O_3 concentrations

The M7 index is used to quantify O_3 exposure for wheat and rice and the M7 (or M12) index is used for soybean (see Table 2-5). The time period for the M7 (7 daylight hours) and M12 (12 daylight hours) calculation is intended to capture the time of the day when both plant sensitivity to O_3 and O_3 concentrations are at their highest (Heck *et al.,* 1983); daylight hours between 09:00 – 16:00 hours and 08:00 – 20:00 hours were used for

applications of this index in North America (Heck *et al.*, 1983). However, conditions in SA will differ from those in North America (e.g. day length, diurnal O_3 concentration profile, plant physiological status) such that the daylight period over which these indices are averaged needs to be redefined. As such, the 7 and 12 hour daylight periods for SA were identified by plotting data describing time of the day during which peak O_3 concentration were observed in India represented by diamonds (Figure 2-7). Figure 2-7 also shows the period when peak O_3 concentrations were found in the US for comparison (Heagle *et al.*, 1987; Hogsett *et al.*, 1987). The circles in Figure 2-7 show the hours of highest physiological activity in Indian wheat (Singh *et al.*, 1987; Kumar *et al.*, 1999; Srivastava *et al.*, 2002); hence it is assumed that wheat physiology activity is broadly representative of other crops studied in this assessment. When defining the 7 and 12 hour periods for SA, more weighting was given to the O_3 concentrations as compared to the plant physiological activity data. Based on these data, the M7 daylight hours are defined as between 09:30 to 16:30 hours IST (Indian standard Time) and the M12 daylight hours are defined as between 07:30 to 19:30 hours IST.

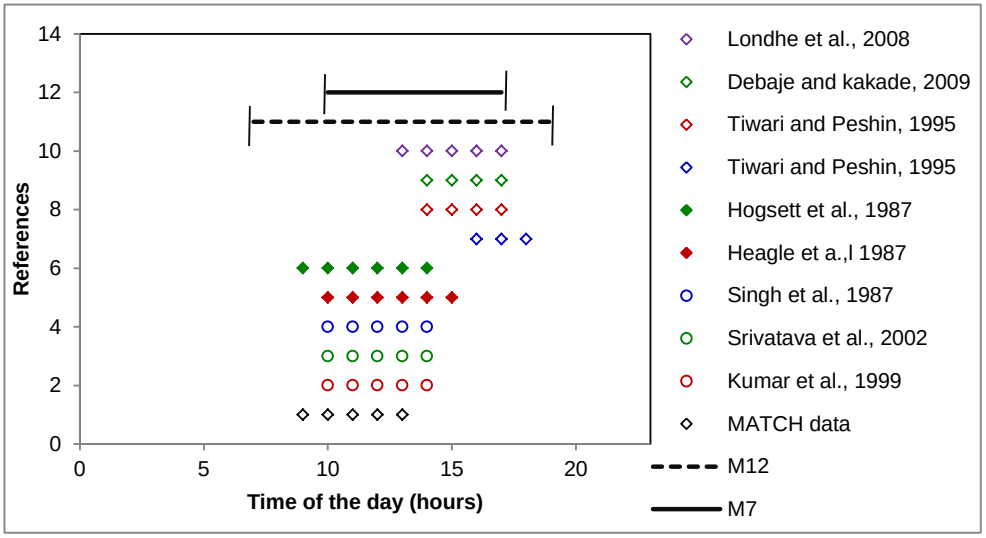

Figure 2-7: Definition of the daylight hour period over which the M7 and M12 indices are calculated based on data from SA describing i) the period of highest O_3 concentration (denoted by diamonds) and ii) the period of highest physiological activity (denoted by circles) for wheat plants as reported in literature. The lines indicate the time window for SA M7 and M12 calculations.

2.2.4.2 Cumulative O_3 concentrations

(a) AOT40

AOT40 is calculated as the accumulated daylight hourly O_3 concentration above a threshold concentration of 40 ppb over a time period of three months during the plant growing season. Daylight hours here are defined as the time when irradiance is greater than 50 W/m^2.

The values are expressed in ppm hours.

$$\text{AOT40} = \sum_{i=1}^{n}(C_{O3} - 40)_i \text{ when } C_{O3} \geq 40 \text{ ppb} \quad [2\text{-}3]$$

Where, C_{O3} is the hourly O_3 concentration (in ppb) during the local daylight hours and n is the number of hours with O_3 > 40 ppb.

AOT40 has been used as an index for O_3 risk assessment in Europe over the past decade (LRTAP Convention, 2004).

(b) W126

W126 is the sum of hourly average O_3 concentrations that have been weighted according to a sigmoid function that is based on a hypothetical vegetation response (Lefofn and Runeckles, 1987; U.S.-EPA, 2006). W126 is calculated during a three month O_3 accumulation period during daylight hours and it is expressed in ppm hours.

The W126 index is calculated as follows;

$$\text{W126} = \sum_{i=1}^{n} C_{O3} \times w_i \quad [2\text{-}4]$$

Where, w_i is the weighing factor for the i^{th} hour and is calculated as;

$$w_i = \frac{1}{(1+4403\times\exp(-0.126\times C_{O3}))} \quad [2\text{-}5]$$

C_{O3} is the hourly O_3 concentration (in ppm v) and n is the number of hours during which the W126 index is calculated

(c) SUM06

SUM06 is the sum of hourly O_3 concentrations when the O_3 concentrations are ≥ 60 ppb v during a three month period of the crop growing season (U.S.-EPA, 2006). It is calculated as,

$$SUM06 = \sum_{i=1}^{n} (C_{O3})_i \text{ when } C_{O3} \geq 60ppb \quad [2\text{-}6]$$

Where, C_{O3} is the hourly O_3 concentration (ppb); n is the number of hours with O_3 > 60 ppb

2.2.5 Exposure-Response (ER) functions

The ER functions used in the current study are presented in Table 2-6 along with the details of the data used to define the ERs. The AOT40 ER is available for all the four crops studied. The AOT40 ERs are based on the experimental data collected from US, Europe and Asia and hence could be argued to be representative of a wider geographical spectrum and cultivars than the M7/M12 ERs which are based on experimental data only from the US (Table 2-6).

The AOT40 ER functions are a linear function described in Mills *et al.* (2007). To derive these functions Mills *et al,* (2007) re-analysed crop response data from a number of experimental studies conducted mainly in Europe (Reference in Table 2-6) but also in the US (Kats *et al..,* 1985) and Asia (Kobayashi *et al..,* 1995), or Asian cultivars grown in Europe (Maggs and Ashmore 1998).

The M7 for wheat were based on the Weibull functions given in Lesser *et al.* (1990) which were derived from an empirical fit of data from open top chamber (OTC) studies carried out in the US under the NCLAN Programme.

The Weibull function is given by equation 2-7:

$$RY = A * \exp\left[-\left(\frac{X}{B}\right)^{C}\right] \qquad [2\text{-}7]$$

Where, X is the O_3 exposure index (i.e. M7, M12, SUM06 or W126), A is theoretical yield at 0 (zero) O_3 concentration, B is the scale parameter for O_3 exposure which reflects the dose at which the expected response is reduced to 0.37A, and C is the shape parameter effecting the change in predicted in the rate of loss in expected response (Lesser *et al.,* 1990).

The reference exposure index or threshold value of O_3 for M7 is 25 ppb, 20 ppb for M12, and 0 ppb for SUM06 and W126 (Heagle *et al.,* 1987; U.S.-EPA, 1996, 2006). It assumes there is a threshold above which damage will occur, i.e. some level of O_3 concentration will be assumed not to cause damage due to antioxidant plant defences (Felzer *et al.,* 2007).

The M7 ER functions for rice and spring wheat are given in Adams *et al.* (1989) which were derived based on the same NCLAN experiments conducted in the US. All these functions have already been used in regional (Wang and Mauzerall, 2004) and global (Dingenen *et al.,* 2009) O_3 risk assessment studies.

Out of the 14 sets of experiments that were used to derive M7 and M12 indices, 3 experiments (1985 & 1986) had proportional O_3 fumigation. One study in 1982 had both proportional and constant fumigation. And the other 10 studies were fumigated with a constant value (additive). Except for the last 3 studies (1985 & 1986) where 12 hours fumigation was done the rest of the studies are based on 7 hour/ day fumigation. The duration ranges from 59 days to 92 days, but in most experiments it is between 80 - 90 days.

The details of ER functions that were used in the present study are given in Table 2-6.

Table 2-6: Details of the Exposure-Response relationships used in this assessment. The W126 and SUM06 were based on the same crop data as M7/M12 but re-analyzed with a weighting function.

Crop	Yield based on weight of	Exposure response function	r^2	No. of data points	No of years (cultivars)	Countries	Stand characteristics (fumigation/ day duration)	References
AOT40 (ppm.hrs)								
Wheat SW-EU WW-US	grain	RY = -0.0161x+0.99	0.89	52	9 (9)	6: Sweden. Denmark. Belgium, Swizerland, USA, Finland	OTC	Fuhrer *et al.*, 1997; Gelang *et al.*, 2000
Rice	grain	RY=-0.0039x+0.94	0.2	32	5(6)	3: Pakistan, Japan,USA	OTC,	Kobayashi *et al..*, (1995), Maggs and Ashmore (1998), Kats *et al..*, (1985)
Potato	tubers	RY =-0.0057x+0.99	0.38	14	7 (3)	6: Sweden. Germany, Belgium, Finland, UK, Italy	OTC, Closed chamber (1)	Skärby and Jönsson (1988), Köllner and Krause (2000), Donnelly *et al..*, (2001), Lawson *et al..*, (2001), Pleijel *et al..*, (2002, 2004), Pell *et al..*, (1988), Finnan *et al..*, (2002)

Table 2-6: Continued.

Soybean	seed	RY =-0.0116x+1.02	0.61	50	(7)		Heagle *et al..*, (1986), Heggestad *et al..*, (1985, 1988), Mulchi *et al..*, (1995)
M7 (ppb)							
Rice	grain	$RY = \frac{\exp\left[-\left(\frac{M7}{202}\right)^{2.47}\right]}{\exp\left[-\left(\frac{25}{202}\right)^{2.47}\right]}$		3	1 (3)	1: US	Wang and Mauzerall, 2004, Adams *et al.*, 1989
Winter wheat	grain	$RY = \frac{\exp\left[-\left(\frac{M7}{136}\right)^{2.56}\right]}{\exp\left[-\left(\frac{25}{136}\right)^{2.56}\right]}$		7	2 (4)	1: US	Wang and Mauzerall, 2004, Lesser *et al.*, 1990
Spring wheat	grain	$RY = \frac{\exp\left[-\left(\frac{M7}{186}\right)^{3.2}\right]}{\exp\left[-\left(\frac{25}{186}\right)^{3.2}\right]}$		3	-	1: US	Wang and Mauzerall, 2004, Adams *et al.*, 1989
Soybean M12	seed	$RY = \frac{\exp\left[-\left(\frac{M12}{107}\right)^{1.58}\right]}{\exp\left[-\left(\frac{20}{107}\right)^{1.58}\right]}$		21	7 (6)	1: US	Lesser *et al.*, 1990

Table 2-6: Continued.

SUM06						
Wheat	grain	$RY = \exp\left[-\left(\frac{SUM06}{52.32}\right)^{2.176}\right]$	-	2 (4)	1: US	Wang and Mauzerall, 2004, U.S.-EPA (1996)
Soybean	seed	$RY = \exp\left[-\left(\frac{SUM06}{101.505}\right)^{1.452}\right]$	-	7(6)	1: US	Wang and Mauzerall, 2004, U.S.-EPA (1996)
Potato	tubers	$RY = \exp\left[-\left(\frac{SUM06}{86.55}\right)^{1.327}\right]$	-	1 (1)	1: US	U.S.-EPA (1996)
W126						
Wheat	grain	$RY = \exp\left[-\left(\frac{W126}{51.2}\right)^{1.747}\right]$	-	2 (4)	1: US	Wang and Mauzerall, 2004, U.S.-EPA (1996)
Soybean	seed	$RY = \exp\left[-\left(\frac{W126}{109.75}\right)^{1.2315}\right]$	-	7 (6)	1: US	Wang and Mauzerall, 2004, U.S.-EPA (1996)

Table 2-6: Continued.

Potato	tubers	RY $= \exp\left[-\left(\frac{W126}{105.10}\right)^{1.15}\right]$	-	1 (1)	1: US	U.S.-EPA (1996)

2.2.6 Crop loss evaluation

To apply these ER functions, the O_3 concentrations for each of the DPs have to be characterised according to the O_3 indices (AOT40, M7/M12, W126 and SUM06). Once the O_3 exposure index is estimated for each DP it can then be used with the appropriate ER function to estimate crop yield loss by;

$$\mathrm{RYL_{DP}} = 1 - \frac{\mathrm{RY_{DP}}}{\mathrm{RY_{base\_DP}}} \qquad [2\text{-}7]$$

Where, RY_{DP} is the RY of each DP estimated based on functions given in Table 2-6 and RY_{base_DP} is the estimated RY at the reference exposure index, set to 1 as described in the previous text.

To calculate the crop production loss (CPL) it is first necessary to estimate crop production for each DP; this calculation assumes an area weighted average of the district level crop production dependent upon the percentage share in area of each DPs and hence assumes that that production is equally distributed across each district. The crop production in each DP (CP_{DP}) is therefore calculated as,

$$\mathrm{CP_{DP}} = \mathrm{PA_{DP}} \times \mathrm{P_D} \qquad [2\text{-}8]$$

where, PA_{DP} is the percentage share in area of the DP and P_D is the actual crop production of the DP.

The CPL in each DP (CPL_{DP}) is then calculated based on relative yield losses, and the actual crop production. As such, if the CP_{DP} is the actual crop production of the DP, CPL_{DP} the crop production loss and CP_{base} the crop production of the DP if there were no O_3 CPL then

$$\mathrm{CPL_{DP}} = \frac{\mathrm{RYL_{DP}}}{\mathrm{RY_{DP}}} \times \mathrm{CP_{DP}} \qquad [2\text{-}9]$$

The CPL for each country (CPL_C) can then be calculated for each individual crop as:

$$\mathrm{CPL_C} = \sum_{n}^{1} \mathrm{CPL_{DP}} \qquad [2\text{-}10]$$

where, n is the number of DPs in each country.

The CPL for SA can then be calculated by,

$$\mathrm{CPL_{SA}} = \sum \mathrm{CPL_C} \qquad [2\text{-}11]$$

The national average RYL for each crop is calculated using Equation [2-12] which is based on Wang and Mauzerall (2004);

$$\text{National average RYL} = \frac{\sum_{i-1}^{n}[\mathrm{CPL}]_i}{\sum_{i-1}^{n}([\mathrm{CPL}]_i+[\mathrm{Output}]_i)} \qquad [2\text{-}11]$$

Where, n is the number of DPs included for each country.

2.2.7 Economic loss (EL)

The CPLs can be translated into economic losses based on the producer price (PP) of the crop. This simple method has been used in previous studies (Wang and Mauzerall, 2004; Van Dingenen *et al.*, 2009). This rather simple approach to estimating economic losses is known to give an overestimate of about 20% as compared to the more sophisticated economic models that incorporate price elasticity and supply and demand statistics (Adams *et al.*, 1982; Westenbarger and Frisvold, 1995). The PP in US $ / tonnes for all four crops for all the countries of SA were obtained from FAOSTAT (2011) and are shown in Figure 2-8. The PP varies for each country by crop and in some countries; relatively high prices can be paid for the same crop. For example, Figure 2-8 shows that the PP of rice in Bhutan is more than double that of the other SA countries. This is because Bhutan produces less than 50% of the country's rice consumption with the remaining rice requirement being met through imports, mainly from India (Ghimiray *et al.*, 2007; IFPRI, 2010). The high demand and low supply lead to a high PP.

The economic loss (EL_C) of each crop for each country is calculated as;

$$\mathrm{EL_C} = \mathrm{CPL_C} \times \mathrm{PP_C} \qquad [2\text{-}13]$$

Where, the PP_C is the PP of the particular crop for the year 2000 in the particular country.

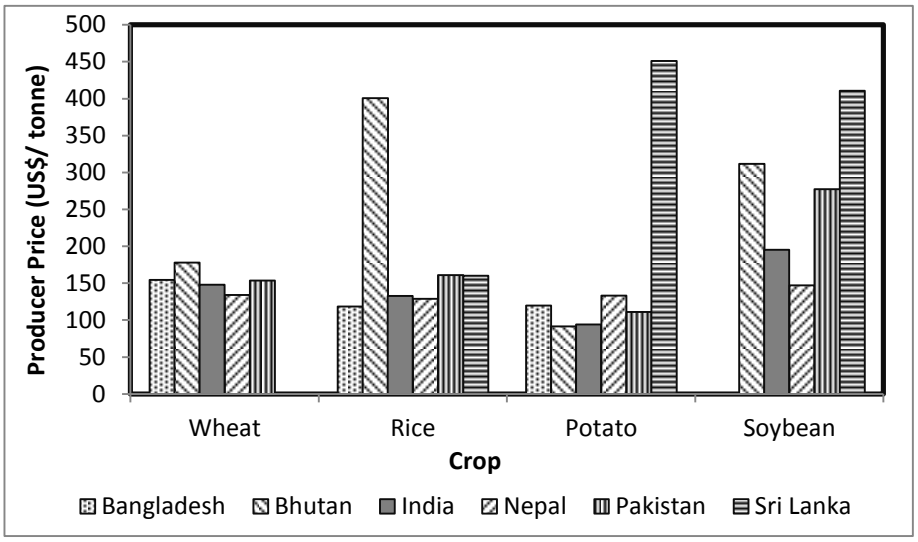

Figure 2-8: Producer price in US $ /tonnes for the four crops in the six countries of SA for the year 2000 (FAOSTAT, 2011)

2.3 Results

Results in this section present the estimates of RYLs, CPLs and ELs for each of the four crops (wheat, rice, soybean and potato) based on the different O_3 exposure indices and associated ER functions. The results are presented as maps, to allow an analysis of spatial patterns to be assessed such that the influence of variations in O_3 concentrations, exposure indices and subsequent RYLs can be assessed in relation to crop distribution and crop production statistics. Results are also presented as summaries of RYL, CPL and EL for each of the different SA countries allowing generalizations to be made in terms of the magnitude of damage resulting from O_3 exposures to be assessed in a broader SA context. The EL for each of the different SA countries is then discussed in terms of its likely effect on the region's GDP.

2.3.1 Relative Yield Loss (RYL)

Figure 2-10 to Figure 2-13 show the spatial distribution of O_3 induced RYLs for each of the four crops by O_3 exposure index and associated ER function. The overriding conclusion from these Figures is that the O_3 induced RYL varies spatially, depending on the crop and also depending upon the ER used to estimate the crop yield loss. RYL estimates using AOT40 indices (RYL_{AOT}) are higher than those estimated by M7 (RYL_{M7}), W126 (RYL_{W126}) and SUM06 (RYL_{SUM}) except for soybean where RYL_{M12} values are higher than the estimates derived using the cumulative indices (Figure 2-9).

The estimated national average yield losses, based on the 4 different O_3 metrics and associated ER functions for each of the four crops, are given in Figure 2-9. The sensitivity of the four crops to O_3 across the SA region based on these estimates ranked according to the highest estimate of yield loss (with the values in brackets giving the range in yield losses estimated using the different ERs) is given below, however, it should be noted that there is substantial variation and overlap in these RYL estimates both between crops and between exposure index and ER functions;

Wheat (0.6-10.6 %) > Rice (0.9-7.4 %) > Potato (2-3.7 %) > Soybean (0.02-4 %)

In all the countries, except Pakistan, RYL_{AOT40} for wheat is higher than rice (Figure 2-9). The higher rice yield loss in Pakistan is because the important rice growing area coincides with regions where high O_3 concentrations are modelled. On the other hand, wheat is more widely grown than rice and not all the important wheat growing regions are associated with high O_3 concentrations (Figure 2-10). In all the four crops, RYL is higher in the IGP (Figure 2-10 to Figure 2-13), the most important cropping region for wheat, rice and potato. In soybean, the important cropping region is the central part of India where the RYL is not very high. Thus, even though soybean has a relatively high O_3 sensitivity, O_3 may not be a threat to this crop as the O_3 concentration tends to be low across the main soybean growing regions.

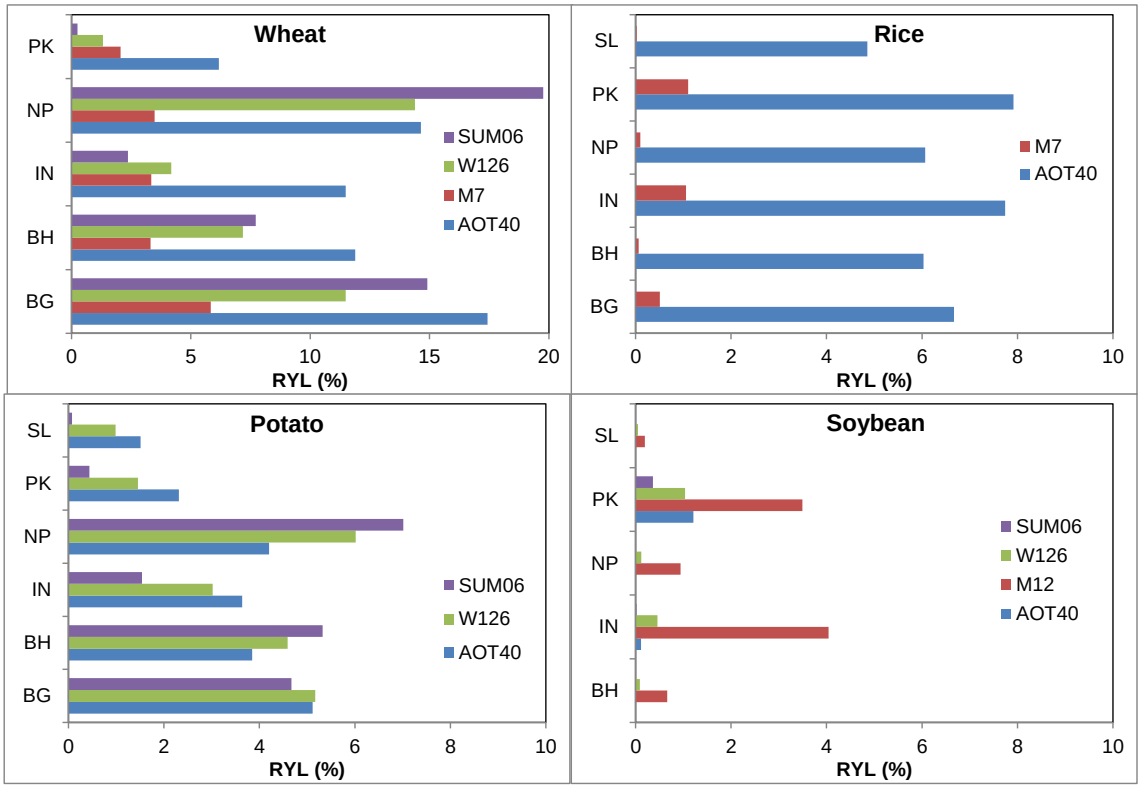

Figure 2-9: O_3 induced RYL (%) for wheat, rice, potato and soybean in different countries of SA based on AOT40, M7 / M12, W126 and SUM06 exposure indices. SL= Sri Lanka; PK= Pakistan; NP= Nepal; IN= India; BH= Bhutan; BG= Bangladesh.

The national average wheat RYL_{AOT40} is the highest of all the indices across all parts of SA. The maximum wheat RYL_{AOT40} was in Bangladesh (17.4 %) followed by Nepal (14.6 %), Bhutan (11.9 %) and India (11.5 %). High RYLs are observed along the IGP (> 20%), the northern border of India and Nepal (> 50%) and along the coastal region of India (> 30%).

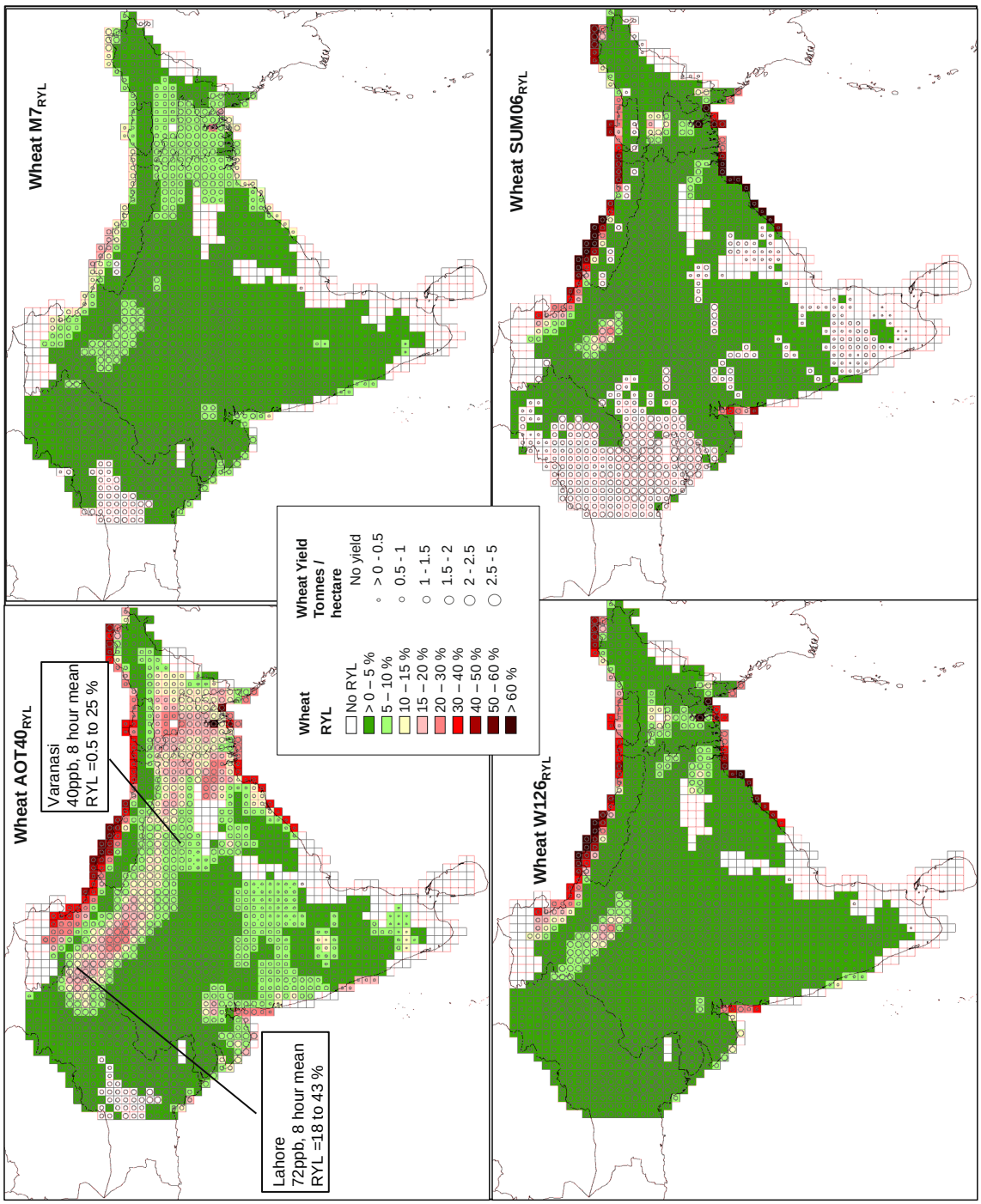

Figure 2-10: Estimates of RYL for wheat based on MATCH O_3 concentration data expressed as different exposure indices (AOT40, M7, W126 and SUM06) and associated ER functions across SA for the cropping year 1999-2000. The circles indicate wheat yield (in tonnes/hectare) in each grid. The annotated boxes provide details of experimentally derived wheat yield losses due to ambient O_3 concentrations in Lahore, Pakistan and Varanasi, India (see Table 1-1 for references).

Wheat RYL_{SUM06} has a different distribution as compared to other indices (Figure 2-10). RYL_{M7} shows a less spatial differentiation in yield losses, with almost the entire region showing RYLs between 5-10 %. By contrast RYL_{AOT40} shows a much larger spatial variation in wheat yield losses and also a larger range of yield losses with values ranging between 0 and 30 %. RYL_{W126} and RYL_{SUM06} fall between RYL_{M7} and RYL_{AOT40} in terms of spatial variation and range of yield losses. Even with this variability in the yield losses, the north western part of the IGP and the area of Bangladesh and its surroundings tend to suffer the highest wheat yield losses; AOT40 also predict yield losses of between 5-10 % across substantial parts of southern India. Some coastal areas also show high yield losses for all indices with the exception of M7. As indicated by the circles, the north-western IGP has the highest wheat yield as well as high RYLs (Figure 2-10). It is interesting to note that the RYLs found from the experimental studies conducted in Lahore, Pakistan and Varanasi, India, which are also shown in Figure 2-10 suggest RYLs of 18-43 % and 0.5-25% respectively (see Table 1-1 for references); both higher than the RYLs estimated using even the AOT40 index and associated ER function.

Figure 2-11 shows similar RYLs estimated for rice using AOT40 and M7 indices and associated ERs (values based on W126 and SUM06 are not available as ERs do not exist for these indices for rice). The RYL_{M7} shows 0-5 % rice yield losses across SA. However, RYL_{AOT40} indices give a higher rice yield loss estimate of 5-8 % across most of SA; in some parts of western IGP and eastern IGP in the state of West Bengal, bordering with Bangladesh, the RYLs are between 10-15 %. The national average RYL_{AOT40} is highest in Pakistan and India with 7.8 and 7.7 % respectively (Figure 2-9). However, there is some spatial variation in the RYL_{AOT40} in India. The highest RYL_{AOT40} values were observed in some parts of Uttar Pradesh and Punjab (parts of the IGP) where the RYL_{AOT40} were above 15 %. Rice RYL_{M7} estimates are lower than RYL_{AOT40} estimates (by ~10%). Pakistan and India has the highest RYL_{M7} (1.1 % each) while Sri Lanka has the lowest RYL_{M7} (0.02%). As for wheat, the experimentally derived rice yield losses found in Faisalabad, Pakistan (Wahid *et al.*, 2011), estimate higher yield losses (at 29-37 %, 75 ppb v 8 hour mean O_3) than were estimated by either the AOT40 or M7 ER functions.

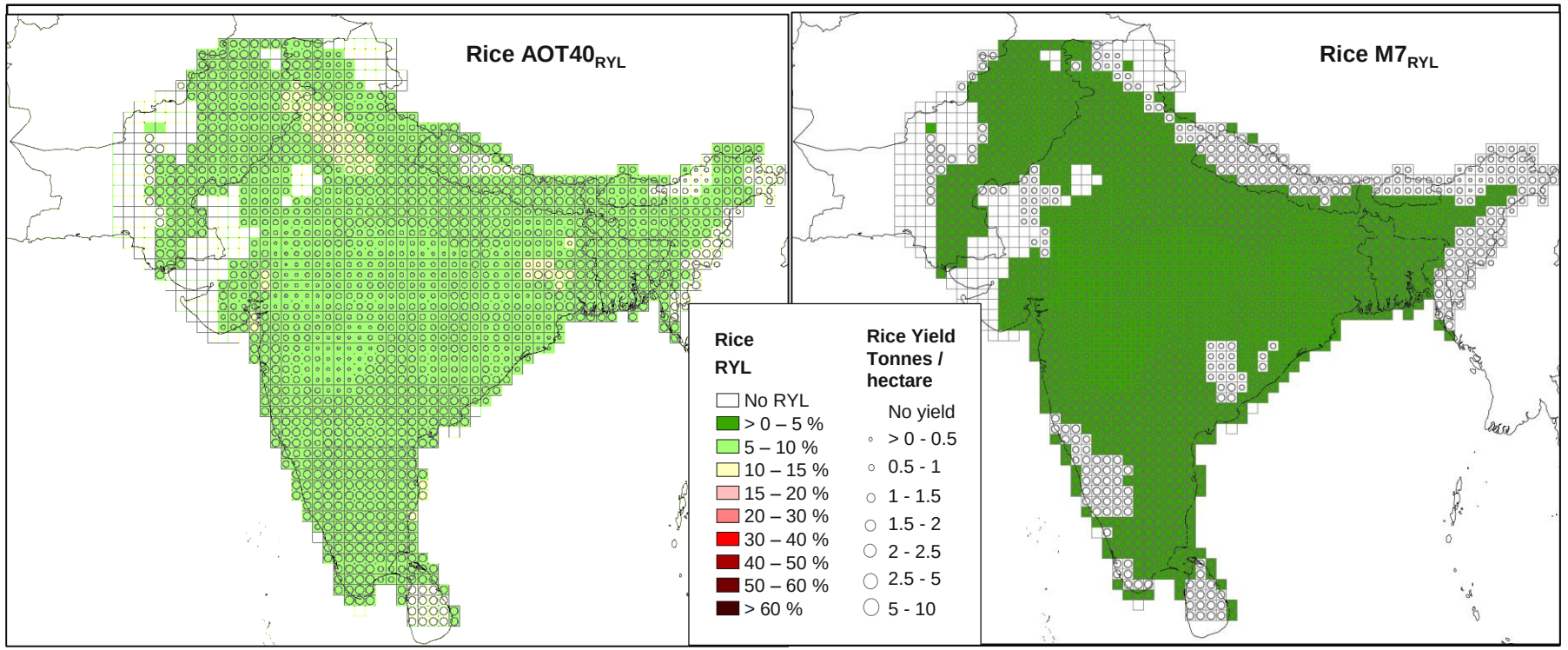

Figure 2-11: Estimates of RYL for rice based on MATCH O_3 concentration data expressed as different exposure indices (AOT40 and M7) and associated ER functions across SA for the cropping year 2000. The circles indicate rice yield (in tonnes/hectare) in each grid. The annotated box provides details of experimentally derived rice yield loss due to ambient O_3 concentrations in Lahore, Pakistan.

Figure 2-12 shows RYLs estimated for potato using the AOT40, SUM06 and W126 indices and associated ERs (values based on M7 are not available as ERs do not exist for this index for potato). Similarly for wheat, the potato RYL_{SUM06} seems to have a different distribution of yield loss compared to RYL_{AOT40} and RYL_{W126}. The RYL_{SUM06} shows more spatial variation in the eastern coastal region near Bangladesh and in the northern border along the Himalayas with yield losses as high as 50-60 % being estimated. Bangladesh has the highest RYL_{AOT40} (5.1%) while Sri Lanka has the least RYL_{AOT40} (1.5%). 80 % of SA's potato is produced from India while 10 % is produced from Bangladesh and the remaining 10% is shared between the four other countries (Figure 2-9). High RYLs are observed along the coastal region and the Himalayas (Figure 2-12); this is due to frequent peak O_3 concentrations that tend to occur in this region as mentioned earlier.

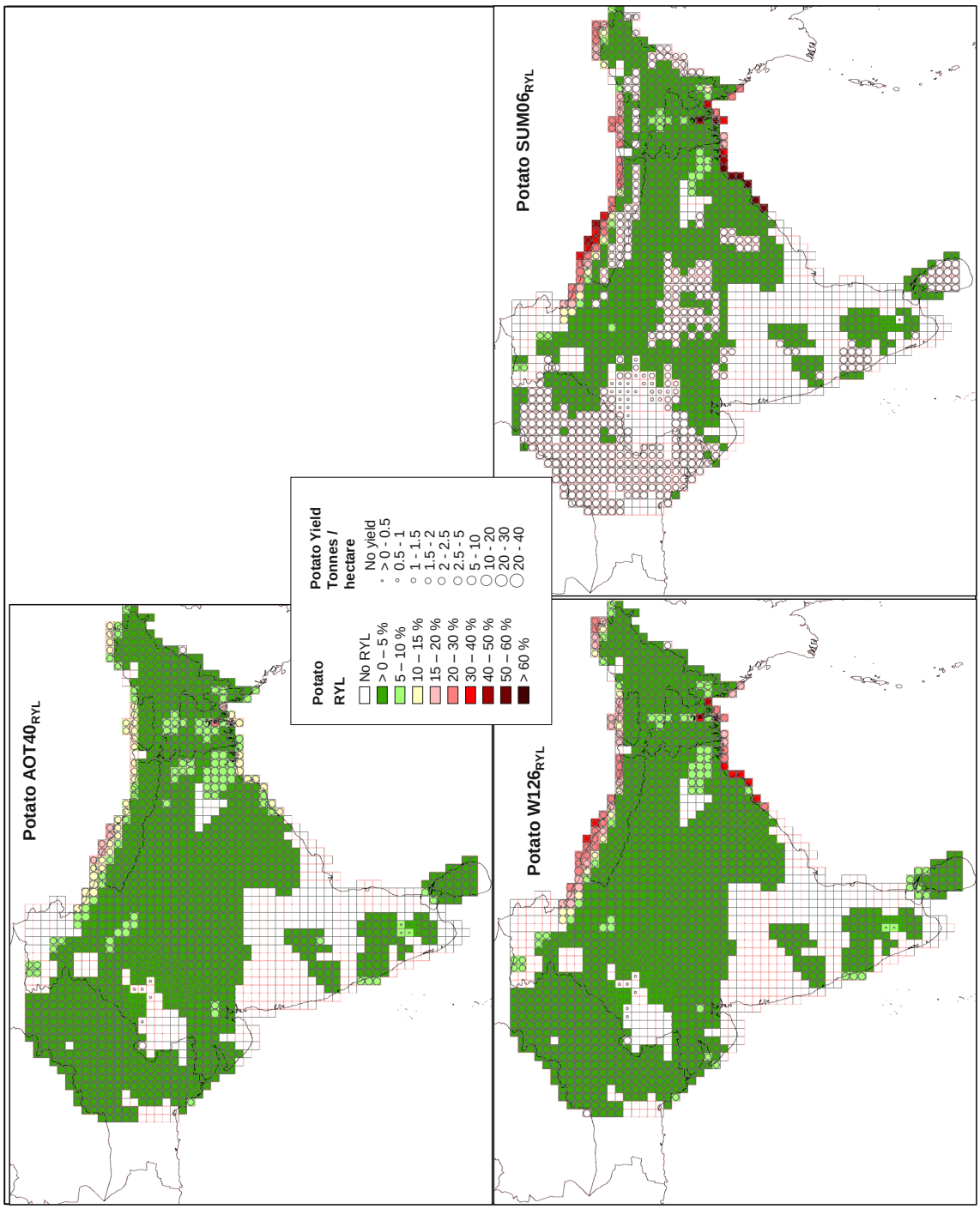

Figure 2-12: Estimates of RYL for potato based on MATCH O_3 concentration data expressed as different exposure indices (AOT40, W126 and SUM06) and associated ER functions across SA for the cropping year 1999-2000. The circles indicate potato yield (tonnes/hectare) in each grid. There are no M7 ER functions for potato and hence no RYL_{M7} for potato were calculated.

Figure 2-13 shows RYLs estimated for soybean using all four indices. The soybean RYLs estimated using these different indices have a rather different spatial distribution. The RYL_{AOT40} shows no crop losses in most parts of India except in the IGP region where it shows a RYL of about 0-5 %. Maximum yield losses are estimated when using the M12 exposure index. RYL_{M12} shows yield losses of 10-15 % in the IGP and 5-10 % in the central part of India. Although in most parts of SA, W126 and SUM06 show no yield losses, in regions where there are yield losses estimated, large spatial variation in these yield losses occurs with values ranging between 0- 60 %. As for both wheat and rice, the experimentally derived soybean yield losses found in Lahore, Pakistan and Varanasi, India both suggest substantially higher yield losses (between 32 - 74 % and 10 – 33 % respectively) than were estimated by any of the ER functions.

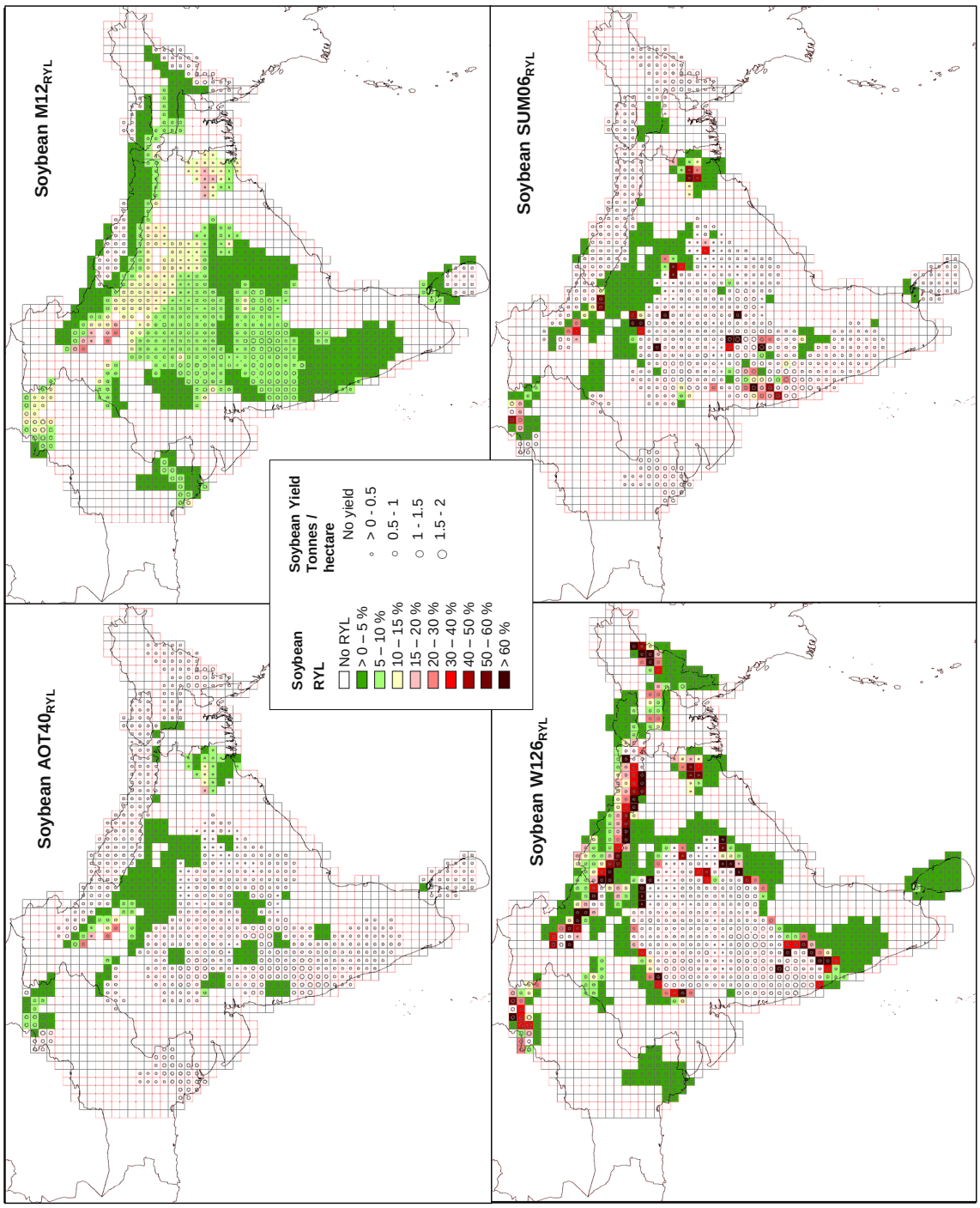

Figure 2-13: Estimates of RYL for soybean based on MATCH O_3 concentration data expressed as different exposure indices (AOT40, M12, W126 and SUM06) and associated ER functions across SA for the cropping year 2000. The circles indicate soybean yield (tonnes/hectare) in each grid. The annotated boxes provide details of experimentally derived soybean yield losses due to ambient O_3 concentrations in Lahore, Pakistan and Varanasi, India.

2.3.2 Crop production loss (CPL) and Economic loss (EL) estimates

The estimate of CPLs incorporates the intensity of the crop growth within a region into an assessment of the damage caused by O_3 exposures thereby giving an indication of where O_3 induced RYLs are likely to translate into substantial agricultural losses. As for the RYLs presented in the previous section, CPLs and Els are presented both as maps as well as national summaries of the loss estimates (Figure 2-14 and Figure 2-15). In terms of maps, CPLs and ELs are presented using only the AOT40 (Figure 2-16) and M7/M12 (Figure 2-17) indices and associated ER functions since only these are available for either all four, or at least three, of the crops studied. In terms of the national summaries, CPLs and ELs are provided using all available ER functions.

Figure 2-16 and Figure 2-17 show that the maximum CPLs in wheat, rice and potato were observed in the IGP region. This is because the IGP region has both high O_3 concentrations during the crop growing seasons as well as intensive cultivation of these crops. On the other hand, for soybean, even though relatively high RYLs were observed in the IGP region, the main cropping area is in the state of Madhya Pradesh (central India) where lower O_3 concentrations translate into lower RYLs and subsequently reduced CPLs.

The largest losses of rice crop production were found in the Punjab, West Bengal and Bangladesh where the cropping intensity is high and the RYL due to O_3 is also high. The states of Punjab (14.4 %), UP (18 %) and Haryana (10 %) experienced the maximum wheat CPL based on the AOT40 index.

The soybean cropping intensity in terms of the area under cultivation and production is highest in Madhya Pradesh where more than 80% of South Asia's soybean is produced (DACNET,2011; FAOSTAT, 2011). This means that even though there is substantial spatial variation in soybean RYL_{M7} (0-10% in Madhya Pradesh region and 10-15% in the IGP; Figure 2-13) there are few differences in CPL_{M7} across SA (Figure 2-17).

Also based on this AOT40 index, the CPLs of wheat, rice, potato and soybean were 11.9, 14.4, 1.2 and 0.001 billion tonnes respectively (Figure 2-14). These CPLs translate into ELs of 1.8, 1.9, 0.1 and 1.2 million US$ respectively (Figure 2-15). CPLs calculated using the M7 indices were very low as compared to those estimated using

AOT40 for all four crops. For rice, the estimates CPL based on AOT40 were more than 6 times those calculated using M7 exposure indices and for wheat it was more than double the amount. The wheat CPL_{W126} and CPL_{SUM06} values were between CPL_{AOT40} and CPL_{M7}.

The maximum RYL_{AOT40} loss was for wheat in Bangladesh (17.4%) while in India it was 11.5%. However the crop production loss (CPL) in absolute terms was not so high in Bangladesh (only 0.4 million tonnes) as compared to that of India (9.9 million tonnes).

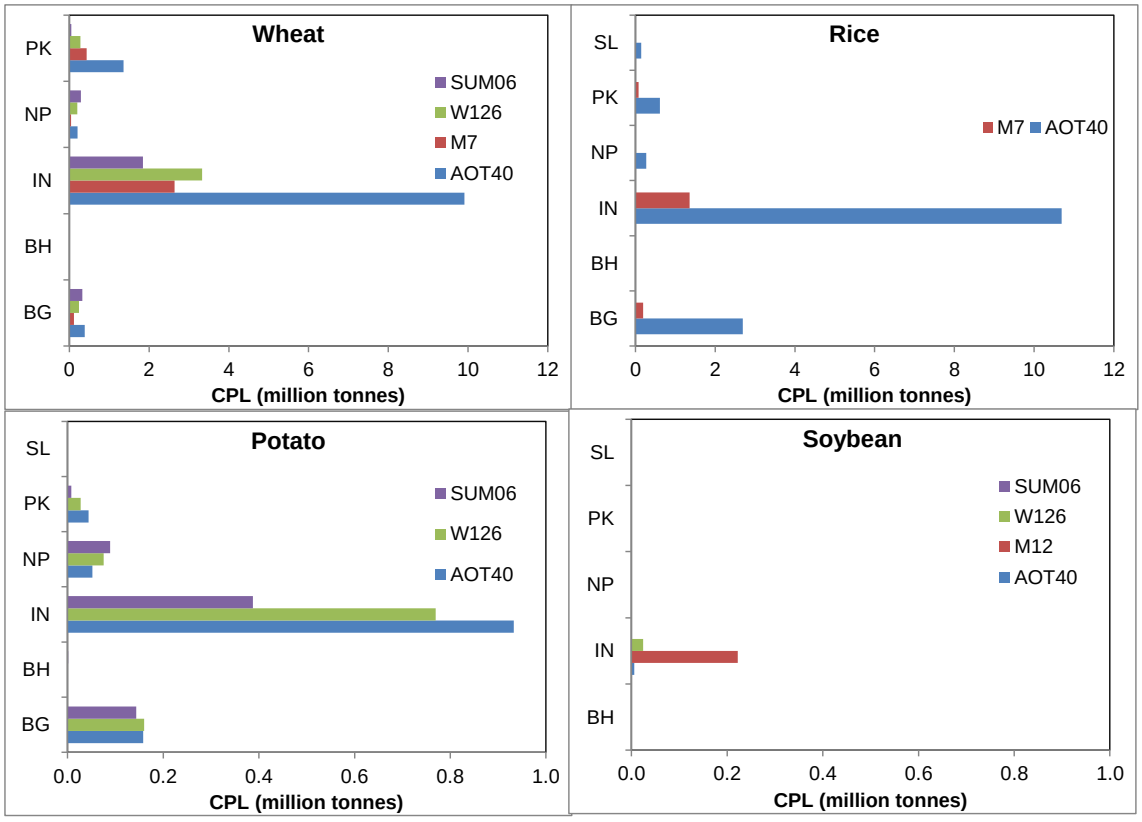

Figure 2-14: O_3 induced crop production loss (CPL) given as million tonnes for countries in SA estimated for wheat and potato during the 1999-2000 cropping year and for rice and soybean during the 2000 cropping year for each of the four O_3 indices; AOT40, M7 / M12, W126 and SUM06. SL= Sri Lanka; PK= Pakistan; NP= Nepal; IN= India; BH= Bhutan; BG= Bangladesh. Note that the x-axis scale for wheat and rice are different from that of potato and soybean.

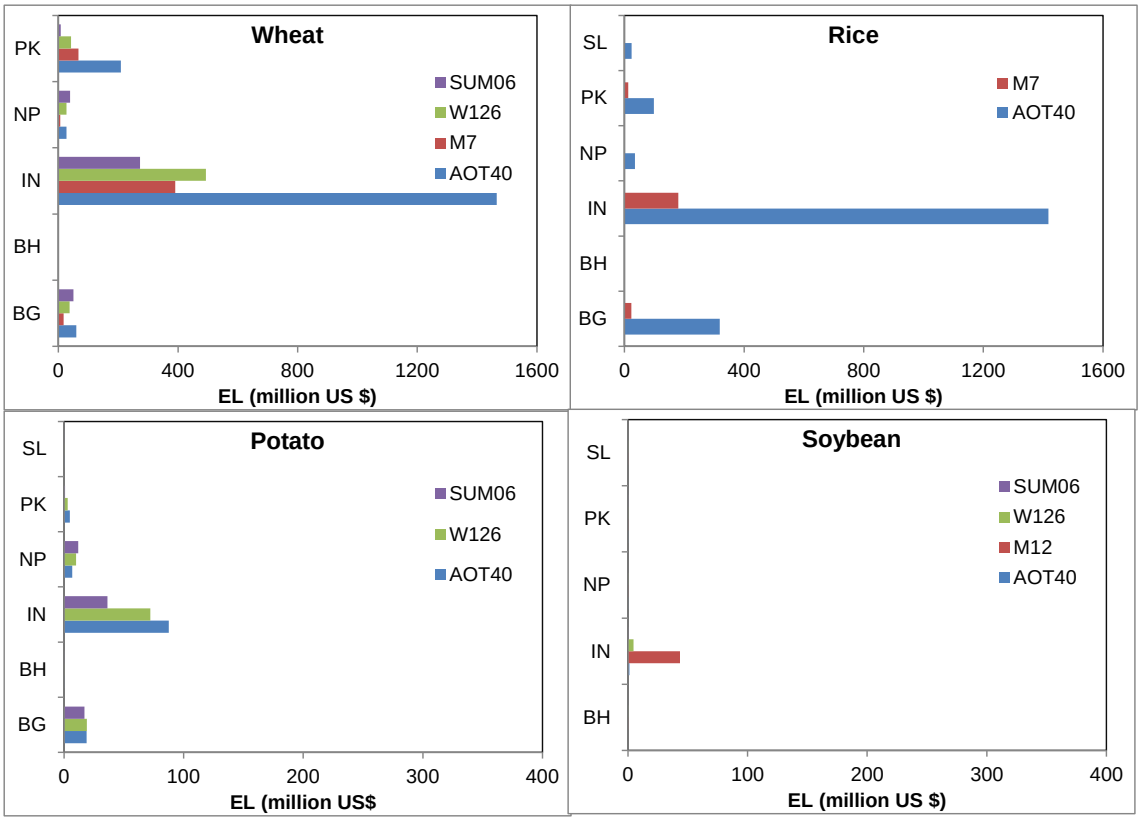

Figure 2-15: O_3 induced economic loss (EL) given as millions of US $ for countries in SA estimated for wheat and potato during the 1999-2000 cropping year and for rice and soybean during the 2000 cropping year for each of the four O_3 indices; AOT40, M7 / M12, W126 and SUM06. Note that the x-axis scale for potato and soybean is 1/4th of that of wheta and potato.

Figure 2-16 shows the CPL of the four crops in SA during the cropping year 2000 (rice and soybean) and 1999-2000 (wheat and potato) using the AOT40 index and associated ER function. In terms of loss, as a fraction of total national / regional production, wheat appears to be the most sensitive crop with an average relative loss of 10.6 % in SA reaching as high as 17.4 % (RYL) in Bangladesh (Figure 2-10). However, in terms of loss in quantity by weight, the maximum loss was observed in rice, with an estimated loss of 14.4 million tonnes in SA. Although the wheat RYL_{AOT40} is higher than the rice RYL_{AOT40} (Figure 2-10 and Figure 2-11), the total rice production losses are more than wheat production losses (Figure 2-16). This is because the total quantity of rice

produced (179 million tonnes) is almost double that of wheat (100 million tonnes). The maximum CPL for all the four crops is observed in the IGP region (Figure 2-16). The largest losses of rice crop production were found in Punjab and West Bengal in India and Bangladesh where the cropping intensity is high and the RYL due to O_3 is also high. The states of Punjab, UP and Haryana in India had the maximum wheat CPL. Wheat and rice production losses extend across almost the entire south Asian region; potato has a slightly more limited range of losses whereas the soybean losses are limited to the northern parts of SA in the IGP. The potato CPL ranges between 0 – 6.2 thousand tonnes per grid in most parts SA except in some parts of eastern IGP, in west Bengal, where the CPL is as high as 50 thousand tonnes per grid (Figure 2-16). Figure 2-18 shows the minimum and maximum range in ELs for all four crops combined resulting from the use of the four different exposure indices. The resulting EL ranged from a minimum of 0.4 billion US$ to a maximum of 3.8 billion US$ estimated using the PP of these crops. Here the maximum EL for wheat, rice and potato is calculated using AOT index while for soybean the maximum EL is estimated using M12 index. The minimum ELs for wheat and rice are from the M7 index while for potato and soybean minimum values are derived from the SUM06 index.

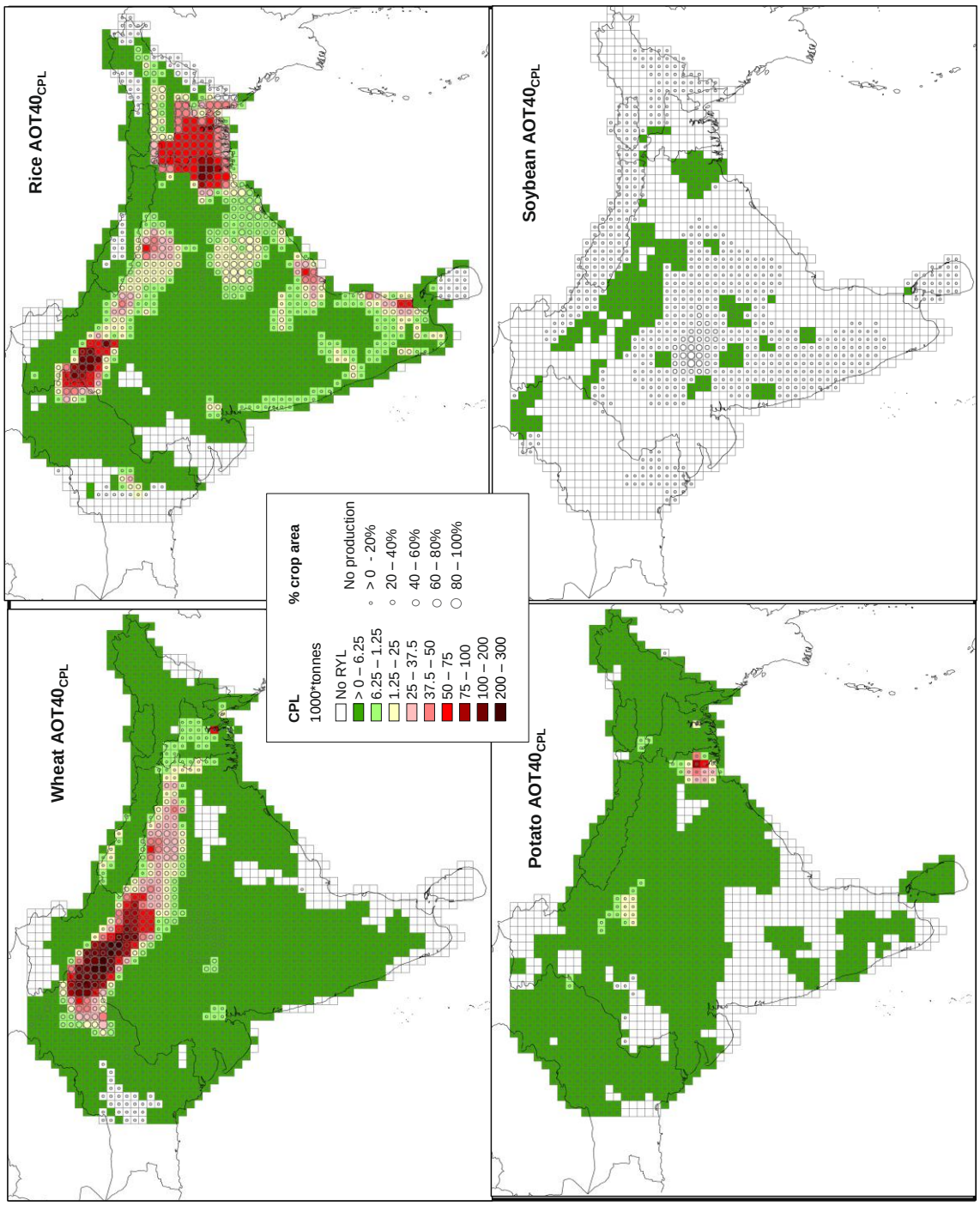

Figure 2-16: Estimates of O_3 induced CPL for wheat, rice, soybean and potato crops grown across SA based on the AOT40 index and associated ER function for the cropping year 1999-2000 for wheat and potato and for the cropping year 2000 for rice and soybean. Also shown is the percentage of the cropping area per grid indicated by the size of the circle symbols.

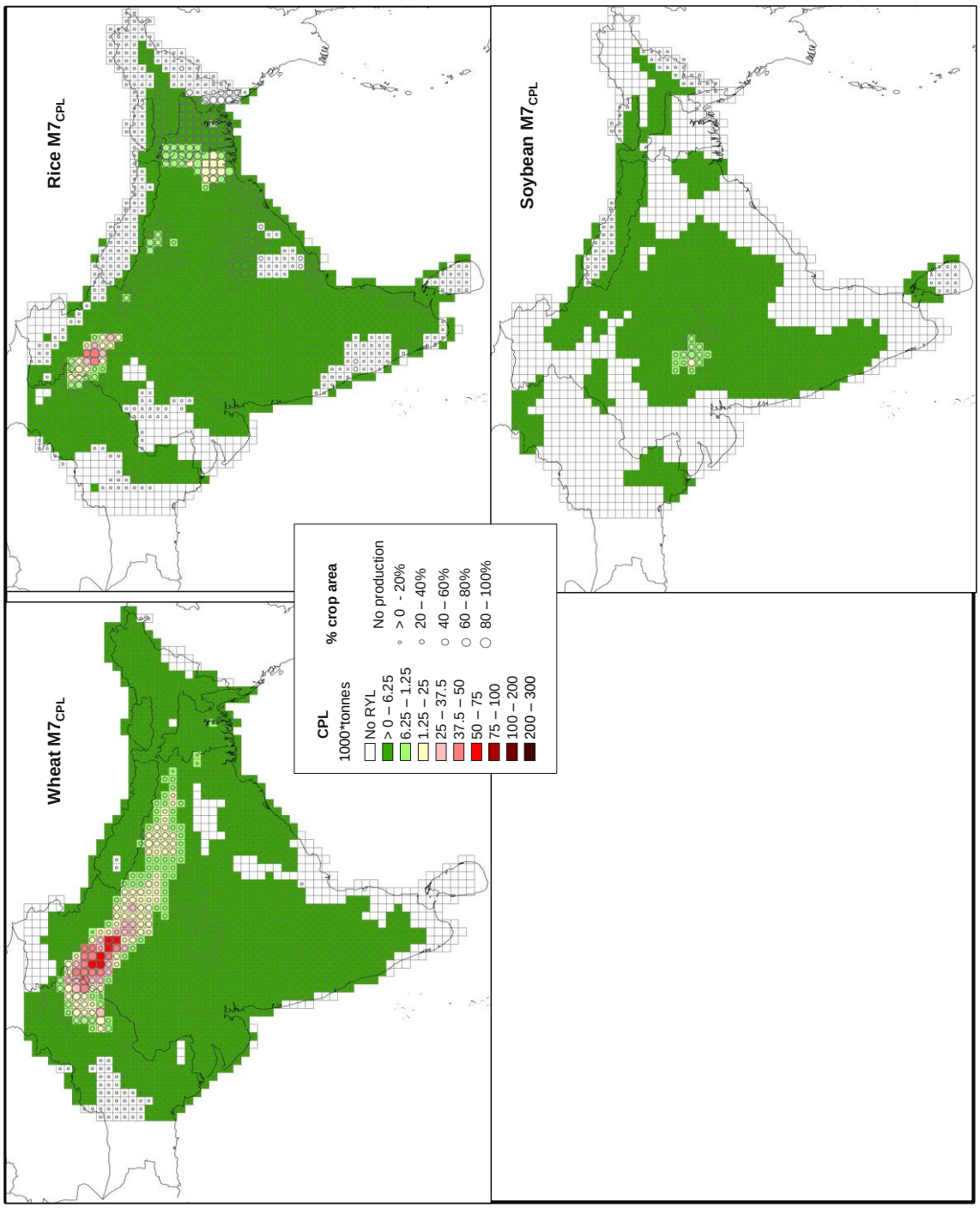

Figure 2-17: Estimates of O_3 induced CPL for wheat, rice and soybean grown across SA based on the M7 (M12 for soybean) index and associated ER function for the cropping year 1999-2000 for wheat and 2000 for rice and soybean. Also shown is the percentage of the cropping area per grid indicated by the size of the circle symbols.

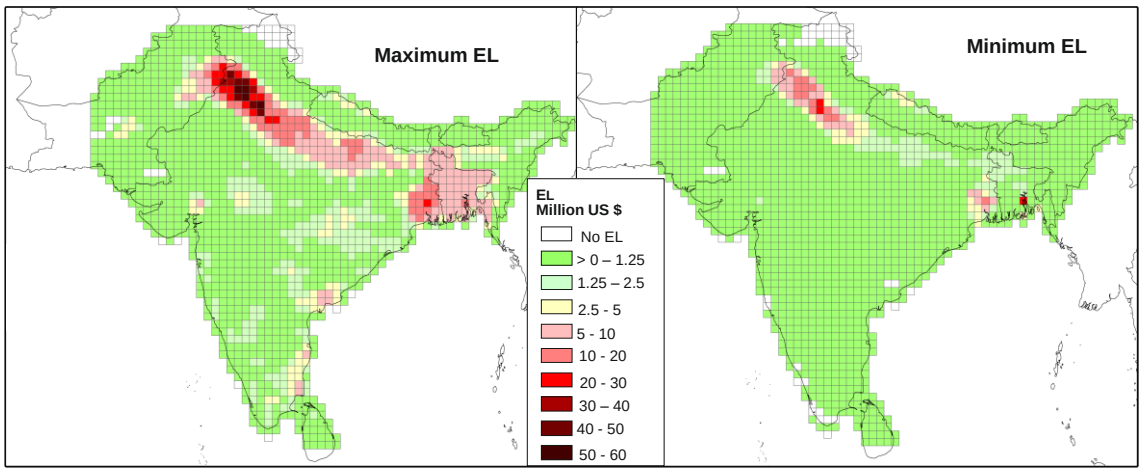

Figure 2-18: Estimates of O_3 induced maximum and minimum economic loss (EL) given in millions of US$ for the four crops in SA for the year 1999/2000 based on AOT40, M7 (M12 for soybean), W126 and SUM06 indices.

The PP varies among the crops and within a crop there is also variation between the countries. In Bhutan the total national wheat CPL (435 tonnes) is half that of potato (812 tonnes). However, when this CPL is converted into EL, the wheat economic loss is US$80,000 which is more than the EL loss for potato (US $ 74, 000). This is because the PP for wheat is double that of potato in Bhutan (Figure 2-15). In terms of CPL, O_3 induced losses for potato in Sri Lanka (726 tonnes) are less than that in Bhutan (812 tonnes). However when these losses are expressed in terms of EL, the Sri Lankan EL for Potato are 4.5 times that of Bhutan due to the high potato PP in Sri Lanka as compared to that in Bhutan. The economic impact of O_3 on crops therefore also depends on the price dynamics of the crop in the region.

2.3.3 Potential effect of O_3 induced EL on the gross domestic product (GDP) of the region

Agriculture in SA plays an important role in the economy of the region and it contributes a major share in the region's gross domestic product (GDP) (25 % of GDP of SA, IFPRI, 2001). Therefore, any effect on the agricultural production will have a substantial impact on GDP and may offset the GDP growth rate. In order to place the impact of O_3 on crop production in the context of the economy of the region, the EL

was compared with the GDP of SA. The potential effect of the EL on the GDP of the region was assessed using the maximum and minimum EL that was calculated based on the four indices. EL as percentage of agricultural GDP and its growth rate in SA is given in Table 2-7.

Table 2-7: O_3 induced economic loss (in millions of US$) for the four crops (wheat, rice, potato, and soybean) and its effect on annual GDP growth and agricultural GDP in SA. The GDP values are average of 10 years (1995-2005) data from United Nations Statistics Division, http://data.un.org/Data.aspx?q=GDP&d=CDB&f=srID%3a29919.

Country	**Annual GPD growth**	**Agriculture GDP**	**Economic Loss (EL)**		**EL as % of GDP growth**		**EL as % Agricultural GPD**	
			Max	**Min**	**Max**	**Min**	**Max**	**Min**
Bangladesh	2209	12246	398	44	18	2	3.2	0.4
Bhutan	53	126	1	0	2.5	0.2	1.1	0.1
India	45057	105846	2972	334	6.6	0.7	2.8	0.3
Nepal	301	2250.9	69	14	23	4.5	3.1	0.6
Pakistan	5066	19227	312	26	6.2	0.5	1.6	0.1
Sri Lanka	1051	3266	24	0	2.3	0	0.7	0
South Asia	53737	142961.9	3776	417	7	0.8	2.6	0.3

The EL for all four crops was between 0.3 to 2.6 % of the total agricultural GDP (in SA for the year 2000 (Table 2-7). The country which has the largest proportion of agricultural GDP lost due to O_3 is Bangladesh (0.4-3.1 %) followed by Nepal (00.6-3.1 %) and the least affected country was Sri Lanka (0-0.7 %). However, in terms of GDP growth rate, Nepal and Bangladesh are most affected by the O_3 induced ELs with effects on the GDP growth rate of 0.6-19.2 % and 0.2-16.3 % respectively. The associated economic loss for these four crops might offset about 0.8-7 % of SA's GDP

growth rate. The effect on India's GDP growth rate (0.7-6.6 %) and agricultural GDP (0.3-2.8 %) is very closely related to effect for SA which suggests that the effect of O_3 induced economic losses on SAs GPD is influenced primarily by effects felt in India.

SAs economy is extremely dependent on the agricultural sector and therefore such an impact will have substantial consequences on the socio-economic conditions of the region.

2.4 Discussion

In this section, the results of the O_3 risk assessment using the four concentration based O_3 exposure indices and associated ER functions are discussed in a wider context comparing the current study results with observed data of yield losses derived both from experiments and other model based O_3 risk assessments.

2.4.1 Comparison of O_3 induced yield and production losses with other experimental and modelling studies

The results from this chapter have shown that O_3 is causing a potential risk to yield and production of some of the most important staple crops grown in India. This O_3 risk tends to be highest in the important crop growing areas, particularly the IGP.

Comparison with experimental studies

The yield loss estimates from the current study are compared with the yield losses observed under ambient O_3 concentrations in SA. Table 2-8 identifies experimental studies conducted on wheat, rice, pulses (no studies were available for soybean so data on mungbean are included instead) and potato. These studies are conducted at 5 different sites across India or Pakistan; the experimentally derived yield losses are compared with this study's modelled RYLs, given as the range of all 4 O_3 exposure indices, for the particular MATCH grid corresponding to the studies location.

The modelled wheat RYLs for Varanasi, India and Lahore, Pakistan ranged between 1-9 % and 1-16% respectively. This is within the range of the yield losses found in the experimental study conducted in Varanasi which was between 0.5-25 % but substantially lower than the yield losses found in Lahore which were between 18-43%. In Lahore, a similar situation was found for rice with modelled RYLs for rice being between 1-8 %, substantially lower than the experimental yield losses that were between 29-37 %. The comparison between modelled estimates and experimental observations are likely to be more robust for wheat in Varanasi as they are based on 8 studies compared to a single study in Lahore. For example, Rai *et al.* (2007) reported yield losses of 21 %, substantially higher than the model estimates; however, the inclusion of the other wheat studies in India with lower yield losses brings the experimentally derived yield losses into the range of the modelled estimates (Table 2-8). By comparison, only 1 experiment each for wheat and rice in Pakistan are available which both happen to show large yield losses. This shows the importance of having more experimental studies with which to compare model results.

There are no ambient O_3 experimental studies on soybean in SA; only fumigation studies. These have used commonly grown soybean cultivars (cv. Bragg and cv. PK-472) and found that fumigation with O_3 concentrations of 70 ppb and 100 ppb in OTCs reduced yield by 10-14 % and 16-33 % respectively (Singh *et al.*, 1998, cf. Agrawal, 2003; Singh *et al.*, 2010). By comparison, at lower O_3 concentrations, this study estimated RYLs between 0.1- 4 %. For comparison, studies on mungbean, another important pulse grown in SA, have shown that ambient O_3 reduced yield by 32 % in Allahabad (Agrawal *et al.*, 2005) and 50-73 % in Varanasi (Agrawal *et al.*, 2003). However, these studies are conducted in the IGP region, which experiences higher O_3 concentrations than the main soybean growing regions in central India.

The first reported O_3 injury to crops in India were in potato and tobacco (Bel-W3) by Bambawale (1986) and later, Bambawale (1989). These studies used EDU treatment methods to assess the impact of O_3 on potato and reported foliar injury in the form of leaf spots due to O_3. These studies were performed in Jalandhar, India and the model estimates in the current study show 2-4 % yield losses in potato for the Jalandhar location (Table 2-8). No further experimental studies have been conducted on potato.

Table 2-8: Comparison of RYL estimates derived in this study with yield losses observed under ambient O_3 as reported from experimental studies.

Crop	Location (latitude_ longitude)	Current study	Experimental study		References
			Yield	Other response	
Cereals					-
Wheat	India	1-11	-	-	
	Varanasi, India (25_83)	1-9	0.5-25	Reductions in photosynthesis, biomass, chlorophyll and ascorbic acid	Agrawal *et al.*, 2003; Ambhast and Agrawal, 2003; Tiwari *et al.*, 2005; Rai *et al.*, 2007; Singh *et al.*, 2009; Singh and Agrawal, 2009, 2010; Sarkar and Agrawal. 2010
	Lahore, Pakistan (31.5_74)	1-16	18-43	Reduced nutritional quality (reduced starch but not vitamin E and proteins)	Wahid, 2006
Rice	Faisalabad, Pakistan (31_72.5)	1-8	29-37	Decreased transpiration rate (10-20%), stomatal conductance (12-23%), net photosynthetic rate (9-22%) and photosynthetic efficiency (6-12%)	Wahid *et al.*, 2011

Table 2-8: Continued.

Pulses					
Soybean	India	0.1-4	-	-	-
Mungbean	Allahabad, India (25.8_81.5)	-	32	reduced growth, biomass accumulation and allocation	Agrawal *et al.*, 2005
	Varanasi, India	-	50-73	Reduced stomatal conductance and reduced chlorophyll content	Agrawal *et al.*, 2003
Tubers					
Potato	Jalandhar, India (31_75.5)	2-4	-	leaf spots were similar to the ozone stipple of potato reported in the U.S.A	Bambawale, 1986, 1989

These comparisons show that for locations where crops have been studied reasonably comprehensively the modelled estimates from this study are within the range of yield losses found in the experimental studies.

It should be noted that in the current study the RYLs are calculated as a percentage of the potential yield under conditions of no O_3 pollution (based on regressions of experimental data used to define the ER functions) while the RYLs from the experimental studies are given i) as a percentage of crop yield in an unpolluted location (i.e. transect study; Agrawal *et al.,* 2003; Ambhast and Agrawal, 2003), ii) as a percentage of yield of EDU treated crops (Tiwari *et al.,* 2005; Singh *et al.,* 2009; Singh and Agrawal, 2009, 2010) or iii) as a percentage of yield of crops in filtered air (OTC; Wahid, 2006; Rai *et al.,* 2007; Sarkar and Agrawal. 2010; Wahid *et al.,* 2011). Hence, the control plant used to calculate the RYLs may not have experienced the same level of pollutant free conditions (Emberson *et al*., 2009).

The experimental studies are also conducted in different years to the modelled 2000 year estimates. Studies have reported inter-annual variations in O_3 to be as high as 10 ppb (Carmichael *et al*., 2003; Tildbald and Das (2006) cf., from Engardt, 2008). Therefore, inter-annual differences in yield losses could be due to differences in O_3 concentrations which are also likely to bring differences in meteorological conditions such as temperature, humidity, etc. which may affect crop sensitivity to O_3.

Further, there can be substantial variations in yield losses even within a few kms of a single study site, for example Agrawal *et al*. (2003) showed differences in RYLs at different sites in Varanasi. Yield losses of 0.5 %, 17 % and 25 % were found for wheat crops at three different locations only a few kms apart with 4 hours mean O_3 concentrations of 29, 34 and 47 ppb v respectively. The MATCH grids encompass an area of approximately 50 x 50 km which will have substantial sub-grid variation in O_3 concentrations; hence the RYLs for each grid represent average values whilst the values from experimental studies are local values for particular conditions. As a result of all these considerations it is expected that there will be some differences in RYLs between the model and experimental studies.

Comparison with other model based O_3 risk assessments

Although modelling based O_3 risk assessments have already been performed for India these have been performed as part of global modelling efforts (Van Dingenen *et al.*, 2009; Avnery *et al.*, 2011a); this is the first study that has performed O_3 risk assessments specifically for SA or countries within SA. Comparisons of the results of this SA study with these other global modelling studies show that all identify O_3 as a substantial threat to yields of important staple crops grown in the region; they also found that different O_3 indices gave rather different estimates of RYLs. In spite of these similarities in the results, Table 2-9 shows that the absolute values of RYL and CPL estimates in this study were significantly lower than those estimated by Van Dingenen *et al.* (2009) and Avnery *et al.* (2011a) with the exception of the RYL predicted for rice which has the same maximum RYL value of 8 % as predicted by Van Dingenen *et al.* (2009).

Table 2-9: Comparison of RYL estimates derived in this study with others based on the application of similar regional O_3 risk assessments. The range of RYL represents the range in RYL values derived from applying different metrics of O_3 exposure and associated ER functions.

Region	**Crop**	**Current study**	**Avnery *et al.*, 2011a**	**Van Dingenen *et al.*, 2009**
RYL				
India	Wheat	0.6-11.5	9-30	13-28
	Rice	1.1-7.7	-	6-8
	Soybean	0.1-4	3-13	5-19
SA	Wheat	3-10.6	8-27	-
	Rice	1-7.4	-	-
	Soybean	0.1-4	3-13	-

The global O_3 risk assessments have used similar methods to those used in this SA study; i.e., they use data derived from O_3 photochemistry transport models to define O_3 exposure indices which can be used in conjunction with appropriate ER functions and information describing crop growth periods and crop distribution to estimate yield losses. These yield losses can then be translated into CPL and EL estimates using crop production and price statistics respectively. However, the global studies differ in the modelling tools and input data they have used; different O_3 photochemical transport models have been used to estimate O_3 concentration fields and, perhaps most importantly, the spatial resolution of the O_3 concentration and crop data are different; this SA study having a much finer spatial resolution. The implications of these differences are discussed in the following sections.

2.4.2 O_3 concentration data

To estimate O_3 concentration fields across SA, the current study uses the MATCH model (Engardt, 2008).while the other global modelling studies have used the TM5 (global geochemistry Transport Model) model (Van Dingenen *et al.,* 2009) and the MOZART-2 (Model of Ozone and Related Chemical Tracers, version 2) model (Avnery *et al.,* 2011a). The main characteristics of the 3 different models are described below along with a description of the emissions data, the resolution (both spatial and vertical and the O_3 dry deposition schemes used by the models. These are discussed in relation to the likelihood that they may have caused differences in surface O_3 concentrations and hence the lower RYLs found in this SA study.

2.4.2.1 Description of MATCH, MOZART-2 and TM5

Table 2-10 gives an overview of the MATCH, TM5 and MOZART-2 photochemical models which are described briefly below.

MOZART-2

The MOZART-2 model is a global chemical transport model (CTM) designed to simulate the distribution of tropospheric O_3 and its precursors (Horowitz *et al*, 2003). The model used in Avnery *et al.* (2011a) has been driven with meteorological inputs (every three hours) using the MACCM3 (National Center for Atmospheric Research Community Climate Model), (Kiehl *et al.,* 1998). MOZART-2 has a horizontal resolution of 2.8° x 2.8° with 34 vertical hybrid levels extending up to 4 hPa (corresponding to an altitude of ~40 km), with a time step of 20 minutes for all the chemistry and transport processes (Horrowitz *et al.,* 2003).

The dry deposition scheme used in MOZART-2 is calculated off-line using a resistance-in-series scheme (Wesley, 1989; Hess *et al.,* 2000). The calculation is perfromed on a 1° x 1° grid and then averaged to the model resolution taking into account the different vegetation types within each grid cell (Horrowitz *et al.,* 2003).

Avnery *et al.* (2009) uses a global emission inventory, Emissions Database for Global Atmospheric Research (EDGAR 2.0; Oliver *et al.,* 1999, 2002). The EDGAR emission inventories are based on global datasets and the calculations are representative for the year 1990 scaled to year 2000 by a ratio of 2000:1990 emission scenarios as specified by IPCC SRES under B1 and A2 scenarios (Avnery *et al.,* 2011).

TM5

The Tracer Model 5 (TM5) is an off-line global chemistry transport model which operates with meteorology from ECWMF. It has 25 vertical layers and 37 chemical

species and includes coupled gas-phase chemistry and bulk aerosol chemistry (Krol *et al.,* 2005). TM5 has a resolution of 1° x 1°. The O_3 concentration from a reference height of 30 meters to the plant canopy height of 1 meter was calculated using a simplified version of the DO_3SE dry deposition model (described in Chapter 3) based on Tuivonen *et al.* (2007).

Van Dingenen *et al.,* 2009 uses a global emission inventory developed by the International Institute for Applied System Analysis (IIASA) available at http://www.iiasa.ac.at/rains/global_emiss/global_emiss.html (Dentenenr *et al.,* 2005). The global totals from this inventory were distributed spatially using the Emissions Database for Global Atmospheric Research (EDGAR 3.2; Oliver and Berdowski, 2001). The EDGAR emission inventories are based on global datasets and the calculations are representative for the year 1995; with NMVOC emissions being estimated assuming they follow the same trend as CO emissions (Dentener *et al.,* 2005).

MATCH

MATCH 4.4 is a regional Eulerian off-line model and in this study, it simulated hourly O_3 concentrations at a 0.5° x 0.5° horizontal resolution. It has a vertical resolution of 30 layers with 10 layers in the lowest 1 km. The MATCH model operates on a gas phase chemical scheme based on Simpson *et al.* (1993) with 60 chemical species and 130 thermal and photochemical reactions. Since MATCH is a regional model, the O_3 boundaries have to be taken from global simulations, the TM5 model was used to provide these boundaries for the year 2000 (Dentener *et al.,* 2006; Stevenson *et al.,* 2006). MATCH, uses an Asian emission inventory (TRACE-P; Streets *et al.,* 2003; Carmichael *et al.,* 2007) which has a database for the year 2000. The O_3 concentration at the plant canopy height of 1 meter was calculated using a surface resistance dry deposition scheme (Wesley, 1989).

Table 2-10: overview of the atmospheric chemistry models used in this study and in other studies that have estimated O_3 risk to crops in SA.

Model	**Resolution**		**Emission inventory (year)**	**Tropospheric chemistry**	**O_3 deposition scheme**	**Underlying meteorology**	**References**
	Latitude x Longitude	**Vertical**					
MATCH 4.4 (Engardt, 2008)	0.5° x 0.5°	30 levels; 10 layers in the lowest 1 km	TRACE-P (2000) (Streets *et al.*, 2003)	~60 chemical species and ~130 thermal and photochemical reactions	Dry deposition is based on a resistance-in-series scheme (Wesley, 1989) and used dry deposition velocity from Anderson *et al.* (2007) O_3 calculated from 10 meter to 1 meter	ECWMF ERA40 reanalysis (Upalla *et al.*, 2005) Original ERA40 resolution ~120 km interpolated to 0.5° x 0.5° grid	Current study and Engardt, 2008
MOZART-2 (Horrowitz *et al.*, 2003)	2.8° x 2.8°	34 levels extending up to approximately 40 km	EDGAR 2.0 1990 emissions scaled to 2000 using	63 chemical species and 167 chemical and photochemical reactions	Dry deposition is based on a resistance-in-series scheme (Wesley, 1989; Hess *et al.*,	MACCM3 (Kiehl *et al.*, 1998)	Avnery *et al.*, 2011a and b

Table 2-10: Continued.

		IPCC SRES scenarios (Olivier *et al.*, 1996)		2000)		
TM5 (JRC) (Krol *et al.*, 2005)	25 levels; Lowest layer, 50m; 5 layers represent the boundary layer, 10 in the free troposphere, and the remaining 10 layers the stratosphere	IIASA (Dentener *et al.*, 2005) spatially distributed using EDGAR 3.2, 1995 (Olivier and Berdowski, 2001)	37 species	A resitance shceme dry deposition schem based on the DO_3SE model (Tuovinen *et al.*, 2007) O_3 calculated from 30 meter to 1 meter	ECWMF	Van Dingenen *et al.*, 2009

Emissions data

To investigate whether the differences in RYLs were due to the differences in emission inventories, the emission inventory used in the current study was compared with that used in Van Dingenen *et al.* (2009) and Avnery *et al.* (2011). The comparisons of emission values for CO, NO_X, NMVOC and CH_4 were made for India and are shown in Figure 2-19. The 2000 TRACE-P emissions used in the current study are similar to the EDGAR 2.0 emissions scaled for 2000 used by Avnery *et al.* (2011); however, there are substantial differences in the CO, NMVOC and CH_4 emissions of the 1995 EDGAR 3.2 emission used by Van Dingenen *et al.* (2009). This comparison would suggest that the lower RYLs found in the current SA study are not due to differences in the emission inventory used by MATCH.

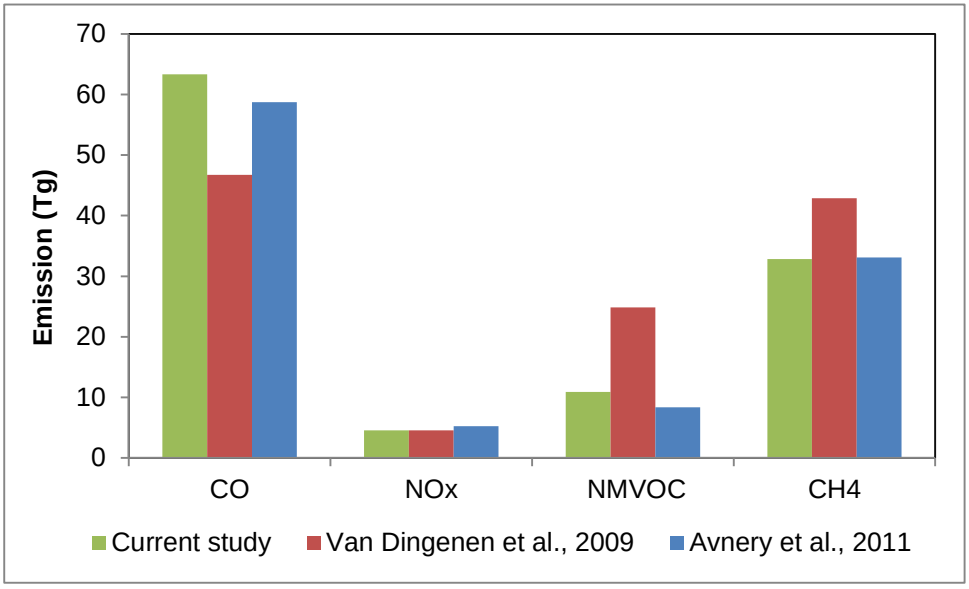

Figure 2-19: Total O_3 precursors emissions in the year 2000 that were used in this SA study (TRACE-P), Van Dingenen *et al.* (2009) (EDGAR 3.2) and Avnery *et al.* (2011) (EDGAR 2.0).

Photochemical model resolution

Studies have shown that when all model parameters are equal, higher resolution models tend to simulate less O_3 formation from the same levels of precursors emissions due to

the lower levels of forced mixing generated when emissions are added to large grid boxes (Esler, 2003; Stevenson *et al.,* 2006). Therefore, lower resolution models can be expected to be inherently more mixed and hence more chemically active than the higher resolution models (Stevenson *et al.,* 2006). Of the three photochemical models the MATCH model has the finest spatial resolution (0.5^o x 0.5^o) and also has a high vertical resolution (30 levels), albeit less than MOZART-2 which has 34 vertical levels. Taken together, this might suggest that the MATCH model would predict lower O_3 concentrations than either MOZART-2 or TM5.

Dry deposition

The MATCH model outputs O_3 concentrations at a height of 10 m above the surface, these are transformed to 1 m heights using an O_3 dry deposition model which follows the resistance scheme of Wesely (1989). Similarly, the TM5 model outputs O_3 concentrations at 30 m above the surface and uses a simplified version of the DO_3SE model to transform these to 1 m height concentrations. Avnery *et al*. (2011) do not mention the height at which O_3 concentrations are output by MOZART-2; the model also uses the Wesley (1989) dry deposition scheme but there is no mention of transforming the O_3 concentrations to heights above the ground surface representative of the canopy. Since O_3 concentrations increases with height this could lead to an overestimation of canopy height O_3 concentrations if the values are not converted. Since the dry deposition schemes are largely similar between the 3 models, following either the Wesley (1989) or DO_3SE resistance schemes, it is unlikely that this would cause much variation in the surface O_3 concentrations. However, though the manner in which surface, and particularly stomatal, resistance is dealt with may cause some variation; the Wesely (1989) scheme defines minimal stomatal resistances for different seasons and land use classes and modifies these resistances as a function of temperature and radiation. The modified DO_3SE dry deposition scheme used by Van Dingenen *et al*., 2009 defines a constant minimum stomatal resistance for the entire season; this may overestimate O_3 deposition reducing surface O_3 concentrations. The underlying land cover which determines the extent of dry deposition may also affect O_3 concentrations though not enough information is documented in either Avnery *et al*., 2011 or Van

Dingenen *et al*., 2009, or their associated references to assess the effect of land cover. As such, it is not possible to be certain the effect of these different dry deposition modelling methods on surface O_3 concentrations and hence RYL estimates of the different model studies.

In summary, these comparisons of the different aspects of the photochemical models would tend to suggest that the lower RYLs found in this SA study may have been most likely due to the higher resolution of the MATCH model since the emission inventories and dry deposition schemes are comparable across models. To assess which of the models seems most capable of estimating surface O_3 concentrations across SA requires evaluation of model against observed data; results of such evaluations for all 3 photochemical models are presented in the following section.

2.4.2.2 Comparison of modelled estimates with monitored O_3 data

All photochemical models (MATCH, TM5 and MOZRT-2) provide an indication of how well the modelled O_3 concentrations compare with observations. Figure 2-20 shows the comparisons of the TM5 and MOZART-2 models. Van Dingenen *et al*. (2009) compared the TM5 modelled monthly O_3 concentrations at 30 and 10 height with observed O_3 data for South India (Ahammed *et al.*, 2006; Beig *et al.*, 2007) and North India (Lal *et al.*, 2000; Satsangi *et al.*, 2004; Jain *et al.*, 2005). Avnery *et al.*, (2011) also compared the MOZART-2 modelled monthly O_3 concentrations with the observed O_3 data for North India (Mittal *et al.*, 2007; Ghude, 2008) as well as South India (Naja and Lal, 2002; Naja *et al.*, 2003; Debaje *et al.*, 2003; Ahammed *et al.*, 2006; Beig *et al.*, 2000; Mittal *et al.*, 2007; Debaje *et al.*, 2010) but do not state the height at which the O_3 data are provided by the model.

Both the studies show the seasonal O_3 profile is captured reasonably well but that O_3 concentrations are overestimated, especially in Northern India (Figure 2-20). For example, Avnery *et al.*, (2011) reported that the O_3 concentrations simulated by MOZART-2 in northern India were significantly overestimated by ~10-18 % throughout the year. The greater overestimates in North India may be due to the use of urban O_3 data for these comparisons since observed urban O_3 concentrations will tend to be lower

than concentrations in rural areas. Overestimates of modelled O_3 would be expected for the Van Dingenen *et al*. (2009) comparisons since modelled data are provided at a height of 30 meter and 10 meters; it should also be remembered that the O_3 indices in the Van Dingenen *et al*., (2009) study are estimated from O_3 concentrations transformed to a 1 m height which would lessen the overestimate.

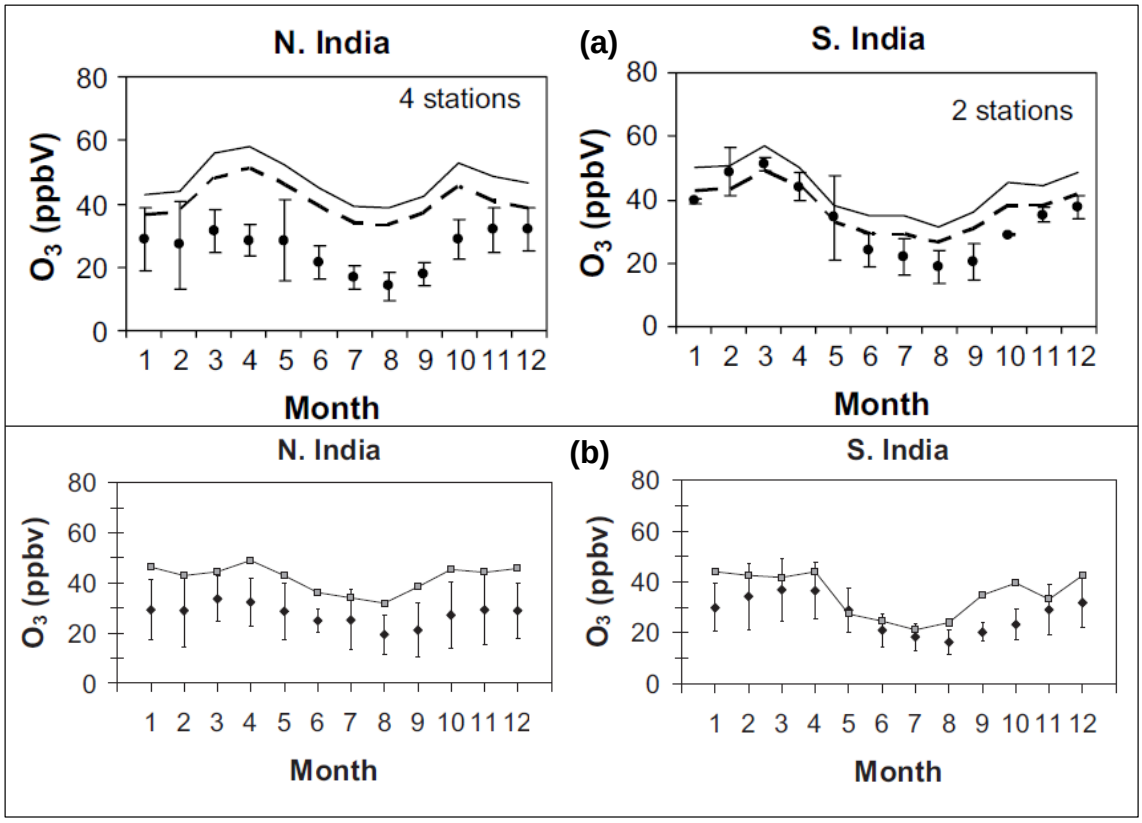

Figure 2-20: Comparisons of annual monthly mean, surface O_3 concentrations for North India and South India. Comparison are made by (a) Van Dingenen *et al.*, (2009) for TM5 modelled O_3 concentrations and data collected from the published literatures (details in text) and (b) Avnery *et al.* (2011) for MOZART-2 modelled O_3 concentrations and data collected from the published literature (details in text). The dot with error bars indicate observed data while the lines indicated the modelled values. In (a), the solid line indicates the modelled O_3 at 30 meter height while the dotted line indicates O_3 at 10 meters.

Engardt (2008) performed an evaluation of the MATCH model with observations of O_3 data collected from 9 rural sites of which 6 were located in Northern SA and 3 in South India. This assessment showed that the MATCH model was able to capture the seasonality in O_3 concentration across SA reasonably well but that the model had a tendency to underestimate the day-time O_3 concentrations ($\leq$ 10%) in rural locations.

As an addition to Engardts (2008) comparison, this study has compared MATCH model data with additional observations of annual O_3 concentration profiles collected from more recent literature (Beig *et al.*, 2007; Ahammed *et al*, 2006; Debaje and Kakade, 2009; Debaje *et al.*, 2010); the results are shown in Figure 2-21 and again indicate that MATCH describes the seasonality in surface O_3 reasonably well. Taken together the evaluation data in Figure 2-21 and Engardt (2008) suggest that in winter (January to March), coinciding with the wheat and potato growth period, MATCH gives a good representation of observed O_3 values. However, during June to September, coinciding with rice and soybean growing season, MATCH tends to overestimate observed O_3 values. During this period all of the photochemical models have a tendency to overestimate O_3 concentrations, Engardt (2008) attributed this over estimation to erroneously specified seasonality of precursor emission or the limited seasonality of the boundary values in the experimental set-up; these problems may well be exacerbated by the monsoon affecting estimates of precursor emissions and photo-chemistry in the models (Beig *et al*., 2006). There are also obvious inter-annual differences in the O_3 concentrations, e.g., in Ahmednagar (Debaje *et al.*, 2010), the O_3 concentration values and pattern for 2006 is different from that of 2007 (Figure 2-21). Engardt (2008) reported that in some months the inter-annual difference between the monthly O_3 concentrations may be as large as 10 ppb. This is useful as a reminder that these evaluation data can only provide an indication of the model performance for any particular year (i.e. the year 2000 that is used in these modelling studies).

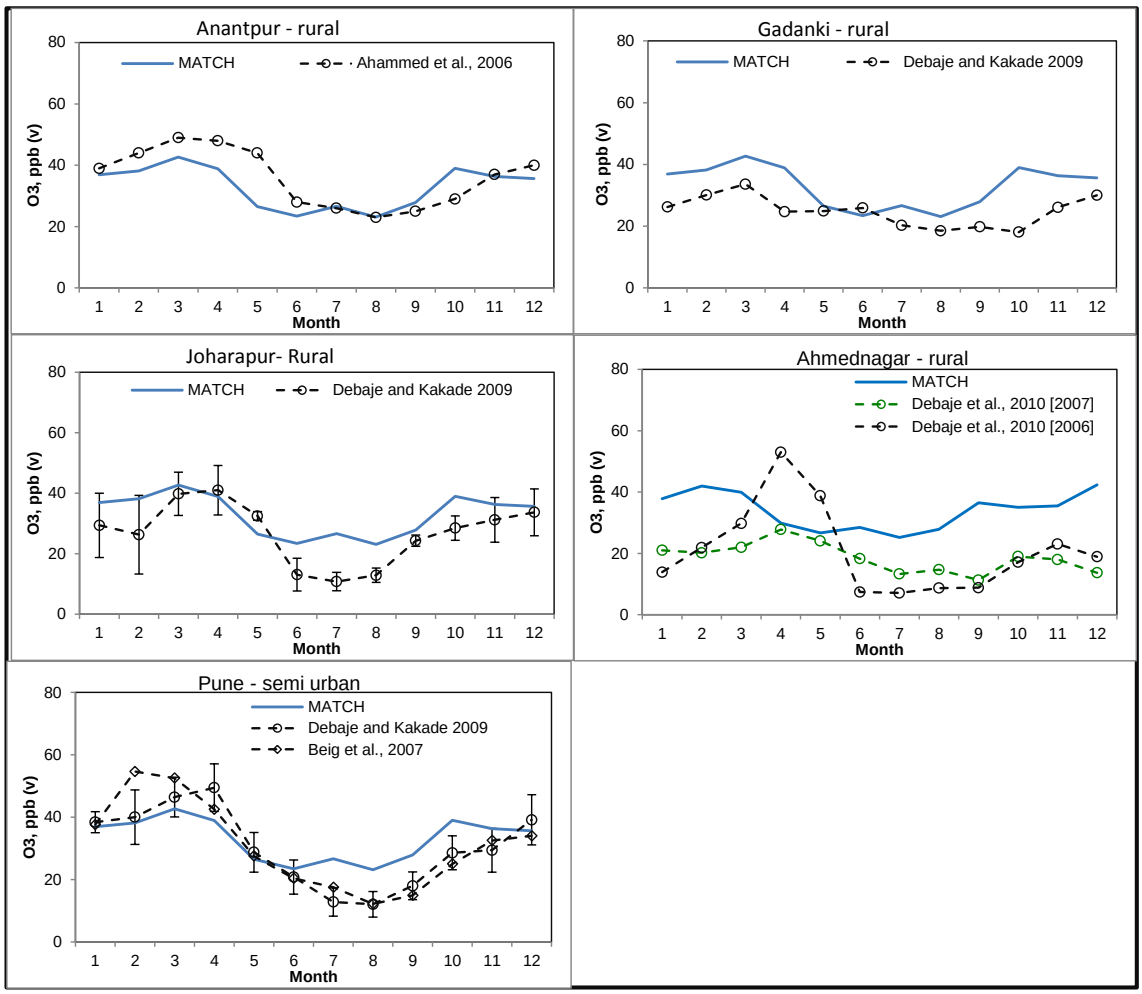

Figure 2-21: Comparisons of annual monthly mean, surface O_3 concentrations for three different rural locations in SA. Comparisons are made between MATCH modelled O_3 concentrations and data collected from the published literature (Ahammed *et al.*, 2006; Beig *et al.*, 2007; Debaje and Kakade, 2009 and Debaje *et al.*, 2010). Error bars are standard deviation values and are added wherever data was available.

While there are uncertainties in these evaluations, mainly due to the limited availability of observed O_3 data from which to validate and improve model performance, the MATCH model has been more extensively assessed for rural SA conditions than the global O_3 photochemical models. These evaluations have tended to show that the MATCH model generally provides a more realistic estimate of absolute O_3 concentrations than either TM5 or MOZART-2, especially in Northern India, though the height at which the modelled O_3 is provided, at least for TM5, may in part explain these

differences. The apparent overestimate of O_3 in Northern India may be especially important in terms of the RYLs since the majority of wheat and rice cultivation occurs in these areas, therefore over estimation of O_3 will magnify losses in this region.

2.4.3 Crop phenology data

The crop phenology used in this study is based on data from national databases that provide details of crop sowing and harvest dates for different regions in India and SA. The phenology used in this study show good agreement with data describing the timing of crop growing seasons available in the peer reviewed literature (Rane *et al.*, 2007; Mitra and Bhatia, 2008). The global modelling studies conducted by both Van Dingenen *et al.* (2009) and Avnery *et al.* (2011a) used crop phenology data for India given by USDA (1994) and hence are likely to exclude within region variations in crop phenology that will be important in determining the exact O_3 concentrations to which crops are exposed.

2.4.4 Crop distribution and production data

Although much of the SA's land is under crop cultivation, there is variation across the region in the types of crops grown and the season within which the crops are grown. Therefore, assessments that are performed using a finer resolution of crop distribution and production data in conjunction with a finer resolution O_3 concentration data should be able to accommodate the local scale variations in these variables hence improving estimates of O_3 risk. The data used in this SA study are likely to be more suited to represent Indian conditions as district and province level crop data are provided for most of the SA region (i.e., India and Pakistan). By comparison the global modelling studies of Avnery *et al.* (2011) and Van Dingenen *et al*. (2009) relied on integration of data at a broader resolution defined by the grid used by the photochemical models.

In summary, it is likely that the finer resolution used in the current SA study in terms of emissions data, photochemical model characteristics, crop distribution and production

data are likely to capture local variations across SA better. This means that systematic bias in any one aspect of the model is less likely to be magnified; the higher O_3 concentrations in Northern India reported by the global modelling studies may have provided such a systematic bias that could in part be responsible for the higher RYLs found in these studies.

2.4.5 Crop RYLs and ER functions

This section highlights important aspects of the different O_3 indices and their associated ER functions that influence estimates of O_3 induced RYLs in relative terms within and between crops.

Crop growth period and crop location determinants of O_3 sensitivity

RYL estimates will be a function of the O_3 concentration, characterized in terms of the particular index, to which the crop is exposed. Since O_3 concentrations show strong seasonality across SA, the timing of the crop growth periods will be important in determining the magnitude of O_3 exposures. Similarly, since O_3 concentrations also show large spatial variability across SA, the location of the crop will also be important in determining O_3 exposure.

The wheat and potato growing periods occur during the winter season which coincides with the time of the year when the monthly average O_3 concentrations are relatively high. In contrast, rice and soybean grow during the monsoon season when the monthly average O_3 concentrations are relatively low (Figure 1-12). Potato and wheat are both winter crops in SA but the potato crop harvest occurs earlier than wheat and hence the 3-month period when the O_3 exposure indices are calculated for potato has a lower O_3 exposure than that of wheat; this helps to explain why, in general, potato shows less sensitivity to O_3 compared to wheat. Similarly, in this study, with the exception of Pakistan, wheat was more sensitive than rice because the O_3 concentrations are lower during the rice growing season (Figure 1-12).

The location of the crop will also determine the O_3 levels to which the crop is exposed. The soybean RYLs are not as high as might have been expected given the sensitivity of the crop as described by the ER functions. This is due to the low O_3 concentrations (average M7 values of only 20-30 ppb) found across the soybean growing regions leading to low RYLs. For example, even though the growing seasons of rice and soybean are similar so that they would be exposed to the same seasonal profile, the geographical distribution of the main soybean cropping region is Madhya Pradesh which is in the central part of India where O_3 concentrations are much lower at the same time of year than across the main rice growing region in the IGP.

Therefore, the differences in RYL values between the crops are in part attributable to the differences in the timing of the different crop growing season and the spatial location of the crop. Van Dingenen *et al.*, (2009) also commented that the sensitivity of the ER function could be due to the differences in the statistical methods used in their derivation caused by differences in the O_3 profiles (frequency and magnitude of O_3 concentrations). Therefore, the timing of the growth period and geographical location of the experimental studies from which the ERs were derived may also affect the sensitivity of the ER function. This will be explored further in the following sections.

ER function determinants of O_3 sensitivity

The current SA study found significant differences in the estimates of O_3 induced yield losses using the different O_3 exposure indices, a finding that has also been emphasized in the global studies (Van Dingenen *et al.,* 2009; Avnery *et al.*, 2011a). Figure 2-22 exemplifies this and shows this SA study estimates of RYLs for wheat, rice and soybean using M7 (M12 for soybean), W126 and SUM06 indices (as available) plotted against estimates made using AOT40. Each data point in the scatter plots represents the values for a single MATCH grid. Figure 2-22 clearly shows that for wheat, rice and soybean, AOT40 gives significantly higher RYLs as compared to M7, W126 and SUM06. RYL_{M7} is always lower whereas RYL_{W126} and RYL_{SUM06} values are higher than RYL_{AOT40} at higher concentration. The largest differences are found between wheat RYL_{AOT40} and RYL_{M7} where the difference is about 90%. In rice due to the AOT40 ER intercept at 0.94, the RYL_{AOT40} shows yield loss > 6% even when there is no RYL_{M7}.

For potato, no averaging (M7/M12) ER function exists; comparison between RYL_{AOT40} and the other cumulative indices (W126 and SUM06) showed AOT40 generally estimated lower yield losses.

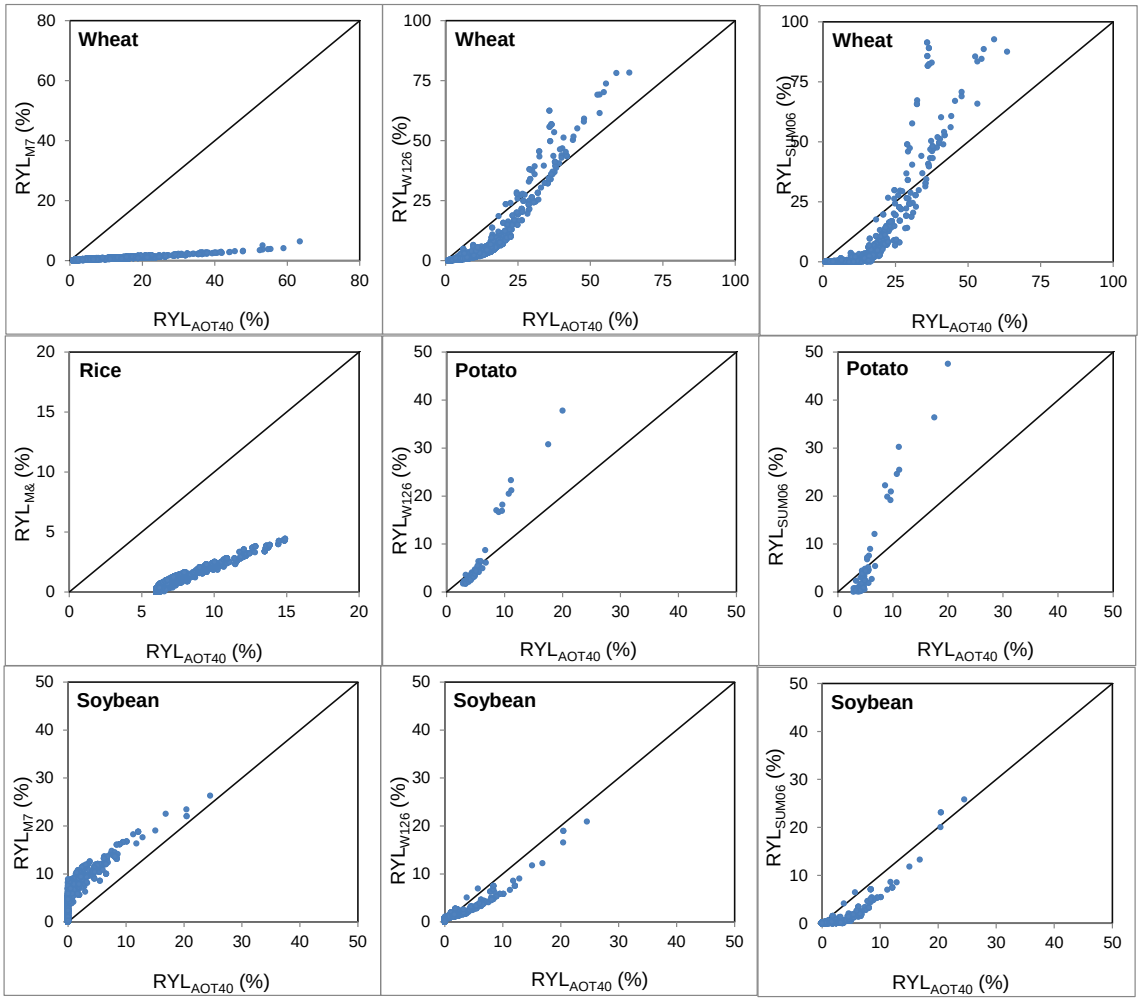

Figure 2-22: RYLs estimated for wheat, rice and soybean using M7 (M12 for soybean), W126 and SUM06 indices (as available) plotted against estimates made using AOT40 for each MATCH grid.

These differences can in part be explained as follows. The cumulative indices will emphasise the higher O_3 concentrations and therefore may be more appropriate for regions where the O_3 concentration profile is represented by high frequencies of elevated O_3 concentrations that exceed the selected threshold. In contrast, the averaging indices may be better suited for locations that suffer more moderate levels of O_3

pollution with less variability in the range of concentrations experienced. The cumulative indices will ignore the lower levels of O_3 concentration which are captured by averaging indices (i.e., M7 and M12). The importance of these different O_3 profiles and the effect of the O_3 exposure index and ER function used to estimate RYL are especially apparent for soybean. In SA, soybean tends to grow in regions where there are low O_3 concentrations during the growing season. In soybean, RYL_{M12} is significantly higher than the RYL calculated using cumulative indices (Figure 2-23). This is because M12 shows O_3 impacts from average O_3 values of above 20 ppb, i.e. well below the 40 ppb threshold used in the AOT40 index. This M12 index therefore suggests that soybean is more sensitive to long term exposure to moderate concentrations of O_3 than frequent exposure to high O_3 levels which are best captured by cumulative index (Wang and Mauzerall, 2004; Betzelberger *et al.*, 2010). In contrast, wheat seems to be more sensitive to frequent exposure to high O_3 levels (Avnery *et al.*, 2011a).

The sensitivity of the four crops to each of the exposure indices is given in Figure 2-23. Wheat is the most sensitive crop in terms of AOT40, SUM06 and W126. However, in terms of the seasonally averaged indices (M7 and M12), soybean is the most sensitive crop. In terms of the AOT40 index, soybean is the second most sensitive crop to wheat. This highlights one important limitation to performing O_3 risk assessments, namely that the ranking of crop sensitivity to O_3 is not consistent between indices and their associated ER functions; this causes a fundamental difficulty in drawing firm conclusions as to which crops in which areas are most likely to be at risk from prevailing O_3 concentrations.

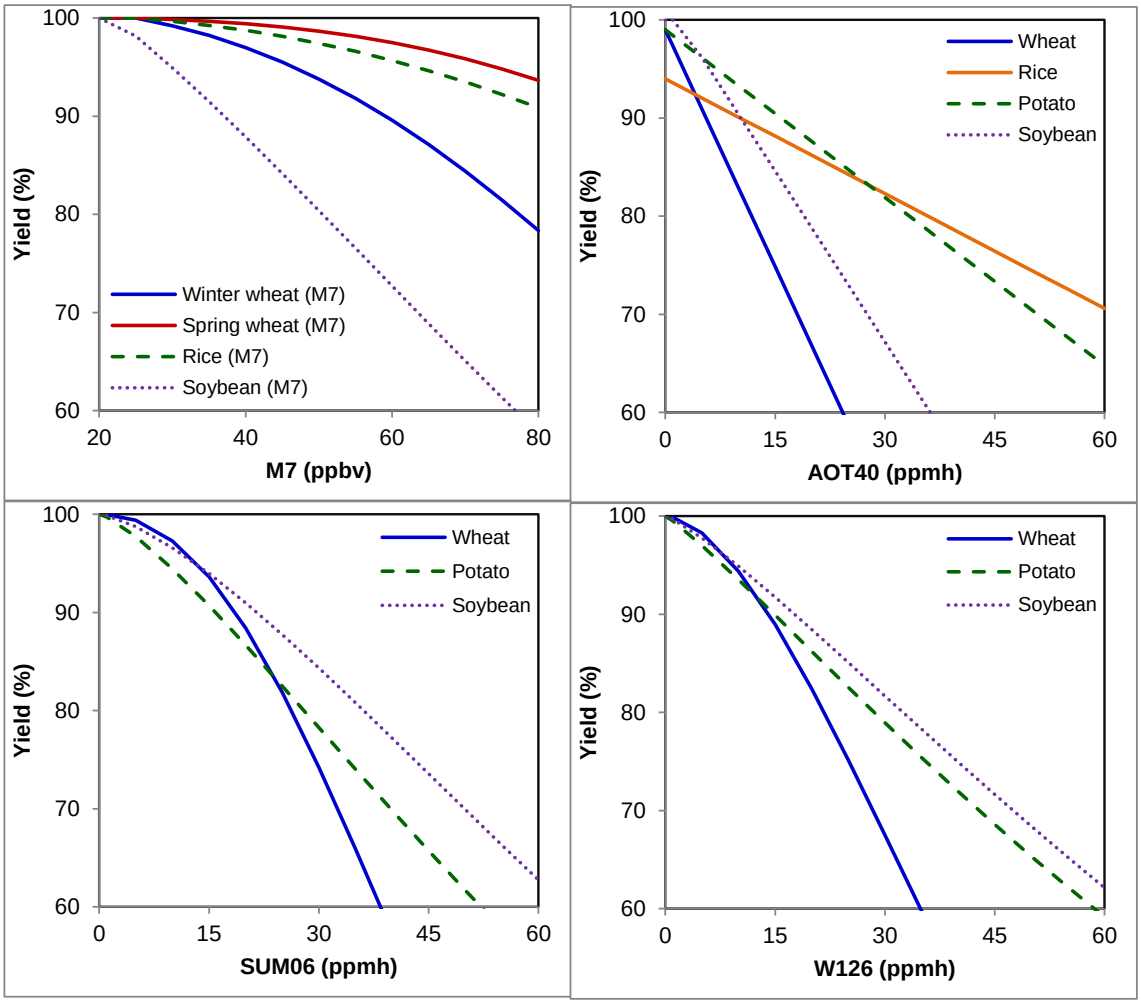

Figure 2-23: O_3 exposure response indices for wheat, rice, potato and soybean.

An additional issue in terms of application of these ER functions is that the intercepts of the AOT40 functions derived from Mills *et al*. (2007) are different from 1 (0.99, 0.94, 0.99 and 1.02 for wheat, rice, potato and soybean respectively) such that the relative yield (RY) can be greater than 1 at low O_3 concentrations or less than 1 even when AOT40 values are zero (Figure 2-23 which shows values as percentage yield losses). This can be explained by the fact that these functions were derived based on recalculation of O_3 exposure data provided as M7/M12 to AOT40. This means, for example, that any yield loss occurring at M7/M12 averaging values of less than 40 ppb can only be captured by assuming that a yield loss will occur at AOT40 values equal to zero and *vice versa*. To avoid the estimation of yield increases in this study a maximum value of 1 for RY was established; however, yield losses at zero AOT40 are allowed to

occur. The uncertainty due to this is particularly significant for rice where the intercept at 0.94 means that 6% yield loss will occur at zero AOT40 values. Van Dingenen *et al.* (2009) overcame this intercept issue by scaling the Mills *et al*. (2007) AOT40 ER functions so that all intercepts were at relative yield of 1; since this may come with its own set of uncertainties (for example, rice yield losses at AOT40 values higher than zero would be underestimated) this study has used the original function provided by Mills *et al*. (2007).

In summary it is clear that there are large uncertainties in the RYL estimates provided by application of the different ER functions. Adding to this uncertainty is the suggestion that SA crops and cultivars may be more sensitive to O_3 than suggested by the North American M7 / M12 averaging ER functions (Emberson *et al*., 2009). Recent experimental studies conducted in Asia also suggest even higher sensitivity to O_3 in the modern Asian wheat cultivars (Biswas *et al*., 2008a; Sarkar and Aggrawal, 2010) and hybrid rice (Shi *et al.,* 2009). There is also a need to assess varietal differences in sensitivity to O_3 of the same crop species. Variability in cultivar sensitivity to O_3 has been found previously for wheat (Barnes *et al*., 1990; Heagle *et al*., 2000; Quarrie *et al*., 2007; Biswas *et al*., 2008a, b) and rice (Ariyaphanphitak *et al*., 2005). Ariyaphanphitak *et al*. (2005) found that the variation of the sensitivity of different Thai rice cultivars to O_3 exposures in closed top chamber experiments was as high as 56%. Quarrie *et al.* (2007) reported that these differences in O_3 sensitivity are genetically linked and that the differences in genetic traits that govern the O_3 sensitivity between the cultivars cause the variations in yield losses due to O_3 exposure. The AOT40 is sensitive to changes and uncertainties in input values (Van Dingenen *et al.,* 2009) and this makes it less robust. M7 is most robust for replication observed O_3 exposure values (Avnery *et al.,* 2011). As such, ideally ER functions would be developed for Indian cultivars growing under Indian conditions (Emberson *et al.,* 2009).

2.5 Conclusions

This study is the first to evaluate O_3 damage to crops specifically for the SA region using fine resolution datasets. The estimates of RYL are within the range of yield losses derived from ambient O_3 concentration experiments conducted across SA. However, the

RYLs are substantially lower than those estimated by global modelling studies; this may be due to differences in the modelling tools and input data but is perhaps more likely due to the application of the model using finer resolution data both in terms of O_3 concentrations and crop distribution and production data. All studies (this SA study and the global studies) have identified problems in applying the concentration based indices due to inconsistencies in inferred crop sensitivity to O_3. This is likely due to the interpretation by different indices of the most important aspect of the O_3 concetration profile in determining O_3 sensitivity. One option to overcome such inconsistencies may be to use flux rather than concentration based indices (Ashmore, 2005) since these integrate O_3 concentrations, prevailing meteorological conditions and crop specific characteristics into a single exposure index. The plausibility of such an approach is investigated further in Chapter 3.

Chapter 3 Stomatal O_3 flux based risk assessment in India

3.1 Introduction

In Chapter 2, the application of concentration-based O_3 risk assessment methods showed that O_3 is a potential threat to important crops grown across many parts of SA, especially in the important crop growing region of the IGP. These findings are in agreement with previous studies of O_3 risk assessments using concentration-based methods (Van Dingenen *et al.,* 2009; Avnery *et al.,* 2011a) as well as experimental field studies that show crop yield loss due to ambient O_3 (Tiwari *et al.,* 2006; Sarkar and Agrawal, 2010; Singh and Agrawal, 2010).

However, a study that collated SA concentration-based ER data (Emberson *et al.,* 2009) suggested that the SA crop cultivars and the SA crop growing conditions show a heightened sensitivity to O_3 than is suggested by ER functions for wheat, rice and legumes derived in North America (Heck *et al.,* 1988) and Europe (Jäger *et al.,* 1992). This was thought either to be due to the differences in sensitivity in SA crop cultivars, due to differences in O_3 concentration profile experienced in SA, or due to the differences in cropping pattern and crop growing conditions influenced by the meteorological conditions that occur in SA (Emberson *et al.,* 2009).

Studies have shown that O_3 damage to crops is more closely related to stomatal O_3 uptake and the amount of O_3 reaching the sites of damage within the leaf (Pleijel *et al.,* 2000, 2007; Emberson *et al.,* 2000; Fowler *et al.,* 2009; Mills *et al.,* 2011). Therefore, quantifying the stomatal O_3 flux (F_{st}) is important for understanding O_3 impacts on plants (Pleijel *et al.,* 2004; Fuhrer, 2009; Fares *et al.,* 2010). This is supported by experimental (Grunhage and Jäger, 2003; Gerosa *et al.,* 2009) as well as modelling (Massman, 2004; Pleijel *et al.,* 2004, 2007) studies both of which suggest that the O_3 flux approach gives a more 'biologically relevant' and robust approach to quantifying O_3 effects on crops than O_3 exposure indices purely based on O_3 concentrations. For example, studies have shown that modelled cumulative O_3 uptake gives a better fit to effects data than O_3 concentration in both crop (Pleijel *et al.,* 2000, 2007; Fiscus *et al.,* 2005; Mills *et al.,* 2010) and forest tree species (Udling *et al.,* 2004; Karlsson *et al.,* 2007a). This is explained by the fact that the periods of high F_{st} do not necessarily

coincide with periods of high external O_3 concentration (Grunhage *et al.,* 1997). Pleijel *et al.,* (2007) showed that the r^2 value for the relationship between relative yield of wheat and different exposure indices was 0.41 when using AOT40 and 0.77 when using cumulative O_3 uptake above a threshold of 5 nmol O_3 m^{-2} PLA s^{-1}, indicating that the flux-based approach represents a better and more relevant approach for quantification of O_3 effects on crop yield.

Importantly, the use of flux also allows aspects related to crop physiology (and therefore crop varietal differences), phenology and meteorology to be incorporated into the risk assessment; all of which are aspects that might have been responsible for the differential sensitivity of SA *vs* European /North American ERs.

Since O_3 flux is strongly dependent on stomatal conductance (g_{sto}), the factors that effect g_{sto} will also influence O_3 impacts on crops (Fiscus *et al.,* 2005). These factors include CO_2 (Morgan *et al.,* 2003; Booker *et al.,* 2005; McKee *et al.,* 1995), a number of meteorological factors such as, temperature, humidity, irradiance, etc., (Collatz *et al.,* 1991; Wilkinson *et al.,* 2001; Gruters *et al.,* 1995; Bunce, 2000; Pleijel *et al.,* 2007) and other pollutants that the crops may be exposed to during the different phases of their development as well as the crop physiology, phenology and the management (e.g. irrigation schedule) and growth conditions of the crop (Fiscus *et al.,* 2005; Fuhrer *et al.,* 1997). Therefore, to understand the stomatal O_3 flux (F_{st}) into the plants, it is essential to understand the variation of g_{sto} according to the influencing factors mentioned above.

Although O_3 may cause damage on the surface of the plant (e.g. changing the chemical composition of waxes (Barnes *et al*., 1988), the main site of damage by O_3 occurs inside the plant (Fowler *et al.,* 2009). Plants have a defence mechanism by which they are able to detoxify a certain amount of O_3 that enters the plant through the stomates; once this detoxification capacity is exceeded plant damage would be expected to occur (Musselman and Massman, 1998). This detoxifying capacity of the plant is species-specific and has also been found to depend upon the age of the plant, the age of the leaf and water stress (Musselman and Massman, 1998). Once inside the plant, O_3 reacts to form reactive oxygen species (ROS) (Fiscus *et al*., 2005). Plants also produce ROS in response to a cultivar of other stresses (e.g. heat and water stress); therefore they have evolved defence mechanisms that use a cultivar of different enzymes to

detoxify these ROSs and hence will have an innate capacity to deal with high F_{st}. Studies have reported an increase in the activity of certain enzymes following exposure to O_3 thereby identifying them as being particularly important in O_3 detoxification; these include ascorbate peroxidase (Ranieri *et al.,* 1996), gluthathione reductase (Pell *et al.,* 1999), peroxidase (Ranieri *et al.,* 2000) and superoxide-dismutase (Calatayud and Barreno, 2004).

Stomatal O_3 uptake is not the only mechanism by which O_3 is deposited to vegetation; non-stomatal O_3 deposition also takes place with O_3 loss to external plant surfaces and the soil surface, as well as through within canopy chemical reactions. Non-stomatal deposition tends to be the smaller component of total deposition though the relative magnitude of these different deposition pathways will vary seasonally depending upon the physiological activity of the vegetation (Pleijel *et al.,* 2004; Tuovinen *et al.,* 2009; Fuhrer, 2009; Bender and Weigel, 2011). For example, some studies have reported that non-stomatal O_3 removal often exceeds stomatal O_3 removal, especially when the plant surface is wet (e.g. Fowler *et al.,* 2009). These studies that have highlighted the importance of considering O_3 absorption to the plant cuticle and soil surfaces (Fowler *et al.,* 2001; Gerosa *et al.,* 2003; Altimir *et al.,* 2006; Cape *et al.,* 2009; Tuovinen *et al.,* 2009), indicating that these surfaces serve as important O_3 sinks (Emberson *et al.,* 2000b). The factors that influence the non-stomatal and stomatal O_3 deposition to vegetation surfaces are described in the following sections.

3.2 Factors determining O_3 deposition to vegetation

O_3 is transferred from the atmosphere to the vegetative surfaces by three main processes: (i) movement from a height within the atmosphere to top of the canopy is determined by atmospheric turbulence caused by wind and thermal heating, (ii) movement across the quasi-laminar leaf boundary layer to the leaf surface is determined by both turbulence and diffusion, and (iii) movement through the stomata is determined by diffusion and assumes that O_3 concentrations reduce almost to zero within the sub-stomatal cavity (Laisk *et al*., 1989). Figure 3-1 gives a diagrammatic representation of the transport of O_3 from the atmosphere to vegetation, highlighting the stomatal and non-stomatal uptake of O_3.

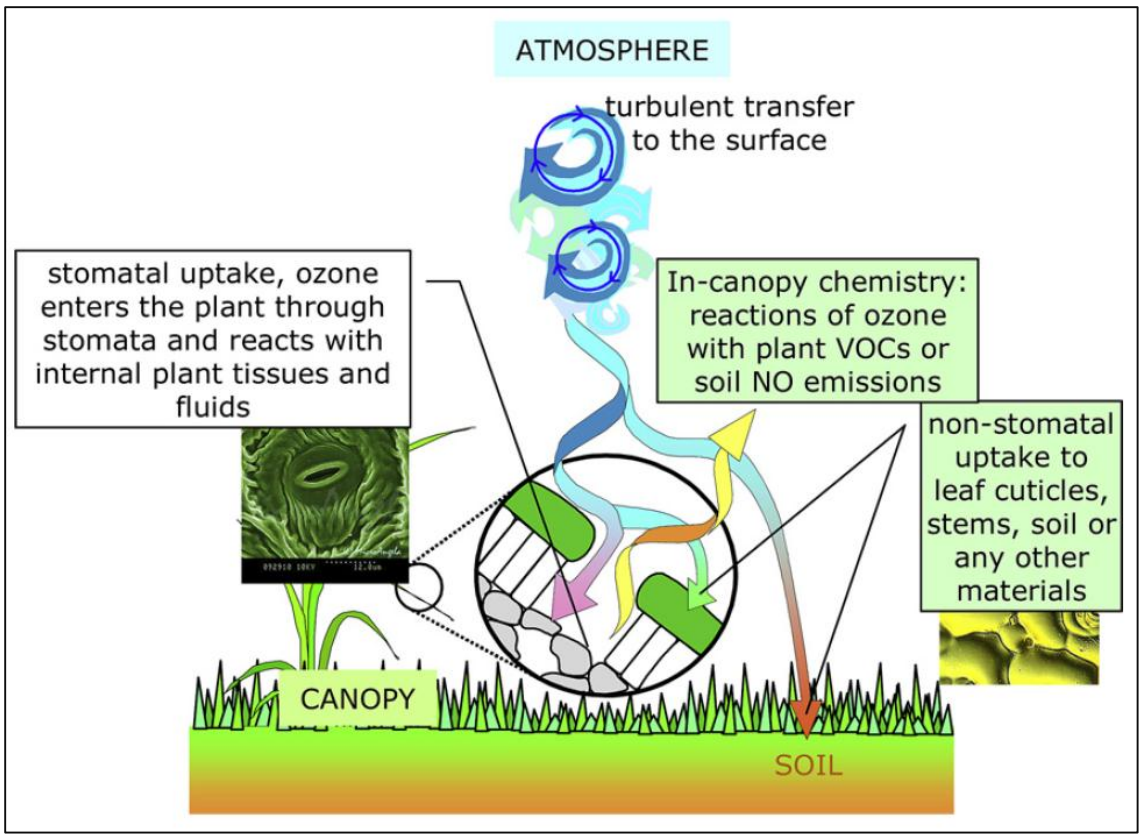

Figure 3-1: Diagrammatic representation of stomatal and non-stomatal uptake of O_3 (Fowler *et al.*, 2009).

3.2.1 Non-stomatal O_3 uptake

The non-stomatal deposition of O_3 onto the plant surface is influenced by factors such as surface wetness (Altimir *et al.*, 2006; Coyle *et al.*, 2009), solar irradiance (Hoggs *et al.*, 2007; Coyle *et al.*, 2009), temperature (Hoggs *et al.*, 2007; Coyle *et al.*, 2009) and wind speed (Fowler *et al.*, 2009), and this has been reported for different vegetation types including crops, grasslands and forest trees. The non-stomatal deposition serves as an important sink and studies have reported that it could account for up to 70% of the total O_3 deposition (Fowler *et al.*, 2001; Altimer *et al.*, 2006; Hoggs *et al.*, 2007; Tuzet *et al.*, 2011).

O_3 is known to react with structures on the leaf surface such as epicuticular waxes; this can cause altered chemical composition of these waxes (Percy *et al.*, 1992, 2002; Della

Torre *et al.,* 1998) and can induce regeneration of waxes increasing the amount of waxes in mature leaves (Percy *et al.,* 1992; Paoletti *et al.,* 2007). Experimental studies have shown that reaction of O_3 with waxes is influenced by temperature, radiation and surface wetness. The thermal decomposition of O_3 on plant surfaces has been reported in many studies (Fowler *et al.,* 2001; Coyle *et al.,* 2009; Cape *et al.,* 2009). Both radiation and temperature increases the thermal decomposition of O_3, while surface wetness may reduce thermal decomposition by forming a thin coating of water on the surface of the leaf. However, the sink capacity of plant surfaces is known to increase with increases in surface wetness (Altimir *et al.,* 2006). Biogenic volatile organic compounds (BVOCs) in the air near the plant surfaces can also serve as O_3 sinks and the emission of BVOCs is influenced by temperature, irradiance and humidity (Altimir *et al.,* 2006).

3.2.2 Stomatal O_3 uptake

Stomatal regulation is important in controlling gas influx through the stomates into the leaf mesophyll; it can also help to exclude O_3 from entering the leaf (Fiscus *et al.,* 2005). As mentioned earlier, the g_{sto} and hence F_{st} are influenced by various factors. The most important g_{sto} influencing factors include temperature (Pleijel *et al.,* 2000; Fowler *et al.,* 2001), VPD (Pleijel *et al.,* 2000; Zhang *et al.,* 2006), soil moisture and bulk leaf water potential (Jarvis and Morison, 1981; Feng *et al.,* 2008; Wilkinson and Davies, 2010; Biswas *et al.,* 2011), irradiance (Gruters *et al.,* 1995; Bunce, 2000), ambient CO_2 concentration (Collaz, 1991; McKee *et al.,* 1995; Booker *et al.,* 2005), salinity of the soil (Katerji *et al.,* 1997: Munns and Tester, 2008), plant species type (Bermejo *et al.,* 2003; Altimir *et al.,* 2006; Mills *et al.,* 2007) and the developmental stage of the plant (Soja *et al.,* 2000; Pleijel *et al.,* 2007). These factors either act independently or in combination with one or more of the other factors. For example, the magnitude of the stomatal response to temperature depends on the corresponding VPD values (Jones, 1993). These factors are discussed briefly in the following sections. High O_3 also affects the g_{sto} of plants indirectly by accelerating leaf senescence which may reduce irradiance interception and thereby reducing food production (Dermody *et al.,* 2008).

3.2.2.1 Temperature

g_{sto} usually has an optimum temperature from which it will decrease as the temperature either reduces or increases. This optimum temperature is species-specific and can also be influenced by environmental factors like humidity. At high temperatures, the stomates close in order to prevent excessive water loss due to increased transpiration (Lange *et al*., 1971). High temperature also affects the photosynthetic mechanism of the leaf, thereby decreasing the photosynthetic rate and subsequently reducing the g_{sto} (Collatz *et al.,* 1991). At very high temperatures this effect can lead to a mid-day depression of g_{sto} (Tenhunen *et al*., 1984). At low temperatures, the uptake of water by plants through the roots is reduced; the stomates will close in order to maintain the leaf water potential, (Cornic and Ghashghaie, 1991). This is achieved either by directly affecting the guard cell osmotic potential (Honor *et al.,* 1995; Ilan *et al.,* 1995) or through increase in ABA biosynthesis (Assmann and Shimazaki, 1999; Wilkinson *et al.,* 2001).

In India, heat stress affects about 13.5 million hectares of wheat under cultivation reducing the yield (Nagarjan, 2005; Joshi *et al.,* 2007b; Rane *et al.,* 2007). These crops are subjected to heat stress towards the end of the growing season which happens to be the grain filling, when the crop is considered most sensitive to O_3 (Younglove *et al.,* 1994). Therefore, under Indian conditions, heat is likely to be a major flux limiting factor occurring at a time of heightened sensitivity to O_3.

3.2.2.2 Vapour Pressure Deficit (VPD)

VPD is a measure of the water status of the atmosphere and is a function of the temperature and water vapour content of the atmosphere; leaf-to-air VPD is a function of leaf temperature and internal leaf water status in relation to atmospheric VPD. VPD plays an important role in influencing the g_{sto} of plants (Lang *et al,* 1971). With increasing VPD levels above a threshold g_{sto} starts to decrease in order to maintain water potential in the leaf cells, which in turn maintains the photosynthetic capacity of the mesophyll cells (Jones, 1993; Xu *et al.,* 1994; Gruters *et al.,* 1995; Pleijel *et al.,* 2007). Once the VPD crosses a certain threshold value (for example a number of studies

have suggested that for wheat this is > 3 kPa; Gruters *et al.,* 1995; Shirke and Padre, 2004), the stomates closes rapidly. The magnitude of stomatal response to VPD depends on the species, growing conditions and plant water status. The stomatal response to VPD is generally smaller at higher temperature (Jones, 1993) and in water stressed plants (Gruters *et al.,* 1995). On the other hand, at high leaf-to-air VPD, the sensitivity of g_{sto} to temperature is not very significant but at low leaf-to-air VPD the g_{sto} is very responsive and increases as temperature rises (Dai *et al*., 1992; Fuhrer, 2009). During the afternoon, the high VPD limits g_{sto}. In the late afternoon, the temperature decreases which in turn usually causes a decrease in the VPD; this would normally allow the stomates to open and result in an increase in g_{sto}. However, stomatal re-opening does not always occur. Re-opening is prevented under conditions when the temperature and VPD of the afternoon period have been high enough to cause the plant to lose water at a higher rate than it can replace water by root uptake. This results in a decrease in the plant water potential (PWP) that prevents the stomates from opening in the late afternoon. The PWP recovers during the following night when the transpiration is low such that normal stomatal functioning returns for the following morning period (Pleijel *et al.,* 2007). Under high predawn leaf water potential (>0.4 MPa), VPD has a higher effect on the g_{sto} than soil water deficit (Ferreira and Katerji, 1992).

3.2.2.3 Soil water content

The amount of water in the soil is very important for plant growth. Field capacity is the amount of water that a well-drained soil can hold against gravitational forces (Allen *et al*., 1998). This is the water in the soil within the plant root zone that is available to the plant, as the plant extracts water from the soil the amount of water in the root zone decreases. As this soil water decreases, the water becomes more strongly bound to the soil particles and makes it more difficult for the plant to extract water. The plant can extract water only up to a certain level. This point is known as the 'permanent wilting point'. When soil water content is low, it causes the stomates to close and reduces transpiration in order to maintain plant water status (Jones, 1992).

Soil water deficit is the amount of available water removed from the soil within the crop's active rooting depth. Likewise it is the amount of water required to refill the root

zone to bring the current soil moisture conditions to field capacity. Soil water decreases as the crop uses water (evapotranspiration) and increases as precipitation (rainfall or irrigation) is added. Expressed in terms of soil water deficit, evapotranspiration increases the deficit and precipitation decreases it. It is usually expressed in 132illimetres of water.

3.2.2.4 Irradiance

Irradiance in the form of photosynthetic photon flux density (PPFD) plays a key role in g_{sto} regulation mainly through its role in determining the rate of photosynthesis and the internal CO_2 concentration (Collatz *et al.*, 1991; Bunce, 2000). At low irradiance the stomates tend to close although there are some studies that suggest low levels of g_{sto} even during night-time (Caird *et al.*, 2007). As irradiance increases the stomata open before normally reaching a maximum g_{sto} at a light saturation point. The light saturation level is species-specific (e.g., in wheat it occurs at about 400 to 500 μmol m^{-2} s^{-1} PPFD; Gruters *et al.,* 1995). The closing response of stomates at low irradiance is more rapid than the opening response (Jones, 1992). The intensity of irradiance varies diurnally and seasonally due to the position of the sun in the sky in relation to the horizon (generally referred to as the zenith angle) and also varies with the geographic location (e.g. variation in intensity of solar radiation with latitude or altitude) and atmospheric condition (e.g. cloud cover or atmospheric aerosol).

3.2.2.5 Phenology

Stomatal conductance varies with the age of the plant and the age of the leaf, the variation in g_{sto} phenology within canopies is particularly high in short-lived species such as annuals and hence many crops. Under optimum conditions, maximum stomatal conductance (g_{max}) for a species is observed only for a specific period of time during the plant growth season (e.g., in wheat during mid anthesis). This is because towards the start and end of the growing period the leaves are either still developing or have started to senesce (Jones, 1994; Emberson *et al.*, 2000b; Pleijel *et al.*, 2007).

3.2.2.6 Carbon dioxide (CO_2)

O_3 induces stomatal closure and this decreases CO_2 uptake thereby decreasing photosynthesis. Studies have shown that higher atmospheric CO_2 concentrations protects plants from adverse effects of O_3 primarily due to reduced F_{st} via reduction of the g_{sto} (McKee *et al.,* 2000) but some studies have reported that increased CO_2 can protect against O_3 injury without substantial reductions in O_3 uptake (Heagle *et al*., 1993; Mulholland *et al*., 1997)

3.2.2.7 Salinity

Salinity is known to reduce g_{sto}, either due to perturbation in the plant water relations or through production of ABA (Katerji *et al.,* 1997: Munns and Tester, 2008). Salinity is an important stress in the western parts of India affecting about 4.5 million hectares of the area under wheat cultivation, especially in the canal irrigated areas (Singh and Chatrath, 2001; Chatrath *et al.,* 2007).

3.3 The benefit of a flux-based O_3 risk assessment.

In Chapter 2 it was made clear that there are some limitations to the use of concentration based O_3 exposure indices in estimating O_3 risk. Perhaps most importantly, these concentration based indices do not allow for the variation in meteorological conditions that might limit O_3 uptake. In addition the indices are unable to accommodate the variability in O_3 profiles that will influence the importance of peak *vs* chronic O_3 exposures experienced by plants. A flux-based approach that bases O_3 risk on the O_3 taken up by plants rather than the O_3 concentration in the ambient air would provide a means of being able to address some of these limiting factors. The estimation of O_3 uptake as a function of both O_3 concentration and meteorological conditions would allow a more realistic indication of the O_3 dose to be obtained. In addition, the use of species-specific parameterization would allow variability between species (e.g. the time during the growth period when the plant is most physiologically active) to be taken into

account in terms of identifying O_3 risk. Therefore, this study will, for the first time, apply the flux based O_3 risk assessment model in India specifically to assess risk to wheat growing across the region.

3.3.1 Methods for estimating O_3 flux

A number of models have been developed for estimating O_3 uptake by plants have been developed in Europe (Grunhage *et al.,* 1997, 2000; Emberson *et al.,* 2000; Nussbaum *et al.,* 2003; Bassin *et al.,* 2004; LRTAP Convention, 2004).

Ideally, a O_3 stomatal flux model would incorporate the important resistances to O_3 deposition and the factors that influence stomatal O_3 uptake into the leaves that have been described above. However, to develop such models requires comprehensive datasets providing information on how each of these factors will affect both stomatal and non-stomatal deposition for a cultivar of important landcover types, species and cultivars. The models currently available do not incorporate all of the factors identified above and may only have been parameterised for species of a particular global region (e.g. Europe). Many of the models are also being continually developed, for example, one such O_3 dry deposition model, the DO_3SE (Deposition of Ozone for Stomatal Exchange) has only recently been updated to include a soil moisture deficit (SMD) module to estimate the influence of soil drying on g_{sto} using the Penman-Monteith approach to estimate plant evapotranspiration (Buker *et al.,* submitted).

To apply the stomatal O_3 flux approach in SA and specifically to crops in India, a flux model would ideally need to incorporate the factors (environmental, plant physiological and phenological) that are most likely to be important in influencing O_3 fluxes to crops grown in this region. However, in the absence of models specifically designed for Indian crop cultivars, this study has chosen to use components of the existing DO_3SE O_3 deposition model developed for European conditions (Emberson *et al.,* 2000b).

The DO_3SE has been selected since it has been widely used and extensively evaluated across Europe and has been shown to perform well in estimating O_3 deposition and stomatal O_3 flux for a number of different species under different climatic regimes

(Emberson *et al.*, 2000c; cf., Simpson *et al.*, 2007; Tuovinen *et al.*, 2004; Pleijel *et al.*, 2007; Karlsson *et al.*, 2007; Simpson *et al.*, 2007; Mills *et al.*, 2010). The DO_3SE model has been embedded in the Eulerian photo-oxidant transport model of the European Monitoring and Evaluation Programme (EMEP) (Simpson *et al.*, 2002, 2003a); this model package will be referred to here as the EMEP photo-oxidant model. This EMEP photo-oxidant model is used within the UNECE LRTAP Convention (United Nations Economic Commission on Long-range Transboundary Air Pollution) for estimating total O_3 deposition. The fact that the model is capable of estimating both stomatal and non-stomatal deposition means that it can also be used to assess O_3 risk, through estimates of leaf level stomatal O_3 flux, to arable crops, forest trees and semi-natural vegetation growing in Europe (Simpson *et al.*, 2007). Use of this model within European has allowed the LRTAP effects-based approach to European air pollution to be applied to develop more effective emission control policies within the region (Goumenaki *et al.*, 2007; Simpson *et al.*, 2007; Tuovinen *et al.*, 2009; Mills *et al.*, 2010).

3.3.2 The DO_3SE model

The DO_3SE model is an O_3 dry deposition model which estimates the total and stomatal flux of O_3 to European agricultural crops, grasslands and forest trees (Emberson *et al.*, 2000b; LRTAP Convention, 2004). The model assumes three key resistances (Figure 3-2), (i) aerodynamic resistances (R_a), (ii) the quasi-laminar sub-layer resistance above the plant canopy (R_b) and (iii) the surface resistance (R_c). R_a accounts for the aerodynamic resistances to O_3 transfer between two heights, the height at which O_3 is measured (reference height; z_r) and a height near the boundary layer surface of the canopy (z_1). R_b is the canopy boundary layer resistance and accounts for the resistance to O_3 passing through the canopy boundary layer. R_c is the canopy resistance and consists of both non-stomatal and stomatal resistances and is calculated as a function of temperature, radiation, relative humidity, phenology and soil water (Tuovinen *et al.*, 2009).

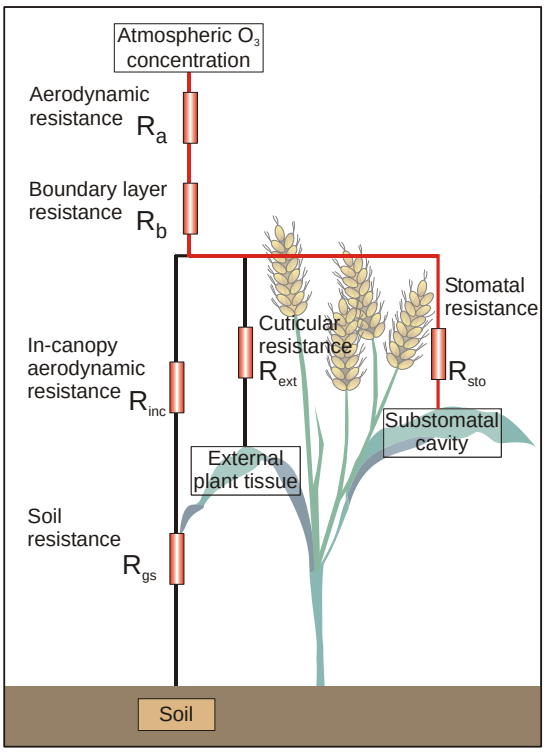

Figure 3-2: The resistances to O_3 transfer from atmosphere to crop canopy include in the DO_3SE O_3 dry deposition model (Emberson, Pers. Comm.).

3.4 Application of the DO_3SE stomatal O_3 flux (F_{st}) model for wheat in India

Wheat was selected for the study because, along with rice, it is the most important staple crop in India. A parameterization of the F_{st} model parameters also exist for wheat, although this parameterization is based on European wheat cultivars. Wheat is a widely grown and studied crop in India; therefore it likely to be able to obtain additional data to re-parameterise the DO_3SE model for Indian wheat. This will be important to allow incorporation of the variable physiology that might exist between Indian and European wheat although its useful to note that, at least in broad terms (i.e. without considering within region climatic variation), the differences in the climatic conditions for the wheat growth period between Europe and India are not so great. The optimum meteorological conditions that are prevalent during the wheat growing season in Europe and India are more or less similar; e.g. optimum temperature for wheat growing in India is 20 to 25°C (DWD, 2011) while for Europe it is 18-24°C (Porter and Gawith, 1999). Detailed description of each of the required data is given below.

For wheat, the O_3 flux to the flag leaf is considered most influential in causing damage to the plant as a whole. This is because about 60-70 % of assimilates transported to the developing wheat grain are derived from photosynthesis occurring in the flag leaf (Wang *et al.,* 1997). As such, the flag leaf and head usually contribute up to 50% of the photosynthate that makes up the grain yield (Simmons *et al.,* 1995). This is in part due to the fact that the flag leaves typically, and rather consistently, constitute a larger amount of projected leaf area (PLA) of the canopy and thus receive most of the direct photosynthetically active radiation (PAR) intercepted by a dense wheat canopy. Lower leaves contribute less to grain filling (Evans and Dunstone, 1970) and are likely to have lower conductance, and thus smaller O_3 uptake than flag leaves due to lower irradiance levels and a higher degree of senescence (Pleijel *et al.,* 2000). Therefore, in this study, as in flux based risk assessments conducted in Europe (LRTAP Convention, 2004), the F_{st} is estimated for the flag leaf only as opposed to the entire canopy.

3.4.1 Data required for the application of the DO$_3$SE F_{st} model in India.

In order to apply the F_{st} model for wheat crops grown in India a number of different datasets are required: i) O_3 concentration data; ii) meteorological data; iii) crop distribution and production data; with the exception of meteorological data these are the same datasets that were used in the analysis described in Chapter 2. Table 3-1 provides details of the meteorological data used in this study. These meteorological data were provided by the ECWMF and include temperature, downwards surface solar radiation (SSRD), VPD and wind speed. These data are also used by the MATCH photo-oxidant model (Engardt, 2008) to provide the O_3 concentration data used both in Chapter 2 and in the flux-based analysis presented here.

The ECWMF temperature, VPD and wind speed meteorological data were provided as instantaneous values recorded every 3 hours while the SSRD is the mean value for the preceding 3 hour period. The F_{st} model requires hourly data for temperature, VPD and windspeed. A simple averaging method was used to derive hourly data from the 3-hourly ECWMF data. The two missing data points, X_1 (value for the first hour) and X_2 (value for the second hour) between the two consecutive three hourly values (defined here as A and B) were calculated using Equations 3-1 and 3-2.

$$X_1 = \frac{(2\times A)+B}{3} \qquad [3\text{-}1]$$

$$X_2 = \frac{2+(2\times B)}{3} \qquad [3\text{-}2]$$

Details of how the SSRD 3-hourly averaged data were converted to hourly data, along with other data derivations necessary to provide the DO_3SE F_{st} data input, are described where appropriate in the description of the full DO_3SE F_{st} model given in the following sections.

Table 3-1: Details of the meteorological data provided by the ECWMF model and the corresponding meteorological data required by the DO_3SE F_{st} model.

ECWMF				**Data required for DO_3SE F_{st} model**			
Meteorological data	**Units**	**Temporal resolution**	**Height above ground surface**	**Meteorological data**	**Units**	**Temporal resolution**	**Height above ground surface**
Temperature	Kelvin	3 hour	2 m	Temperature	^{o}C	1 hour	2 m
Solar radiation (SSRD)	W/m^2	3 hourly average	-	Photosynthetic photon flux density (PPFD)	$\mu mol\ m^{-2}\ s^{-1}$	1 hour	-
VPD	Pa	3 hour	2 m	VPD	kPa	1 hour	2 m
Air pressure	Pa	3 hour	2 m	Air pressure	Pa	1 hour	2 m
Wind speed	m/s	3 hour	10 m	Wind speed	m/s	1 hour	1 m

SSRD = surface solar radiation downwards

The MATCH modelled O_3 concentration data and ECWMF meteorological data are provided at a spatial resolution of 0.5° latitude x 0.5° longitude as described in Figure 3-3 which shows the MATCH model grid for the area across India under wheat cultivation. The wheat distribution is defined using crop production data described previously in Chapter 2. The O_3 concentration data are provided at a height of 1 m above the ground surface, assumed equivalent to the top of the canopy of wheat. These O_3 concentrations have been derived on application of the MATCH O_3 dry deposition model which follows the resistance scheme of Wesely (1989). This is similar to the DO_3SE dry deposition scheme using the same formulations to estimate R_a and R_b, in part this is due to the MATCH model being a modified version of the EMEP photo-oxidant model. The main difference in the dry deposition scheme is in the method used to estimate g_{sto}; in MATCH, the Wesley (1989) scheme defines a maximum g_{sto} for different seasons and landuse classes and modifies these g_{sto} values as a function of radiation and temperature. In this application, the MATCH dry deposition model has been used rather than the DO_3SE model for practical reasons; it is outside the scope of this thesis to incorporate DO_3SE within the MATCH model. However, it should be recognized that the small differences in the estimates of g_{sto} will confer some inconsistency in the MATCH estimate of O_3 concentration at the 1m canopy height and the DO_3SE estimate of F_{st} to wheat. However, given that the aims of this study are to assess the spatial patterns in the magnitude of F_{st} values and compare with concentration based approaches this difference would not be expected to unduly affect the results.

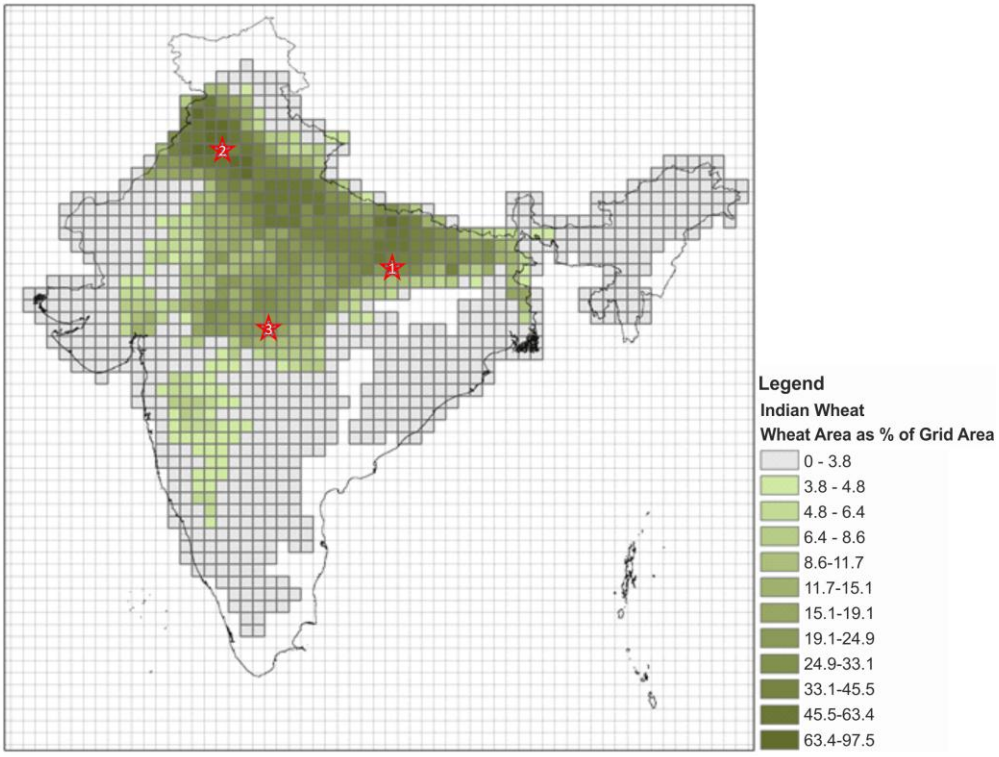

Figure 3-3: Grids with wheat cultivation. The green and grey colours indicate the percentage of wheat area per total grid area. Data source; FAOSTAT (2011).

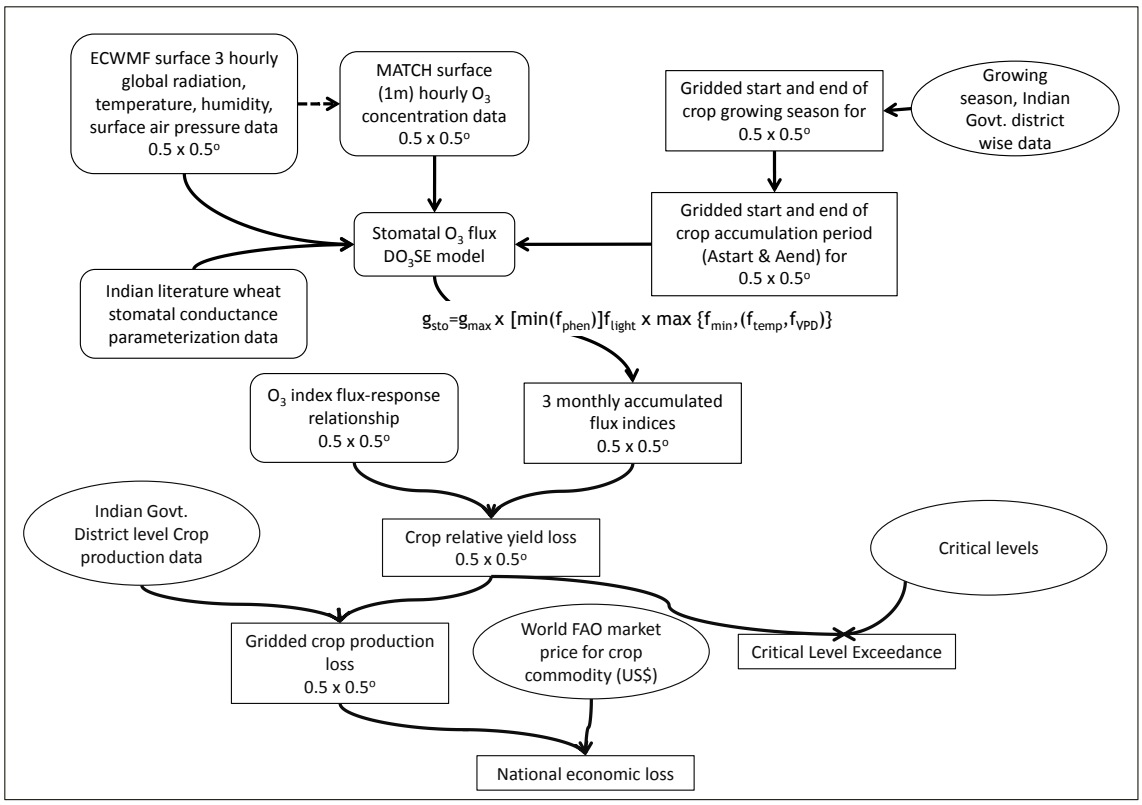

Figure **3-4** provides an overview of how these different datasets were combined to estimate F_{st} to wheat growing across India. The ECWMF data are used to estimate both the MATCH modelled O_3 concentration data and the g_{sto} that forms one of the key components of the DO_3SE stomatal O_3 flux (F_{st}) model. The growing season data for wheat (described in Chapter 2) are used to estimate the wheat growth period over which F_{st} is calculated and accumulated to provide a single end of growth period values of accumulated F_{st} above a threshold (y), referred to here as the 'phyto-toxic O_3 dose' (POD_y). The resulting POD_y values is then used in conjunction with a flux-response relationships to estimate wheat yield losses and subsequent production and economic losses using crop production data and price data described previously in Chapter 2.

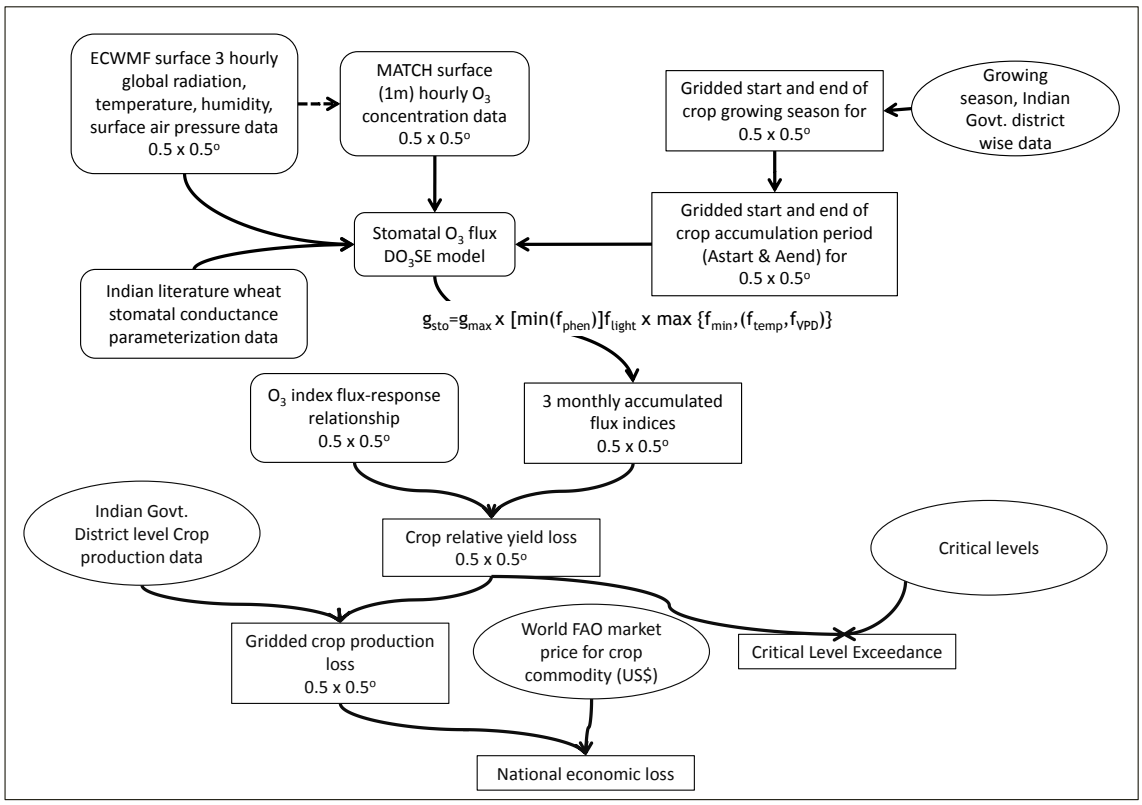

Figure 3-4: Broad outline of the steps that are involved in applying the flux based O_3 risk assessment for wheat in India.

The exact methodology for application of this flux based approach for wheat grown across India is described in more detail in the following sections.

The stomatal O_3 flux to wheat crops grown in India is calculated for the entire wheat growing region in India. The wheat growing region is indicated by the green and grey shaded grids in Figure 3-3. Although wheat is cultivated across India, 95 % of the total area under wheat cultivation and 97 % of the total wheat produced in India is produced in the green shaded region shown in Figure 3-3 which lies along the IGP.

3.4.2 Description of the DO_3SE F_{st} model

The calculation of F_{st} for wheat flag leaf is based on the formulations for the DO_3SE model given in the LRTAP Convention (2004) provided here in Equation [3-3]. The calculation assumes there are two resistances to O_3 flux into the leaf; the leaf boundary layer resistance (r_b), and leaf surface resistance (r_c). The F_{st} is calculated assuming a zero or negligible and O_3 concentration inside the leaf (Laisk *et al.*, 1989). F_{st} is in nmol m^{-2} PLA s^{-1} and calculated as;

$$F_{st} = c(z_1) * g_{sto} * \frac{r_c}{r_b + r_c} \qquad [3\text{-}3]$$

Where, c (z_1) is the O_3 concentration at canopy height (height= z_1; unit = m) in nmol m^{-3}; g_{sto} is the hourly stomatal O_3 conductance; r_c is leaf surface resistance given in Equation [3-4]; r_b is the quasi laminar resistance given in Equation [3-5].

R_c /(r_b + r_c) represents the transfer of O_3 across the leaf boundary layer.

$$r_c = \frac{1}{g_{sto} + g_{ext}} \qquad [3\text{-}4]$$

Where, g_{ext} = 1/2500 (m s^{-1})

$$r_b = 1.3 \times 150 \times \sqrt{\frac{L}{u(z_1)}} \ (s\ m^{-1}) \qquad [3\text{-}5]$$

Where, L is the cross wind leaf dimension; u (z_1) = wind speed at height z_1; and the factor 1.3 accounts for the differences in diffusivity between heat and O_3.

The wind speed data from the EMCWF model is provided at a height of 10 m. This wind speed has been converted to wind speed at the canopy (1 m) height; this is done using Equation [3-6] which assumes stable atmospheric conditions.

$$u(z1) = \frac{u*}{k}\left[ln\left(\frac{h-d}{zo}\right)\right] \quad [3\text{-}6]$$

Where $u*$ is the friction velocity, k is von Karmen's constant (k= 0.41), h is the canopy height (h=1 m), d and zo are the displacement and canopy roughness heights respectively where d= 0.7 x h and zo=0.1 x h. $u*$ describes the coupling of the vegetation to the atmosphere and is estimated as described in Equation [3-7]:

$$u* = \frac{k.u_{(zRef)}}{ln\left(\frac{h-d}{zo}\right)} \quad [3\text{-}7]$$

Where $u_{(zRef)}$ is the wind speed at the reference height in the atmosphere, in this case 10 m, the height at which wind speed is provided by the EMCWF model.

3.4.3 The DO_3SE multiplicative g_{sto} algorithm

The g_{sto} model is the core of the DO_3SE F_{st} model and is represented by a multiplicative algorithm based on principles introduced by Jarvis (1976). The DO_3SE model was first described in Emberson *et al.* (2000b) and has since been continually refined (Emberson *et al.*, 2001, 2007, LRTAP Convention, 2004; Büker *et al.*, submitted); the multiplicative algorithm is defined as follows in Equation [3-8].

$$g_{sto} = g_{max} \times f_{phen} \times f_{light} \times \max\left[f_{min}, \left(f_{temp} \times f_{VPD}\right)\right] \quad [3\text{-}8]$$

where, g_{sto} is the actual stomatal conductance to O_3, g_{max} is the maximum stomatal conductance of the plant, f_{min} is the minimum stomatal conductance (g_{min}) as a fraction of g_{max} while f_{phen}, f_{light}, f_{temp} and f_{VPD} allow for the influence of phenology, irradiance, temperature and vapour pressure deficit (VPD) on g_{sto}. G_{sto} and $g_{\max}$ are expressed in

mmol O_3 m^{-2} PLA s^{-1} while the remaining parameters are expressed in relative terms, varying between 0 and 1 relative to g_{max}. Thus this model allows the F_{st} to be calculated allowing for the influence of plant phenological and physiological characteristics and the prevailing meteorological conditions that modify the g_{sto} of plants (Tuovinen *et al.*, 2009). G_{max} and f_{min} are species-specific fixed values and the other f factors can be viewed as largely controlling either seasonal (f_{phen}) or diurnal (f_{light}, f_{temp}, f_{VPD}) modification of g_{max}. The seasonal parameter is calculated on a daily basis to capture the daily variation over the crop growing season while the diurnal parameters are calculated on an hourly basis in order to capture the diurnal variation in each of the parameters and its influence on g_{sto}. Each of these model formulations are described in more detail below.

3.4.3.1 g_{max} and f_{min}

g_{max}

As mentioned earlier, $g_{\max}$ is the species-specific maximum stomatal conductance under optimal conditions and forms a ceiling value that is modified by the other f factors listed in Equation [3-8] (Emberson *et al.*, 2000b; Mills *et al.*, 2011). It is a constant value and the units are expressed in mmol O_3 m^{-2} PLA s^{-1}. G_{max} is known to occur only for a specific period of time during the crop growing period and for wheat, this period is typically around the time of anthesis, close to mid-anthesis (Pleijel *et al*., 2007).

F_{min}

The g_{min} represents the baseline g_{sto} that may occur during the course of the growing season under field conditions. F_{min} is g_{min} as a fraction of g_{max}. Using this function in the model allows for the occurrence of stomatal O_3 uptake, although limited, even in the presence of severe environmental stress (Emberson *et al.*, 2000b).

3.4.3.2 Seasonal parameters

f_{phen}

g_{max} occurs only for a specific period during the plant growing season, especially in crops. Towards the start and end of the growing season, the g_{sto} will be lower than g_{max} even under optimal environmental conditions as during this period the leaves are either developing or have started to senesce (Emberson *et al.*, 2000b). For wheat, F_{st} is calculated only for a specific period of time (referred to as the accumulation period) when g_{sto} and subsequent photosynthesis is crucial for crop productivity. The start and end of this accumulation period are termed as A_{start} and A_{end}.

The phenology function (f_{phen}) allows for the influence of leaf phenology on g_{sto} based on the fact that the flag leaf requires some time to reach g_{max} after emergence and that prior to senescence g_{sto} will decline (Jones, 1994; Emberson *et al.*, 2000b; Pleijel *et al.*, 2007). The f_{phen} function is expressed in relative terms between 0 to 1, where the value given to g_{max} is 1.

F_{phen} can be based on either a fixed number of days or an effective temperature sum accumulation and has a similar shape for both approaches. The correlation between thermal time and wheat growth is well defined (McMaster and Wilhelm, 1997) and the use of effective temperature sum is generally accepted to describe plant development more accurately than using a fixed time growth period since it allows for the influence of temperature on growth (Cambell and Norman, 1998; Pleijel *et al.*, 2007).

Flag leaf f_{phen} based on thermal time as given in LRTAP Convention (2004) is calculated using Equations [3-9] and [3-10]:

When $A_{start} \leq T_{\text{sum}} < (A_{start} + f_{phen\_e})$

$$f_{phen} = 1 - \left(\frac{1-f_{phen\_a}}{f_{phen\_e}}\right)\left(\left(A_{start} + f_{phen\_e}\right) - T_{sum}\right) \qquad [3\text{-}9]$$

When $(A_{start} + f_{phen\_e}) \leq T_{sum} \leq (A_{end} - f_{phen\_f})$

$$f_{phen} = 1$$

When ($A_{end} - f_{phen\_f}$) < $T_{sum} \leq A_{end}$

$$f_{phen} = 1 - \left(\frac{1-f_{phen\_b}}{f_{phen\_f}}\right)\left(T_{sum} - \left(A_{end} - f_{phen\_f}\right)\right) \qquad [3\text{-}10]$$

Where T_{sum} is the cumulative growing degree days (GDD) in °C days accumulated from day of sowing, f_{phen_a} and f_{phen_b} represent the maximum fraction of g_{max} that g_{sto} takes at A_{start} and A_{end}, $f_{\text{phen\_e}}$ and $f_{\text{phen\_f}}$ are thermal time in GDD (°C) between A_{start} and mid-anthesis, and mid-anthesis and A_{end} respectively.

The different components of f_{phen} in terms of fixed day as well as GDD are illustrated in Figure 3-5 f_{phen} is calculated on a daily basis.

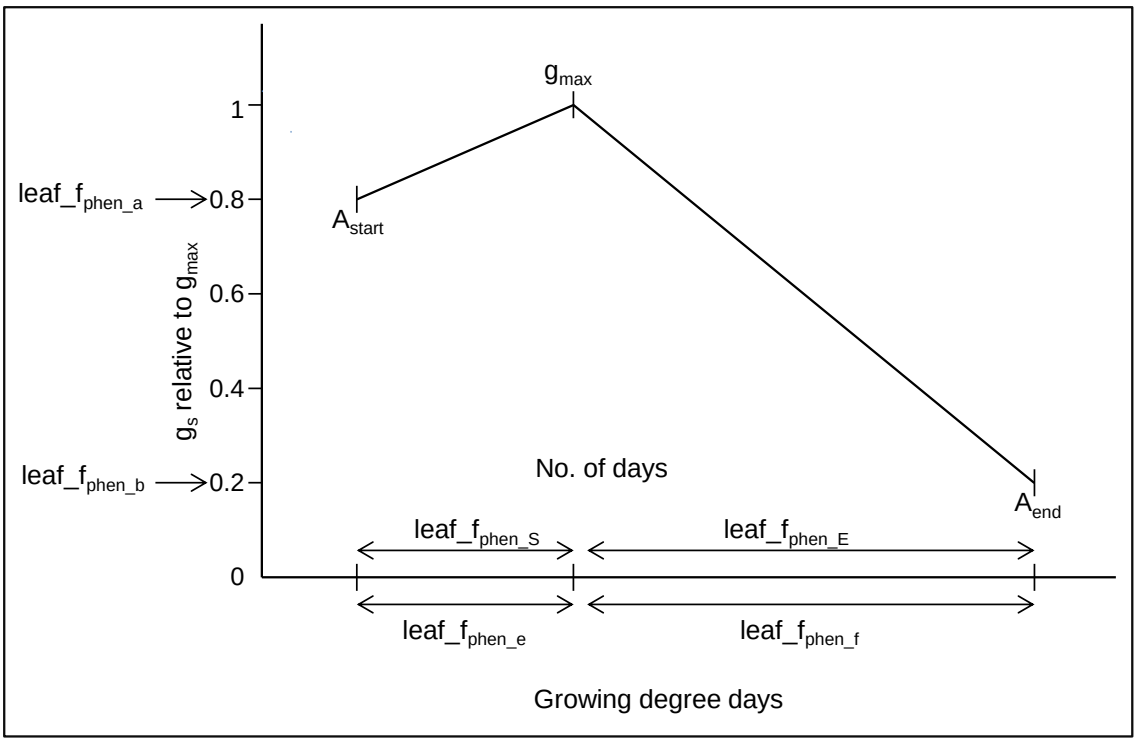

Figure 3-5: The f_{phen} profile in relation to the different f_{phen} components; growing degree days is GDD in °C; g_{sto} relative to g_{max} is f_{phen}.

3.4.3.3 Diurnal parameters

f_{light}

To account for the influence of the irradiance on the g_{sto} of wheat, the f_{light} function is used. The f_{light} function is described using an exponential function given in Equation [3-11];

$$f_{light} = 1 - \exp(-\text{light}_a . \text{PPFD}) \qquad [3\text{-}11]$$

Where, light_a = is the species-specific irradiance constant and PPFD is in units of μmol m^{-2} s^{-1}.

The ECWMF model provided irradiance data as total solar radiation directed downward at the surface of the earth (SSRD). This includes both the visible and infrared fraction of the radiation. However, as mentioned in Equation [3-11], the f_{light} function is calculated based on photosynthetic photon flux density (PPFD). PPFD is in the visible range of total radiation, and has to be calculated from the SSRD. The SSRD data was also provided as a 3-hourly average of the preceding 3 hours; therefore the simple averaging method used to extrapolate hourly values from three hourly data for the other meteorological data was not appropriate (see Equations 3-15 and 3-16). Therefore, a different method was employed to extrapolate hourly PPFD values from 3-hourly average SSRD data.

This method first involved converting SSRD values into photosynthetic active radiation (PAR). A ratio of total visible PAR (PAR_{total}) to total solar radiation (SSRD) of 0.50 was used in the present study based on Weiss and Norman (1985) as given in Equation [3-12]

$$\text{PAR}_{\text{total\_3hour}} = 0.5 \times \text{SSRD} \qquad [3\text{-}12]$$

To provide an indication of how irradiance would be expected to vary on an hourly basis over the course of a day the potential PAR total ($pPAR_{total}$) is calculated. This estimate of hourly $pPAR_{total}$ can then be used in conjunction with the 3-hourly averaged SSRD to provide an indication of cloudiness of the sky, here referred to as the sky

transmissivity (*ST*), over each 3-hour period. This *ST* value can then be used to estimate an hourly actual PAR value (PAR_{total}). $pPAR_{total}$ is estimated as described in Equation [3.13].

$$pPAR_{total} = pPAR_{dir} + pPAR_{diff} \quad [3\text{-}13]$$

Where $pPAR_{dir}$ and $pPAR_{diff}$ are the potential direct and diffuse values of PAR respectively in W/m^2; these are estimated based on Weiss and Norman (1985) as described in Equations [3-14] and [3-15].

$$pPAR_{dir} = 600 \times exp\left\{-0.185 \times \left(\frac{P_{surf}}{sea_p}\right) \times m\right\} \times sin\beta \quad [3\text{-}14]$$

$$pPAR_{diff} = 0.4 \times (600 - pPAR_{dir}) \times sin\beta \quad [3\text{-}15]$$

where P_{surf} is air pressure and sea_p is the atmospheric pressure at sea level, both in Pa; *m* is the optical air mass (the ratio of the mass of atmosphere traversed per unit cross-sectional area of the actual solar beam to that traversed for a site at sea level if the sun were overhead) and is estimated as $\frac{1}{sin\beta}$ and $sin\beta$ is the solar elevation.

Sinβ is the sun's angle of elevation and is calculated based on the formulations given in Campbell and Norman (1998) as follows in Equation [3-16].

$$sin\beta = \{[sin(deg2rad \times \emptyset)] \times sin\delta\} + \{[cos \times (deg2rad \times \emptyset)] \times cos\delta \times cos(hr_{angle})\} \quad [3\text{-}16]$$

where, *deg2rad* is the conversion factor for degrees to radians (*deg2rad* = 0.017453292519943295), $\emptyset$ is the latitude and δ is the solar declination estimated as described in Equation [3-17]

$$\delta = deg2rad \times \left\{-23.4 \times \cos\left[deg2rad \times \left(360 \times \left(\frac{dd+10}{365}\right)\right)\right]\right\} \quad [3\text{-}17]$$

Where *dd* is the year day. The hr_{angle} is calculated by Equation [3-18]

$$hr_{angle} = deg2rad \times [15 \times (\mathrm{hr} - t_0)] \quad [3\text{-}18]$$

Where t_o is calculated in Equation [3-19] by

$$t_0 = 12 - LC - e \quad [3\text{-}19]$$

Where *LC* is the longitude correction [Equation 3-20] and *e* is the solar noon correction calculated as described in Equation [3-22]

$$LC = \frac{(lon - lon_m)}{15} \quad [3\text{-}20]$$

where *lon* is longitude and $\mathrm{lon_m}$ is calculated by Equation [3-21] as

$$\mathrm{lon_m} = \mathrm{nint}\left(\frac{\mathrm{lon}}{15}\right) \times 15 \quad [3\text{-}21]$$

$$e = \left(\frac{(-104.7 \times \sin f) + (596.2 \times \sin 2f) + (4.3 \times \sin 3f) - (12.7 \times \sin 4f)}{-(429.3 \times \cos f) - (2.0 \times \cos 2f) + (19.3 \times \cos 3f)} \over 3600 \right)$$

[3-22]

Where, $f = deg2rad \times \left(279.575 + (0.9856 \times dd)\right)$ [3-23]

The *ST* is specifically the fraction of the total extra-terrestrial solar radiation that reaches the earth's surface. It is a function of the optical air mass of the atmosphere. The hourly *ST* is calculated from the $pPAR_{total}$ and three hourly SSRD values using Equation [3-24].

$$ST = \min\left\{0.9, \max\left(0.21, \frac{0.5 \times \mathrm{SSRD}}{\mathrm{pPAR_{total}}}\right)\right\} \quad [3\text{-}24]$$

The use of this ST value in combination with the hourly $pPAR_{total}$ then provides an indication of the hourly PAR_{total}, calculated as described in Equation [3-25].

$$PAR_{total} = pPAR_{total} \times ST \quad [3\text{-}25]$$

The PAR_{total} value is then converted into PPFD using a conversion factor of 4.57 as given in Jones (1992).

F_{temp}

The air temperature at the 2 m height provided by the ECWMF model is assumed to represent the air temperature at the plant canopy and is used to estimate f_{temp}. The validity of this will depend to some extent on how the f_{temp} function has been parameterised and therefore is discussed further in Chapter 4.

The f_{temp} is included in the model to account for the limiting role that the air temperature plays on wheat g_{sto}. The function represents a normal curve and is described in Equation [3-26] and [3-27];

when $T_{\min}<T<T_{\max}$

$$f_{\text{temp}} = \max\left\{f_{\min}, \left[\frac{(T-T_{\min})}{(T_{\text{opt}}-T_{\min})}\right] \times \left[\frac{(T_{\max}-T)}{(T_{\max}-T_{\text{opt}})}\right]^{\text{bt}}\right\} \qquad [3\text{-}26]$$

when $T_{min} >T>T_{\max}$

$f_{temp} = f_{min}$

Where T is the air temperature in °C, T_{min} and $T_{\max}$ are the minimum and maximum temperatures below and above which minimum g_{sto} occurs and beyond which g_{sto} is equal to $g_{\min}$. The optimum temperature (T_{opt}) is the temperature at which g_{max} is likely to occur in the absence of other limiting factors. *Bt* is defined as described in Equation [3-27];

$$bt = \frac{(T_{max}-T_{opt})}{(T_{opt}-T_{min})} \qquad [3\text{-}27]$$

f_{VPD}

The f_{VPD} function is used to account for the effect of VPD on g_{sto} described. F_{VPD} is calculated based on the formulations given in Equation [3-28];

$$f_{VPD} = \min\left\{1, \max\left[f_{\min}, \left((1 - f_{\min}) \times \left(\frac{(\mathrm{VPD}_{\min} - \mathrm{VPD})}{(\mathrm{VPD}_{\min} - \mathrm{VPD}_{\max})}\right)\right) + f_{\min}\right]\right\} \qquad [3\text{-}28]$$

where, VPD_{min} and VPD_{max} are the minimum and maximum VPD.

The f_{VPD} function is calculated on an hourly basis during the course of the day to capture the effect of VPD on stomatal conductance. To account for the effect of high transpiration on leaf water potential which may result in a stronger limitation of g_{sto} than that included in Equation [3-4], an additional VPD sum function (∑VPD) is included. This assumes that if the ∑VPD during the course of day increases above a certain critical value, then the stomatal re-opening in the afternoon will not occur. ∑VPD is calculated based on the formulations given by Pleijel *et al.* (2007) described in Equation [3-29]

If $\sum \mathrm{VPD} \geq \sum \mathrm{VPD}_{\mathrm{crit}}$, then,

$$g_{sto\_hour\_n+1} \leq g_{sto\_hour\_n} \qquad [3\text{-}29]$$

Where, $g_{sto\_hour\_n}$ and $g_{sto\_hour\_n+1}$ are the g_{sto} values for hour *n* and hour *n+1* respectively calculated using Equation [3-8].

The ∑VPD is calculated hourly during the course of the day and the ∑VPD at a given hour (n) is used to calculated g_{sto} for the following hour.

3.4.4 Estimating yield, production and economic loss from DO_3SE F_{st}

Using the methods described above the DO_3SE F_{st} model can be used to calculate hourly F_{st} values above a threshold value (Y) which can be accumulated over the O_3

accumulation period (A_{start} to A_{end}) to estimate an accumulated 'phyto-toxic O_3 dose' (POD_Y) value. The accumulation period is the period when the crop is actively growing and considered most sensitive to F_{st} in terms of its effect on yield (Pleijel *et al.*, 2007), this period is between the time when the wheat flag leaf is fully unrolled and when the crop attains physiological maturity (LRTAP Convention, 2004). The Y threshold value represents the plants detoxification capacity. The Y threshold value was defined as that which gave the best statistical fit between POD_Y and yield loss (Danielsson *et al.*, 2003; Pleijel *et al.*, 2007). For wheat, the strongest POD_Y-yield loss relationships were obtained when using Y= 6 nmol O_3 m^{-2} PLA s^{-1} (r^2=0.83). Thus, the threshold Y is likely to represent a detoxification threshold below which it can be assumed that any O_3 absorbed by the plant will be detoxified (Pleijel *et al.*, 2007; Mills *et al.*, 2011). Therefore, F_{st} values above 6 nmol O_3 m^{-2} PLA s^{-1} are accumulated over the accumulation period to calculate POD_6. These POD_6values can then be used in conjunction with O_3 flux response relationships to estimate relative yield losses.

Figure 3-6 shows the relationship between POD_6 and relative yield of wheat (LRTAP Convention, 2004). A relative yield of 1 represents the absence of O_3 effects. This relationship was established using the data from Danielsson *et al.* (2003) on field grown wheat exposed to different concentrations of O_3 in open-top chambers from four different countries (Belgium, Finland, Italy and Sweden) for five cultivars of European wheat.

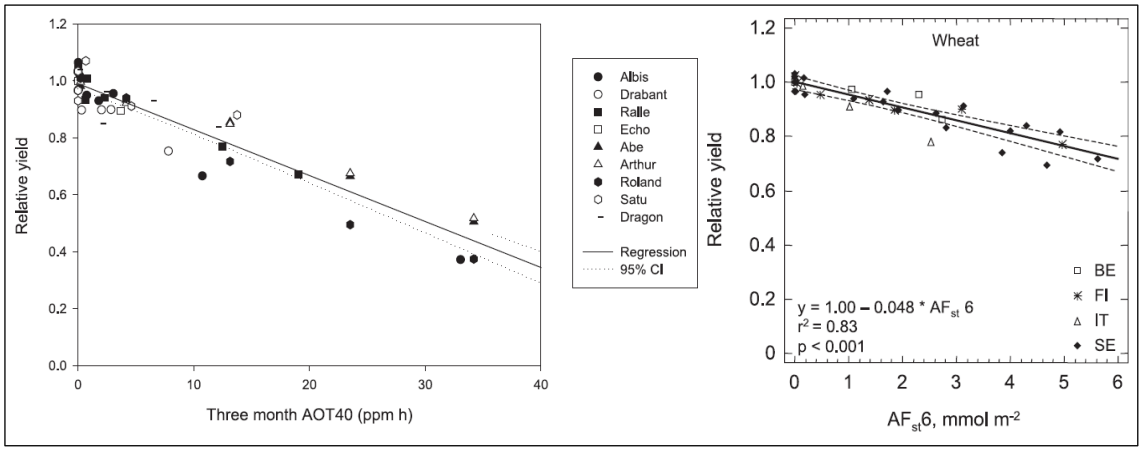

Figure 3-6: O_3 Exposure response relationship using AOT40 and flux response relationship using POD_6 for European wheat (LRTAP Convention, 2004). R^2 for AOT40 = 0.89, data based on Fuhrer *et al.*, 1997 and Gelang *et al.*, 2000).

The flux-response relationship of wheat is given in Equation [3-30]. According to this, RYL is given as;

$$RY = 1.00 - (0.048 \times POD_6) \quad [3\text{-}30]$$

RYL values were calculated for each MATCH grid where, RY is the relative yield of wheat and RYL is 1-RY.

Flux based CPLs were calculated for each MATCH grid using the RYLs and the crop production data for the cropping season 1999-2000 that is described in Chapter 2. The CPL was then translated into Els using the same methods described in Chapter 2.

3.4.5 Estimating relative exceedance of critical levels (R_{CL})

Critical levels are statistically derived values above which direct adverse effects on vegetation will not occur according to current knowledge (Simpson *et al.,* 2007). Under the UNECE LRTAP Convention (1996), a 5% yield loss was used as the loss criterion for estimation of the flux based critical level for wheat (LRTAP Convention, 2004). A flux-based critical level of POD_6 of 1 mmol m^{-2} PLA for wheat crops was established (LRTAP Convention, 2004). Critical levels can be used for mapping and quantifying O_3 impacts at both national and regional scales.

Critical levels have also been defined for the AOT40 concentration based O_3 index. Therefore, it is possible to compare the AOT40 and the POD_6 O_3 indices by estimating a relative exceedance of the critical level (R_{CL}). The R_{CL} is calculated based on the formulations given by Simpson *et al.,* (2007) and described in Equation [3-31];

$$R_{CL}(M) = \frac{M}{CL_M} \quad [3\text{-}31]$$

Where, M = O_3 metric (AOT40 and POD_6)

CL_M = Critical level for M metric

3.5 Methods to parameterize the DO_3SE F_{st} model.

The previous sections have described the formulations of the DO_3SE F_{st} model. However, to be able to apply the model the parameterization of these different formulations needs to be defined. The DO_3SE F_{st} model has been parameterised for European wheat; this parameterization is described in detail in LRTAP Convention (2004). This parameterization has been achieved using a combination of primary and secondary data. Here, primary data represents data provided directly from experimental or observational campaigns whilst secondary data represents data that is available only from the published literature.

Primary data, when provided as g_{sto} measurements and associated meteorological conditions, can be analysis using boundary line analysis techniques to estimate the limiting influence of various factors on g_{sto}. The boundary line technique, originally introduced by Webb (1972), is commonly used to describe relationships for biological data where one independent variable is considered to have some limiting effect on the other (dependent) variable (Milne *et al.,* 2006a,b). This assumes that these independent factors influence the dependent variable independently and multiplicatively (Pleijel *et al.,* 2007). A boundary line is fitted between the relative maximum g_{sto} and each of the factors thought to influence g_{sto} (temperature, VPD, light, SWP, etc.) to approximate the response of relative g_{sto} to the factor assuming no limitation from the other factors and excluding obvious outliers. This boundary line represents the different f functions for the corresponding variables described in Equation (3.4). This boundary line method has also been used to develop multiplicative style g_{sto} models to assess the influence of environmental variables on g_{sto} (Jarvis, 1976; Chambers *et al.,* 1985; Pleijel *et al.,* 2007). Such an approach requires a substantial amount of experimental data describing how each factor influences g_{sto}.

Secondary data can be used to provide additional support to the derivation of the f functions from primary data. Where primary data are not available, secondary data from a number of different studies may provide data that can be pooled and from which a boundary line can be inferred. For both primary and secondary data these boundary lines tend to be fitted by eye since the tendency for uneven distribution of data points across the full range of environmental conditions (the number of data points tend to be

reduced at the more extreme environmental conditions) preclude the use of more sophisticated line fitting techniques such as probability distributions.

The details of the parameterizations of the F_{st} model for European wheat cultivars are given in Table 3-2. The wheat g_{max} parameterizations described in the LRTAP Convention (2004) was established from wheat g_{sto} experiments conducted in Denmark, Spain, Germany, Austria and Sweden. The experiments were carried out in the field as well as open top chambers (OTC) on 6 spring wheat, 1 durum wheat and 1 US winter wheat cultivars. The data used for establishing the parameterizations for the f functions were a mixture of both secondary data from Austria, Denmark, Germany, Spain, USA and China (LRTAP Convention, 2004) and primary data from experiments conducted for wheat in Sweden (Danielson *et al.*, 2003).

The f_{light} is derived from experimental data from 4 references and the data seem to be fairly robust. The f_{temp} function is parameterized using both primary and secondary data from 3 references, giving g_{sto} data on both spring and winter wheat and gives a good representation of the T_{opt} but there are still data missing for g_{sto} at temperatures close to T_{min} and T_{max}. The same situation exists for f_{VPD}, where the parameterizations are derived using both primary and secondary data from 4 references but g_{sto} data corresponding to high (> 2.5 kPa) and low VPD (<1 kPa) are missing.

Table 3-2: Summary of the parameterization of the different DO_3SE F_{st} model parametersations of the g_{sto} algorithm for wheat flag leaves grown in Europe (LRTAP Convention, 2004).

Parameter	Units	Parameterization	No. of References	Types of data	No. of cultivars	No. of countries	Growing conditions
g_{max}	mmol O_3 m^{-2} PLA^{-1}	450	7	P = 1; S = 6	7	5	AA; OTC
f_{min}	fraction	0.01	1	P	1	1	AA; OTC
f_{phen_a}	fraction	0.8	-	-	-	-	-
f_{phen_b}	fraction	0.2	-	-	-	-	-
f_{phen_c}	Days	15	-	-	-	-	-
f_{phen_d}	Days	40	-	-	-	-	-
f_{phen_e}	°C days	270	-	-	-	-	-
f_{phen_f}	°C days	700	-	-	-	-	-
$light_a$	(constant)	0.0105	5	P = 1; S = 4	5	4	AA; OTC; GH
T_{min}	°C	12	3	P=1; S=2	3	3	AA; OTC; GH;
T_{opt}	°C	26	-	-	-	-	-

Table 3-2: Continued.

T_{max}	°C	40	-	-	-	-	-
VPD_{max}	kPa	1.2	4	P=1; S=3	3	3	AA; OTC; GC
VPD_{min}	kPa	3.2	-	-	-	-	-
$\sum VPD_{crit}$	kPa	8	-	-	-	-	-
SWP_{max}	MPa	-0.3	6	P=1; S=5	6	6	AA; OTC; CC
SWP_{min}	MPa	-1.1	-	-	-	-	-

S= secondary data from literature; P = primary data; AA= ambient air; OTC= open top chamber; GH = green house; GC= growth Chamber; cc=Closed chamber.

As described previously, the flux based approach has greater potential than the concentrations based approach to O_3 risk assessment to be applied to different wheat cultivars under different geographical and or climate conditions. However, care has to be taken in such applications to ensure that the appropriate components of the model are modified for particular regional conditions. The parameterization of the g_{sto} module is potentially the most important aspect in the F_{st} model as it reflects some of the most important differences in cultivars response to meteorological and crop growing conditions that will influence O_3 uptake. Therefore, a large effort has been made to derive a g_{sto} parameterisation specifically for Indian conditions. The derivation of this Indian parameterization is described in Chapter 4 while the results of the F_{st} modelling are described in the Chapter 5.

Chapter 4 Parameterization and application of the O_3 flux model for wheat in India

4.1 Introduction

The DO_3SE F_{st} model requires information on certain plant phenological and physiological characteristics to parameterize the g_{sto} component of the model. Parameterization of this component of the model for wheat growing in Indian will ensure that the F_{st} model can produce results more likely to reflect different cultivars of this Indian crop growing under Indian meteorological and agro-climatic conditions.

The re-parameterization of the g_{sto} model, and the application of the F_{st} model using Indian meteorology will together improve the transferability of the flux-based risk assessment method to the SA region as compared with the concentration based risk assessment approaches (see also Chapter 2 and 3).

An important consideration when parameterising the wheat g_{sto} model is to define whether the wheat commonly grown across the region being investigated is the 'winter' or 'spring' wheat cultivar.

In Western Europe 'spring' wheat occupies < 10 % of wheat area, the rest is winter wheat (Curtis, 2002); by contrast, in India, mostly 'spring' wheat is grown (Curtis, 2002; Sayre, 2002). 'Winter' wheat in Europe and North America (NA) is sown in autumn and harvested in late spring or early summer, while 'spring' wheat is sown in early spring and harvested in late summer. In India 'spring' wheat is sown in autumn and harvested in spring. This is because the warm growing conditions during the autumn, winter and spring in India are similar to spring and summer conditions in Europe and NA, which are most suited for 'spring' wheat. In view of this the Indian wheat parameterization will be based on 'spring' wheat types. The winter season is chosen as more than 95 % of the wheat crop in India is grown during the winter season, summer wheat crops only account for 5% of the total crops (DWD, Government of India). In India, more than 85% of the area under wheat cultivation is irrigated (CWC, 2006). Hence, the parameterizations were also developed for irrigated Indian wheat crops with the assumption that all wheat crops in India are irrigated.

At present, the DO_3SE model has been parameterized for crops that include wheat, potato and tomato cultivars grown in Europe (LRTAP Convention, 2010). However, parameterisations for crop cultivars that are grown in India are yet to be established. As such, the model has to be re-parameterized for Indian crop cultivars to take into account the differences in crop phenological and physiological characteristics between the cultivars and the differences in the cropping pattern between the two geographic regions. The parameters that are included in the multiplicative algorithm in Equation [3-8] require knowledge of how these dose-modifying factors influence the g_{sto} of wheat cultivars grown in India and how changes in these factors would change the g_{sto} and subsequently the F_{st}. This requires a comprehensive study of the g_{sto} of wheat cultivars grown in India under varied meteorological and crop growing conditions common in the wheat growing regions in India. It is also important to define the accumulation period during which the F_{st} to wheat should be calculated.

In this Chapter, efforts to establish parameterizations of the DO_3SE model functions for wheat cultivars grown in India are described. A comprehensive literature review was performed to identify and collate data on g_{sto} and phenology of wheat cultivars that are grown in India searching the literature using literature search engines both in the UK and in India, the latter was achieved through visits to a number of University libraries in India to gain access to journals only available from SA. These data were then collated to parameterize the various components of the DO_3SE model. A detailed description of the data used, methods to define the accumulation period, methods to obtain the g_{sto} relationships and the parameterization of each component of the F_{st} algorithm are described in the following sections.

From Chapters 1, 2 and 3 it is clearly evident that most wheat growing regions lie in the IGP, although there are wheat crops grown in other parts of India. Based on the prevailing growing conditions such as climate, soil etc., the DWD, Government of India has divided the wheat growing regions into five agroclimatic zones (AGZ; Table 4-1; Figure 4-1). In each of these zones wheat cultivars are cultivated that have been adapted for growing under the zone-specific climatic conditions (Table 4-1; list of cultivars from Mishra *et al.,* 2007). New wheat cultivars are continuously being released that are adapted for growing under the climatic conditions that are prevalent in each of these AGZs. These cultivars are also able to cope with certain levels of biotic (e.g., rust disease) and abiotic (e.g., drought, heat, etc.) stresses that are prevalent in the region. Of

these five AGZs, three AGZs, namely NWPZ, NEPZ and CZ, are the main wheat growing zones having 93 % of India's total wheat area and contributing 96 % of India's total wheat production (Table 4-1).

Table 4-1: Wheat agro-climatic zones (AGZs) in India as outlined by the Directorate of Wheat Development (DWD, Government of India), along with wheat area cultivated, production and yield during the cropping season 1999-2000.

Sl. No.	**Zone name**	**Wheat production (Million tonnes)**	**Area under wheat (Million hectares)**	**Yield (tonnes/ hectare)**
1	North-Western Plains Zone (NWPZ)	33.6	12.0	2.8
2	North-Eastern Plains Zone (NEPZ)	31.7	8.9	3.6
3	Central Zone (CZ)	8.6	4.7	1.8
4	Peninsular Zone (PZ)	1.6	1.3	1.2
5	Northern Hill Zone (NHZ)	1.1	0.7	1.7
6	Southern Hills Zone (SZ)	0.0	0.0	-

Figure 4-1: Wheat growing agro-climatic zones (AGZs) in India as defined by the Directorate of Wheat Development (DWD, Government of India). The map is from Expert System on Wheat Crop Management, Indian agricultural Statistics and Research institute, http://www.iasri.res.in/expert1/General/zonewise.asp.

4.2 Stomatal ozone flux (F_{st}) accumulation period for wheat crops grown in India

Experimental data from Europe has found that the O_3 effect on wheat yield loss is greater during the reproductive stage than during the vegetative stage with a maximum sensitivity to O_3 exposure occurring after ear emergence, during the anthesis stage (Soja, 1996; Younglove *et al., 1994*). The mid-anthesis period (defined as growth stage 65 according to Zadoks *et al.,* 1974) is the time when maximum g_{sto} (g_{max}) can occur; the increased sensitivity to O_3 during this period being centred on anthesis has also been reported in other studies (Lee *et al.,* 1988; Pleijel *et al.,* 1998; Soja *et al.,* 2000; Harmens *et al.,* 2007).

To capture this period of heightened O_3 sensitivity, here referred to as the accumulation period (see also Chapter 3), the start (A_{start}) and end (A_{end}) of the period within the growing season needs to be defined. Anthesis occurs when the flag leaf is fully developed, and since the model estimates F_{st} to the flag leaf, the accumulation period is placed around the flag leaf stage of the wheat crop, i.e. the period between ear emergence (when the flag leaf is fully developed) and the maturity stage (about 2 weeks before the harvest). During the last 10-15 days prior to harvesting, the flag leaf turns yellow and as such the green leaf area index decreases to almost zero (Peltonen-Sainio *et al.,* 1997; Acevedo *et al.,* 2002). Therefore, the omission of the O_3 exposure 2-3 weeks prior to harvesting should not introduce large errors in the O_3 risk assessment. The same period is used in the model parameterizations for F_{st} in the flag leaf of European wheat cultivars (Pleijel *et al.,* 2000; LRTAP Convention, 2004). The following sections describe the phenological data collection and methods to define the Indian wheat phenological stages to define this F_{st} accumulation period.

4.2.1 Phenological data collection

In order to understand the various phenological stages of Indian wheat cultivars, data on phenology were collected from various published data sources listed in Table 4-2. These phenological data were collected based on strict criteria which are as follows:-

i. Only observed phenological data from spring wheat cultivars in India under field

conditions were used.

ii. The wheat cultivars had to be grown in winter in accordance with the typical growing season for wheat in the region. As discussed in Section 4.1, wheat is predominantly grown during the winter season in India.

iii. The period between the different phenological stages can either be described using days after sowing (DAS) or cumulative growing degree days (GDD, °C days). To use GDD, a base temperature has to be defined since GDD is calculated according to the formulation provided in Equation [4-1] given by Bishnoi *et al.*, (1995). In India many studies have shown that wheat crops in India show noticeable growth at temperatures above 5°C; therefore there is strong consensus that this value be used as the base temperature for wheat.

$$\mathrm{GDD} = \sum \left[\frac{T_{max} - T_{min}}{2}\right] - T_b \qquad [4\text{-}1]$$

Where, $T_{\min}$ and T_{max} are daily minimum and maximum temperature respectively and T_b is the base temperature (5°C). In comparison, for European wheat cultivars the base temperature is 0°C (LRTAP Convention, 2004).

The DAS and GDD for different phenological stages were defined based on observed data published in the literature. These values are summarised in Table 4-2 which also provides information on the number of studies, cultivars and locations as well as the growing conditions under which these data were obtained. Table 4-2 lists study-specific ranges of DAS and GDD in relation to different phenological stages which were: flag leaf emergence, ear emergence (assumed equal to A_{start}), mid-anthesis and physiological maturity or end of grain filling period (assumed equal to A_{end}). The methods used to estimate the wheat sowing date and to select and parameterise the most appropriate measure of phenological period (i.e. either DAS or GDD) for use in defining the F_{st} accumulation period, based on the data provided in Table 4-2, are explained in the following sections.

Table 4-2: Literature used to extract wheat phenology data. Listed are the publication-specific range of values of both DAS and GDD for wheat phenological stages. The table also show the AGZs where the location of study is situated.

References	**Growth stages in GDD (°C) and days after sowing (DAS). ***			**No. of experimental sets**	**Location / AGZ [No. of locations]**	**Cultivars [No. of cultivars]**	**Growing conditions**
	A_{start}	**Mid-anthesis**	A_{end}				
Bishnoi *et al.*, 1995	GDD: 669-884 DAS: 74-94	GDD: 817-1044 DAS: 84-111	GDD: 1258-1687 DAS: 108-154	15	Hisar / NWPZ [1]	WH-147 [1]	Field
Gosh and Patra, 2004	DAS: 68-73	DAS: 71-77	DAS: 105-109	4	Purulia, / NEPZ [1]	K-9107; Rajlaxmi; UP-262; Sonalika [4]	Field
Kant *et al.*, 2004	DAS: 66-85	DAS: 86-104	DAS: 121-131	8	Hisar / NWPZ [1]	PBW-343; Raj-3765; Sonak; UP-2338 [4]	Field
Kichar and Niwas 2005	N.A.	GDD: 848-948 DAS: 89-108	GDD: 1452-1618 DAS: 104-131	4	Hisar / NWPZ [1]	WH-711 [1]	Field
Rajput *et al.*, 1987	N.A.	GDD: 820-982 DAS: 63-76	GDD: 1531-1772 DAS: 83-100	8	Rewa/ CZ, Kathulia [2]	Sonalika [1]	Field

4.2.2 Wheat sowing date

Table 4-2 provides data for DAS and GDD measures of different phenological periods. To be able to use these data to define the timing of these different periods requires first the identification of the sowing date.

The recommended sowing time of irrigated wheat in India is between 10 to 25th of November (DWD, Government of India (http://dacnet.nic.in/dwd/); Rane *et al.,* 2007; Joshi *et al.,* 2007b; Pal *et al.,* 2001; Pal *et al.,* 2001; Tyagi *et al.,* 2003; Ladha *et al.,* 2003; Karla *et al.,* 2008). Studies conducted across the important wheat growing geographical regions in India, i.e. NEPZ (Bihar and Eastern U.P.), NWPZ (Western U.P., Eastern Rajasthan, Haryana and Punjab) and CZ (Western M.P.) have shown that the optimum yield is achieved when the wheat sowing date is close to the 16th November (year day 320) (Karla *et al.,* 2007; see also Figure 4-2, Karla *et al.,* 2008; Mehla *et al.,* 2000). Therefore, in this study it is proposed to use a fixed sowing date, i.e. 17th November (year day 321), which represents the average of the dates recommended by DWD, Government of India, as the sowing date.

However, it should be noted that in many parts of northern India, there are frequent delays in wheat sowing mainly due to the delay in the rice harvest; in these regions sowing often takes place between 25th November and 25th December (DWD, 2010a; Rane *et al.,* 2007); the implications of variations in the timing of the important phenological periods are assessed further in Chapter 5.

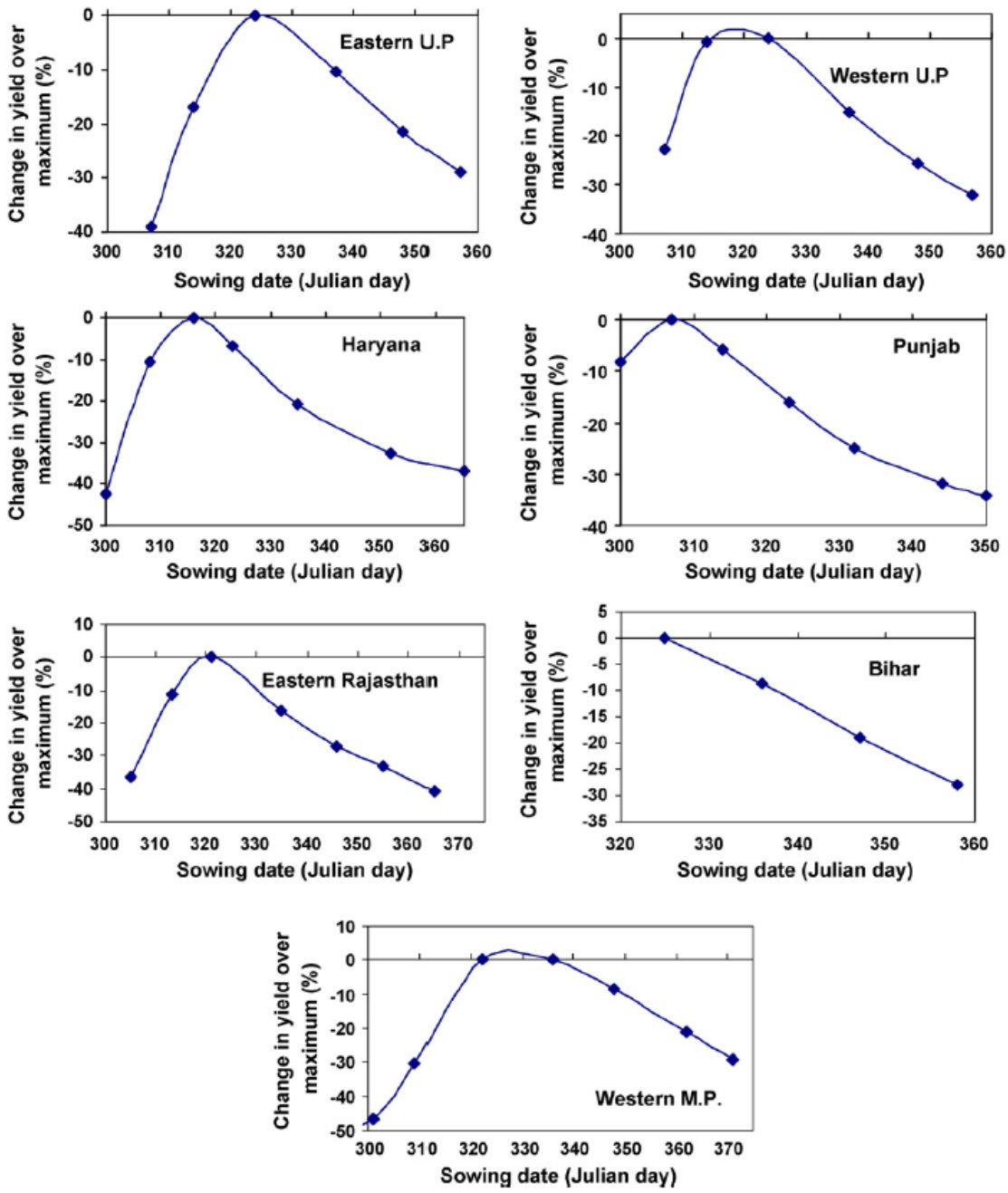

Figure 4-2: Effect of different sowing dates on wheat yield under different meteorological subdivisions in NWPZ, NEPZ and CZ agroclimatic zones in India (Karla *et al.*, 2007).

4.2.3 Defining the phenological stages in the F_{st} accumulation period

As shown in Table 4-2 phenological periods can be defined as either DAS or GDD. Ideally, the F_{st} accumulation period will be identified using the most robust of either of these methods. This section analyses data from the literature to determine which measure of phenology should be used in the DO_3SE F_{st} model.

4.2.3.1 Fixed day (DAS) accumulation period

Table 4-3 summarises the data from Table 4-2 to show the average and median values of DAS of the different phenological stages calculated for wheat cultivars grown in India. The median value for ear emergence (A_{start}) is 79 days (rounded to 80 days), mid-anthesis is 98 days (rounded to 100 days) and days to physical maturity (A_{end}) is 130 days.

Table 4-3: Days after sowing (DAS) for different phenological stages of wheat grown in India. References are listed in Table 4-2.

Phenological stage	**DAS**	
	Average ±standard deviation	**Median**
Flag leaf emergence	62±9	65
A_{start}	79±7	79
Mid-anthesis	97±6	98
A_{end}	129±13	130
Accumulation period	50	51

4.2.3.2 Thermal time (GDD) accumulation period

Table 4-7 gives the median and average values of GDD required to attain the different phenological stages calculated from phenological data listed in Table 4-2.

Table 4-4: Cumulative growing degree days (GDD, °C days) for different phenological stages of wheat grown in India. References are listed in Table 4-2.

Phenological stage	**Observed GDD (°C days)**	
	Average ±standard deviation	**Median**
Flag leaf emergence	514±97	486
A_{start}	761±78	743
Mid-anthesis	906±69	907
A_{end}	1509±142	1530
Accumulation period	748	787

4.2.3.3 Comparison of DAS and GDD for defining F_{st} accumulation period

Figure 4-3 (a) and (b), shows values derived for A_{start}, mid anthesis and A_{end} using DAS and GDD respectively plotted along with observed phenological data for different cultivars from individual experiments obtained from the published literature listed in Table 4-2.

The DAS values for A_{start}, mid-anthesis and A_{end} are very similar for both average and median values; these values are rounded to 80, 100 and 130 DAS respectively to compare cultivar data in Figure 4-3 (a). The GDD comparison uses values of 800 ^{o}C days GDD for the entire F_{st} accumulation period with A_{start} at 700 ^{o}C days after sowing and A_{end} at 1500 ^{o}C days. The value of A_{start} of 700 ^{o}C days was chosen over 750 ^{o}C days, which is closer to the median value, in order to make sure the accumulation period

captures the time when the flag leaf is fully developed, this will mean that for cultivars that have early ear emergence, the F_{st} accumulation period will start before the flag leaf is fully developed. The value for A_{end} of 1500 ^{o}C days is selected since it gives a better representation of the average and median A_{end} values.

Figure 4-3 (a) and (b) shows there is substantial variation between cultivars in the timing of phenological periods measured both in terms of DAS and GDD. However, for DAS there is a substantial overlap between different phenological stages; for example, approximately 10 out of the 40 cultivars investigated have an A_{end} value of approximately 100 DAS whilst approximately 15 of the cultivars have an A_{start} value of approximately 100 DAS. In contrast, all cultivar A_{end} values estimated using GDD finish later (between 1300 and 1700 ^{o}C days) than A_{start} and mid-anthesis. This would suggest that GDD captures the timing of the different phenological stages more consistently between cultivars than DAS.

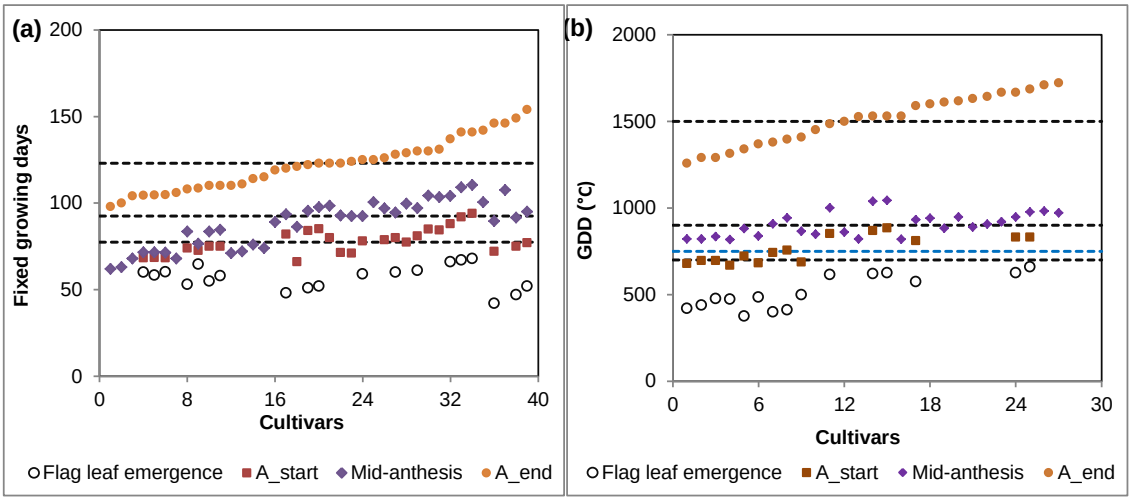

Figure 4-3: Wheat accumulation period. (a) based on DAS. The dotted lines indicate A_{start} = 80 days; Mid-anthesis = 100 days and A_{end} = 130 days. (b) based on GDD. The dotted lines indicate A_{start} = 700 GDD; Mid-anthesis = 900 GDD and A_{end} = 1500 GDD. The values are from Table 4.2. The blue dotted line indicates GDD=750.

Published studies have also reported similar observations which highlighted the influence of temperature on wheat growth and where the thermal time method was able to define wheat phenology better than the fixed day method for wheat crops grown in India (Ghadekar *et al.,* 1992; Hundal *et al.,* 1997; Kichar and Niwas, 2007; McMaster *et al.,* 2008) as well as in Europe (Pleijel *et al.,* 2000). McMaster and Wilhelm (1997) commented that the use of the effective temperature sum is generally accepted to describe plant development more accurately than using a fixed time period since it allows for the influence of temperature on growth. Sandhu *et al.* (1999) reported that the coefficient of variation for growth duration measured in days was higher than growth duration in thermal time (e.g., GDD, °C days) for the different phenological stages of Indian wheat. Pleijel *et al.* (2000) also found less variation in phenology between different experiments when thermal time was used as compared to using fixed duration for European wheat cultivars (Pleijel *et al.,* 2000).

However, neither method is able to capture the full range of cultivar phenological periods; using an A_{end} of 1500 ^{o}C days for the shorter duration cultivars causes the F_{st} accumulation period to extends beyond the physiological maturity when the green flag leaf area is low and photosynthesis is not likely to have significant contribution to grain development with the consequence of overestimating F_{st}. For longer duration crops, the F_{st} accumulation period starts before the flag leaf is fully developed but ends before physiological maturity. Due to this, towards the start of the accumulation period, the F_{st} may be overestimated while towards the end of the accumulation period it may be underestimated. The over estimation towards A_{start} is likely to be compensated by the underestimation of the O_3 flux that may occur towards A_{end}.

Based on the analysis presented here this study will use the GDD method to estimate the F_{st} accumulation period with A_{start}, mid-anthesis and A_{end} defined as 700, 900 and 1500 ^{o}C days after sowing and a total F_{st} accumulation period of 800 ^{o}C days.

4.3 Parameterization of the g_{sto} model for Indian wheat

A literature review was performed using online search portals such as Web of Science and Sciencedirect. In addition, a visit to libraries in India was made to access the literature that is available only in journals and books published in India. To derive g_{max}, data describing g_{sto} of Indian wheat cultivars were collected from published studies of experiments carried out in India using strict criteria that were based on those used to derive the European g_{max} wheat parameterisation defined in LRTAP Convention (2004). These criteria can be summarised as described below and were used to ensure that, as far as possible, the data collected from different experimental studies and observations in India (or some cases SA) were as comparable as possible.

1. Only data obtained from g_{sto} measurements made on cultivars grown either under field conditions or in open top chambers in India were considered. If not enough information was found, potted plants were also taken into account.

2. The g_{sto} measurements used to define g_{max} had to be made on fully mature leaves of the wheat canopy, and ideally the wheat flag leaf; during those times of the day and year when g_{max} would be expected to occur (i.e. between ear emergence and physiological maturity periods of wheat development). Although the F_{st} model is parameterised for the flag leaf, the data search was extended to all mature canopy leaves in an attempt to capture as much g_{sto} data as possible for further consideration.

3. Full details had to be given of the gas for which g_{sto} measurements were made (e.g. H_2O, CO_2, O_3).

4. Details of the leaf surface area basis upon which the g_{sto} measurements were expressed (e.g. total or projected) had to be provided. Ideally these would be specifically stated; alternatively, they could be inferred from provision of details of the g_{sto} measurement apparatus used to collect g_{sto} data.

5. Only g_{sto} measurements made using recognized g_{sto} measurement apparatus were considered. Such apparatus included IRGAs and porometers.

6. Only g_{sto} measurements made on wheat grown during the winter season (between

November and March/ April months in India) were considered.

14 experimental studies (see Table 4-5) were identified that provided information on the g_{sto} of flag leaves for 22 wheat cultivars growing under Indian conditions; of these only 5 experiments clearly described the leaf area basis for measuring the g_{sto}. Due to this, certain assumptions had to be made based on the type of instruments that were used to measure g_{sto} in order to derive the values for g_{sto} based on projected leaf area (PLA). PLA is the leaf area projected onto a horizontal plane, while total leaf area (TLA) is the total surface area of the leaves including the upper and the lower leaf surface (Chapin *et al.*, 2002). Unless otherwise stated, it was assumed that:-

1. Data from an IRGA represents conductance from both sides of the leaf expressed on a PLA basis.

2. Data from a porometer represents conductance from the higher conducting side of the leaf (in wheat the adaxial surface; see Table 4-6 describing data collected from Indian studies that provide data on the adaxial:abaxial ratio) on a TLA basis.

The ratio of adaxial to abaxial g_{sto} of 0.53 to 0.47 was taken from Agarwal & Singh (1984) and used to convert from TLA to PLA; this ratio was supported by data describing adaxial and abaxial stomatal frequency distribution (Table 4-6).

Table 4-5: Details of the conditions under which the g_{sto} data used for deriving maximum stomatal conductance (g_{max}) in wheat were collected.

References	g_{max} (mmol O_3 m^{-2} PLA s^{-1})	g_{max} derivation	Location	Cultivar	Time of the day	Stage of crop	g_{sto} measuring apparatus	Gas/ leaf area basis	Growing conditions	Leaf
Agrawal and Singha, 1984; Ghildiyal *et al.*, 2001	232	From graph showing g_{sto} at different days after showing stomatal resistance of both adaxial and abaxial side of the leaf. Adaxial=2.23 s/cm and abaxial=2.35 s cm^{-1}; n=3	New Delhi (NWPZ)	Kalyansoni	10.30-12.00	109 days after sowing	Diffusive resistance meter (LI 65, Licor)	H_2O /PLA	Field	Flag
Ghildiyal *et al.*, 2001	171	Value in table. g_{sto} = 0.281 (mol H_2O m^{-2} s^{-1}); value of n not given but least significant difference (LSD) values given so assumed n≥3.*	New Delhi (NWPZ)	B 449	10:00 – 11:00 hours	Anthesis	IRGA (Li-Cor 6200, Lincoln, NE, USA)	H_2O / not mentioned but IRGA so assumed to be PLA	OTC	Flag
Ghildiyal *et al.*, 2001	186	Value in table. g_{sto} = 0.173 (mol H_2O / m^{-2} s^{-1}); value of n not given but least significant difference (LSD) values given so assumed n≥3.*	New Delhi (NWPZ)	HD 4502	10:00 – 11:00 hours	Anthesis	IRGA (Li-Cor 6200, Lincoln, NE, USA)	H_2O / not mentioned but IRGA so assumed to be PLA	OTC	Flag

Table 4-5: Continued.

Ghildiyal *et al.*, 2001	101	Value in table. g_{sto} = 0.165 (mol H_2O m^{-2} s^{-1}); value of n not given but least significant difference (LSD) values given so assumed n≥3.*	New Delhi (NWPZ)	Kundan	10:00 – 11:00 hours	Anthesis	IRGA (Li-Cor 6200, Lincoln, NE, USA)	H_2O / Not mentioned but IRGA so assumed to be PLA	OTC	Flag
Kumar *et al.*, 2005	168	From graph showing stomatal conductance plotted against irradiance (PPFD); 275.3264 (mol H_2O m^{-2} s^{-1}); n= 4	Palampur (NHZ)	VL-116	not mentioned	85 days after sowing	IRGA (LI-6400, Lincoln, NE, USA)	H_2O/ Not mentioned but IRGA so assumed to be PLA	assumed to be field	Flag
Rai *et al.*, 2007	583	Value in table. g_{sto} = 2.33 (cm s^{-1}); n =3.	Varanasi (NEPZ)	HUW-234	9:00 - 10:00 hours	60-64 DAG	IRGA (LI-6200, LI-COR, USA)	H_2O/ not mentioned but IRGA so assumed to be PLA	OTC	Flag
Saharan and Singh, 1984	90	Value in table. g_{sto} = 0.36±0.01 (cm s^{-1}); g_{sto} = abaxial + adaxial; value of n not given but std. deviation values given so assumed n≥3.*	Hissar (NWPZ)	C-306	11:00 hours	14 days after anthesis	Diffusion porometer (LAMDA, IC, Lincoln, Nebraska)	Assumed H_2O as it is measured with Porometer/ PLA	Field	Flag
Saharan and Singh, 1984	110	Value in table g_{sto} = 0.43±0.01 (cm s^{-1}); g_{sto} = abaxial+adaxial; n not	Hissar (NWPZ)	C-591	11:00 hours	14 days after anthesis	Diffusion porometer (LAMDA, IC,	Assumed H_2O as it is measured	Field	Flag

Table 4-5: Continued.

		given but std. deviation values					Lincoln, Nebraska)	with Porometer/ PLA		
Saharan and Singh, 1984	88	Value in table g_{sto} = 0.34±0.01 (cm s^{-1}); g_{sto} = abaxial+adaxial; n not given but std. deviation values given so assumed n≥3.*	Hissar (NWPZ)	HD-2009	11:00 hours	14 days after anthesis	Diffusion porometer (LAMDA, IC, Lincoln, Nebraska)	assumed H_2O as it is measured with Porometer/ PLA	Field	Flag
Saharan and Singh, 1984	93	Value in table. g_{sto} = 0.35±0.02 (cm s^{-1}); g_{sto} = abaxial+adaxial; n not given but std. deviation values given so assumed n≥3.*	Hissar (NWPZ)	WH-157	11:00 hours	14 days after anthesis	Diffusion porometer (LAMDA, IC, Lincoln, Nebraska)	Assumed H_2O as it is measured with porometer/ PLA	Field	Flag
Singh and Datta, 2010)	116	Value in table. g_{sto} = 0.19 mol H_2O m^{-2} s^{-1}; n=20.	New Delhi	RKGR-1	-	fully opened flag leaf	IRGA (LICOR-6400 , USA)	H_2O/ Not mentioned but IRGA so assumed to be PLA	Flag leaf	Field
Singh *et al.*, 1993	122	From graph showing g_{sto} plotted against irradiance (PPFD); 3.8565 s cm^{-1}; n=3	Hissar (NWPZ)	WH-147	12.00-13.00	99 days after sowing	Steady state porometer , (Li-Cor 1600)	Assumed as H_2O since it is measured with porometer	Field	Flag

Table 4-5: Continued.

Ashraf and Bashir, 2003	84	Value from line graph showing g_{sto} at different days after anthesis. g_{sto} = 137.9817 (mmol H_2O m^{-2} s^{-1}); n not given.	Faisalabad, Pakistan	Barani-83	10:00 - 11:35 hours	12 days after anthesis	IRGA (ADC, England)	H_2O/ Not mentioned but IRGA so assumed to be PLA	Flag leaf	Potted
Ashraf and Praveen, 2002	60	Value from line graph showing g_{sto} at different days after anthesis. g_{sto} = 97.7361 (mmol H_2O m^{-2} s^{-1}); n not given	Faisalabad, Pakistan	Potohar	10:00 - 13:00 hours	8 days after the start of anthesis	IRGA (ADC, England)	H_2O/ Not mentioned but IRGA so assumed to be PLA	Flag leaf	Potted
Ashraf and Praveen, 2002	74	Value from line graph showing g_{sto} at different days after anthesis. g_{sto} = 120.7762 mmol H_2O m^{-2} s^{-1}. n not given	Faisalabad, Pakistan	SARC-1	10:00 - 13:00 hours	8 days after the start of anthesis	IRGA (ADC, England)	H_2O/ Not mentioned but IRGA so assumed to be PLA	Flag leaf	Potted
Sawney and Singh, 2002	92	Value in table. g_{sto} = 151.0±15.00 mmol CO_2 m^{-2} s^{-1}; n not given but std. deviation values given so assumed n≥3.*	Hissar (NWPZ)	LOK-1	-	13 days after anthesis	IRGA (CIRAS-1, UK)	CO_2/ Not mentioned but IRGA so assumed to be PLA	Flag leaf	Potted; natural growing conditions
Sawney and Singh, 2002	84	137.0±14.40 mmol CO_2 m^{-2} s^{-1}; n not given but std. deviation values given so assumed n≥3.*	Hissar (NWPZ)	WH-533	-	13 days after anthesis	IRGA (CIRAS-1, UK)	CO_2/ Not mentioned but IRGA so assumed to be PLA	Flag leaf	Potted; natural growing conditions

Table 4-5: Continued.

Sharma *et al.*, 2005	36	Value in table. g_{sto} = 37.26±2.87 mmol CO_2 m^{-2} s^{-1}; n=3	Jobner (NWPZ)	HD-2395	10:00 - 11:00 hours	anthesis stage	IRGA (CID-301, USA)	CO_2/ Not mentioned but IRGA so assumed to be PLA	Flag leaf	potted
Uprety and Sirohi, #1987a&b; Agrawal *et al*., 2009	590	Value in table. Stomatal resistance = 0.88 s cm^{-1}. value of n not given but since critical difference (CD) values are given therefore assumed ≥3.*.	New Delhi (NWPZ)	Sonalika	10:00 - 16:00 hours	anthesis	porometer (LI 1600)	Not mentioned but Porometer so assumed to be for H_2O/ one sided	Flag leaf	Potted; natural growing conditions
#Wahid, 2006; Ashraf and Bashir, 2003	229	From graph showing bar graph of g_{sto} = 229.25 (mmol O_3 m^{-2} s^{-1}), n≥16.	Lahore, Pakistan	Inqilab-91	not mentioned	70 days after sowing	IRGA (LCA-2) (ADC, Herts, UK)	O_3/ Not mentioned but IRGA so assumed to be PLA	Flag leaf	OTC potted
Wahid, 2006	226	From graph showing bar graph of g_{sto} = 226 (mmol O_3 m^{-2} s^{-1}) , n≥16.	Lahore, Pakistan	Pasban-90	not mentioned	70 days after sowing	IRGA (LCA-2) (ADC, Herts, UK)	O_3/ Not mentioned but IRGA so assumed to be PLA	Flag leaf	OTC potted

Table 4-5: Continued.

Wahid, 2006	229	From graph showing bar graph of g_{sto} = 228.82 (mmol O_3 m-2 s-1) , n≥16.	Lahore, Pakistan	Punjab-96	not mentioned	70 days after sowing	IRGA (LCA-2) (ADC, Herts, UK)	O_3/ Not mentioned but IRGA so assumed to be PLA	Flag leaf	OTC potted

Mean = 182; Median = 145; 90th Percentile = 232; Range = 88 – 583; all values are in mmol O_3 m^{-2} PLA s^{-1}; n= number of replicates. * n value is not given in the literature but the g_{sto} values are given along with LSD or std.dev values which require n≥3 for analysis and therefore n is assumed to be ≥3. In cases where two or more references are available, the reference from which the g_{max} for that cultivar came is indicated by #.

Table 4-6: Data collected from Indian studies used to define the relative adaxial and abaxial g_{sto} and stomatal frequency of wheat.

Parameter	Adaxial	Abaxial	References
Stomatal conductance	0.53	0.47	Agarwal and Singha, 1984
Stomatal frequency	0.53	0.47	Hattali *et al.*, 1993
Stomatal frequency	0.58	0.42	Saharan and Singh, 1984

4.3.1 g_{max} and f_{min} of wheat crops grown in India

4.3.1.1 g_{max}

There were only 12 experimental studies providing data on g_{sto} of Indian wheat cultivars that fit the criteria set in the previous section to estimate g_{max}. Therefore, g_{sto} data were also collected from potted wheat plants which were grown under natural conditions and met all the other criteria. This also gave an opportunity to check how different the g_{sto} of potted wheat is from the non-potted field grown wheat. Data on wheat g_{sto} were also collected from experimental pot-based studies that were performed in Lahore (Wahid, 2006) and Faisalabad (Ashraf and Praveen, 2002) in Pakistan. Both Lahore and Faisalabad are located close to the Pakistan – India border; they are part of the Punjab province in Pakistan. The Punjab state in India is one of the most important wheat growing regions in India and due to the close proximity of Lahore and Faisalabad to this region; therefore it was assumed that the wheat growing conditions in Lahore are similar to those of India, especially in the NWPZ region and the Wahid (2006) experimental data could be used in the Indian wheat parameterisation.

After taking account of all the considerations mentioned above, g_{sto} data for 22 wheat cultivars from 14 experimental studies were collected to derive the g_{max} for Indian wheat (Table 4-5). The publications give g_{sto} data either as g_{sto} of water vapour (H_2O), CO_2 or O_3. In cases where the g_{sto} was given for H_2O or CO_2, the values were converted to O_3 using a factor of 0.61 and 0.96 respectively (Pleijel *et al.*, 2007). The values 0.61 and 0.96 represent the ratios of coefficient of molecular diffusivity of H_2O and CO_2 to that

of O_3 respectively. The value of g_{max} (mmol O_3 m^{-2} PLA s^{-1}) for each cultivar was derived as the maximum value of g_{sto} for each of these cultivars collected from one or more experimental studies listed in Table 4-5. Table 4-5 also gives the g_{max} values for each of the 22 cultivars.

To capture the maximum g_{sto} for Indian wheat, the 90th percentile of the g_{max} values of flag leaf of the 22 cultivars listed in Table 4-6 (g_{max} = 232, rounded to 230 mmol O_3 m^{-2} PLA s^{-1}) was used as the g_{max} of Indian wheat flag leaf. The 90th Percentile was used instead of the absolute maximum in order to avoid the outliers in the data. The g_{max} of the 22 cultivars, potted as well as field crops, used to derive the g_{max} of wheat flag leaf for the stomatal flux model is plotted in Figure 4-4.

Studies have reported that growing plants in pots affects the rooting system due to limited soil volume and this may affect the transpiration of the plant and subsequently g_{sto}. Ray and Sinclair (1998) reported a decrease in transpiration of potted soybean and maize plants with decrease in the pot size. This suggests that pots may reduce the transpiration and g_{sto} of plants. Surprisingly, there was no significant difference between the g_{max} values of the field grown wheat and potted wheat, and adding the g_{max} values of the potted wheat to the field wheat g_{max} values did not change the 90th percentile values g_{max} significantly. The 90th percentile of field wheat g_{max} was 227 mmol O_3 m^{-2} PLA s^{-1}, while the 90th percentile of the potted and field grown wheat flag leaves was 232 mmol O_3 m^{-2} PLA s^{-1}.

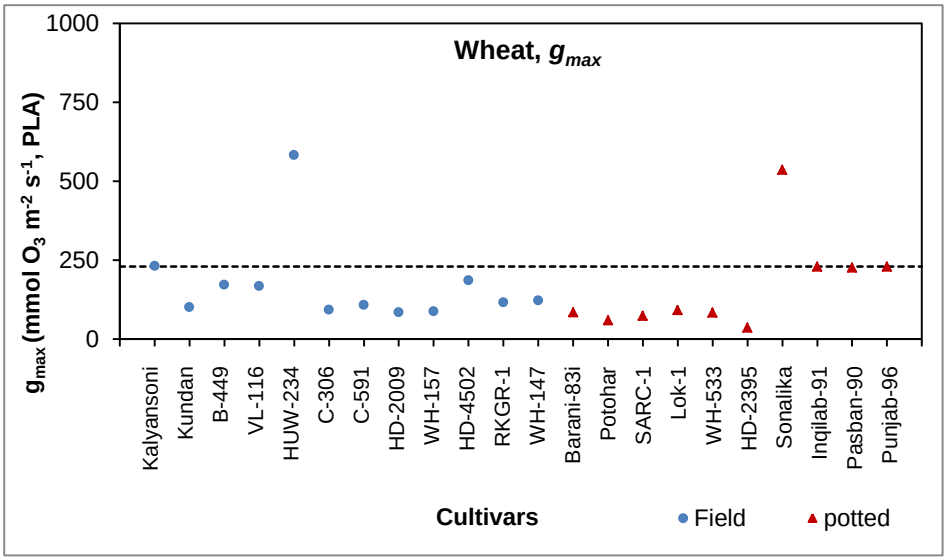

Figure 4-4: Parameterisation of g_{max} for wheat stomatal conductance model. Each data point represents the maximum g_{sto} that was observed for each cultivar, either from a single or more than one study and the dashed line indicates the 90th percentile, g_{max} = 230 mmol O_3 m^{-2} PLA s^{-1}. The references of the g_{max} data are listed in Table 4-5.

4.3.1.2 f_{min}

The absolute minimum g_{sto} was selected as the g_{min} based on the g_{sto} data from literature listed in Table 4-6. The published literature from which the g_{sto} data were collated allowing the derivation of g_{min} were the same as those from which the g_{max} value was derived (Table 4-6). From these data, the g_{min} was found to be 1% of g_{max}. Therefore, f_{min} value of 0.01 is used for the Indian wheat.

In the European wheat cultivars, Pleijel *et al.* (2003) and Danielsson *et al.* (2003) reported that f_{min} under field conditions frequently reached values as low as 1% of g_{max}. Hence the Indian parameterisation for f_{min} seems consistent with the European.

4.3.2 Seasonal g_{sto} parameters

Seasonal parameters are those that show variability in influencing g_{sto} over the growing season but do not vary during the course of the day, e.g., f_{phen}.

4.3.2.1 g_{sto} as a function of wheat phenology (f_{phen})

The variation in wheat flag leaf g_{sto} with leaf age has been reported in Indian wheat cultivars (Agrawal and Sinha, 1984; Ashraf and Praveen, 2002). To derive an f_{phen} function that accounts for this variation due to phenology, wheat flag leaf g_{sto} measured during different stages of the F_{st} accumulation period were obtained from literature. The data was collected following strict criteria similar to the ones set for deriving g_{max}, with slight modifications to suit the requirements for the f_{phen} function, i.e. the g_{sto} had to be measured on the flag leaf, grown under natural conditions, and the data should have measurements of g_{sto} in at least three stages of the F_{st} accumulation period. The data used for deriving the f_{phen} function are listed in Table 4-7.

Table 4-7: List of literature for deriving f_{phen} values for Indian wheat. DAA= days after anthesis; DAS= days after sowing.*Values are obtained during anthesis so are assumed to be for the flag leaf.

References	Location	Cultivars	Time of the day	Stage of crop	g_{sto} measuring apparatus	Growing conditions	Leaf
Ashraf and Bashir, 2003	Faisalabad, Pakistan	Inqlab-91, Barani-83	10:00 - 11:35 hours	2, 4, 6, 8, 10, 12 DAA	IRGA (ADC, England)	Potted	Flag leaf
Ashraf and Parveen, 2002	Faisalabad, Pakistan	SARC-1, Potohar	10:00 – 13:00 hours	2, 4, 6, 8, 10, 12 DAA	IRGA (ADC, England)	Potted	Flag leaf
Singh and Singh, 1989	Hissar, NWPZ_2	WH-157	07:00-19:00 hours at every two hour interval	Jointing, flowering (anthesis) and dough stage	Leaf diffusive resistance meter (Porometer)	Field	Fully developed leaves exposed to sunlight of main tiller
Uprety and Sirohi, 1987b	Delhi, NWPZ_1	Sonalika	10:00 - 16:00 hours	Pre-anthesis, anthesis and post-anthesis	Porometer (LI 1600)	Field	Flag
Aggarwal and Sinha, 1984	Delhi, NWPZ_1	Kalyansoni	10.30-12.00	80, 87, 95, 101, 109, 116, 123 DAS	Diffusive resistance meter (LI 65, Licor)	Field	Flag
Saharan and Singh, 1984	Hissar, NWPZ_2	C-306, C-591, HD-2009, WH-157	11:00 hours	7, 14, 21 and 28 DAA	Diffusion porometer (LAMDA, IC, Lincoln, Nebraska)	Field	Flag

The phenology data in these literatures were described in days and not in GDD (Table 4-7) and therefore fixed days were used to define f_{phen_c} and f_{phen_d} values (Figure 4-5), which represent g_{sto} at the A_{start} and A_{end} in relation to g_{max}. A boundary line analysis was used to establish the f_{phen} function. A similar method was also used to establish f_{phen} for European wheat. The f_{phen} relationship for Indian wheat given in Figure 4-5a is very similar to that derived for European wheat (Figure 4-5b). Therefore, the relative g_{sto} of 0.8 at A_{start} and 0.2 at A_{end} from European wheat were used to define the f_{phen} for Indian wheat. Assuming g_{max} is at mid-anthesis, the leaf f_{phen} at A_{start} is 20 days before anthesis and A_{end} is at 30 days after mid-anthesis (based on values in Table 4-3).

For the Indian parameterization of the F_{st} accumulation period, GDD is used to define crop phenology. There the fixed days over which f_{phen} is described have to be converted into GDD before this function can be used in the model. A_{start} in GDD has been defined as 200 ^{o}C days before mid-anthesis and A_{end} is 600 ^{o}C days after mid-anthesis. These GDD values replaced the fixed day values. Thus at 200 ^{o}C days before mid-anthesis, relative g_{sto} is 0.8 while at 600 ^{o}C days after mid-anthesis the relative g_{sto} is 0.2.

Figure 4-5 shows the parameterisation of f_{phen}. The A_{start} is taken as 20 days before mid-anthesis (assuming g_{max} to be at mid anthesis) and A_{end} as 30 days after mid anthesis (Table 4-3).

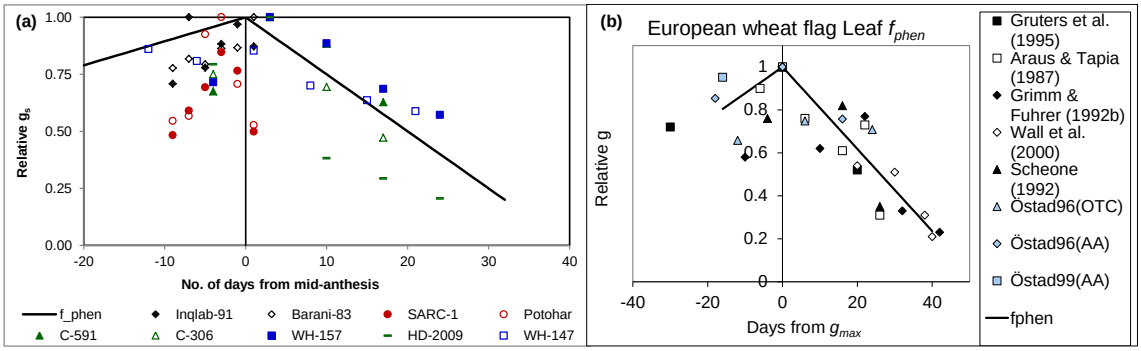

Figure 4-5: Parameterisation of f_{phen} for the wheat g_{sto} model; a) representing the Indian, b) representing the European parameterization. Each data point represents the g_{sto} in relation to the relative maximum g_{sto} (i.e. g_{max}) for each cultivar, either from single or multiple experimental datasets. The references for a) are listed in Table 4-7.

4.3.3 Diurnal parameters

Diurnal parameters are those parameters that vary in their limiting influence on g_{sto} over the course of the day.

4.3.3.1 g_{sto} as a function of irradiance (f_{light})

There was only one dataset that gave g_{sto} measurements for Indian wheat at different levels of irradiance (Kumar *et al.,* 2005). This experimental study was conducted at two places, Palampur and Kibber, and it measured the g_{sto} on flag leaves at different levels of irradiance from PPFD 0 μmol m^{-2} s^{-1} to 2700 μmol m^{-2} s^{-1} (Table 4-8 and Figure 4-6).

Table 4-8: List of literature for deriving f_{light} values for Indian wheat.

References	**Location**	**Cultivars**	**Irradiance**	**Stage of crop**	**g_{sto} measuring apparatus**	**Growing conditions**	**Leaf**
Kumar *et al*., 2005	Palampur and Kibber (AGZ 1)	VL-116	PPFD 0-2700 μmol m^{-2} s^{-1}	85 DAS	IRGA (LI-6400, Lincoln, NE, USA)	Not mentioned	Flag

The relative g_{sto} values were plotted together with the respective PPFDs to establish the f_{light} relationship for wheat (Figure 4-6). A logarithmic function was used to fit the boundary line function for f_{light} using Equation [4-7]. The f_{light} function for European wheat (f_{light_EU}) is based on an exponential function which is represented by the dotted line in Figure 4-6. Although the g_{sto} data here is limited, the f_{light} is a better representation of these g_{sto} data than the f_{light_EU}. Therefore, this logarithmic function of f_{light} was used to represent the light functions for Indian wheat in the model.

The f_{light} using a logarithmic function is given in Equation [4-2],

$$f_{light} = \left(\text{light}_a \times \text{Ln}(\text{PPFD})\right) - 0.3 \qquad [4\text{-}2]$$

Where, light_a = 0.1661 and, PPFD = photosynthetic photon flux density in units of µmol m^{-2} s^{-1}.

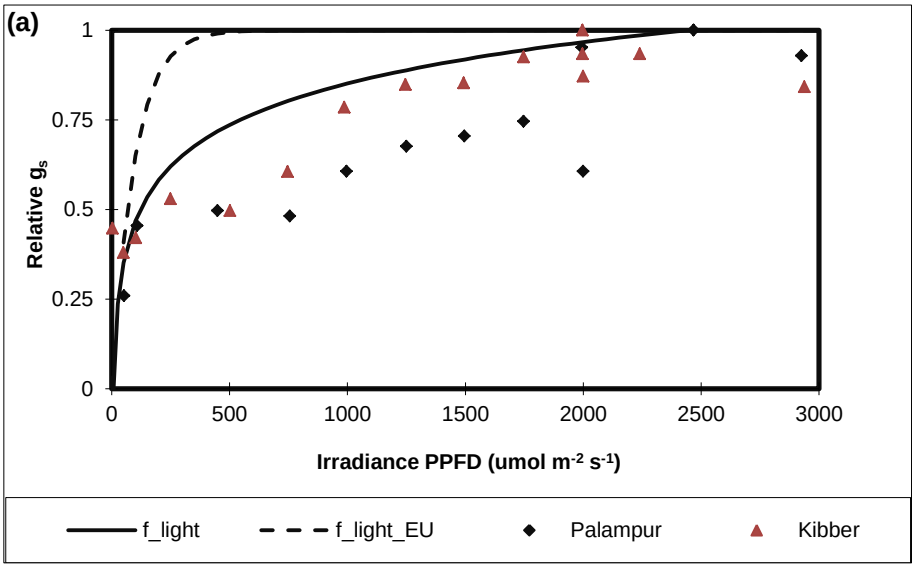

Figure 4-6: Parameterization of f_{light} for wheat. The data points on the primary axis represent observed g_{sto} of a single wheat cultivar, VL-116, at different irradiance levels (Kumar *et al.*, 2005).

The European f_{light} parameterization (f_{light_EU}) is shown for comparison in Figure 4-6; this assumes an exponential function and saturates at PPFD values below 400 µmol m^{-2} s^{-1}; therefore the limitation to g_{sto} of f_{light} would be substantially greater using the Indian parameterisation.

4.3.3.2 g_{sto} as a function of temperature (f_{temp})

To establish the f_{temp} function that describes the influence of temperature on g_{sto} of wheat flag leaves, data on wheat g_{sto} and its relationship were collected from experimental data in the literature following criteria that were similar to that for g_{max}, f_{phen} and f_{light} but with modifications to suit the requirements of the f_{temp} parameterizations, i.e. the data should have measurements of g_{sto} for at least three different temperature values.

There were only two studies that fit the criteria given above, Uprety and Sirohi (1987b) and Singh *et al.* (1993). The details of these two studies are given in Table 4-9.

Table 4-9: Details of data available on the influence of temperature on g_{sto} of wheat crops grown in India.

References	**Location**	**Cultivar**	**Temperature data**	**No of replicates**	**Time of g_{sto} measurements**	**Stage of crop**	**g_{sto} measuring apparatus**	**Growing conditions**	**Leaf**
Singh *et al.*, 1993	Hissar NWPZ_2	WH147	Canopy temperature at the time of measurement	3	12.00-13.00	20-119 DAS	Porometer LI-1600	Field	Well-developed leaves at top of canopy
Uprety and Sirohi, 1987b	IARI, Delhi NWPZ_2	Sonalika	Hourly temperature at the time of measurement	3	10.00-16.00	Anthesis, 7 days before anthesis and 15 days after anthesis	Porometer LI-1600	Potted, ambient conditions	Flag

The relative g_{sto} values from the data in Table 4-9 were plotted in Figure 4-7. It is clear that only limited data describing the response of g_{sto} to either air or leaf temperature for wheat grown in India were available (Figure 4-7) and these were deemed insufficient to establish a robust function that would describe f_{temp} for wheat under Indian conditions. In the absence of such data one possibility was to use the f_{temp} relationship established for European conditions (LRTAP Convention, 2004). The parameters for the f_{temp} function of European wheat cultivars are T_{min} = 12°C, T_{opt} = 26°C and T_{max} = 40°C; this function is shown in Figure 4.9 (f_temp_EU)

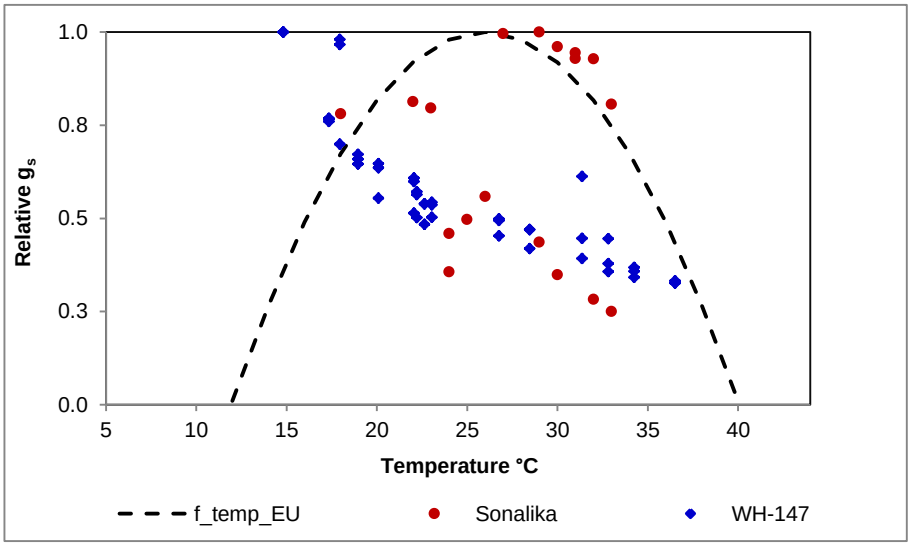

Figure 4-7: Available g_{sto} data for parameterisation of f_{temp}, based on Equations [3-11] and [3-12]. Each data point represents the g_{sto} in relation to the relative maximum g_{sto} for each cultivar according to the corresponding temperature. The source of g_{sto} data is given in Table 4-9. The dotted line indicates the European wheat f_{temp} parameterization from LRTAP Convention (2004).

The other option is to identify the T_{min}, T_{opt} and T_{max} parameters for the Indian wheat flag leaf f_{temp} relationship based on 30 year climate data of the wheat growing region during the wheat F_{st} accumulation period. This is based on the assumption that (i) the wheat cultivars selected for cultivation in India will be physiologically suited to these average climatic conditions and; (ii) the relationship between temperature and g_{sto} is represented by a curve with a normal Gaussian distribution (Jarvis and Morrison, 1981; Jarvis, 1980); the maximum and minimum temperatures as the T_{max} and T_{min} and the average temperature as the T_{opt}.

Having defined the f_{temp} function in this way will mean that g_{sto} will be limited when the temperature deviates from the climatic average; it also reduces reliance on the need to accurately define leaf to air temperature differences since these will be integrated in the approach that is merely trying to identify the effect of cooler and hotter periods from the norm. In view of this, an attempt was made to define the f_{temp} based on the actual temperature range the wheat crops would experience during their growth period across the region.

Collection of 30 years of temperature data

Analysis of daily average, maximum and minimum hourly temperature will give an idea of the range of temperatures prevalent during the Indian wheat growing period. These data were obtained from the National Oceanic and Atmospheric Administration (NOAA, 2009; http://www.ncdc.noaa.gov/oa/mpp/freedata.html) who have recorded data at various locations across the important wheat growing regions of India for 30 years, from 1979 to 2008. For many of these stations there are gaps in the data; therefore a comprehensive screening of the NOAA (2009) datasets was performed to identify 4 stations from each of the 3 main wheat growing AGZs (see Chapter 2) that had < 5% of the data missing during the F_{st} accumulation period; these station data (see Table 4-10) were used to define the f_{temp} parameters.

In order to be able to use these 24 hour temperature data to define f_{temp} it is important to ensure that the statistics provided are representative of daylight conditions. This requires that the T_{min} and T_{max} parameters used to define f_{temp} should correspond with the maximum and minimum average 24 hour temperature data provided by NOAA (2009). In India, the maximum temperature occurs during the daylight hours between 14:00 – 16:00 hours (Agri Info, 2011; Deosthali, 1999; Singh *et al.*, 1997; Jain, 2005); therefore the 24 hour maximum temperature is assumed to be equivalent to the daytime maximum temperature. The diurnal profile of temperature in India (Deosthali, 1999; Singh *et al.*, 1997; Jain, 2005) as well as in other parts of the world (Boni *et al.*, 2001; Purcell, 2003; Tejeda, 1991) indicates that the hourly minimum temperature is reached shortly after sunrise (5:30 – 6:00 hours) which means that the 24 hour minimum temperature will be equivalent to the minimum temperature during daylight hours.

The 5th and 95th percentile of the daily 24 hour minimum and maximum hourly temperatures were used to define T_{min} and T_{max}; T_{opt} was defined as the mean of the 24 hour average temperature. Percentiles were used in order to exclude outliers in the data. Since the temperature ranges vary between the different AGZs of India the need for separate f_{temp} profiles for different AGZs was investigated.

Table 4-10 gives the T_{opt}, T_{min} and T_{max} values calculated from the NOAA (2009) temperature data in the 3 AGZs: NEPZ, NWPZ and CZ. ANOVA on the data showed that there was no significant difference in mean temperature data between the three AGZs. Therefore a common T_{opt}, T_{min} and T_{max} value was used for the three AGZs and these same values for f_{temp} were applied for the entire wheat growing region in India. The resulting values for the Indian f_{temp} parameterisation were T_{opt} = 22°C; T_{max} =36°C; and, T_{min} = 9°C.

Table 4-10: T_{opt}, T_{min} and T_{max} values for the three AGZs: NEPZ, NWPZ and CZ. T_{opt} = average; T_{min} =5th Percentile and T_{max} = 95th Percentile of average, minimum and maximum daily 24 hour temperature data respectively. These data were based on the 30 year temperature data from NOAA (2009).

Location	T_{opt} **°C**	T_{max} **°C**	T_{min} **°C**
NEPZ			
Patna	22	34	10
Gorakpur	22	34	10
Gaya	22	35	10
Varanasi	22	34	11
NWPZ			
Lucknow	22	36	10
New Delhi	22	34	11
Hissar	22	36	11
Jaipur	22	34	9
CZ			
Bhopal	20	32	8
Gwalior	23	37	10
Kota	22	35	11
Jabalpur	22	35	10

Comparison of the calculated with observed data

To assess the reliability of using the NOAA (2009) 30 year climate data, the maximum, minimum and average temperatures from these datasets were compared with site-specific temperature data observed during the wheat growing season, which coincided with the period when the F_{st} accumulation period is likely to occur (Table 4-11). The observed data were from Varanasi and Ahmadnagar. Both the maximum and minimum temperature from the NOAA (2009) climate data lies within the range of the observed minimum and maximum data.

Table 4-11: The calculated T_{max} and T_{min}, and the F_{st} accumulation period average minimum and maximum temperature in Varanasi and Ahmadnagar.

Reference	**Location (Latitude_Longitude)**	**Daily Temperature °C**		**No. of years**	**Period of measurement**
		Minimum	**Maximum**		
NOAA (2009)	India	9	36	30	O_3 accumulation period*
NOAA (2009)	Varanasi	11 (5th Percentile)	34 (95^{th} Percentile)	30	O_3 accumulation period *
Tiwari *et al.*, 2005; Rai *et al.*, 2007; Singh *et al.*, 2009; Sarkar and Agrawal, 2010	Varanasi (25°N 83°E)	6.25 - 21.5	16.15 – 38.1	4	December to March 2002 – 2003 2004 – 2005 2007 – 2008 2008 - 2009
Debaje *et al.*, 2010	Ahmadnagar (19°N 75°E)	10.2 – 17.5	30.1 – 36.2	2	January, February, March and December 2006 and 2007

*the O_3 accumulation period occurs between January to March.

To see whether the 30 year climate data f_{temp} parameterization corresponds to the measured g_{sto} values for different temperatures in India, f_{temp} was plotted against observed g_{sto} data from publications listed in Table 4-8; these data were also compared with the European f_{temp} relationship (Figure 4-8). From Figure 4-8 it is difficult to judge whether the f_{temp} from the 30 years temperature data (f_{temp_IN}) or the European parameterization (f_{temp_EU})is better suited to define the f_{temp} relationship for Indian wheat. The use of the f_{temp_EU} is supported by the fact that these values are derived based on studies conducted to establish relationships between wheat g_{sto} and temperature. However, the limitation of using the f_{temp_EU} would be the fact that the physiology and hence the g_{sto} of Indian wheat cultivars is likely to be different from that of the European wheat cultivars.

The use of f_{temp_IN} is supported by the fact that the T_{opt} is similar to the optimum temperature given for Indian wheat. In addition, the T_{opt} value of 22°C is similar to the average of the optimum temperature for wheat growth and yield in India which is 20-25°C (DWD, 2011).

In Figure 4-8, the frequency of the hourly daytime temperature data (°C) from the MATCH model during the F_{st} accumulation period in the 3 AGZs was plotted along with the f_{temp_IN} and the f_{temp_EU}. The MATCH model temperature data was collected from one location for each of the 3 AGZs. The hourly temperatures that are prevalent during the F_{st} accumulation period lie within the maximum and minimum boundary set by the f_{temp_IN}. whereas some of the lower temperatures lie outside the f_{temp_EU}. The hourly temperatures seem to lie way below the T_{max} value of 40 °C. This does not indicate that the f_{temp_IN} is better suited or the f_{temp_EU}. However, it shows that when using f_{temp_IN}, temperature will not be as limiting to g_{sto}. Using f_{temp_EU} will be more limiting of g_{sto} at lower temperatures and less limiting at higher temperatures.

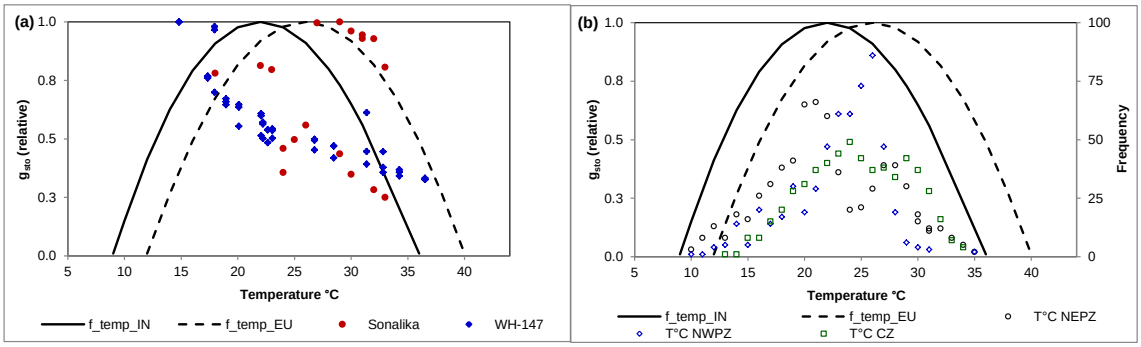

Figure 4-8: Parameterisation of f_{temp} for the wheat g_{sto} model. f_{temp_IN} and the f_{temp_EU} plotted along with, (a) observed relative g_{sto}. Each data point represents the g_{sto} in relation to relative maximum g_{sto} for each cultivar; either from a single or multiple experimental set (see Table 4-9 for data source), (b) the frequency of hourly temperatures during the O_3 flux accumulation period for wheat crops in the three AGZs, the temperature data from MATCH model.

4.3.3.3 g_{sto} as a function of VPD (f_{VPD})

There are no data upon which to parameterize the f_{VPD} function for Indian wheat; the only g_{sto} data that have been recorded with simultaneous measurements of VPD are for wheat cultivar Kalyansoni measured at very low VPD levels (ranging from 0 to 0.2 kPa); these data are from Aggarwal and Sinha (1984); see Figure 4-9 (a)). These VPD values have been calculated from relative humidity and temperature data. Unlike temperature, the VPD values at which g_{sto} will start to decline and reduce to f_{min} are difficult to establish from 24 hour climate data since maximum and minimum VPDs do not necessarily occur when at the same time as daily temperature extremes. Therefore, the VPD parameterization of European wheat is used in the present study.

Figure 4-9 (b) shows the European wheat f_{VPD} plotted along with the frequency of hourly VPD values from the MATCH model during the F_{st} accumulation period in the 3 AGZs. From Figure 4-9 (b) it is clear that VPD during the F_{st} accumulation period is likely to exceed the VPD_{min} threshold of 3.2 kPa fairly frequently. Therefore, using the European wheat f_{VPD} function will cause limitation of the g_{sto}.

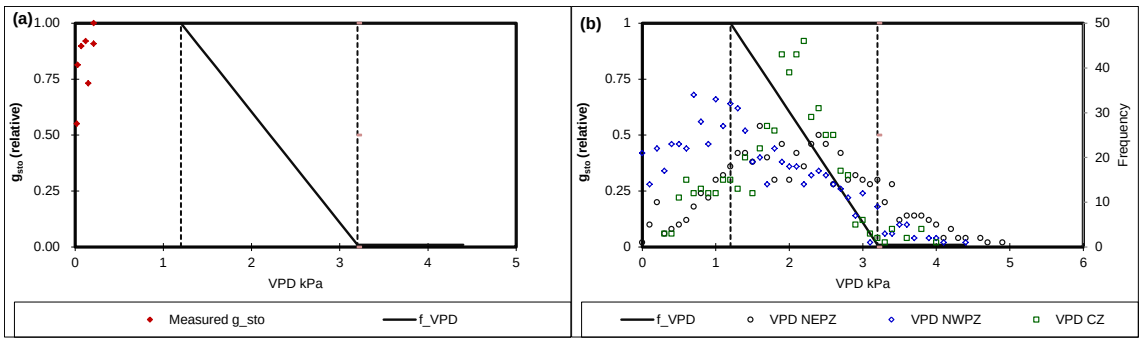

Figure 4-9: Parameterisation of f_{VPD} for the European wheat g_{sto} model, represented by black line and the VPDmax. And VPDmin represented by the dotted line. These are plotted along with, (a) The data points represent observed g_{sto} data of wheat cultivar Kalyansoni at different VPD levels (Aggarwal and Sinha, 1984). (b) The data points represent the frequency of hourly VPD during the F_{st} accumulation period in the 3 AGZs in India obtained from the MATCH model.

4.3.3.4 g_{sto} as a function of soil water

Since more than 85 % of the area under wheat cultivation in India is irrigated, it was assumed that during the entire growing season wheat was not water-stressed. As such it was not considered necessary to include a component in the g_{sto} algorithm that would allow for the influence of variable water status on g_{sto}. Application of the F_{st} model in Europe has also assumed soil water not to be limiting g_{sto}. However, since the environmental and management situation for wheat cultivation is rather different in India as compared to European, the consequences of making this assumption are discussed further Chapter 5.

4.4 Summary of the parameterization of the g_{sto} model for India

The different parameters of the DO_3SE F_{st} model that will be used to simulate O_3 uptake to the flag leaves of wheat grown in India are summarized in Table 4-12.

Table 4-12: Summary of the parameterization of the different parameters of the DO_3SE F_{st} model for wheat flag leaves grown in India.

Parameter	Units	Parameterization
g_{max}	mmol O_3 m^{-2} PLA^{-1}	**230**
f_{min}	fraction	**0.01**
f_{phen_a}	fraction	**0.8**
f_{phen_b}	fraction	**0.2**
f_{phen_c}	Days	**20**
f_{phen_d}	Days	**30**
f_{phen_e}	°C days	**200***
f_{phen_f}	°C days	**600***
$light_a$	(constant)	**0.1661****
T_{min}	°C	**9**
T_{opt}	°C	**22**
T_{max}	°C	**36**
VPD_{max}	kPa	1.2
VPD_{min}	kPa	3.2
$\sum VPD_{crit}$	kPa	8

The DO_3SE F_{st} model described in Chapter 3 will be applied with the parameterization described in Table 4-12 to provide estimates of F_{st} for wheat across India. These results are presented in Chapter 5.

Chapter 5 Results of the O_3 flux based risk assessment

5.1 Introduction

This chapter describes the results generated on application of the stomatal O_3 flux (F_{st}) model. The formulations of the F_{st} model and the combination of datasets necessary to apply the model for Indian conditions have been described in Chapter 3; the parameterization of the model for Indian conditions has been described in Chapter 4.

The analysis of the F_{st} results focuses on the following i) an assessment of the spatial differences in risk estimated using flux compared with a concentration based method (AOT40) described in Chapter 2; ii) an assessment of how these different estimates of risk translate into yield and production losses; iii) an assessment of factors most influential in determining flux both seasonally and diurnally; iv) an assessment of whether the prevailing climate under which wheat is grown (i.e. the AGZ) substantially influences flux and finally; v) consideration of the robustness of the flux model (and particularly the parameterization of the model) such that flux-modifying factors can be reliably determined; this last part compares the Indian with the European parameterization and performs a simple sensitivity analysis to define those parameters most important in determining flux.

In order to perform these various assessments F_{st} values have been calculated using either the Indian parameterization (IN) or the European parameterization (EU); for example, the latter allowed analysis of the importance of parameterisation on F_{st} estimates. In order to compare the cumulative O_3 fluxes, POD_y, directly with accumulated O_3 concentrations (AOT40) it has been necessary to estimate AOT40 over the same O_3 accumulation period used for F_{st} (i.e. A_{start} to A_{end}); this AOT40 is termed $AOT40_A$. These $AOT40_A$ values are therefore different to the AOT40 values estimated in Chapter 2 which were accumulated over a fixed length 3 month growing season. Comparisons of estimates of yield and production losses are made using AOT40 values accumulated over this 3 month period such that the values are comparable to those used to derive the AOT40 yield response functions. Flux based estimates of yield loss for crop production is made using the EU parameterization so that the estimates of flux are consistent with the means of deriving the 'European' flux-response relationship.

The model results are presented as maps to describe the spatial distribution of F_{st} and PODy across India such that the regions that are potentially most at risk from O_3 impacts can be identified. The modelling domain and the distribution of wheat cultivation is shown in Figure 5-1; the maps presented in later sections show F_{st} for the entire Indian land surface area, with the grids where wheat is grown identified by circle symbols whose size gives an indication of the percentage grid area under cultivation. In addition, individual grid squares have been selected from each of the main wheat AGZs (see Figure 4-1 in Chapter 4 for AGZs) in order to analyse the temporal characteristics of F_{st}. The three AGZs are: North-eastern plains zone (NEPZ), North-western plains zone (NWPZ) and Central zone (CZ). The grids within these AGZs were selected such that they had the largest percentage of grid area under wheat cultivation; this and other details related to wheat productivity in these grids are provided in Table 5-1.

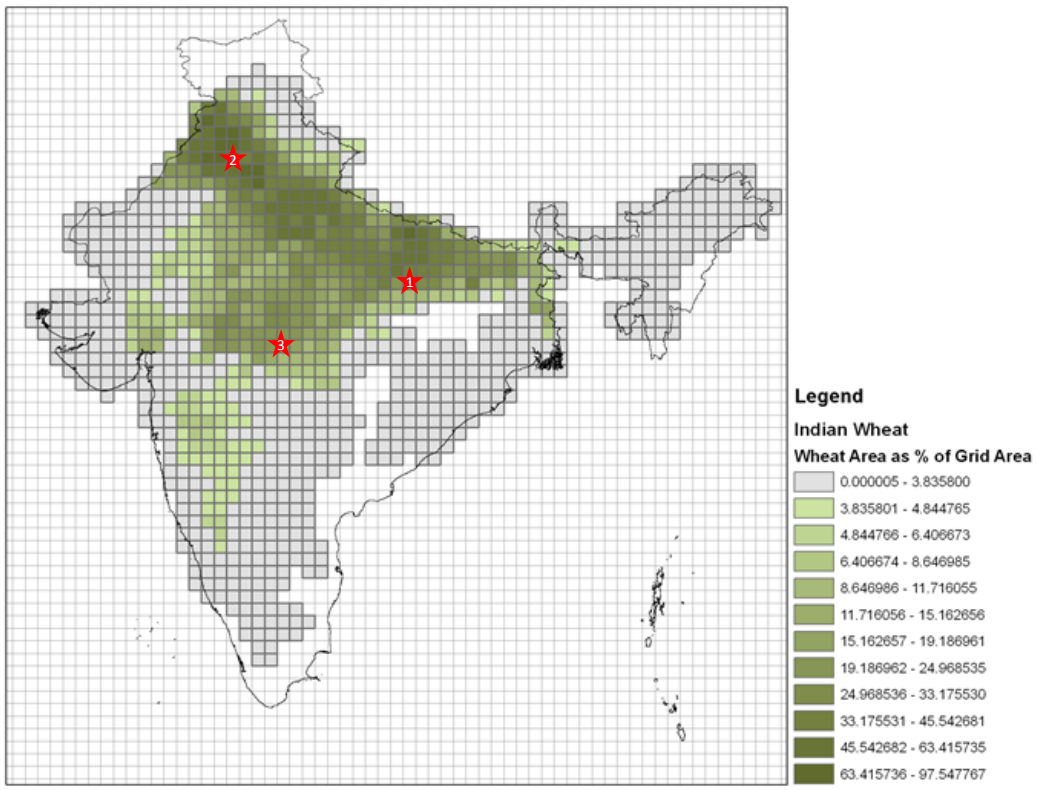

Figure 5-1: MATCH model grids under wheat cultivation, defined as fraction of wheat area per grid. The data to define the wheat cropping area were described in Table 2-2. The stars indicate the location of the three grids; 1= NEPZ; 2= NWPZ; 3=CZ. This figure is same as Figure 3-3**.**

Table 5-1: Details of the location, grid fraction area, production and yield of wheat for the cropping year 1999-2000 for the three grid cells selected for further analysis in each of the AGZs.

Agro-climatic zone (AGZ)	**Latitude_ Longitude**	**Area** **% of grid area**	**Production** **1000 tonnes**	**Yield** **t/ha**
NEPZ	25°N _ 83°E	25.3	71	2.2
NWPZ	30°N _ 76°E	84.5	229	4.7
CZ	22.5°N _ 78°E	22.4	64	2.2

The average temperature and VPD meteorological conditions and average O_3 concentrations defined according to the MATCH data for the year 1999-2000 are provided in Figure 5-2 for each of the three grids; these values represent daytime averages during the F_{st} accumulation period estimated using the Indian phenology parameterization. Figure 5-2 shows that CZ has the lowest average O_3 concentration (~35 ppb v) but the highest temperature (~ 23 ^{o}C) and VPD (~ 2 kPa) values of all grids. By contrast, the NEPZ and NWPZ grids have similar mean O_3 concentrations (~ 42 ppb v), VPDs (~1.5 kPa) and lower temperatures that range between ~19 and 22 ^{o}C). In the following section, a detailed analysis of F_{st} characteristics for these individual grids is provided to identify the seasonal and diurnal variation in F_{st} and how these characteristics might vary between AGZs. This analysis also helps identify the most important model components that modify F_{st}.

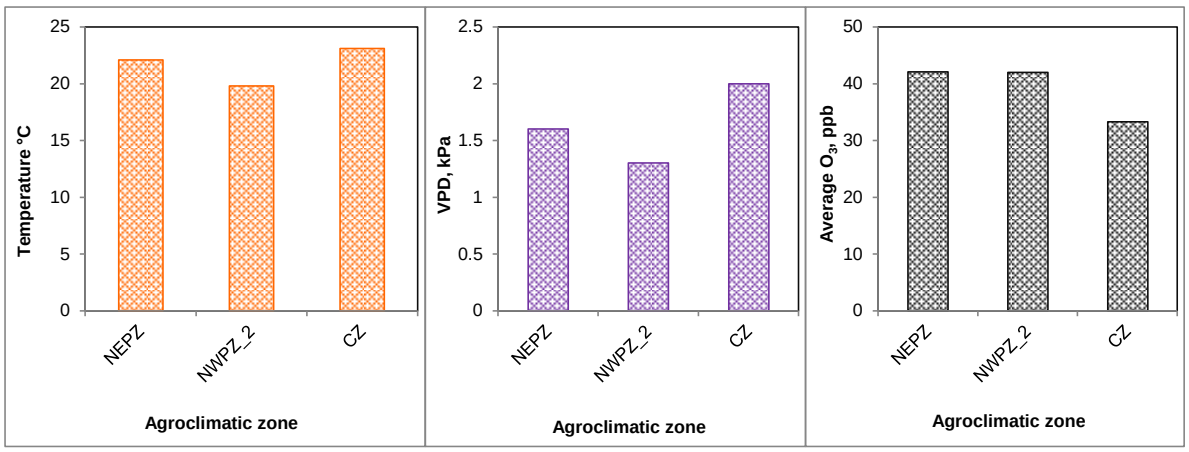

Figure 5-2: Hourly daytime average meteorological conditions and average O_3 concentrations during the O_3 accumulation period calculated using the Indian wheat phenology (IN) with the MATCH data for the cropping year 1999-2000 for the three AGZs in India.

In order to study the seasonal and diurnal trends in F_{st} and the influence of f_{temp}, f_{light} and f_{VPD} at different stages of wheat development, the wheat O_3 accumulation period was divided into three periods (Stage I, II and III) based on GDD (Figure 5-3). The reason for using GDD was to have the greatest consistency in the different stages of wheat development between the periods (see Chapter 4). The stages were divided based on the GDD in the following way;

(i) Stage I- the period between A_{start} and mid-anthesis which will capture the first half of the anthesis period.
(ii) Stage II – the period between mid-anthesis and mid-way between mid-anthesis and A_{end} which captures the second part of anthesis.
(iii) Stage III – the period between mid-way between mid-anthesis and A_{end}, and A_{end} This stage is during the grain filling period.

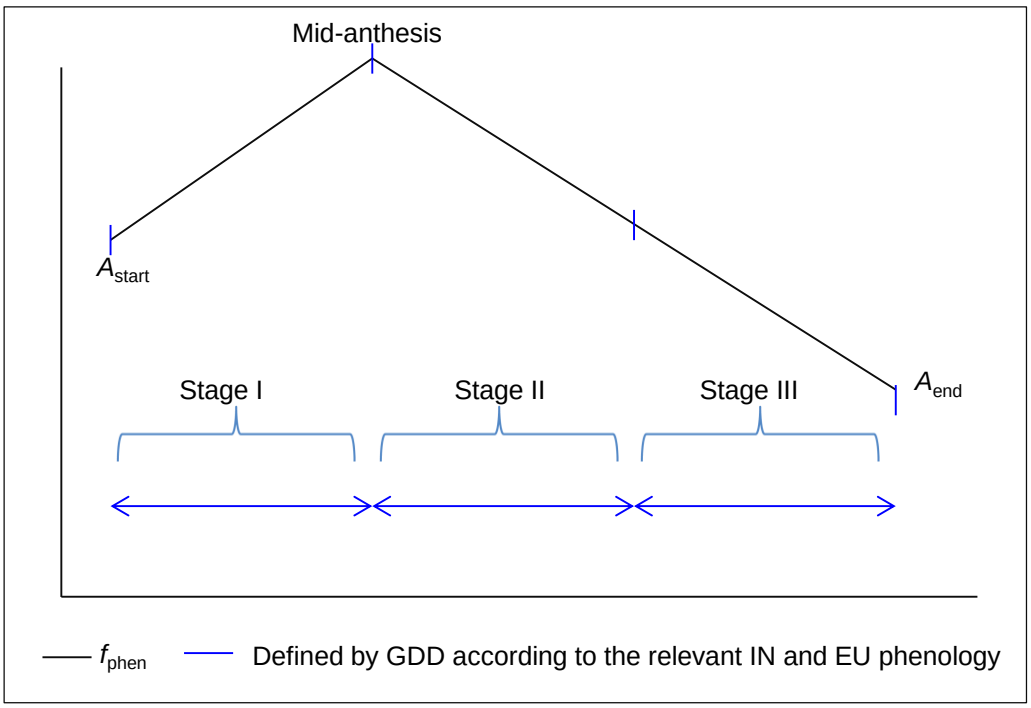

Figure 5-3: The 3 different stages of the O_3 accumulation period that have been used for further analysis of F_{st} characteristics; these periods are defined by GDD.

The results are presented here with a focus on addressing the research aims listed earlier; as such, results are divided into three main sections; the first compares the F_{st} results with corresponding estimates of AOT40 in terms of spatial distribution of risk and an analysis of how these indices accumulate over the course of the growing season; the second focuses on identifying key model components (g_{max}, phenology, and environmental conditions) that are most influential in modifying F_{st} and the third addresses the robustness of the F_{st} parameterization by comparing F_{st} results derived using IN and EU parameterisations.

5.2 Comparison of F_{st} and AOT40 risk assessment methods for India.

This section compares the F_{st} results with corresponding estimates of AOT40 in terms of risk assessment. This is achieved by comparing the spatial and temporal distribution of POD_6 and comparable $AOT40_A$ values; relative exceedances of POD_6 and AOT40 critical levels; and the variation in estimates of yield and crop production losses

estimated using both indices. This latter analysis is intended to provide an indication of how spatial variations in indices scale to effects on production. To assess differences in the temporal accumulation of POD_6 and AOT40 between AGZs over the wheat growth period, data from the 3 AGZs are analysed.

5.2.1 Spatial variation in F_{st} and AOT40 across India

Chapter 4 described the parameterization of the IN wheat F_{st} model; one of the most difficult parameters to define was flag leaf g_{max}. The g_{sto} data collected for Indian wheat indicated that, when considering all canopy leaves, an average maximum g_{sto} of 350 mmol O_3 m^{-2} PLA s^{-1} could be defined. However, when the g_{sto} data for flag leaves only were considered a g_{max} of 230 mmol O_3 m^{-2} PLA s^{-1} was obtained. The g_{sto} data are not extensive enough to really be sure which of these values is most likely to represent g_{max} for wheat cultivars growing in India. Given the uncertainties in this parameterization the analysis in this section has been performed using two different g_{max} values i) the Indian flag leaf g_{max} value of 230 mmol O_3 m^{-2} PLA s^{-1} established from analysis of Indian g_{sto} data presented in Chapter 4 (defined as IN_{230}) and ii) the European flag leaf g_{max} value of 450 mmol O_3 m^{-2} PLA s^{-1} (LRTAP, 2008) (defined as IN_{450}).

Figure 5-4 maps the POD_6 results on the application of the F_{st} model using both IN parameterizations (IN_{230} and IN_{450}) and comparable $AOT40_A$ values for the entire Indian modelling domain. The POD_6 values calculated using the IN_{230} parameterization show very low values with very little exceedance of the flux critical level (see Chapter 3) of 1 mmol O_3 m^{-2} PLA across India, only in the states of West Bengal and Assam, which both fall within the NEPZ AGZ are values greater than 1 mmol O_3 m^{-2} PLA found though exceedances are less than 1 mmol O_3 m^{-2} PLA. Across much of central and western India POD_6 values are zero. The POD_6 values calculated using the IN_{450} parameterization are rather different, there is more spatial variability and a larger range of POD_6 across India. In the IGP region and the south-east coastal region the POD_6 values show high variability ranging between 1 to >8 mmol O_3 m^{-2} PLA. Across much of western (south-west NWPZ) and central India (CZ), the POD_6 values are greater than 0 but still remain below the flux critical level of 1 mmol O_3 m^{-2}. The higher POD_6 values highlight the importance of g_{max} in determining F_{st} and hence POD_6. .

By comparison, high $AOT40_A$ values were also observed across the IGP region with values in the range of 3 ppm h to above 8 ppm h. For example, in both NWPZ and NEPZ AGZs of the IGP region, the $AOT40_A$ values vary between 3 ppm h to > 8 ppm h $AOT40_A$. $AOT40_A$ values are also high, frequently between 2 and 3 ppm h, in the south-eastern coastal area. There are also coastal regions, especially along the east coast of India with high $AOT40_A$ values frequently reaching highs of between 5 and 6 ppm h (Figure 5-4). Although the spatial pattern and range of $AOT40_A$ values are broadly similar to IN_{450} POD_6 values there are some subtle differences. For example, POD_6 values range from 3 to > 8 mmol O_3 m^{-2} PLA in the NEPZ, while in NWPZ the highest POD_6 values only reach 6 mmol O_3 m^{-2} PLA. The higher NEPZ values could be attributed to high O_3 concentrations, however, the NWPZ shows lower POD_6 values but higher $AOT40_A$ values suggesting that other factors may be limiting F_{st} in this NEPZ. $AOT40_A$ is high in both west (reaching 4 ppm h) and east (reaching 6 ppm h) coastal areas; by comparison POD_6 values are higher only in the eastern coastal areas (reaching 4 mmol O_3 m^{-2} PLA). The high POD_6 values in east coastal regions could be attributed to the high O_3 concentrations but the low POD_6 values in the west coast (<0.5 mmol O_3 m^{-2} PLA) again suggest that factors other than O_3 concentration are limiting F_{st}.

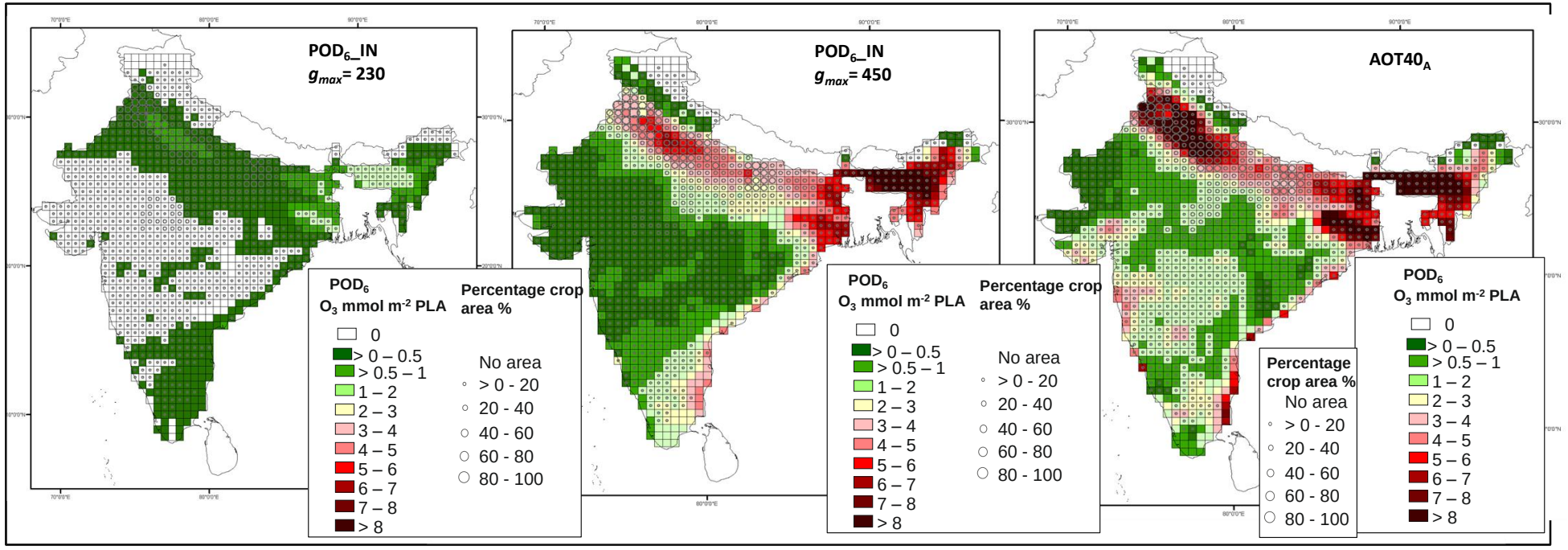

Figure 5-4: Flux- and concentration-based O_3 risk to wheat in India (a) Indian parameterization with a g_{max} of 230 mmol O_3 m^{-2} PLA s^{-1} (IN_{230}); (b) Indian parameterization with a g_{max} of 450 mmol O_3 m^{-2} PLA s^{-1} (IN_{450}) and (c) the $AOT40_A$ in ppm h. All risk indices are estimated for the O_3 accumulation period for the cropping year 1999-2000. Also shown by the circle symbols are the wheat production areas, the size of the circle $AOT40_A$ indicates the extent under wheat cultivation within each MATCH grid.

5.2.2 Variation in relative critical level exceedance, yield and production losses based on F_{st} and *AOT40* across India

The previous section has shown that there are differences in the spatial distribution of risk identified using the flux- and concentration-based methods. Although both $AOT40_A$ and POD_6 indices are high in the NEPZ and NWPZ AGZs, which form a large part of the important wheat growing IGP region, there are subtle differences in the relative magnitude of these two indices, these differences also occur across other parts of India. In order to investigate the true relative difference in the magnitude and spatial distribution of these indices it is necessary to standardize the index values; this can be done either by using their respective critical levels or through translating the potential risk (i.e. as indicated through POD_6 and AOT40) into estimates of yield and production loss. Estimates of production losses have the added benefit of assessing the implications of spatial differences in potential O_3 risk in relation to the location of the important wheat production areas across India. Currently, critical levels, and the concentration- or flux-response relationships from which they have been derived, have been established using European parameterisations. Therefore, in the analysis presented in this section it has been necessary to use the EU flux model parameterization and AOT40 calculated over the full three month growth period to derive the indices. For comparison, the POD_6 values calculated using the IN_{450} are also shown; section 5.3 of this Chapter investigates the differences in the EU and IN_{450} parameterisations in more detail to help interpretation of these results in the discussion.

5.2.2.1 Relative critical level exceedance (R_{CL})

One means of comparing the spatial differences in the relative magnitude of these two indices is to standardize the indices according to their respective critical levels (see Chapter 3). The results of such standardization are presented in Figure 5-6, here the R_{CL} for POD_6 values (R_{CL_POD6}) are estimated using the EU parameterisation and the R_{CL} for AOT40 values (R_{CL_AOT40}) are estimated for the full 3 month growth period (as defined in Chapter 2).

Comparing the EU R_{CL_POD6} and the R_{CL_AOT40} it is clear that the critical levels of both indices (1 mmol O_3 m^{-2} PLA for R_{CL_POD6} and 3 ppm h for R_{CL_AOT40}) are exceeded across almost all of India. Figure 5-5 shows a scatter plot of POD_6 values calculated using the EU parameterization against 3 month AOT40 values for all grids. When the R_{CL_POD6} exceedances are low (< 2.5) there seems to be no particular trend in the relationship between in exceedances of the two indices but at R_{CL_POD6} > 2.5, the R_{CL_POD6} gives higher exceedances than R_{CL_AOT40}. There are some grids in the Northern Plain Zone where R_{CL_POD6} shows no exceedance while R_{CL_AOT40} shows high exceedance, ranging from 3 to 8 times the critical level. There are also differences in the magnitude and spatial distribution of exceedances (and hence potential impact) across the region between the two indices R_{CL_AOT40} and R_{CL_POD6}; although both show high exceedances in the IGP region the R_{CL_POD6} index suggests higher exceedances across more of the IGP region, especially the NEPZ, than the R_{CL_AOT40}. Estimation of R_{CL_POD6} also estimates the largest exceedances to occur in the north eastern part of India with frequent occurrences of values above 7 times the critical level, in contrast the R_{CL_AOT40} values in this region are relatively low only reaching 4 to 5 times the critical level. Finally, the central and western parts of India which include the CZ region show some areas having higher R_{CL_AOT40} of 1 to 2 times the critical level whilst the corresponding R_{CL_POD6} critical level is always below 1.

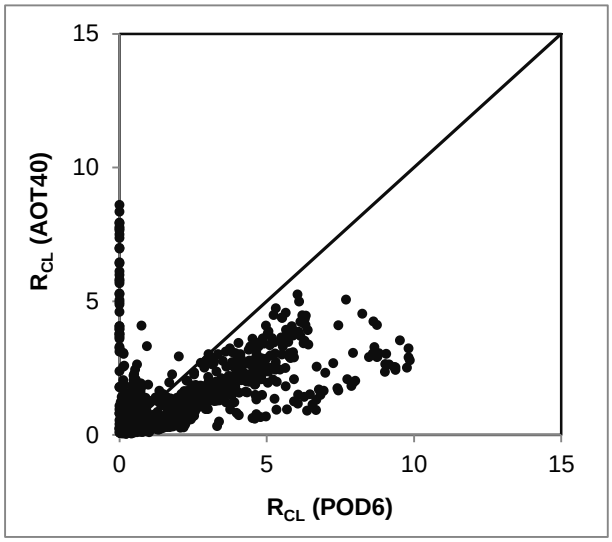

Figure 5-5: Relationship between R_{CL_POD6} and R_{CL_AOT40}. The data points represent all the grids in India.

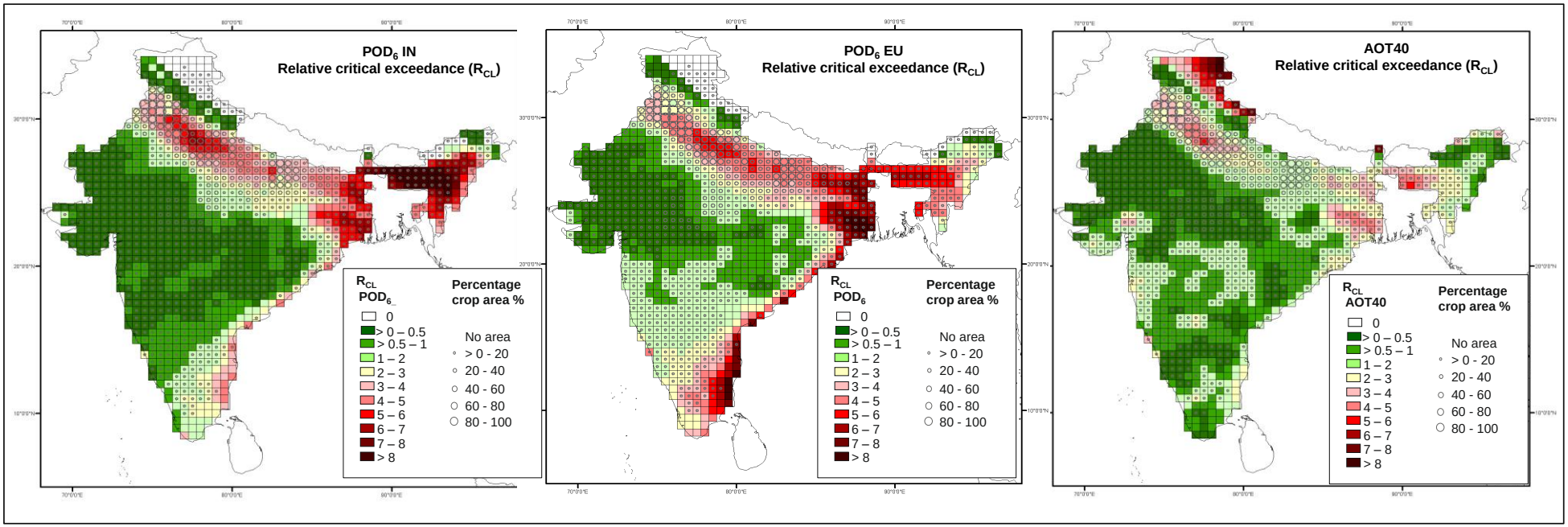

Figure 5-6: The relative exceedances of the respective critical levels for POD_6 (R_{CL_POD6}; estimated using the both EU and IN_{450} model) and AOT40 (R_{CL_AOT40}; accumulated over the 3 month growth period defined in Chapter 2) for wheat across India during the cropping year 1999-2000.

5.2.2.2 Relative yield loss (RYL) and crop production loss (CPL)

The differences seen in the spatial distribution of POD_6 (based on the EU parameterization) and three month AOT40 are translated into RYLs. Results are shown as a scatter plot in Figure 5-7 and spatially in Figure 5-8 with values derived on application of the respective flux- or concentration-response relationship (see Chapter 3). These figures provide an indication of how the yield loss estimates across India vary dependent upon the risk index used. The RYL was assessed using POD_6 values based on the EU parameterization and the AOT40 index. The POD_6 indices tend to show higher RYLs than AOT40 (Figure 5-7). However, there are exceptions, some grids show high RYL_{AOT40} (as high as 40 %) whilst RYL_{POD6} show no losses. The RYL is estimated to be highest in the IGP region (Figure 5-8), which includes the NEPZ and NWPZ regions (with yield losses of 10 to 35%), RYLs are also high in the eastern Coastal region (again with losses between 10 to 35%). The average RYL for the entire wheat producing area estimated according to the POD_{6_EU} and POD_{6_IN} values is 11.7% and 11.5% respectively, while using AOT40 it is 8.5%.

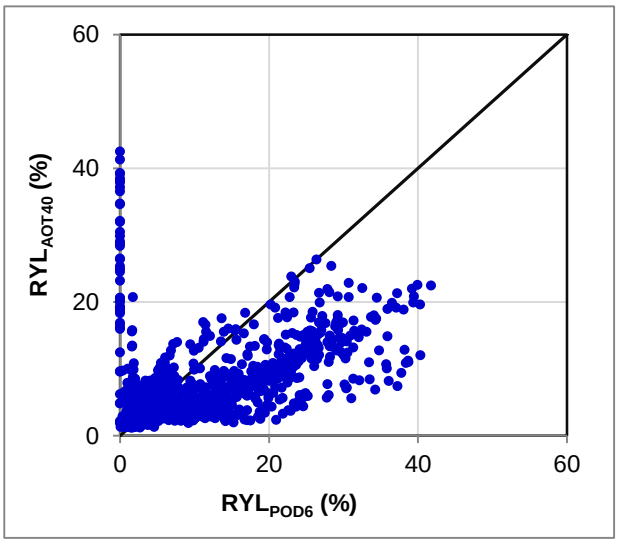

Figure 5-7: Relationship between RYL_{POD6} and RYL_{AOT40}. The data points represent all the grids where wheat is grown.

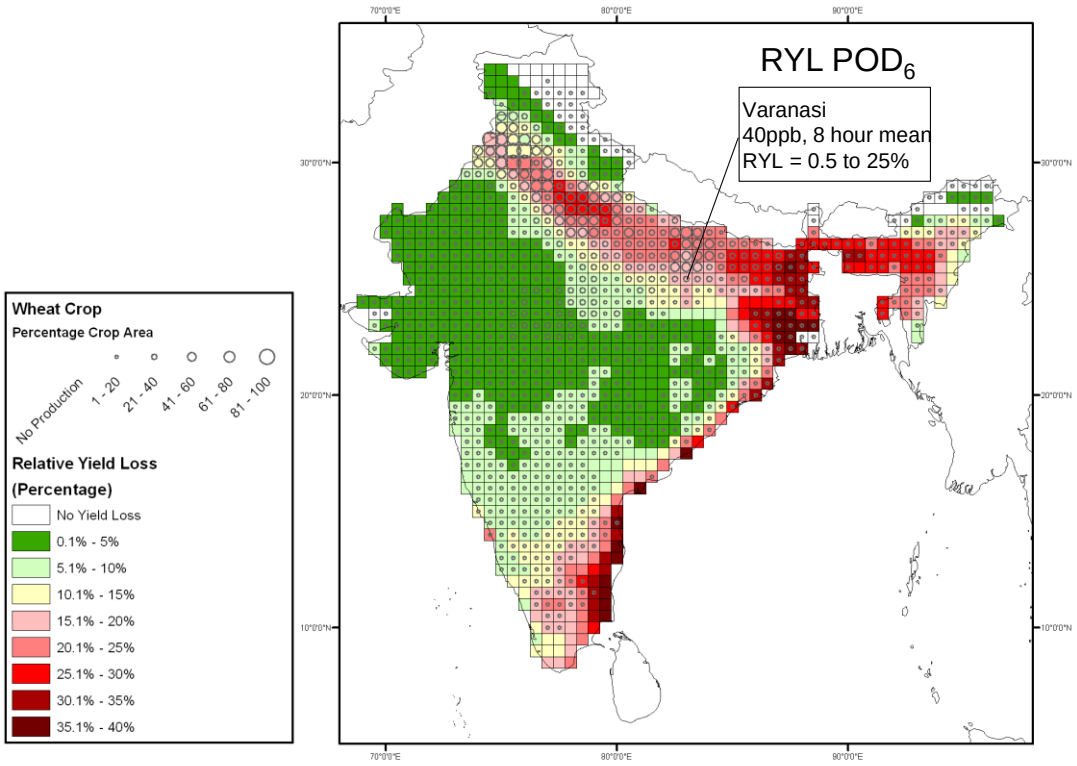

Figure 5-8: Estimates of RYL for wheat for the cropping year 1999-2000 based on POD_6 calculated using the EU parameterization and associated European wheat O_3 flux-response functions. The POD_6 is calculated for all the grids in India. The circles indicate percentage of grids under wheat cultivation in the POD_6.

The RYL based on POD_6 and three month AOT40 are translated into CPLs. Results are shown as a scatter plot in Figure 5-9 and spatially in Figure 5-10. These figures provide an indication of how the risk posed by O_3 to crop production across India depends not only on yield loss estimates but also on cropping intensity in the region. The relationship between POD_6 and AOT40 in terms of CPL is different from that of RYLs. The scatter plot shows that CPL_{POD6} estimates are always higher than CPL_{AOT40} but in grids with high CPL, CPL_{POD6} and CPL_{AOT40} give more or less similar values.

In Figure 5-10 both the indices clearly show that the IGP region is at risk with CPLs of > 12 thousand tonnes per grid across the region and reaching as high as 2000 to 300 thousand tonnes of losses. In the NWPZ, the extent of CPL_{POD6} is quite similar to that of CPL_{AOT40} while in the NEPZ, CPL_{POD6} is significantly greater than CPL_{AOT40}. The total wheat production loss due to O_3 estimated according using the EU parameterization in conjunction with the European wheat flux-response relationship (Pleijel *et al.*, 2007) is

14.6 million tonnes which is 19% of the total wheat production in India for the year 2000 as compared to 13% yield losses calculated using AOT40.

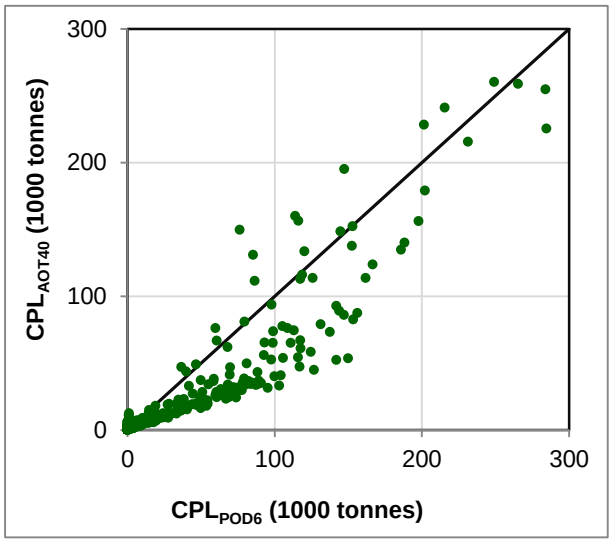

Figure 5-9: Relationship between RYL_{POD6} and RYL_{AOT40}. The data points represent all the grids where wheat is grown.

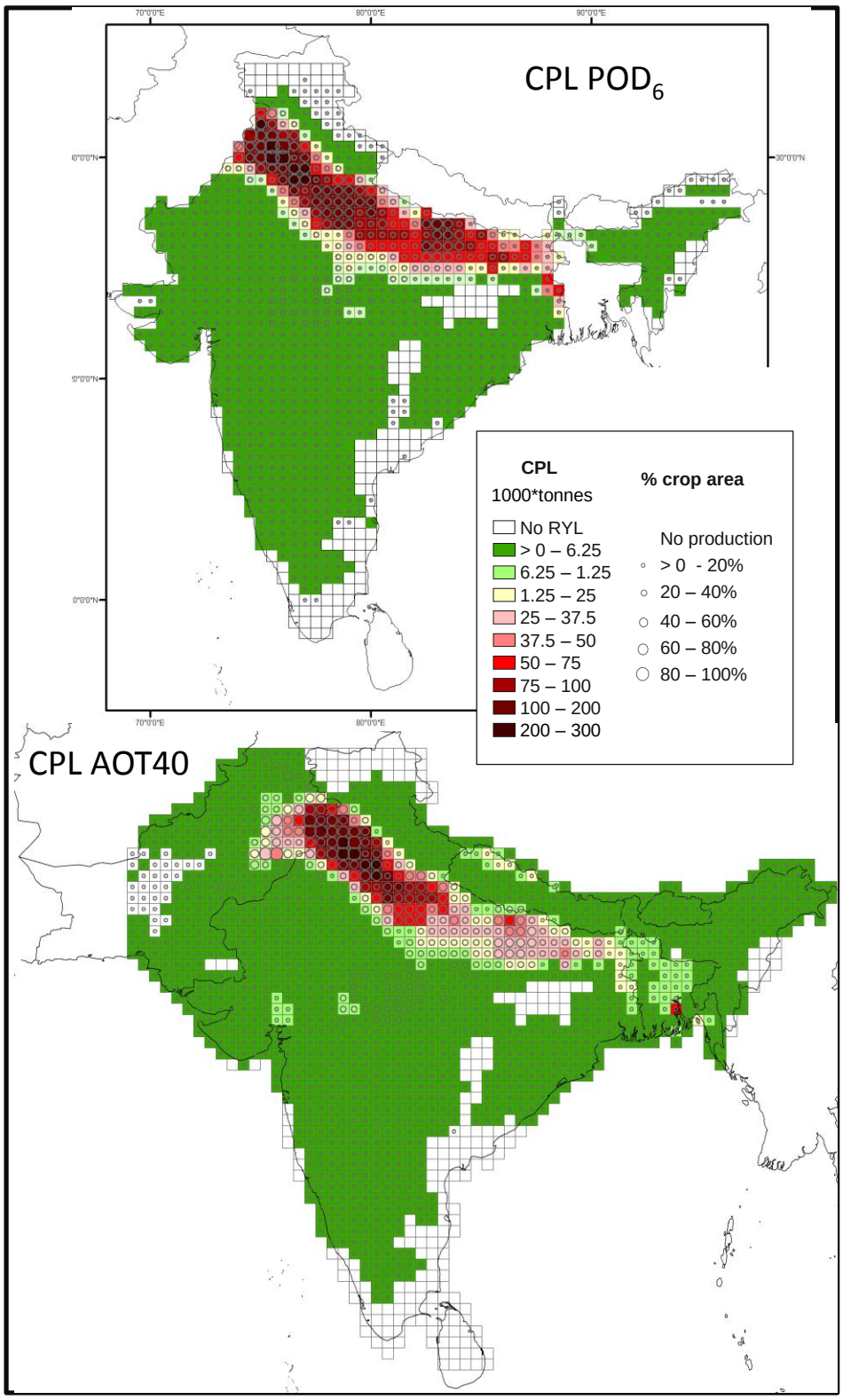

Figure 5-10: Estimates of CPL for wheat for the cropping year 1999-2000 based on (a) POD_6 (CPL_{POD6}) calculated using the EU parameterization and associated European wheat O_3 flux-response function and (b) AOT40 (CPL_{AOT40}) accumulated over the 3 month growth period defined in Chapter 2. The POD_6 is calculated for all the grids in India. The circles indicate percentage of grids under wheat cultivation in the POD_6.

5.2.3 Temporal variation in F_{st} and AOT40 within the important wheat growing AGZs

The previous section has shown that spatial variation exists between the the flux and AOT40 based indices, both in terms of potential as well as estimated actual risk. This implies that factors other than O_3 concentration are important in determining F_{st}. and hence POD_6. To investigate this, the variation in temporal characteristics of both POD_6 (here calculated using the IN_{450} parameterisation) and $AOT40_A$ are compared for the three grids that were selected for further investigation within the important wheat growing AGZs. The IN_{450} F_{st} and POD_6 values are compared with the $AOT40_A$ values since these are considered more likely to reflect the index for Indian conditions both in terms of the timing of the growth period and g_{sto} response to prevailing environmental conditions. These comparisons aim to assess how the evolution of the two indices may vary both over the entire O_3 accumulation period as well during the daytime period in an effort to identify those periods when F_{st} has a greater tendency to diverge from $AOT40_A$.

The end of growth period $AOT40_A$ and POD_6 values for these three grids are given in Table 5-2; both indices suggest the same ranking of sensitivity with NWPZ > NEPZ > CZ in terms of greatest risk from O_3 The $AOT40_A$ and F_{st} values are highest in NWPZ (9.6 ppm h and 5 mmol O_3 m^{-2} PLA respectively) and lowest in CZ (0.8 ppm h and 0.3 mmol O_3 m^{-2} PLA respectively).

Table 5-2: POD_6 (using the IN_{450} model parameterization) and $AOT40_A$ estimates for the three AGZs.

Agro-climatic zone (AGZ)	**POD_6 mmol O_3 m^{-2} PLA**	**$AOT40_A$ ppm h**
NEPZ	2.4	4.0
NWPZ	5.0	9.6
CZ	0.3	0.8

In order to identify key differences in the general relationship between AOT40 and F_{st}, hourly F_{st} values were plotted along with corresponding hourly O_3 concentration; the results are presented in Figure 5-11. Figure 5-11 firstly emphasizes the variation in O_3 concentration that exists between the three AGZ grids with a high number of O_3 concentrations above 60 ppb occurring in NWPZ whilst in contrast concentrations barely exceed 40 ppb in CZ. Although there is an obvious relationship between O_3 concentration and F_{st}, with highest F_{st} values are only possible under higher O_3 concentrations there are also many instances where higher concentrations do not translate into higher F_{st} values, as evidenced by the cloud of data points within the boundary limits of the relationship (e.g. for NWPZ O_3 concentrations above 60 ppb can results in F_{st} values that range between 0 and almost 20 nmol O_3 m^{-2} s^{-1}. The even distribution of points within these clouds seem common to all AGZs though for NEPZ and CZ there are far fewer instances of low F_{st} values below 30 ppb than in NWPZ. This would suggest that in NWPZ there are conditions that occur for any O_3 concentration that will limit F_{st} whilst for NEPZ and CZ, limits to F_{st} tend to be associated with O_3 concentrations above 30 ppb. It is the relationship between O_3 concentrations above 40 ppb and F_{st} values above 6 nmol O_3 m^{-2} s^{-1} that is of most interest when considering the POD_6 and AOT40 indices. In this respect the figures clearly show that there are substantial number of hours in all grid cells when O_3 concentrations are lower than 40 ppb yet F_{st} values are greater than 6 nmol O_3 m^{-2} s^{-1} and conversely, when O_3 concentrations are higher than 40 ppb but F_{st} values are lower than 6 nmol O_3 m^{-2} s^{-1}. These conditions will lead to differences in the rate of accumulation of the two indices and ultimately differences in the spatial pattern seen in Section 5.2.1.

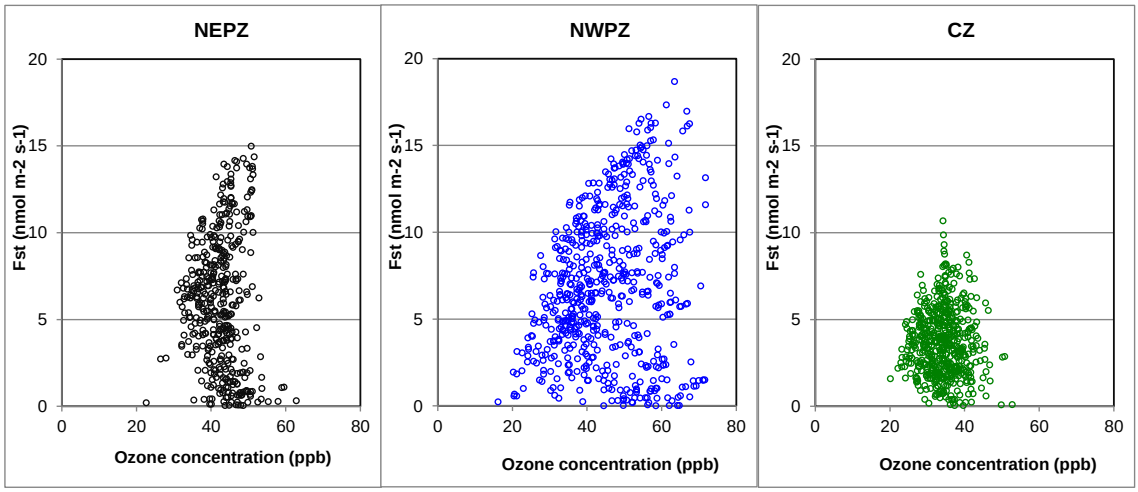

Figure 5-11: Relationship between hourly O_3 concentrations and F_{st} values for the three AGZ grids during the O_3 flux accumulation period. Also show are dotted lines that indicate the O_3 concentrations and F_{st} values that contribute to the AOT40 and POD_6 indices.

5.2.3.1 Seasonal variation in F_{st} and $AOT40_A$ for the three AGZ grids

The accumulation of POD_6 and $AOT40_A$ for each of the three AGZs is shown in Figure 5-12; these show large variability between the three grids in the relationship between POD_6 and the corresponding $AOT40_A$ values. Most striking is the fact that most of the accumulation of POD_6 occurs at the beginning of the growth period whilst the opposite is true for $AOT40_A$. For example, in the NEPZ grid, the POD_6 values increase rapidly to a value of 2.4 mmol O_3 m^{-2} before the accumulation period is halfway through at the halfway mark of the accumulation period; in contrast the $AOT40_A$ values accumulate slowly during this period reaching only 1.9 ppm h. The $AOT40_A$ then continues to increase doubling to a value of 4 ppb h while there is no further increase in POD_6 values. Similar trends are observed in the NWPZ and CZ grids.

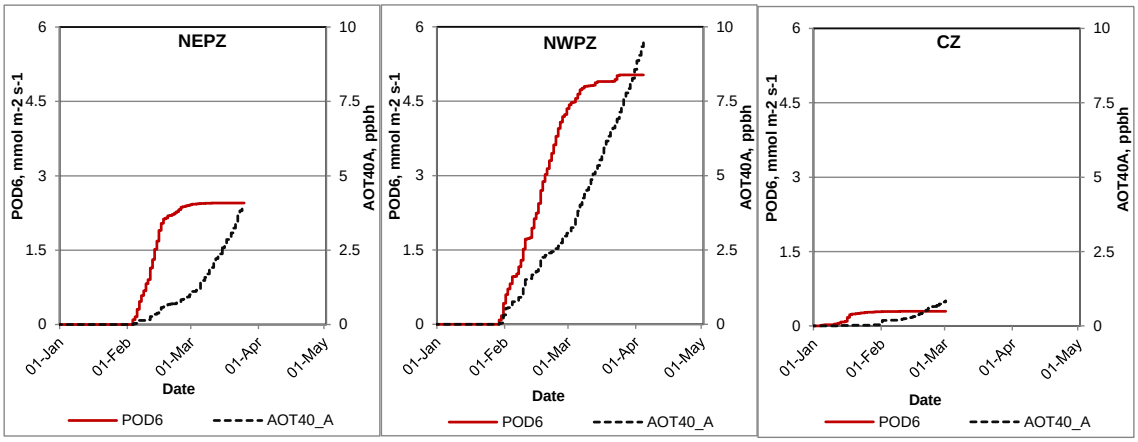

Figure 5-12: Accumulation of POD_6 and $AOT40_A$ during the O_3 accumulation period for the three selected grids of each AGZ (NEPZ, NWPZ and CZ). The figure starts from 1st Jan but the accumulation period starts from a different date.

This shows that for all three grids the higher O_3 concentrations above 40 ppb tend to occur more frequently later in the growth period, in contrast the O_3 concetrations and environmental conditions most likely to lead to higher F_{st} occur at the beginning of the growth period and that, towards the end of the growing season, environmental factors limiting F_{st} will reduce the stomatal uptake of the higher O_3 concentrations. The reasons for these differences in the accumulation of POD_6 and $AOT40_A$ are clearly evident from Figure 5-13; this shows daily maximum F_{st} values plotted along with the corresponding 3 day moving average O_3 concentrations for the three grids, NEPZ, NWPZ and CZ.

All three grids show the same general trend with daily average O_3 concentrations increasing gradually over the course of the O_3 accumulation period; in contrast, the daily maximum F_{st} initially increases but after a relatively short length of time shows a rather rapid decline as to reach its lowest values at the end of the growth period (Figure 5-13). Although the pattern of these F_{st} and O_3 concentration profiles are the same across all AGZs the magnitudes of the variables are quite different. In addition, the timing and length of the O_3 accumulation periods vary by AGZ. The NWPZ grid experiences the longest accumulation period; the average O_3 concentrations are broadly similar those that occur in NEPZ although the values at the start of the accumulation period are slightly higher at ~ 30 ppb in NEPZ compared with ~20 ppb in NWPZ; this may be due to the earlier in the year start to the accumulation period in NWPZ.

However, the maximum F_{st} values are rather different; in NEPZ values increase from ~ 10 to 14 nmol O_3 m^{-2} PLA s^{-1} and then past 80 days after sowing decrease rapidly to values less than 6 nmol O_3 m^{-2} PLA s^{-1} after ~110 days after sowing. By contrast NWPZ shows more frequent occurrences of high F_{st} values from 80 to 100 days after sowing with a less steep decline such that only after 120 days after sowing are maximum F_{st} values always below 6 nmol O_3 m^{-2} PLA s^{-1}. The CZ grid is quite different from both the other grids in terms of the magnitude of O_3 concentrations and F_{st} values; average O_3 concentrations never exceed 40 ppb and maximum F_{st} values only exceed 6 nmol O_3 m^{-2} PLA s^{-1} up until ~80 days after sowing and then decline; this grid also experiences a shorter O_3 accumulation period, though not too dissimilar to the NEPZ grid.

The occurrence of increasing O_3 concentrations associated with a tendency for decreasing F_{st} values again indicates that factors other than O_3 concentration are influencing F_{st}; the analysis presented in this section has shown that such divergences are particularly influential at O_3 concentrations higher than 60 ppb v.

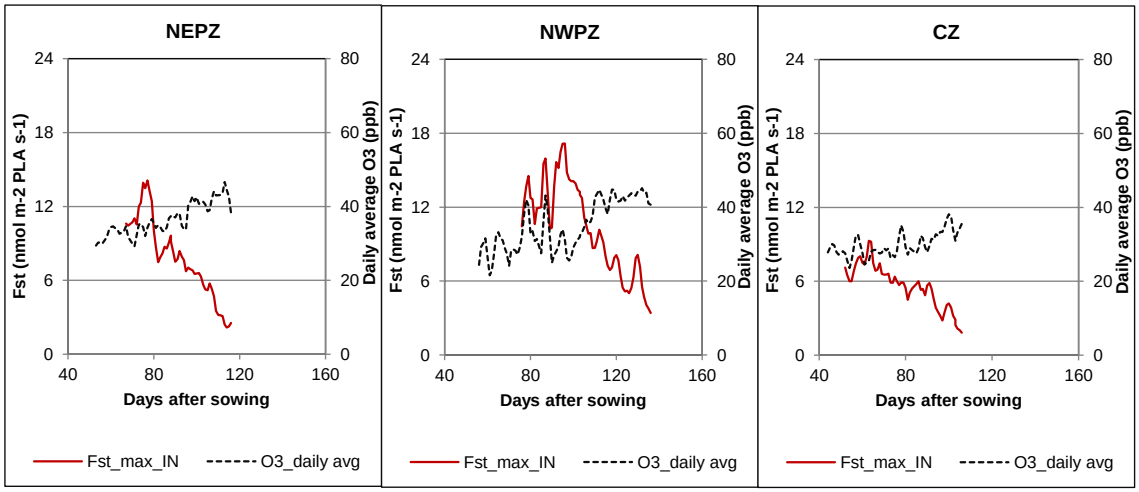

Figure 5-13: Daily maximum stomatal O_3 flux (F_{st}) calculated using IN parameterization, and the corresponding daily average O_3 concentration for grids of the three AGZs. The O_3 concentrations are given as 3-day moving averages.

5.2.3.2 Diurnal variation in F_{st} and $AOT40_A$ for the three AGZ grids

This section investigates the co-variation in changes in O_3 concentration and g_{sto} and their influence on F_{st} over the course of the diurnal period. Figure 5-14 describes a diurnal profile where each hour represents the average O_3, g_{sto} or F_{st} of all hours during the accumulation period; plots are made for all three AGZ grids. From Figure 5-x it is apparent that there is a general pattern to the O_3 concentration profile which is broadly replicated across AGZs. All O_3 concentrations are reduced over the nighttime period such that early morning values are ~20 ppb v; O_3 concentrations have a tendency to increase from this low which occurs at around 6:00 hours over the course of the daylight period; however the rate of increase differs between AGZs. It is also worth noting the O_3 concentrations remain high for some hours after the sunset such that the f_{light} function limits F_{st} during these periods; this is discussed in more detail in Section 3.2. The NWPZ grid has the highest rate of increase with O_3 concentrations reaching ~ 60 ppb v in the evening (18:00 hours); NEPZ follows the same profile but the end of day O_3 concentrations are lower with average values reaching slightly less than 50 ppb v; CZ has the lowest end of day values at only 40 ppb v and also shows a slight midday dip in O_3 concentrations. In contrast, the g_{sto} values show a rather different profile; in NWPZ, the g_{sto} values rapidly increase in the morning (7:00 to 9:00 hours) reaching a peak at 11:00 hours (>200 mmol O_3 m^{-2} PLA s^{-1}) and then start to gradually decrease in the afternoon hours sharply decreasing between 17:00 to 18:00 hours. In NEPZ and CZ the g_{sto} is highest during the morning hours before 11:00 hours when values reach ~ 165 mmol O_3 m^{-2} PLA s^{-1}) and then start to decrease gradually over the course of the day. As such, in NEPZ and CZ, during the morning hours the O_3 concentrations are lower but the g_{sto} values are high, leading to higher F_{st}. However, during the late afternoon, even though O_3 concentrations continue to increase, g_{sto} is reduced which limits the flux of O_3 into the leaves. In NWPZ, the O_3 concentrations as well as g_{sto} remains relatively high over the entire course of the daylight period and therefore the F_{st} values are higher for this grid than the others. In all the three grids it is clear from Figure 5-14 that the diurnal trend in O_3 flux tends to be more closely related to the diurnal trend in g_{sto} than O_3 concentration.

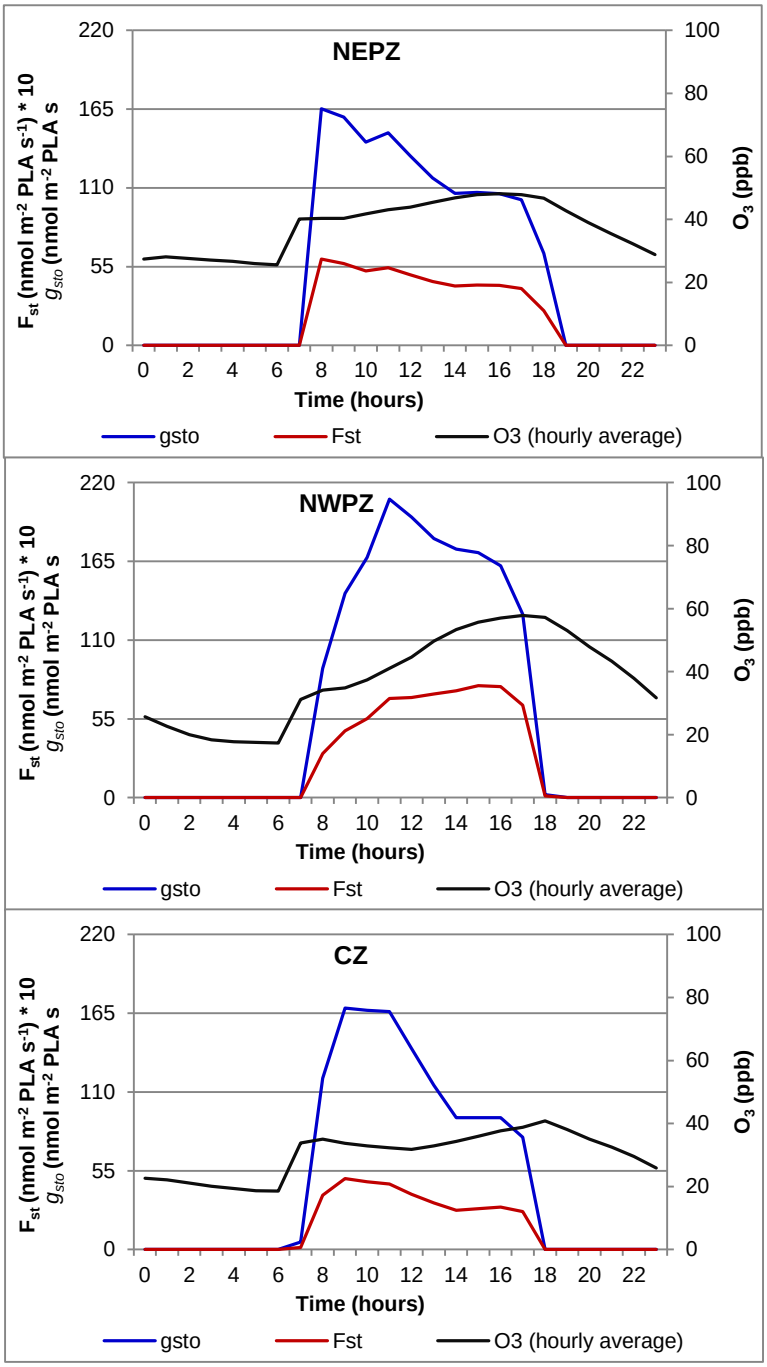

Figure 5-14: Hourly diurnal O_3 concentration g_{sto} and F_{st} values averaged for the O_3 accumulation period for the NEPZ, NWPZ and CZ grids.

The analysis shown in Figure 5-14 provides a broad indication of co-variation between O_3 concentrations, g_{sto} and resulting F_{st} values for the entire O_3 accumulation period. It is also useful to consider whether such co-variation is likely to differ within different stages of this period since the environmental conditions are known to will change over

time. To investigate this Figure 5-15 shows differences in diurnal variation of F_{st} for each of the stages I to III with the aim of understanding the diurnal characteristics of flux.

Figure 5-15 shows that the restrictions to F_{st} increase during the O_3 accumulation period with stage I showing high F_{st} values during the bulk of the daylight period and with F_{st} values decreasing in stage II and further decreasing in stage III. The limitation to F_{st} also becomes more severe in the afternoon periods as the stages progress. There are also differences between the AGZ grids; stage I for NEPZ and NWPZ show little limitation to F_{st} with values ranging between 9 to 14 nmol O_3 m^{-2} PLA s^{-1}, in stages II and III the NEPZ limitation increases, especially in the afternoon period when F_{st} values decrease to 3 nmol O_3 m^{-2} PLA s^{-1} or below whilst in NWPZ limitations to F_{st} occur more consistently across the entire daylight period. In CZ all stages show a decreased F_{st} in the afternoon period which extenuates as the stages progress.

This again suggests the presence of factors effecting F_{st} especially during the afternoon hours. The following section explores the reasons for both the seasonal and diurnal limitations to F_{st} that have been shown in this section.

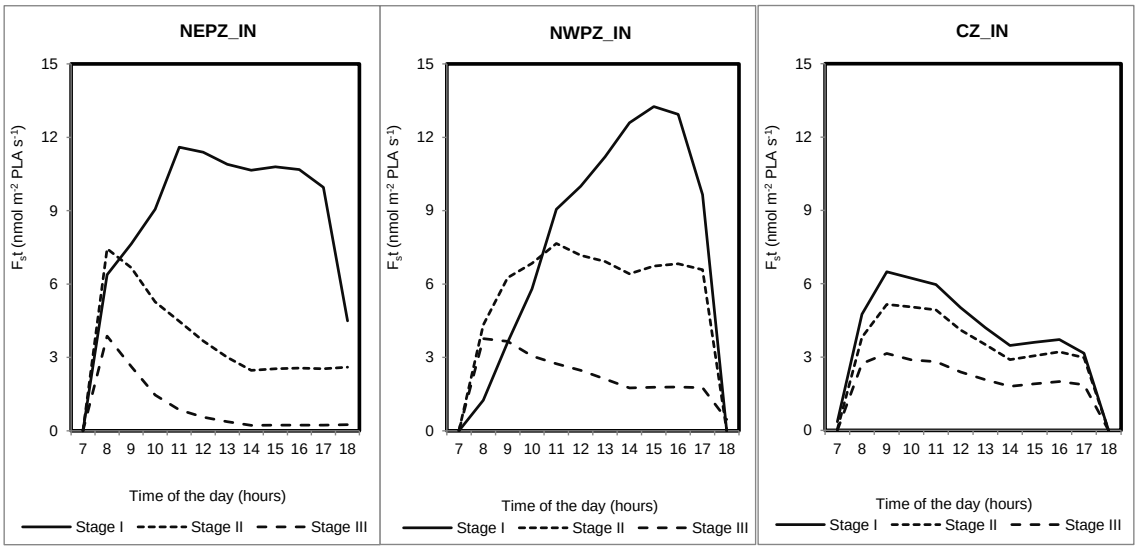

Figure 5-15: Hourly diurnal F_{st} (nmol O_3 m^{-2} PLA s^{-1}) values averaged for each of the three stages (I to III) of the O_3 accumulation period for the NEPZ, NWPZ and CZ grids.

5.3.2 Factors limiting F_{st}

The previous section has clearly demonstrated that high O_3 concentrations do not necessarily translate into high F_{st} values; similarly, F_{st} values that contribute to the accumulation of the POD_6 index are not always associated with O_3 concentrations above 40 ppb v. This indicates that there is some substantial variation in the O_3 concentrations contributing to the POD_6 and AOT40 indices which is reflected in the differences seen in the spatial patterns of these two indices across India. Since these differences affect the assessment of risk and subsequent yield and production losses due to O_3 it is important to try to gain a better understanding of what is driving these differences. Initial analysis has shown that high O_3 concentrations and high F_{st} diverge both over the crop growth period as well as over the course of a day and that the F_{st} closely follows g_{sto}. Therefore, it is important to investigate those aspects of the g_{sto} model that control both seasonal and diurnal F_{st} values to understand which model components are most limiting under particular conditions. As such the following section focuses on each of the g_{sto} model components, taking each in turn to identify the importance of the component in determining F_{st} and the time (either seasonally or diurnally) when the component is having greatest effect.

5.3.2.1 g_{max}

Section 5.3.1 demonstrated the substantial influence of g_{max} on F_{st} and subsequent POD_6 values through the spatial comparison of POD_6 values calculated using the IN_{230} and IN_{450} parameterisations (see Figure 5-4). The POD_6 values calculated using the IN_{230} were on average about 3% of those calculated using the IN_{450} parameterization based on the European wheat g_{max} value. The substantial differences obtained in POD_6 values when g_{max} value is changed clearly show that g_{max} is an important parameter that influences F_{st}. However, the influence is one that scales equivalently for all F_{st} estimates; i.e. it will not directly affect the co-variation in O_3 concentrations and environmental conditions and as such will not differentially limit F_{st} in relation to different levels of O_3 concentration. Therefore, the selection of g_{max} is extremely important in defining the overall magnitude of O_3 risk but not in understanding the more subtle deviations between AOT40 and POD_6.

5.3.2.2 Seasonal factors limiting F_{st}

Crop phenology, determined by the SGS, EGS and the timing and length of the O_3 accumulation period, and hence the shape of the f_{phen} function is all components of the model that affect F_{st}. This crop phenology can be considered to influence F_{st} in two ways; termed here as direct and indirect.

Direct influence

As seen in the previous section, even though the O_3 concentration increases towards the end of the O_3 accumulation period, F_{st} values show a decline as the growth period progresses (Figure 5-13). This is predominantly due to the the phenological function in the model (f_{phen}) which causes g_{sto} to increase gradually to the point at the time of mid-anthesis when g_{max} is attainable and then start to decrease from then until the end of the growth period (see Figure 5-16). Therefore, even though there are higher concentrations towards the later part of the accumulation period the F_{st} decreases due to the decrease in g_{sto} as the flag leaf ages. Although this general trend is true for all AGZs there are some important differences in the f_{phen} profile that can be seen in the three AGZ grid cells in Figure 5-16. Firstly, the differences in the start of the O_3 accumulation period are evident with CZ starting almost a month earlier than NEPZ and NWP; similarly the accumulation period finishes earlier in CZ around beginning of March whilst NEPZ finishes end of March and NWPZ early April. Hence the timing and length of the accumulation periods are very different. In addition, the profile of f_{phen} varies with a more rounded profile in NWPZ and a more peaked profile in both NEPZ and NWPZ; this reflects the lower temperatures and slower accumulation of GDD in the NWPZ grid which will impart a slightly reduced f_{phen} limitation to the F_{st} of the days within the O_3 accumulation period for this location compared to the other two.

Indirect influence

The O_3 concentration and the environmental conditions that are considered important in modifying g_{sto} and hence F_{st} (i.e. radiation, VPD, temperature, etc.) vary with time. Hence, the timing of the O_3 accumulation period is also important in determining the

prevailing O_3 concentrations and environmental conditions to which the crop is exposed and which can limit F_{st} (Figure 5-16). The importance of the influence of f_{phen} timing and prevailing environmental conditions can be seen in Figure 5-16 which, as well as showing f_{phen}, also describes the daily maximum VPD and temperature values for each AGZ grid. For comparison the f_{VPD} parameters VPD_{max} (1.2 kPa) and VPD_{min} (3.2 kPa) and the $f_{temp.}$ T_{opt} parameter (22^oC) are shown to indicate the model constraints in relation to these prevailing environmental conditions. Figure 5-16 shows that in the CZ grid, temperature and VPD value remain relatively constant throughout the O_3 accumulation period with VPD staying close to VPD_{min} throughout. However, in NWPZ and NEPZ, the temperature and VPD values increase towards the end of the accumulation period (Figure 5-16). In NWPZ and NEPZ, the daily maximum VPD values at A_{start} are close to VPD_{max} allowing full g_{sto} but these gradually increase; in the case of NEPZ the increase is so great that the maximum VPD values exceed VPD_{min} for almost a full month before the end of the growth period (Figure 5-16). The pattern is similar with temperature.

Thus in the NWPZ and NEPZ grid cells phenology in terms of the timing and length of the accumulation period is such that high temperatures and VPDs limit F_{st} more towards the end of the O_3 accumulation period even though O_3 concentrations are higher. In CZ, relatively constant conditions of high VPD, temperature and low O_3 are maintained throughout the growth period such that it is the length rather than the timing of the phonological period that is more important in this AGZ. In the CZ the effect of the temperature on the duration of the accumulation period is clear with the higher temperatures, and therefore rapid accumulation of GDD, leading the shorter O_3 accumulation period which will also limit F_{st} (Figure 5-16).

This analysis has focused on how F_{st} is limited over the course of the growth period but it is also important to understand how F_{st} is affected by changes in environmental conditions over the course of a day, especially since Figure 5-13 has shown that the co-variation between g_{sto} and O_3 concentration plays an important role in determining F_{st}. Identifying the environmental conditions and hence model components that are most crucial in limiting F_{st} diurnally will help assessment of O_3 risk; this is discussed in the following section.

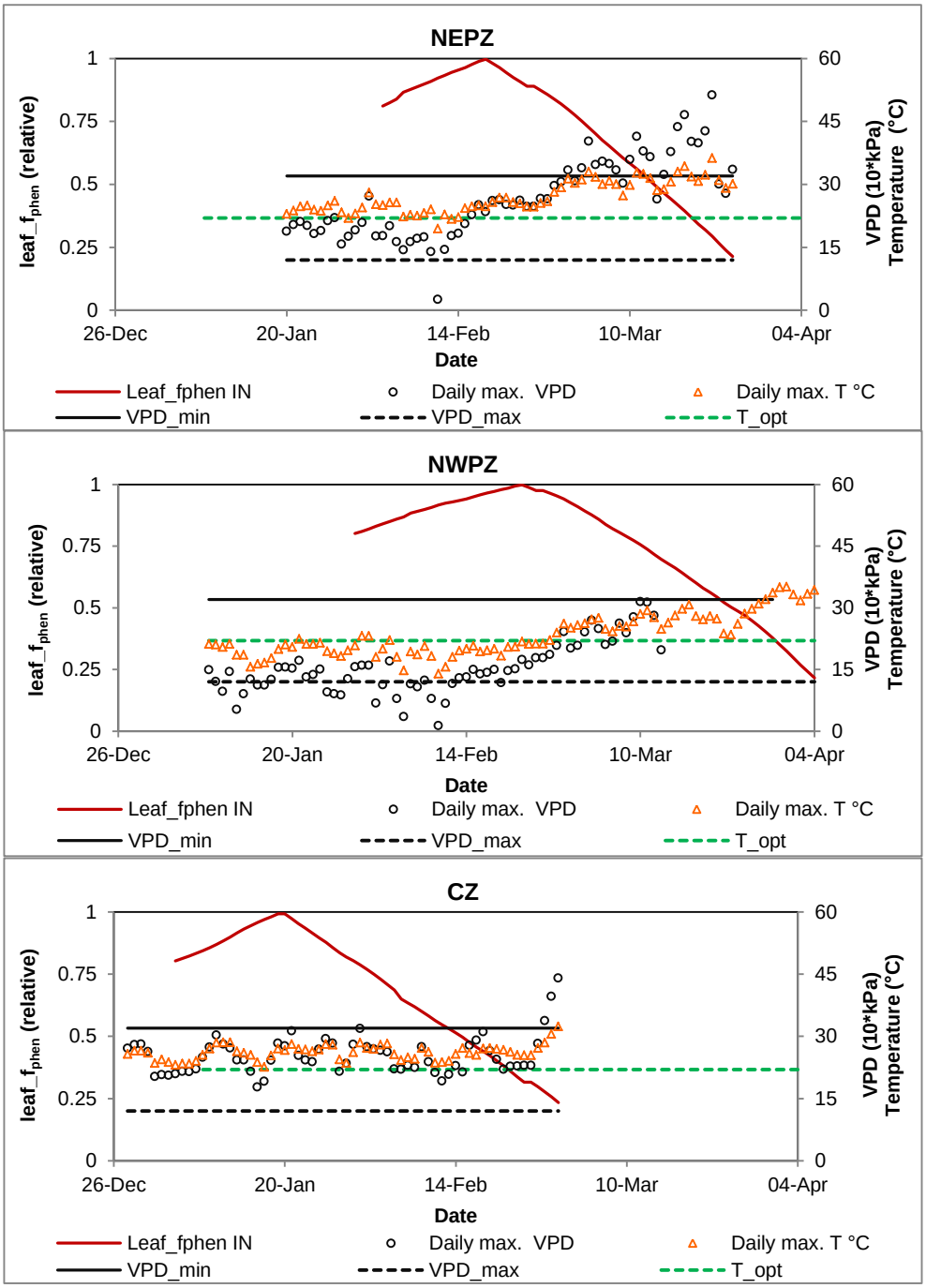

Figure 5-16: Daily maximum VPD (10*kPa) and daily maximum temperature (°C) during the O_3 accumulation period plotted in relation to f_{phen} for the three grids of each AGZs. Also shown are the key parameters of the f_{VPD} (VPD_{min} and VPD_{max}) and f_{temp} (T_{opt}) functions to provide an indication of the prevailing environmental conditions in relation to the constraints set within the model.

5.3.2.3 Diurnal factors limiting F_{st}.

In order to study the model components that limit F_{st} diurnally, the hourly values that describe relative g_{sto} and represent f_{temp}, f_{VPD} and f_{light} during the course of the day were plotted along with the hourly F_{st} values. These diurnal variations were studied for each of the stages I to III and are presented in Figure 5-17.

The limiting factor of temperature and VPD are different between the three stages and also between the different AGZ grids. f_{phen} has a big influence on all the three stages in setting the upper limit of g_{sto} and subsequently the F_{st}.; this has been dealt with in the previous section and therefore not considered in detail here.

During most stages, the temperature and VPD are more limiting during the midday when temperature and VPD are are high. On the other hand, irradiance is limiting at the start and end of the day after sunrise and before sunset. In most of the grids, the temperature and VPD increases during the course of the day reaching a maximum during the afternoon hours (13:00 to 15:00 hours). This increases the limiting influence on F_{st} as can be seen by the f_{temp} and f_{VPD} profiles and often results in an afternoon dip in F_{st} in most of the grids during all the three stages. In all the stages of CZ and NEPZ, the temperature (20 to 30°C) and VPD (close to the VPD_{min} of 3.2 kPa) is high during the afternoon period resulting in a strong limiting influence on g_{sto} and subsequently F_{st}. This is not seen in stage I of NWPZ where there is very little limitation by VPD and temperature during the afternoon and therefore here the F_{st} gradually increases during the course of the day with highest values attained during the afternoon between 14:00 to 16:00 hours.

In stage III of all the three grids, a combination of a decrease in g_{sto} with leaf age (f_{phen}) plus high VPD and temperature results in lower F_{st} especially during the 12:00 to 16:00 hour period. It is clear from Figure 5-17 that the limitation to O_3 flux in stage III is predominantly due to VPD as f_{VPD} values are 0.3 or below. Temperature provides a less severe limitaition with lowest f_{temp} values of between 0.8 and 0.5. . Stage II represents an intermediate period between stages I and II; unaffected by phenological limitation but having high VPDs that cause the lowest f_{VPD} values to reach between 0.5 and 0.2; temperature is less limiting than in stage III

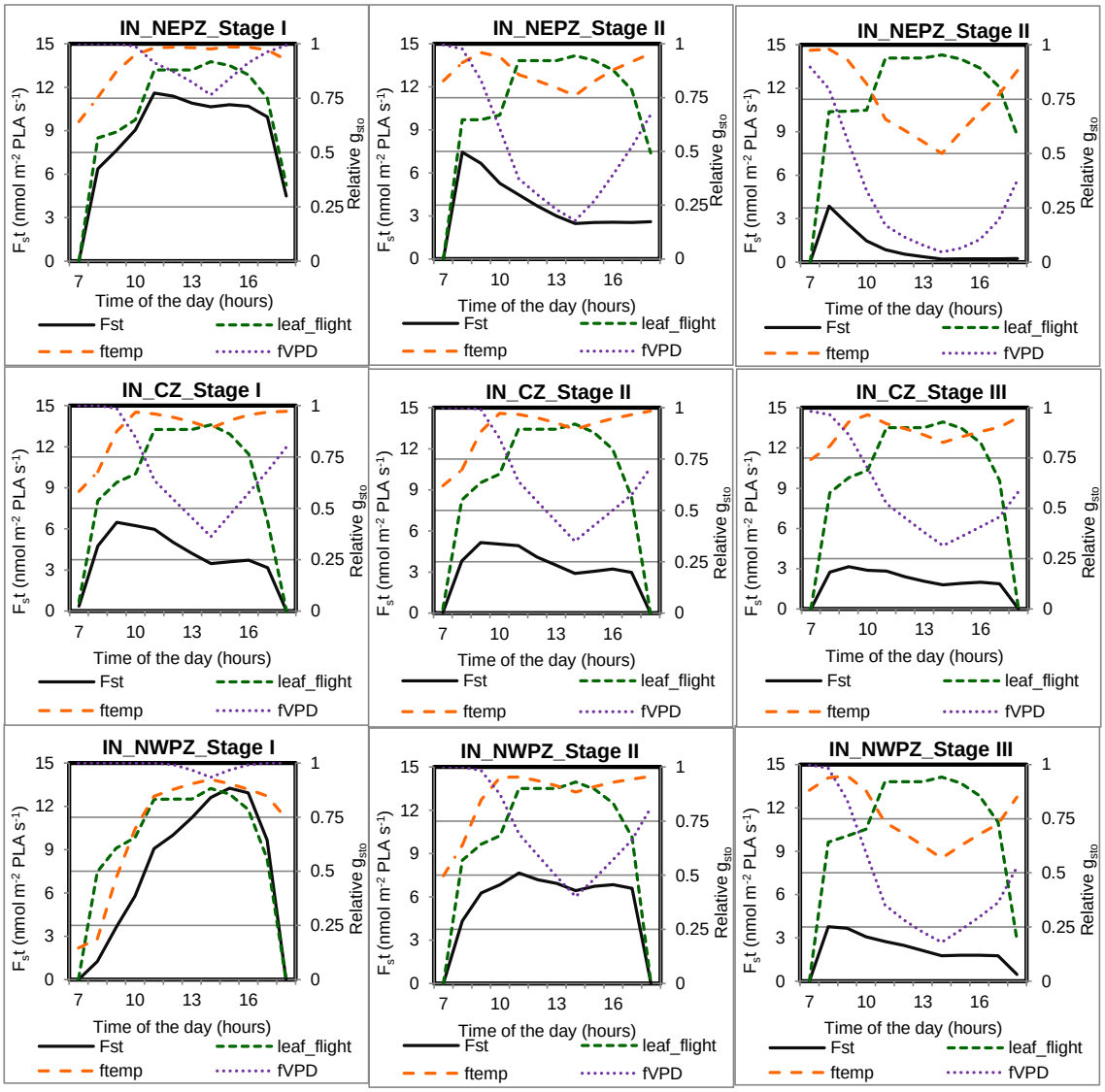

Figure 5-17: Diurnal profiles of F_{st}, f_{temp}, f_{VPD} and f_{light} during the three stages of the O_3 accumulation period estimated using the IN_{450} wheat parameterizations for the three grids in NEPZ, NWPZ and CZ. The values represent diurnal hourly averages for the particular stage of the O_3 accumulation period.

Phenology is also an important factor that influences the seasonal trend in O_3 flux and towards the end of the accumulation period, f_{phen} functions limits the g_{sto} and subsequently limiting F_{st} even under high O_3 concentrations. Diurnal factors like Temperature, VPD and light also play an important flux limiting role.

5.3.2.4 Factors limiting uptake of O_3 above 60 ppb

From previous analysis it is clear that at the high end O_3 concentrations (classified here as those above 60 ppb v) there are very few instances of F_{st} greater than 6 nmol O_3 m^{-2} PLA s^{-1} and hence that will contribute to the POD_6 index. In order to identify which component of O_3 uptake is most limiting when O_3 concentrations are higher than 60 ppb v, further analysis of the relationship between F_{st} and O_3 concentrations were conducted with the results presented in Figures 5-14 to 5-17. This analysis divides the dataset using three thresholds: 40 and 60 ppb v for O_3 concentrations and 6 nmol O_3 m^{-2} PLA s^{-1} for F_{st}. The two O_3 concentrations categories are selected to represent moderately high O_3 concentrations (40 to 60 ppb v) since previous analysis has shown higher F_{st} values tend to be associated with this O_3 level; and > 60ppb v to represent extremely high O_3 levels. The F_{st} thresholds categorize the data into < 6 nmol O_3 m^{-2} PLA s^{-1} and ≥ 6 nmol O_3 m^{-2} PLA s^{-1}. For each of these category combinations the extent of the environmental variables limiting g_{sto} is indicated by calculating the average f_{light}, f_{temp} and f_{VPD} values for the hours corresponding to that category.

There were no O_3 fluxes observed when the O_3 concentrations were above 60 ppb in the NEPZ grid while in the CZ grid the O_3 concentrations are very low and hence there are no O_3 flux values for O_3 concentrations above 60ppb.

The results are shown in Figure 5-18 to Figure 5-20; when O_3 concentrations are between 40 to 60 ppb v, values of F_{st} below 6 nmol O_3 m^{-2} PLA s^{-1} are largely due to the limiting effect of VPD with average f_{VPD} values varying from 0.2 to 0.5; the higher value occurring in the CZ grid. For all AGZ grids except NWPZ this combination occurs more frequently than instances of O_3 > 60 ppb v resulting in F_{st} values > 6 nmol O_3 m^{-2} PLA s^{-1}. During those instances when moderately high O_3 concentrations do translate into higher F_{st} (> 6 nmol O_3 m^{-2} PLA s^{-1}) it is under conditions when environmental conditions are no more limiting than 0.8 relative g; this is with the exception of f_{light} in CZ which limits to 0.6. Finally it is interesting to note that the NWPZ is the only grid cell that has O_3 concentrations in exceedance of 60 ppb v and F_{st} values greater than 6 nmol O_3 m^{-2} PLA s^{-1} though admittedly the chance of such occurrences is heightened as this grid also experiences more instances of > 60 ppb v concentrations; in these situations the main limitation comes from light. This is likely due to these conditions being more likely to occur in the late afternoon hours when the

O_3 concentration is likely to be high and environmental conditions less limiting (cooler temperatures and lower VPDs) to g_{sto}.

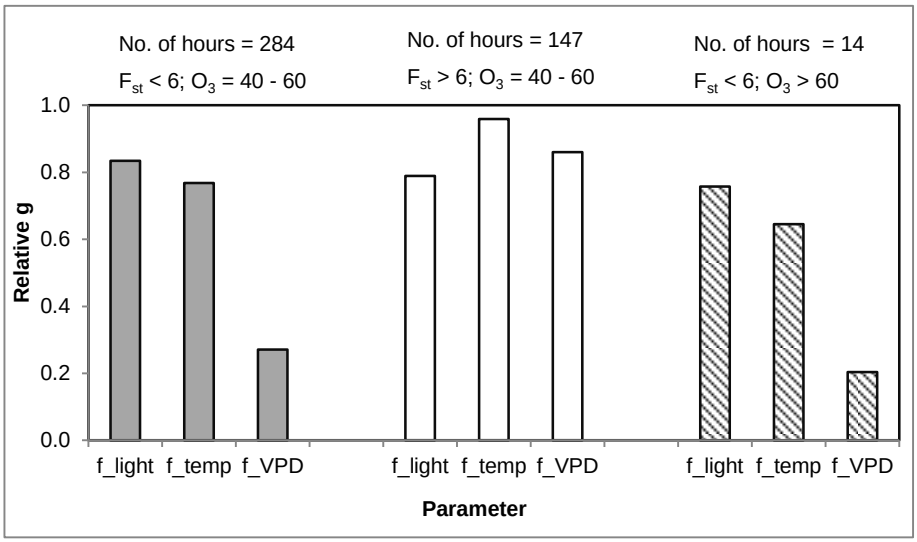

Figure 5-18: Average values for f_{light}, f_{temp} and f_{VPD} for a combination of conditions categorized as O_3 concentrations either between 40 to 60 ppb v or above 60 ppb v and F_{st} values either below or above 6 nmol O_3 m^{-2} PLA s^{-1} in the NEPZ grid. Also shown are the number of hours during for which each of the conditions occurs during the O_3 accumulation period

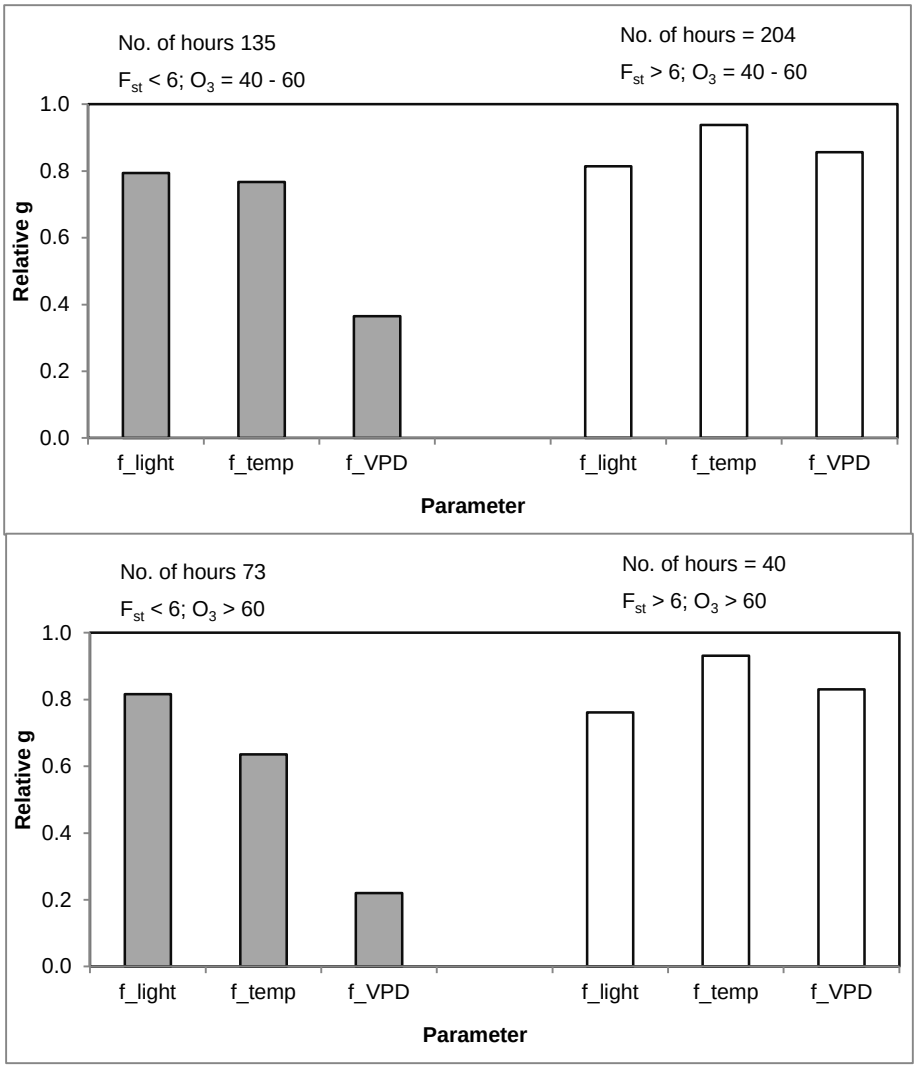

Figure 5-19: Average values for f_{light}, f_{temp} and f_{VPD} for a combination of conditions categorized as O_3 concentrations either between 40 to 60 ppb v or above 60 ppb v and F_{st} values either below or above 6 nmol O_3 m^{-2} PLA s^{-1} in the NWPZ grid. Also show are the number of hours during for which each of the conditions occurs during the O_3 accumulation period.

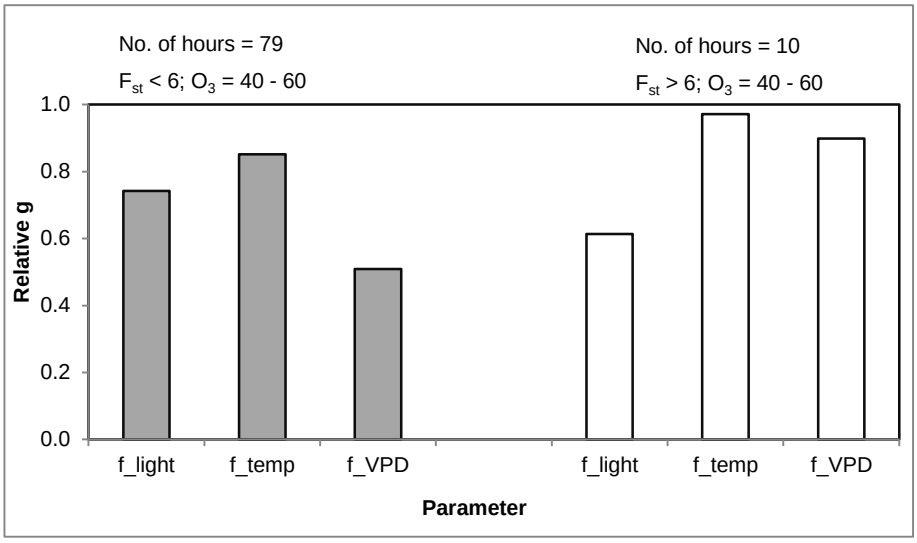

Figure 5-20: Average values for f_{light}, f_{temp} and f_{VPD} for a combination of conditions categorized as O_3 concentrations either between 40 to 60 ppb v or above 60 ppb v and F_{st} values either below or above 6 nmol O_3 m^{-2} PLA s^{-1} in the CZ grid. Also show are the number of hours during for which each of the conditions occurs during the O_3 accumulation period.

5.3.3 Comparison of different DO_3SE model parameterizations

The rationale for parameterizing the F_{st} model for Indian wheat was to develop a model based on the wheat cultivars that are grown in India, essentially one that would best describe the physiological and phenological characteristics of Indian wheat growing under Indian climatic conditions. Due to limited data describing g_{sto} responses to environmental conditions it was not possible to parameterize all aspects of the model (e.g. f_{VPD}); those parameterizations that were defined were also variable in the quantities and types of data used in their parameterization and hence are subject to varying degrees of uncertainty.

In order to assess the necessity of parameterizing the F_{st} model for Indian wheat it was considered useful to compare F_{st} and POD_6 values estimated using the IN_{450} model against those calculated using the EU model parameterization. Using the same g_{max} (450 mmol O_3 m^{-2} s^{-1}) in both the EU and IN parameterizations removes the differences in F_{st} due to g_{max} but and allows the influence of other parameters on O_3 flux to be more easily

compared. The differences in these model parameterization have been described in detail in Chapter 4 but to summarise, in terms of phenology, both models assume the same SGS (sowing) date but assume different GDD to reach particular phenological periods, additionally the EU and IN models use a base temperature of 0^oC and 5^oC respectively. The f_{light} and f_{temp} parameterizations are different, with the f_{temp} T_{min}, T_{opt} and T_{max} parameters being lower in the IN_{450} parameterisation (see Figure 4-8); the f_{VPD} parameterization is the same. Comparisons were made both in terms of the spatial and temporal variation in F_{st} values as described below.

5.3.3.1 Spatial variation in F_{st} values estimated using the IN_{450} and EU model parameterization across India

Figure 5-22 shows the POD_6 results calculated using the IN_{450} and EU parameterizations and the comparable $AOT40_A$ values for the entire Indian modelling domain. To aid this comparison, Figure 5-21 provides a scatter plot of POD_6 values calculated for all grids using the IN_{450} and EU parameterisations. This clearly shows that the EU parameterization can estimate almost double the POD_6 values compared to the IN_{450} parameterization. However in some grids the IN_{450} shows almost double the POD_6 values compared to EU. Comparison of the spatial distribution of IN_{450} and EU shows that across most of northern India the spatial distribution in relative risk between the EU and IN_{450} parameterisations is very similar. Along the east coast of India, the IN POD_6 values range between 1 to 5 mmol O_3 m^{-2} PLA while the EU POD_6 values are considerably higher ranging between 2 to 8 mmol O_3 m^{-2} PLA s^{-1}. In two AGZs namely, Peninsular zone (PZ) and the CZ, except in the east coast, the IN POD_6 values are below 1 mmol O_3 m^{-2} PLA s^{-1} while they frequently reach up to 3 mmol O_3 m^{-2} PLA s^{-1} when using the EU parameterization. In north-east India, IN POD_6 values (0.001 to >8 mmol O_3 m^{-2} PLA s^{-1}) are higher than EU POD_6 (0.001 to 7 mmol O_3 m^{-2} PLA s^{-1}).

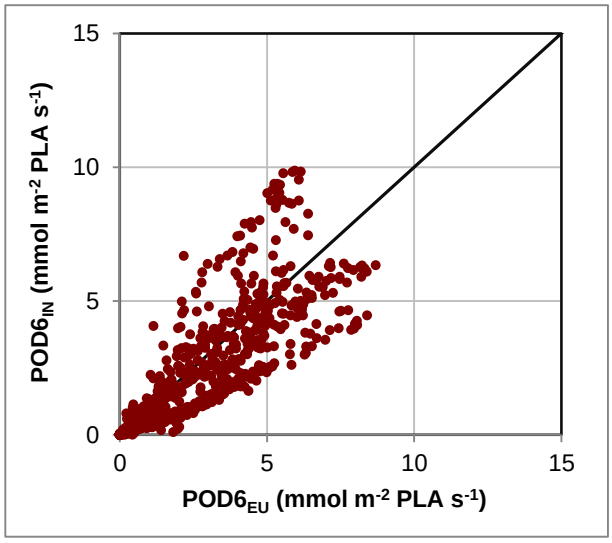

Figure 5-21: Relationship between $POD6_{IN}$ and $POD6_{EU}$. The data points represent all the grids in India.

To establish what the main drivers are causing the differences between these two parameterisations data from the three grids of the different AGZs are analysed; this compares the parameterisation effects on both seasonal and diurnal F_{st}.

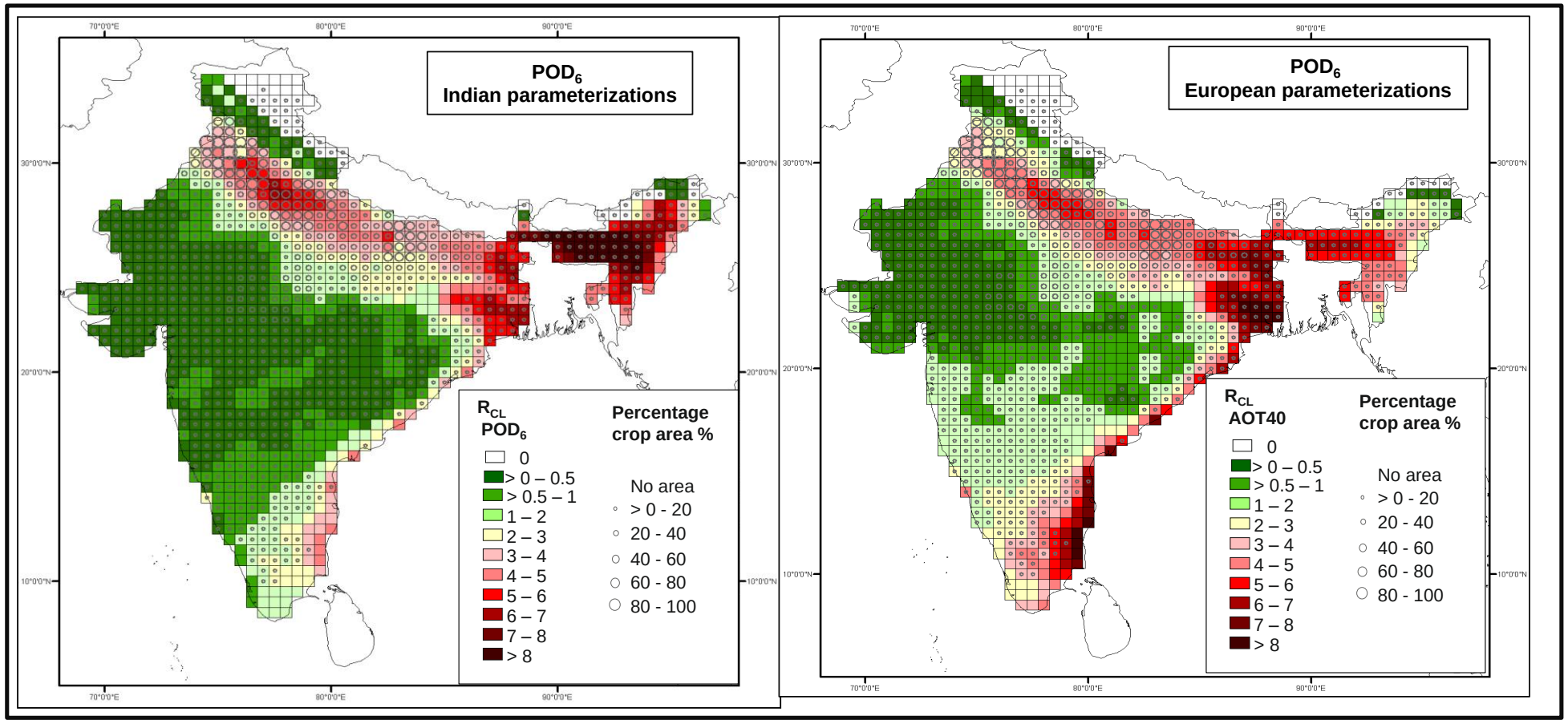

Figure 5-22: POD_6 values for wheat in India estimated during the O_3 accumulation period using (a) the parameterization and IN450 (b) the EU parameterization for the cropping year 1999-2000.

5.3.3.2 Temporal variation in fluxes within the important AGZs

Figure 5-23 shows the POD_6 values calculated using the IN450 and EU parameterizations for the three AGZ grids. This shows variation in the relationship between IN_{450} and EU parameterization with NEPZ and CZ showing higher POD_6 values, and NWPZ lower POD_6 values, when calculated using the EU parameterization.

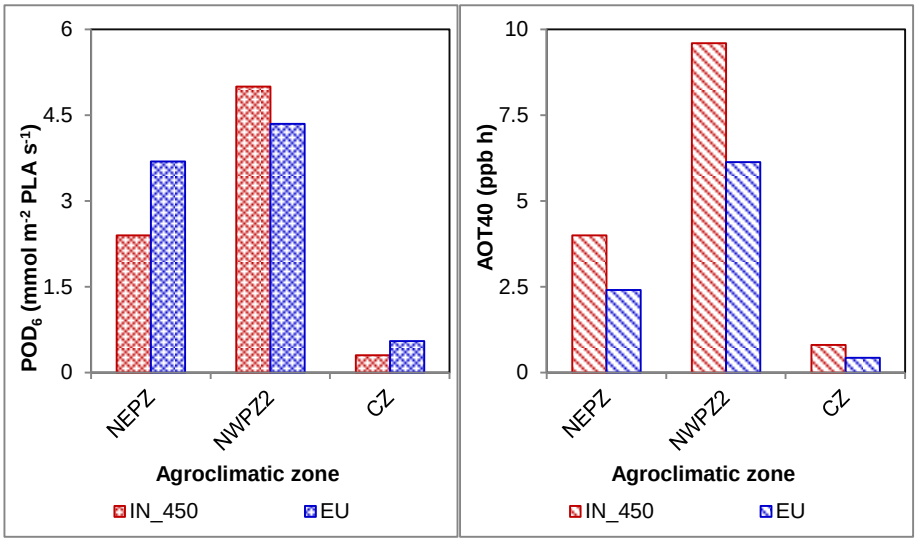

Figure 5-23: POD_6 values estimated using IN_{450} and EU model parameterizations during the O_3 accumulation period for the three AGZ grid cells.

To understand the reasons for these variations it is useful to first investigate the differences in environmental conditions and O_3 concentrations that occur during the different O_3 accumulation periods calculated using each parameterization. Figure 5-24 shows firstly that the average O_3 concentrations are always a little lower (approximately 2 to 3 ppb v) for the EU parameterization. The same is true for temperature (approximately 1 to 2^{o}C lower) and the VPD (about 0.2 kPa lower) for the EU compared to the IN_{450} parameterisation. This information is used to help understand the influence that the variable parameterization has on F_{st} in the following sections.

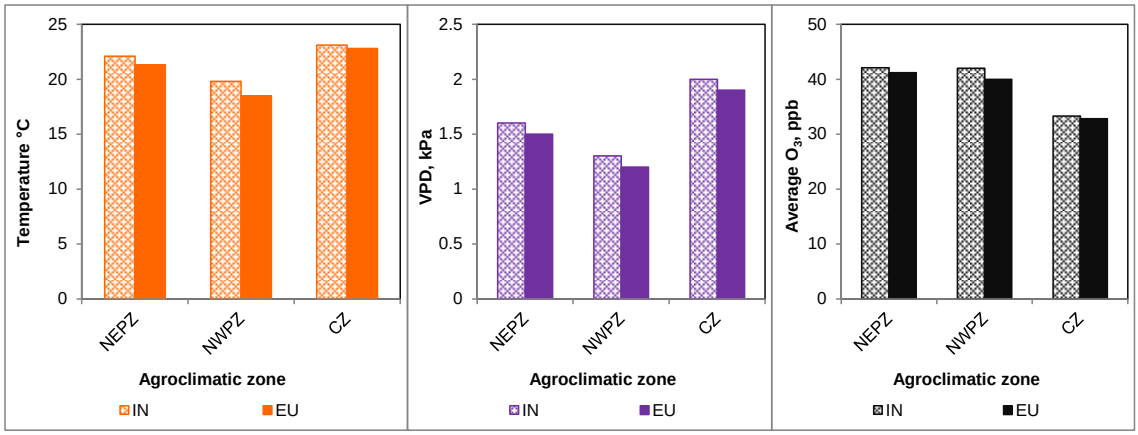

Figure 5-24: Hourly average meteorological conditions and average O_3 concentrations during the O_3 accumulation period calculated using both the Indian phenology (IN) and European phenology (EU) with the MATCH model data for the cropping year 1999-2000 for the three AGZs in India.

3.5.1 Seasonal variation in F_{st} and POD_6 using the IN_{450} and EU model paramterisations.

Figure 5-25 shows how the POD_6 values estimated using both IN_{450} and EU parameterisations increase over the course of the O_3 accumulation period. Of note here is the fact that use of the EU parameterization leads to an earlier start during the year of the O_3 accumulation period. The O_3 accumulation period is also shorter and ends earlier using the EU parameterization. For the NEPZ and CZ grid cells this shift in the accumulation period allows a faster increase in POD_6 at the beginning of the period and a less severe tailing off of POD_6 accumulation towards the end of the period resulting in higher POD_6 values for the EU model. By contrast, the earlier start in the NWPZ grid cell is associated with a slower increase in POD_6 which is not compensated for towards the end of the period such that POD_6 is reduced using the EU model.

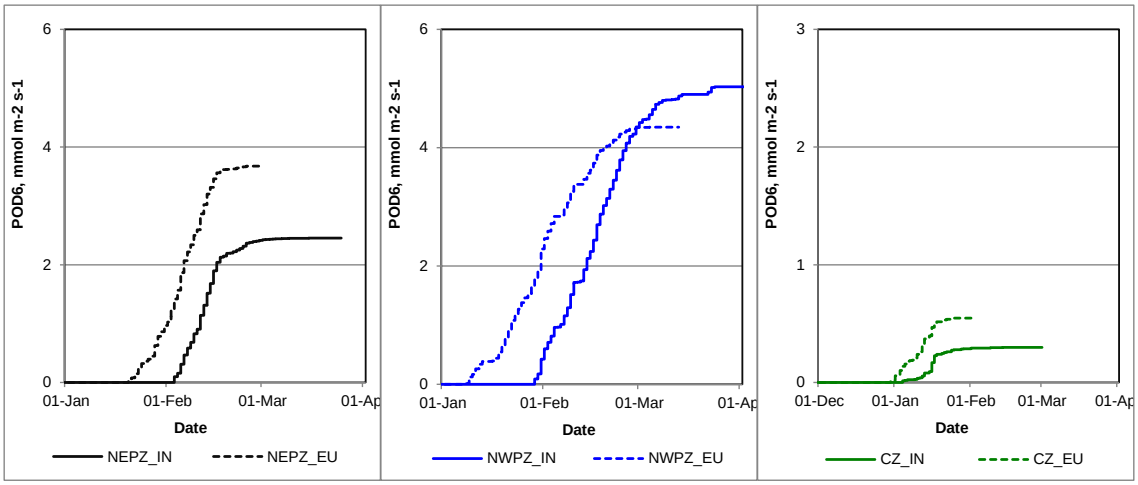

Figure 5-25: Evolution of POD_6 calculated using IN_{450} and EU parameterizations over the course of the O_3 accumulation period for the three AGZ grids. N.B. The scale for CZ is increased by a factor of 4.

This analysis has shown the importance of the timing of the start of the O_3 accumulation period, as such it is useful to see how the different base temperatures (0°C and 5°C for EU and IN_{450} respectively) influence the start of different phenological stages. Figure 5-26 shows the accumulation of the GDD from SGS (day of sowing) along with daily average temperatures for the NEPZ grid. The average daily temperatures during January and February are around 15 to 20^{o}C and are therefore high enough not to limit the accumulation of GDD; however, the lower 0^{o}C base temperature of the EU parameterisation means that GDD accumulates more quickly such that the A_{start} and A_{end} of the accumulation period occur approximately 20 to 25 days days earlier than the EU parameterisaion.

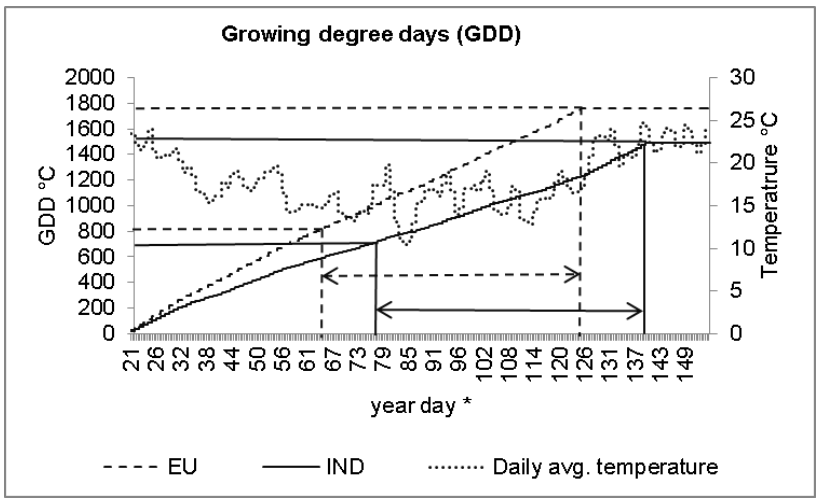

Figure 5-26: GDD calculated from SGS until A_{end} using a base temperature of 0°C (EU) and 5°C (IN_{450}) for the NEPZ grid. The arrows indicate the respective O_3 accumulation period from A_{start} to A_{end}. Also shown are the average daily temperatures.

This shift in O_3 accumulation period has important implications for the O_3 concentrations to which the plants will be exposed. Since the O_3 concentrations tend to increases as the year progresses from February to March and April the use of the IN_{450} wheat phenology will lead to exposure of plants to higher O_3 concentrations. This is clearly shown in Figure 5-27 which shows daily average O_3 concentrations and corresponding F_{st} values estimated using both IN_{450} and the EU parameterisations. This figure shows that for NEPZ and NWPZ the earlier start of the accumulation period leads to higher F_{st} in the initial period, however as the limitation caused by f_{phen} and increasing temperatures and VPDs towards the end of the period starts to occur, F_{st} values decline; this also means the EU parameterization leads to an avoidance of the higher O_3 concentrations. As such, whether the shifted accumulation period leads to a higher or lower final POD_6 value will largely depend upon whether the early period exposure to optimal environmental conditions (which allow more O_3 uptake even though O_3 concetrations are lower) outweighs the end of period restrictive environmental conditions and reduced f_{phen} that limit O_3 uptake, even though O_3 concentrations will tend to be higher.

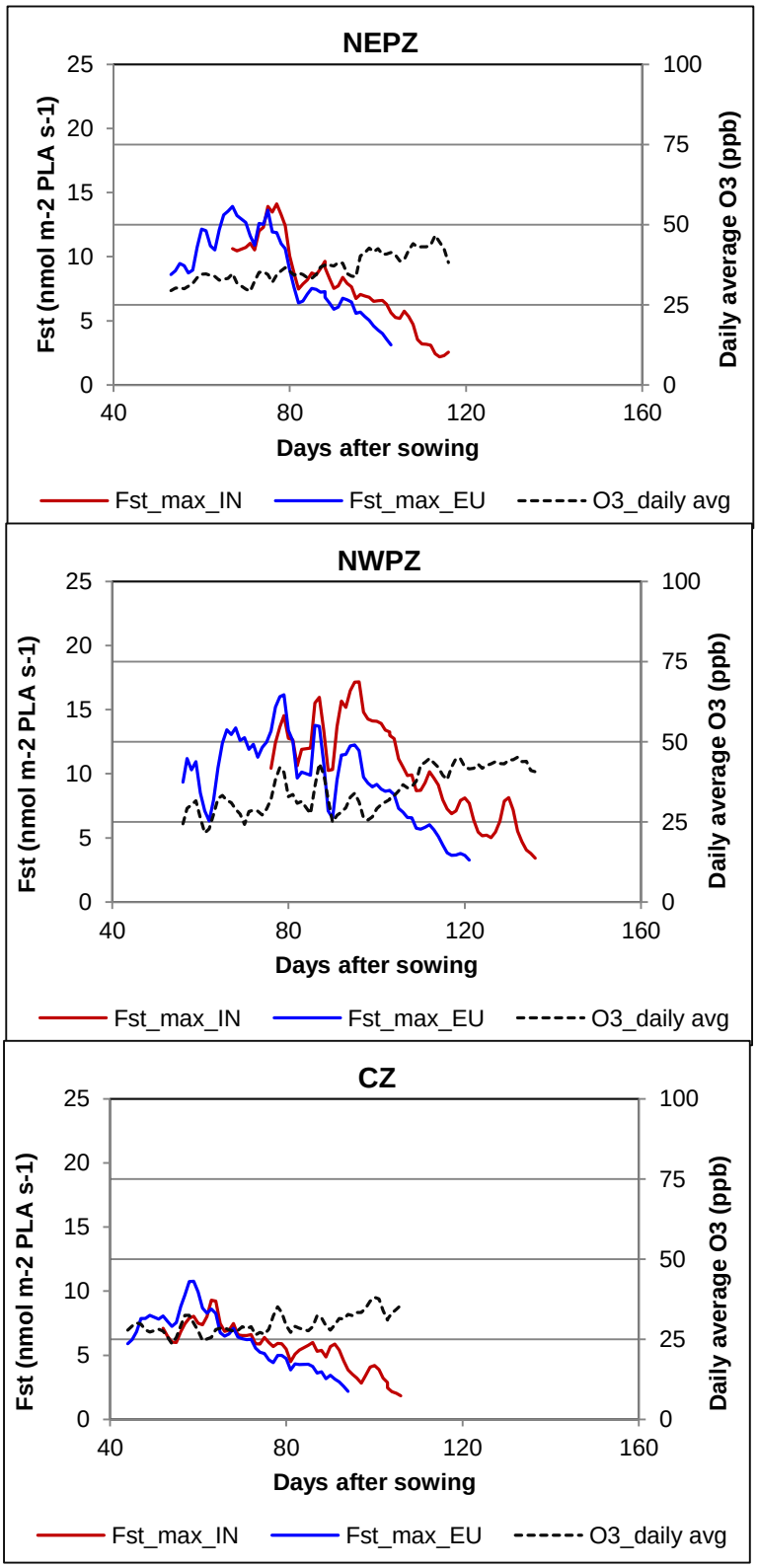

Figure 5-27: Daily maximum F_{st} values calculated using the IN_{450} and EU parameterizations. Also shown are the corresponding daily average O_3 concentrations for the three AGZs. The values for all variables are given as 3-day moving averages.

The fine line of this balance can be seen in Figure 5-28 which shows the f_{phen} (estimated using the IN_{450} and EU parameterisations) and associated daily maximum temperature and VPD values. Figure 5-28 shows that for the NWPZ grid cell, the maximum temperatures during the later part of the accumulation period of the IN_{450} parameterization remain relatively cool (between 25 and 30^{o}C) leading also to lower VPD maxima (within the limits of VPD_{min}). This allows higher g_{sto} values under the higher O_3 concentrations that occur later in the season and hence higher F_{st}. By contrast, the f_{phen} estimated using the IN450 parameterization in the NEPZ grid forces the O_3 accumulation period towards relative hot temperatures (around 30^{o}C) which also lead to higher VPDs (exceeding the VPD threshold of 3.2 kPa). As such, g_{sto} is more limited leading to lower F_{st} values even though O_3 concentrations are higher; thus the EU parameterization for this location provides higher POD_6 estimates. Finally, the temperature and associated VPD climate for the CZ grid remain relatively constant throughout both the EU and IN_{450} estimated accumulation period, hence there is less difference between the estimated POD_6 values in this grid than the other two.

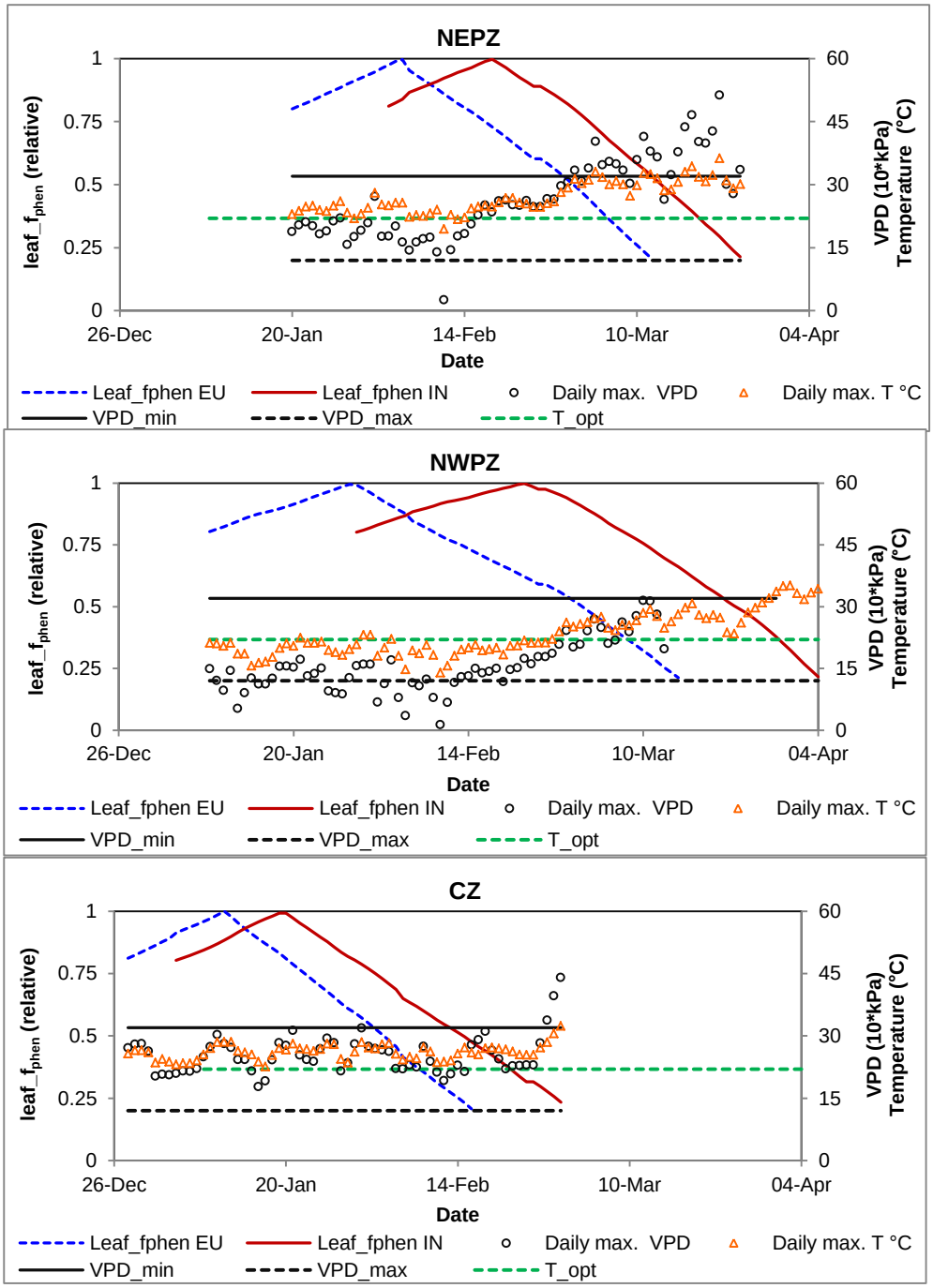

Figure 5-28: Daily maximum VPD (10*kPa) and daily maximum temperature (°C) during the O_3 accumulation period plotted in relation to f_{phen} values based on IN_{450} and EU parameterizations for the three AGZ grids.

This shows that the phenology is very important in determining the O_3 flux especially in areas where there is substantial variation in meteorological conditions (i.e. temperature and VPD) and O_3 concentrations over the course of the O_3 accumulation period.

3.5.1 Diurnal variation in F_{st} using the IN_{450} and EU model parameterizations

The influence of a variable length and timing of the growth period in determining the environmental conditions, and hence limitations to g_{sto}, to which the plants are exposed can be further analysed by investigating the variations in each of f_{light}, f_{temp} and f_{VPD} in relation to F_{st} for Stages I to III of the O_3 accumulation period (see Figure 5-29 to Figure 5-31).

For the NEPZ grid, for which the EU parameterization gave the highest POD_6 values, there is little difference in the f variables during all three stages. The most obvious difference occurs in Stage III where the f_{temp} for the IN_{450} parameterisation is more limiting (with values down to 0.5) than the EU parameterization (values only reducing to 0.6). Since the f_{temp} parameterization is similar between IN_{450} and EU this is most likely due to exposure to higher temperatures as a consequence of the later growth period estimated using the IN_{450} phenology.

Of all the grids the biggest differences in f variables occurs for the NWPZ location. Here there are substantial differences in the f_{light} values which are more limiting in the IN_{450} parameterisation for all stages due to the less sensitive f_{light} relationship to increasing PAR. There are also substantial differences in the f_{temp} relationship with values being lower in the EU parameterization, this is most likely driven by the earlier timing of the accumulation period resulting in exposure to cooler temperatures below the T_{opt}; only in Stage III does f_{temp} not limit g_{sto}, which is in contrast to the IN_{450} parameterisation in which during this growth stage the higher temperatures experienced in the later set accumulation period lead to g_{sto} limitation down to almost 0.5. A similar pattern is reflected in f_{VPD} with only stage I being similar between parameterizations. In stages II and III the increased limiting influence of f_{VPD} is apparent for the IN_{450} parameterisation, with values decreasing to 0.5 and 0.25 in comparison to the EU f_{VPD} values of 0.9 and 0.45 for the two respective growth stages. Since the f_{VPD} relationships are the same between the two parameterization types this is due to the later growth period leading to exposures to higher VPDs.

Finally, Figure 5-31 showing the CZ grid confirm conclusions from the previous phenological analysis that there is little difference in the F_{st} values predicted using each parameterization this grid since the f variables are broadly similar. Slight differences

occur for f_{light} which is again lower in the IN_{450} parameterisation and the f_{temp} which shows a small mid-day depression in the IN_{450} parameterisation that is not seen in the EU model.

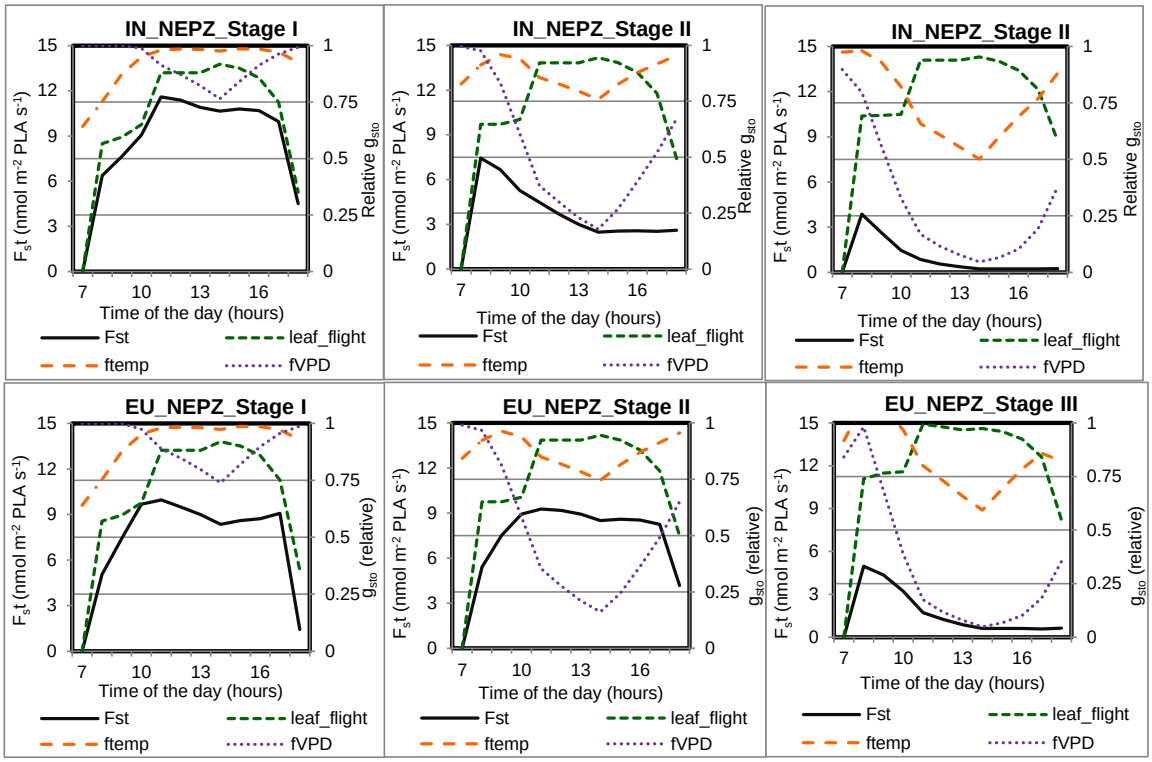

Figure 5-29: Diurnal profile of F_{st}, f_{temp}, f_{VPD} and f_{light} during the three stages of O_3 accumulation period calculated using the IN_{450} and EU wheat parameterizations for the NEPZ grid. The values are hourly averages for each of Stages I to III of the O_3 accumulation period.

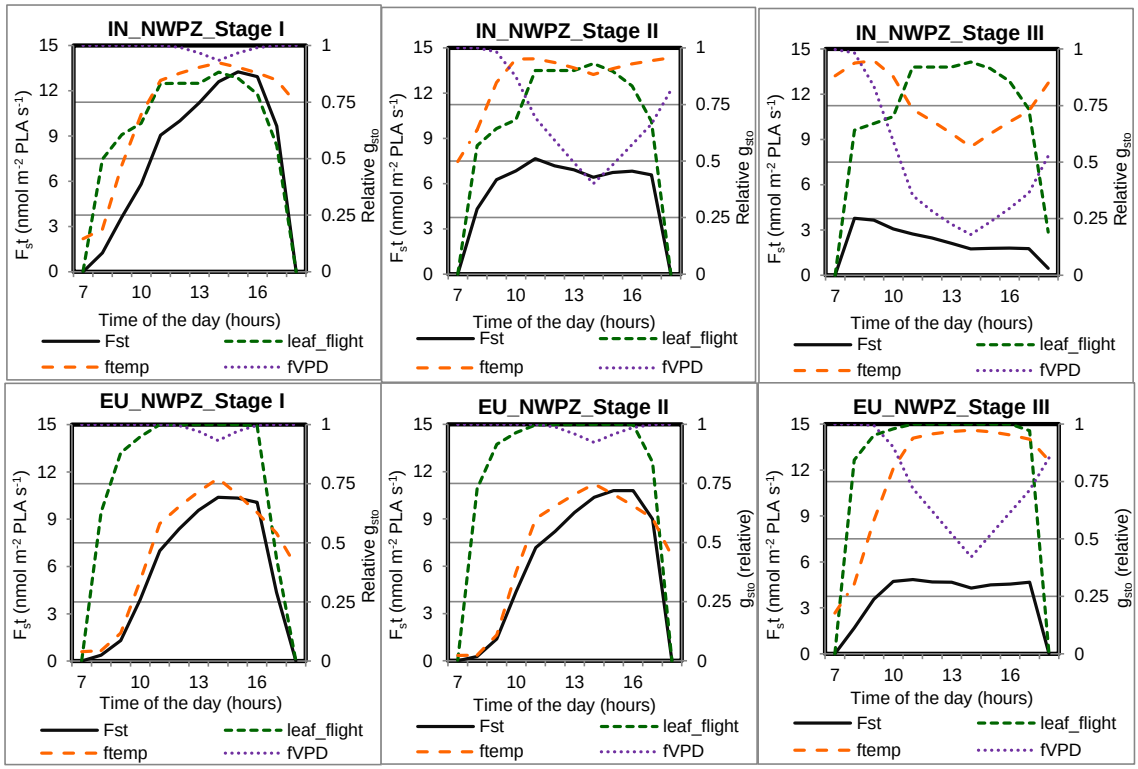

Figure 5-30: Diurnal profile of F_{st}, f_{temp}, f_{VPD} and f_{light} during the three stages of O_3 accumulation period calculated using the IN_{450} and EU wheat parameterizations for the NWPZ grid. The values are hourly averages for each of Stages I to III of the O_3 accumulation period

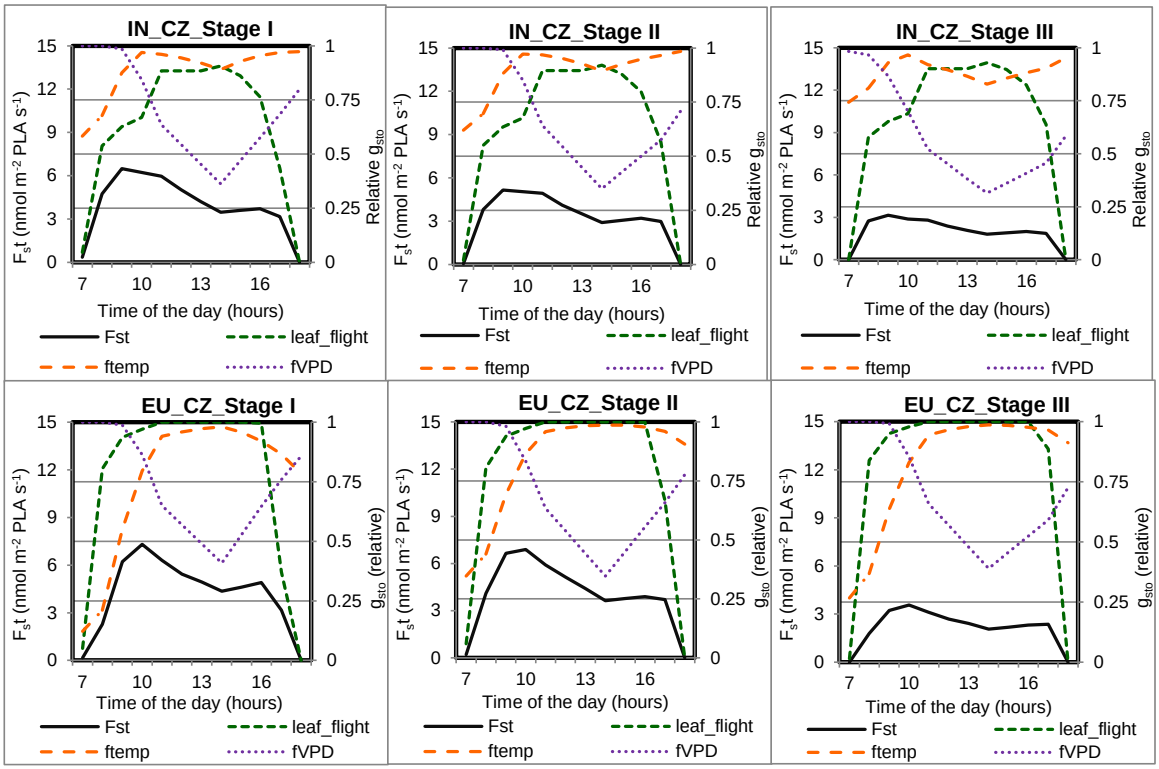

Figure 5-31: Diurnal profile of F_{st}, f_{temp}, f_{VPD} and f_{light} during the three stages of O_3 accumulation period calculated using the IN_{450} and EU wheat parameterizations for the CZ grid. The values are hourly averages for each of Stages I to III of the O_3 accumulation period

This analysis has shown the effect that the different IN_{450} and EU parameterisations have on the timing and length of the growth period is the most important factor influence F_{st} and hence POD_6 values. This is important both because it determines the O_3 exposures to which the plants will be exposed, with the earlier EU parameterization meaning that exposure to lower O_3 concentrations during the O_3 accumulation period is likely; but also because it determines the prevailing environmental conditions, in particular temperature and VPD that also increase during the growth periods. As such, the net effect on F_{st} and hence POD_6 depends on which of these factors (higher O_3 concentrations or more limiting environmental conditions) is most influential in determining O_3 uptake. Although the f_{light} relationship is substantially different between IN_{450} and EU this is likely to have less influence in determining F_{st} since both parameterizations allow close to maximum g_{sto} values.

5.4 Sensitivity analysis of the stomatal flux model

Chapter 4 describes the first attempt to parameterize the F_{st} model for Indian wheat; as mentioned in this chapter there are substantial limitations to the IN model parameterization which could only be overcome through the availability of more data describing the g_{sto} response to Indian wheat cultivars. This would involve a substantial amount of work, ideally with well co-ordinated experimental studies being used to examine the g_{sto} and other physiological and yield parameters of wheat under different meteorological conditions across the wheat growing regions in India. Such work is expensive in terms of time and resources. In order to make a first attempt at assessing which of the model parameterisations is most important in determining F_{st} and POD_6 a simple sensitivity analysis is conducted here. This may help to target future parameterization of the F_{st} model.

The F_{st} model is a deterministic model whose output depends entirely on the model structure and parameters, and the input variables (Marino *et al.,* 2008). Sensitivity analysis is a useful tool to identify influential model parameters (Breierova and Choudhari, 1996; Simpson *et al.,* 2003; Marino *et al.,* 2008).

There are different types of sensitivity analysis, ranging from simple one-at–a-time (OAT) local sensitivity analysis, which help in studying the influence of individual parameters to more complex global sensitivity analysis (e.g., Monte Carlo analysis) that help in quantifying the relative importance of the parameters and also investigate the interactive effects of the different parameters (Morris, 1991; Hamby, 1994; Cariboni *et al.,* 2007, Saltelli *et al.,* 2006).

The more complex global sensitivity analyses require a high number of model runs and are expensive to perform (Campolongo *et al.,* 2007) and it is beyond the scope of this work to apply these here. Therefore, in this Chapter a simple one-at-a-time (OAT) local sensitivity analysis is used to investigate which are the most influential parameters. In this study all, the model parameters are changed one at a time by a fixed ±20% of the actual value to study how these changes influence the variability in the model output. Eleven model parameters were defined to allow investigation of the influence of ; i) g_{max}; ii) stomatal conductance as a function of wheat phenology; iii) irradiance; iv) temperature and v) VPD on the model output. These sensitivity tests were conducted for

the three AGZ grids such that 72 model runs (24 tests per grid) on 3 grids belonging to the important wheat growing AGZs were conducted. The model outputs are presented in terms of POD_6 and POD_0, the latter allowing an assessment of how the sensitivity of the model may change with an altered POD threshold. A summary of the sensitivity tests conducted for each of the model parameters investigated is given in Table 5-3.

Table 5-3: Summary of the sensitivity tests on model parameters.

Tests		**Description**
g_{max} ±20%		Changes in maximum stomatal conductances (g_{max}) by ±20%
f_{phen}	f_{phen_a} ±20%	Changes in relative g_{sto} at A_{start} (f_{phen_a}) by ±20%
	f_{phen_b} ±20%	Changes in relative g_{sto} at A_{end} (f_{phen_b}) by ±20%
	f_{phen_e} ±20%	Changes in GDD at A_{start} (f_{phen_e}) by ±20%
	f_{phen_f} ±20%	Changes in GDD at A_{end} (f_{phen_f}) by ±20%
f_{light}	$light_a$ ±20%	Changes in light constant by ±20%
f_{temp}	T_{max} ±20%	Changes in maximum temperature for g_{sto} by ±20%
	T_{opt} ±20%	Changes in optimum temperature for g_{sto} by ±20%
	T_{min} ±20%	Changes in minimum temperature for g_{sto} by ±20%
f_{VPD}	VPD_{max} ±20%	Changes in minimum temperature for g_{sto} by ±20%
	VPD_{min} ±20%	Changes in minimum temperature for g_{sto} by ±20%

The results of the sensitivity analysis are presented in Figure 5-32 and Figure 5-33. The values obtained using IN_{450} parameterizations provide the base values to which the sensitivity analysis results are compared. The results in terms of POD_6 and POD_0 were compared with the base value in terms of percentage differences. These percentage differences were calculated using Equation 5-1.

$$\%\ Difference = \frac{test-base}{base} \times 100 \qquad [5\text{-}1]$$

The sensitivity analysis shows that out of the 11 model parameters, g_{max} and f_{light} have the biggest effect on the model output. Changes in f_{VPD} (19-22%) and T_{opt} (12-31%) of f_{temp} parameters also had a significant influence on the output. Changes in the f_{temp} and f_{phen} parameters did not have a very substantial influence on the output (<5%) as compared to g_{max}, f_{light} and f_{VPD} parameters (> 20 % and as high as 250% in light_a in CZ grid). Differences due to changes in these parameters were more important when considering POD_6 as compared to POD_0, with effects on POD_6 being twice as much as that of POD_0. Except in tests using f_{light} parameters, most of the tests with 20% change in the model parameters showed <10% changes in POD_0 values and in many tests it was <5% (Figure 5-33). This suggests that estimates of F_{st} for Indian wheat cultivars made using a threshold value of 6 nmol O_3 m^{-2} PLA s^{-1} may be more sensitive to changes in the model parameters.

Out of the 3 AGZs, CZ has the maximum difference in output (Figure 5-32). Changes in VPD play an important role in CZ with the effects more than double that of the effect in the other 3 AGZs. Changes in relative g_{sto} at A_{start} (f_{phen_a}) and GDD after mid anthesis (f_{phen_f}) had little effect on outputs for the NEPZ and NWPZ grids but double the effect in the CZ grid.

Using a more complex global sensitivity analysis model as well as identifying the important input parameters (variables) would be ideal in order to understand the sensitivity of the model. Although sensitivity of the model to input variables is equally important but in this thesis the main focus is on the parameterization of the model and not the model results therefore in this chapter the sensitivity analysis is limited only to model parameters. It is to be noted that for future analysis, to have a more robust estimation of stomatal flux using this model, a sensitivity analysis as well as uncertainty

analysis of the input variables is necessary. However, identification of potentially important parameters from this work will be helpful for future multi-criteria global sensitivity analysis.

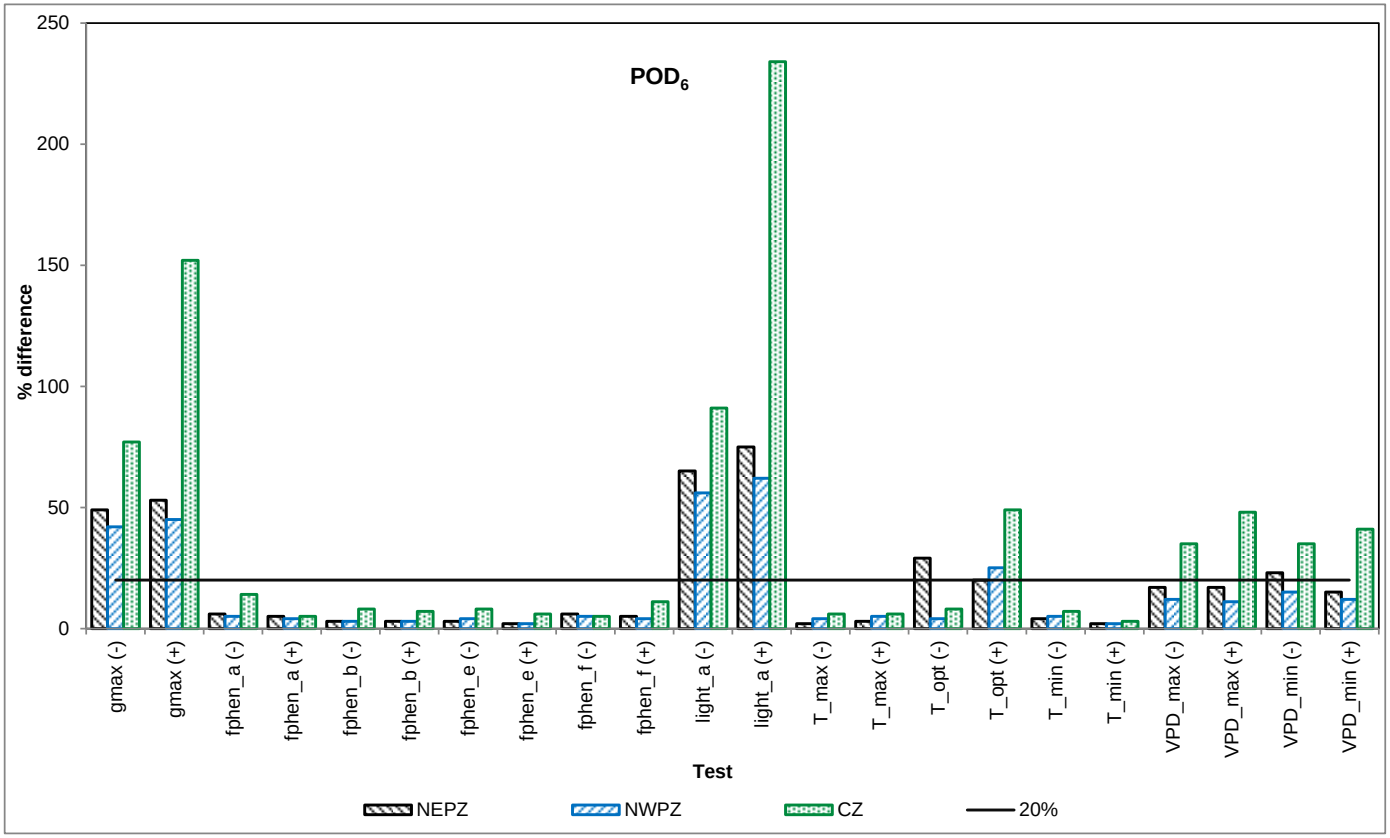

Figure 5-32: Results of sensitivity analysis for stomatal flux model parameters when the values of each parameter are changed by 20%. The values are percentage difference in POD_Y between the base case and sensitivity test ($100 \times \frac{\text{test}-\text{base}}{\text{base}}$).

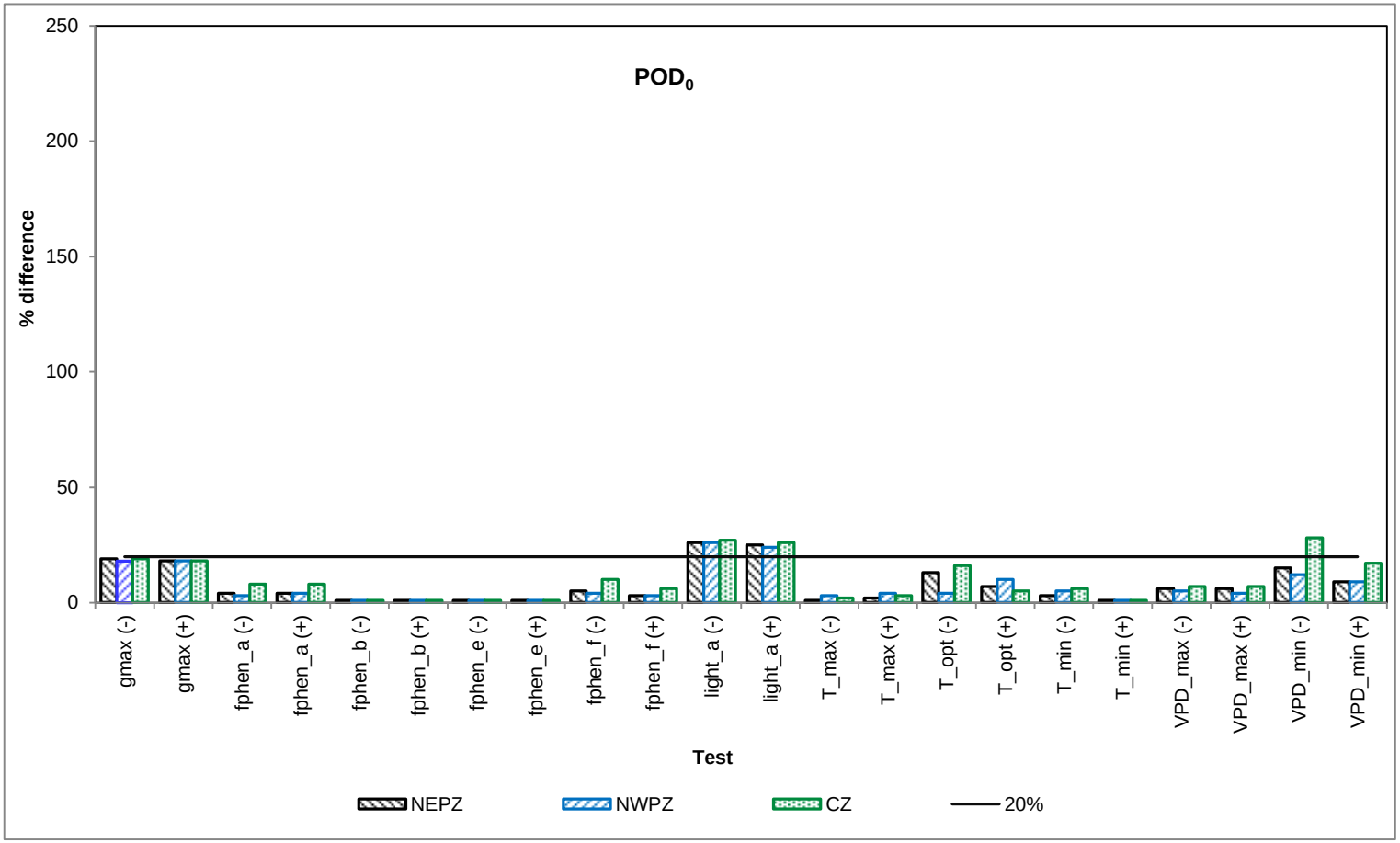

Figure 5-33: Results of sensitivity analysis for stomatal flux model parameters when the values of each parameter are changed by 20%. The values are percentage difference in POD_y between the base case and sensitivity test ($100 \times \frac{\text{test}-\text{base}}{\text{base}}$).

5.5 Discussion

The results from this thesis study clearly show that both indices indicate rather different spatial patterns of risk for certain locations across India though it is clear that the IGP region is identified as being particularly at risk from O_3 by both flux and concentration based indices. It was also found that the relative risk to wheat is estimated to be greater when using the flux based approach compared to the AOT40 approach. Figure 5-34 compares the spatial pattern between POD_6 and AOT40 found in the current thesis study with a similar flux based modelling study conducted in Europe (Simpson *et al.*, 2007). The figure shows that, in Europe, both metrics showed highest impacts in regions with higher O_3 concentrations while in areas with low O_3 concentration, characterized by moderate temperature and moist climate, flux showed O_3 impacts even when AOT40 values were below the critical level (Simpson *et al.*, 2007; Karlsson *et al.*, 2009). Thus the differences between flux and AOT40 are less in humid and moderate environments while in dry, warm regions where high VPD and temperature are likely to be more limiting of O_3 uptake differences between flux and AOT40 will be even greater. Figure 5-34 shows that F_{st} to wheat in most parts of Europe ranged between 1.2 to 6 mmol m^{-2} PLA s^{-1} with highest fluxes over Italy where most of the region has POD_6 values of ~6 mmol m^{-2} PLA s^{-1}. AOT40 values ranged from 1.2 to 6 ppm h. The range of POD_6 values was quite similar in India, with values between 1 to 8 mmol m^{-2} PLA s^{-1}. AOT40 values were as high as ~5 ppm h but in most parts of India the AOT40 values ranged between > 0 to 2 ppm h. The results in Chapter 5 shows that although the O_3 concentration increases towards the end of the wheat growing season, the relatively higher temperature and VPD values and the phenological factor limits the O_3 flux and thereby reducing the impact of O_3 on crops. In such situations the concentration based methods will tend to over estimate the O_3 impact as it is purely based on the O_3 concentration. On the other hand, the flux-based model gives more realistic estimates as it incorporates the influence of meteorological factors as well as crop physiology and phenology.

Although the data from field experiments describing wheat yield loss responses to O_3 in India are limited, these data show that the flux model results are consistent with results from experimental studies and the magnitude of the effects indicated by flux based approaches is similar to the observed crop loss estimates from the field experiments in

SA. For example, in Varanasi, experimental studies have reported wheat yield losses ranging between 0.5 to 25% under ambient O_3 (see Table 2-8) while RYL_{POD6} shows 15 to 20 % loss in the grid cell where Varanasi is situated (Figure 5-8). Other studies have also reported that field grown wheat showed reductions in biomass and under ambient O_3 concentrations in Varanasi (Ambasht and Agrawal, 2003; Tiwari *et al.,* 2005; Rai *et al.,* 2007; Singh *et al.,* 2009; Singh and Agrawal, 2009, 2010; Sarkar and Agrawal. 2010) and in Allahabad (Singh *et al.,* 2003). Both the locations are situated in NEPZ.

Given the evidence presented in Chapter 3 and 4 and from the results in this Chapter, it is therefore clear that on the weight of evidence, the flux based approaches are better than concentration based methods. These findings are also in agreement with findings from Europe. Mills *et al.* (2010) compared the location of observations of O_3 induced damage with estimates of O_3 risk based on modelled AOT40 and flux indices (the latter used a simplified method designed to reduce uncertainties in the estimation of flux by using a lower threshold of Y equal to 3 rather than 6 nmol O_3 m^{-2} PLA s^{-1}) and found data on ~30 species of agricultural and horticultural crops and ~15 semi-natural species showed that flux in Europe gave a better fit to effects data than AOT40; O_3 effects being found in many areas where AOT40 values were below the critical level of 3 ppm h (Mills *et al.,* 2010). The better performance of cumulative O_3 fluxes over AOT40 indices in indicating O_3 effects have also been reported for studies deriving flux-response relationships for crops (Pleijel 2007), semi-natural vegetation (Karlsson *et al.,* 2004) and forest trees (Uddling *et al.,* 2004; Matyssek *et al.,* 2007) with stronger regressions found between flux rather than AOT40 indices and response data. Hence, flux based methods have now been adopted for both crops and forest trees as the preferred O_3 risk assessment method of the UNECE LRTAP Convention in Europe (LRTAP Convention, 2010).

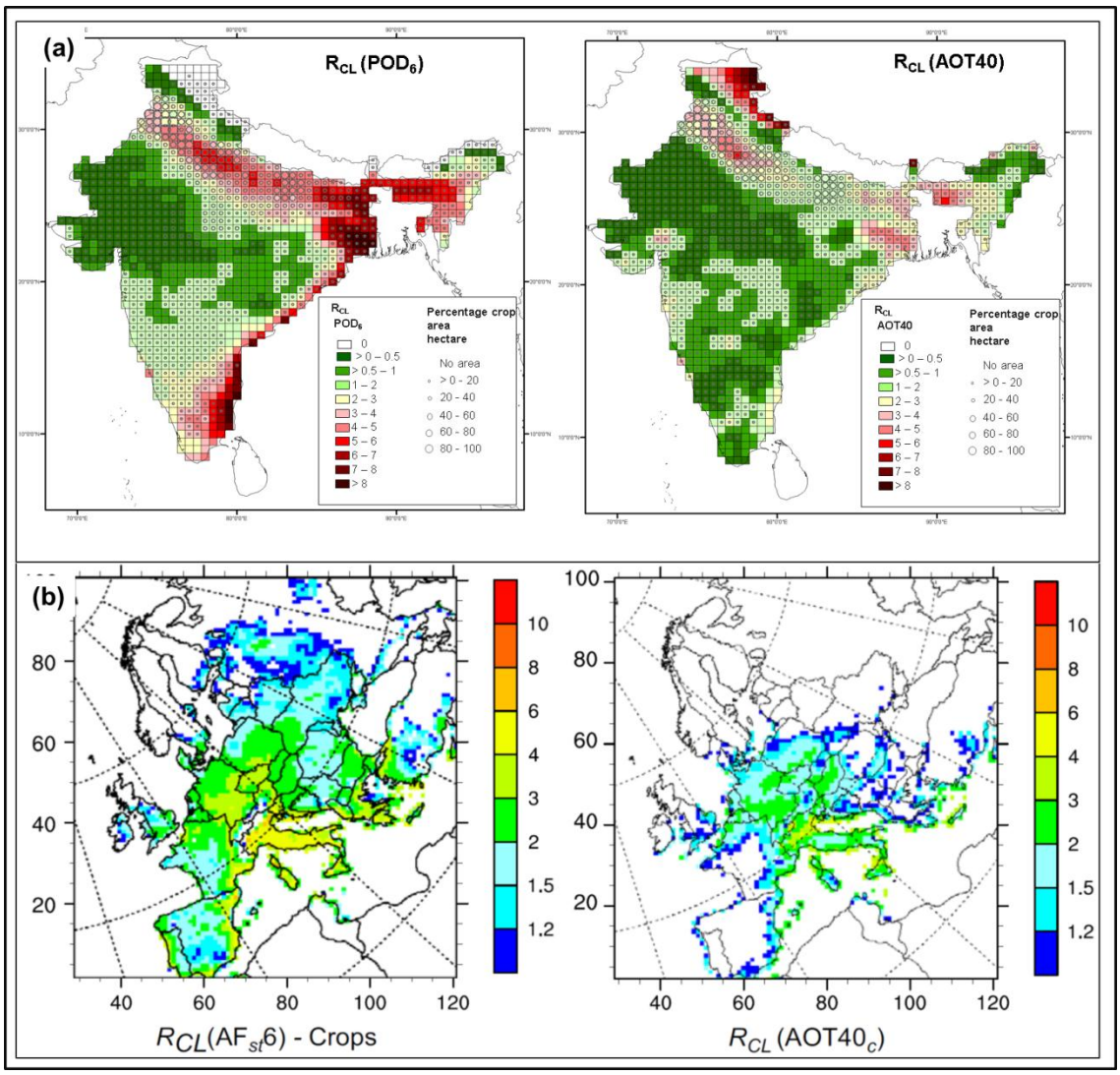

Figure 5-34: Comparison of the difference in spatial pattern between flux and AOT40 in (a) the current study and (b) Simpson *et al.* (2007)

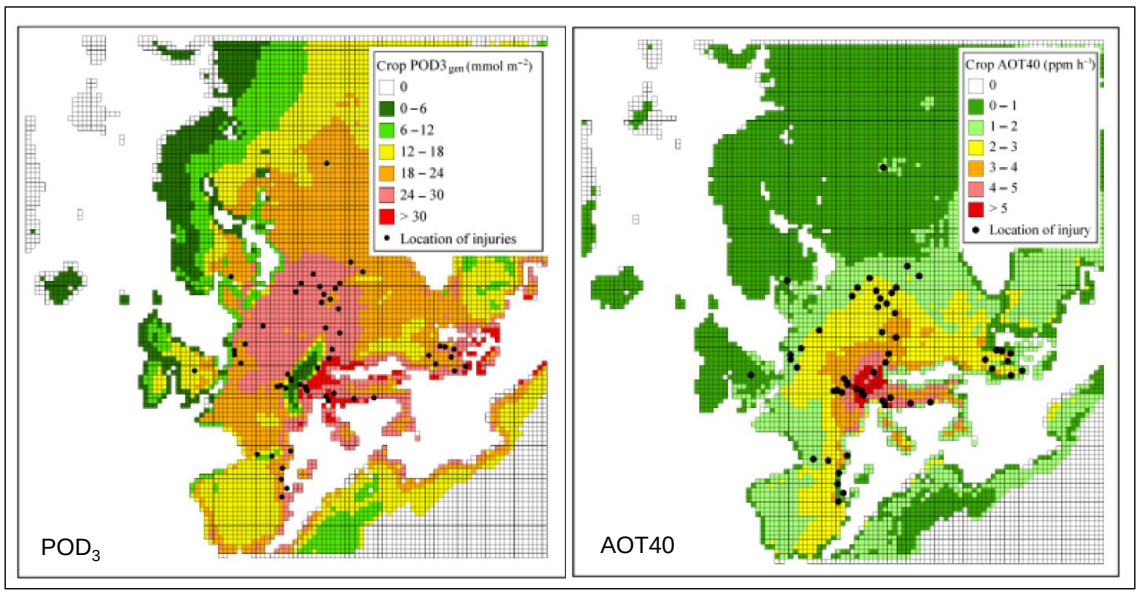

Figure 5-35: Comparison of the difference in spatial pattern between flux and AOT40 (Mills *et al.,* 2010)

In this thesis study, wheat was assumed to be irrigated, however in reality even though > 85 % of wheat area is irrigated, only two thirds receives full irrigation (Aggarwal *et al.,* 2008; FAOSTAT, 2011). Almost the entire wheat area in NWPZ is irrigated; NEPZ there is a mixture of rain-fed and irrigated wheat production (Ladha *et al.,* 2000; see Figure 1-6 in Chapter 1). In irrigated areas, the meteorological and environmental conditions are more favourable for O_3 uptake by stomates and therefore in reality, NWPZ is likely to have more O_3 flux than in NEPZ. But the warm temperatures and high VPDs in this region, especially toward the end of the growing period when O_3 flux is accumulated, may limit O_3 flux by reducing g_{sto}. If soil water restrictions were incorporated the assessment, F_{st} estimates are likely to be lower as drought is likely to limit the stomatal O_3 uptake in the warm, dry weather often associated with high O_3 and hence high AOT40 (Simpson *et al.,* 2007).

In India, the cultivar response may be different to the responses of European wheat to the same F_{st} due to differing physiologies (e.g., g_{max}), innate sensitivities (e.g., detoxification capacities) and different crop management practices. These are likely to add extra uncertainties to the flux-based RYL estimates under Indian conditions. Nonetheless, the use of flux and flux-response relationships attempts to allow for local meteorological conditions and O_3 concentration profiles in the assessment of O_3 risk which is not possible when using concentration based O_3 indices.

Flux incorporates important flux modifying factors like temperature, VPD, phenology and light which are also important crop growth limiting factors in India. Temperature stress is a major problem in India especially towards the end of the wheat growing season commonly referred to as terminal heat stress (Rane *et al.*, 2000; Rane and Nagarjan, 2004; Chauhan *et al.*, 2005). Salinity (see Chapter 3 Section 3.2.2.7) and soil fertility, etc., are important factors that affect wheat crops growing in India (Singh and Chatrath, 2001; Chatrath *et al.*, 2007). Salinity affects stomatal O_3 flux through changes in g_{sto} (Katerji *et al.*, 1997: Munns and Tester, 2008) and therefore future efforts to develop flux based indices for Indian conditions should consider incorporating these modifying factors.

In order to study how robust the Indian parameterization of the wheat g_{sto} model used in the estimates of F_{st} it is useful to compare against the European wheat parameterization as described in LRTAP Convention (2004). This comparison assess the robustness of the parameterizations in terms of the number of data points, number of cultivars and locations of the experimental plots used for deriving the parameterization for each g_{sto} model parameter. These comparisons are given in Table 5-4.

Table 5-4: Comparison of the Indian wheat parameterization (IN) with the European wheat parameterization (EU). *an alternative method was applied to derive f_{temp} (see Chapter 4); **denotes where the EU parameterization was used for the IN parameterization.

Parameter	**Units**	**Parameterization**		**No. of cultivars**		**No. of references**		**No. of data points**		**No. of locations**	
		IN	**EU**	**IN**	**EU**	**IN**	**EU**	**IN**	**EU**	**IN**	**EU**
g_{max}	mmol O_3 m^{-2} PLA^{-1}	230	450	22	7	15	7	22	7	7	5
f_{min}	fraction	0.01	0.01	63	1	15	2	67	2	7	1
f_{phen}				11	6	6	6	67	25	3	6
f_{phen_a}	fraction	0.8	0.8	-							
f_{phen_b}	fraction	0.2	0.2	-							
f_{phen_c}	Days	20	15	-							
f_{phen_d}	Days	30	40	-							
f_{phen_e}	°C days	200	270	-							
f_{phen_f}	°C days	600	700	-							

Table 5-4: Continued.

f_{light}											
$light_a$	(constant)	0.1661	0.0105	1	5	1	5	27	> 100	2	4
f_{temp}					3		3	*	> 100		3
T_{min}	°C	9	12								
T_{opt}	°C	22	26								
T_{max}	°C	36	40								
f_{VPD}		**			3		4		> 100		3
VPD_{max}	kPa		1.2								
VPD_{min}	kPa		3.2								
$\sum VPD_{crit}$	kPa		8								

The applicability of each of the model parameters for Indian wheat is discussed below.

i) g_{max}

From this chapter it is clear that g_{max} is the single most important parameter in the O_3 flux model as it defines the maximum level of F_{st} for a species. The g_{max} of 230 mmol O_3 m^{-2} PLA m^{-1} for wheat flag leaves was derived from a reasonable amount of data (22 data points representing the same number of cultivars from 15 different experiments; Table 5-4) available in the Indian literature. However, this value is very low compared to the g_{max} of non-flag leaves of Indian wheat (~ 430 mmol O_3 m^{-2} PLA m^{-1}; see Chapter 4) and the g_{max} of European wheat (which is based on fewer data; Table 5-4). g_{max} is a difficult parameter to define when relying on experiments or observations that are not specifically targeted towards its derivation, for example, although strict criteria were established and followed to ensure that g_{sto} values were repsentative of g_{max} (see Chapter 4); in the field g_{max} rarely occurs, due to phenological and environmental (CO_2, VPD, soil moisture, temperature etc.) constraints on g_{sto} (Korner, 1994; Breuer *et al.*, 2003; Pleijel *et al.*, 2007). As such, although these criteria were followed there is no guarantee that the 230 mmol O_3 m^{-2} PLA m^{-1} g_{max} value is indeed representative. Even within Europe, there has been a slow evolution in the definition of wheat flag leaf g_{max} with values of 296 mmol O_3 m^{-2} PLA s^{-1} being initially defined (Emberson *et al.*, 1998; Pleijel *et al.*, 2000) and subsequently increased to 485 mmol O_3 m^{-2} PLA s^{-1} (Pleijel *et al.*, 2004), 450 mmol O_3 m^{-2} PLA s^{-1} (LRTAP Convention, 2004; Pleijel *et al.*, 2007) and most recently 500 mmol O_3 m^{-2} PLA s^{-1} (LRTAP Convention, 2010).

To try to get an idea of the factors likely to be affecting g_{sto}, and hence the likelihood of measureing g_{max}, g_{sto} data was also collected for leaves other the the flag leaf to provide a larger dataset. A number of studies had measured g_{sto} on the 3rd fully expanded leaf. These g_{sto} data were grouped accoring to different variables; namely, type of leaf (either flag or non-flag leaf), stand characteristics (potted or field), type of g_{sto} measuring instrument (IRGA or Porometer) and research group making the measruremtns (Figure 5-36).

Figure 5-36 shows no substantial differences between the g_{sto} of potted and non-potted flag leaves. In general the g_{sto} of non-flag leaves is higher than that of the flag leaves. The 90th percentile value of the non-flag leaves was 360 mmol O_3 m^{-2} PLA s^{-1} which is more than the g_{max} of flag leaves (230 mmol O_3 m^{-2} PLA s^{-1}; 90th percentile); it is also evident that there are a few studies that show high g_{sto} values (up to 750 mmol O_3 m^{-2} PLA s^{-1}) which shows that if g_{max} had been defined by the highest value rather than an average maximum statistical value the result would have been quite different.

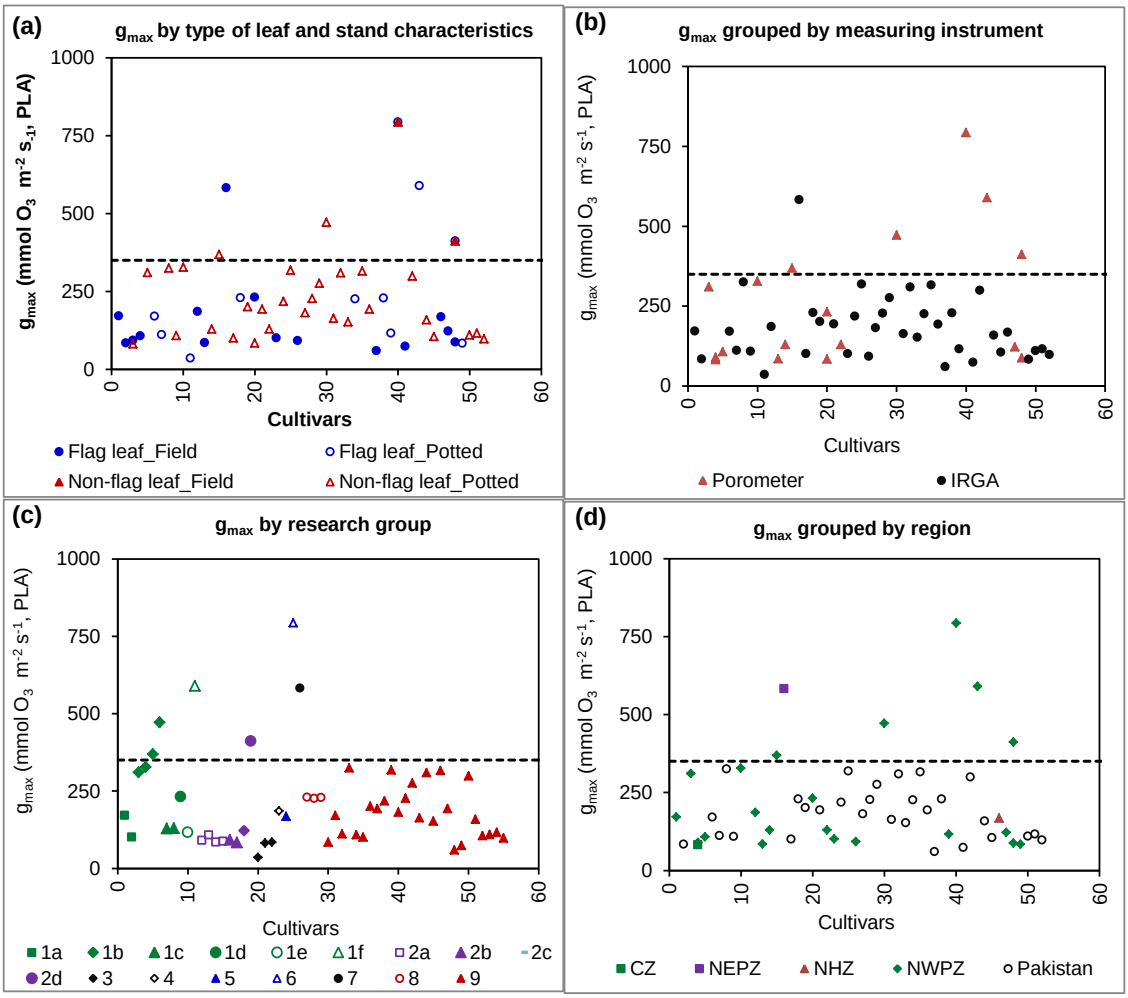

Figure 5-36: Stomatal conductance of wheat grown in India grouped by (a) type of leaf and stands characteristics, (b) measuring instrument, (c) region and (d) research group. Each data point represents the maximum g_{sto} that was observed for each cultivar either on both flag and non-flag leaves, either from a single or more than one study; the dashed line indicates the 90th percentile g_{sto} value.

There are no obvious differences in g_{sto} due to the type of measuring instrument used, though the highest values are often measured with a porometer (Figure 5-36b). Similarly, g_{sto} measreuemnts made in the different regions (AGZs and Pakistan) show a good range of values though the NWPZ region records the highest g_{sto} values (Figure 5-36d). However, there seem to be differences in the g_{sto} values measured by research group (Figure 5-36c). In Figure 5-36c, the colour represents region, the symbol shape the institute and the number the individual research group. These differences between the research groups could possibly be the reason for the differences between flag and non-flag leaf g_{sto} values rather than the actual differences in g_{sto} that exist between the flag leaves and non-flag leaves. Two studies that have already been used to derive g_{max} in (Table 4-6), Ashraf and Parveen (2002) and Ashraf and Bashir, (2003) measured g_{sto} on flag leaves and non-flag leaves simultaneously during the period which is within the O_3 accumulation period on four wheat cultivars. In these two studies, the g_{sto} measurements were performed on the flag leaf, the first leaf from the top and second leaf from top between 2 to 12 days after anthesis. The study shows that in all the four cultivars, the flag leaf g_{sto} was higher than the non-flag leaf g_{sto}. This suggest that it is not possible to conclude from the currently available data, that g_{sto} of non-flag leaves is higher than that of the flag leaves in Indian wheat as the difference in g_{sto} observed in the data in Figure 5-36a could possibly be due to the differences in measuring methods of the different research groups (Figure 5-36c).

ii) Phenology (A_{start}, A_{end}, f_{phen})

This study also clearly indicates that phenology is an important factor in modelling F_{st}. In this thesis study the wheat phenology, both in terms of timing of the wheat growth period and the variation in g_{sto} with leaf age (used to define f_{phen}) have been defined based on a number of extensive wheat phenological databases and supported by data in peer reviewed literature (see Chapter 2) and therefore can be considered to be fairly robust. In fact the IN growing season and f_{phen} parameterization are based on more substantial datasets than the European parameterization of these parameters (Table 5-5).

However, in this thesis study the derivation of the f_{phen} function requires GDD to be calculated from observed fixed day values which is likely to introduce uncertainty into

the estimate of thermal time defined growth stages. As phenology is such an important factor having as robust a parameterization of f_{phen} is important and ideally this should be derived with observed GDD values. The f_{phen} function in this study is similar to the f_{phen} function for European wheat (LRTAP Convention, 2004). However, the recent revision (LRTAP Convention, 2010) defines a plateau in f_{phen} around the mid anthesis period. Further g_{sto} data are required to establish whether a similar f_{phen} relationship would be suitable for Indian conditions.

iii) f_{temp}

Since f_{temp} is estimated form 30 year average temperature data for the wheat growth period it gives a good representation of the temperature conditions that are present when the wheat crop is actively growing. There is also little difference between the EU and IN f_{temp} parameterisations. It should be noted that to get a more robust model parameterization, more data would be required describing the relationship between g_{sto} and the Indian temperature conditions to which wheat is exposed in the different AGZs. However, obtaining such data was beyond the scope of this PhD. In the absence of such robust data, the f_{temp} parameterization at least modifies F_{st} when surface air temperatures fall outside of the mormal AGZ climatic conditions.

The relationship between g_{sto} and temperature is generally a normal Gaussian distribution with the optimum temperature close to the mean temperature. f_{temp} relationships for European wheat also show a curve similar to a Gaussian curve (Emberson *et al.*, 2000; Pleijel *et al.*, 2007). However, there are also studies that show a skewed f_{temp} relationship in other crops, e.g., in lettuce (Goumenaki *et al.*, 2007), in trees (Marzuoli *et al.*, 2008).

iv) f_{light}

The IN f_{light} function is based on just one experimental study and therefore is less robust than the EU parameterization of the model component (Table 5-5). Observational

studies have also shown that during the main wheat growing period (December to March) in India, especially in the IGP region, atmospheric aerosol loads are particularly high (Ramanathan *et al.,* 2008; Badarinath *et al.,* 2011; Verma *et al.,* 2011). Aerosols absorb the incoming solar radiation and therefore alter the amount and quality of radiation at the surface. Future studies could investigate alterations to the calculation of sky transmissivity (ST; see Chapter 3) as well as the manner in which variable fractions of diffuse and direct radiation affect g_{sto} (Mercardo *et al.,* 2009) since this may influence the F_{st} light limitation.

v) f_{VPD}

This study also identifies VPD as an important F_{st} limiting factor. Due to the unavailability of data from which to establish the f_{VPD} function, the EU parameterization for f_{VPD} has been used. In India, the wheat growing areas are mainly on lowlands with a combination of dry tropical areas with VPD usually > 1 kPa and humid tropical areas with VPD values usually < 0.8 kPa; most of the wheat areas are dominated by dry tropical areas which are irrigated (Dubin and Rajaram, 1996). Shirke and Padre (2004) reported that plants exposed to variable levels of VPD in different seasons in India showed differences in g_{sto}, with g_{sto} declining under high VPD (>3 kPa); the plants water use efficiency remained constant. This suggests that the EU f_{VPD} parameterization may provide a reasonable estimate for Indian conditions however it will be important to gain an IN parameterization of this function in the future. Understanding the co-variation in f_{temp}, f_{VPD} and water use (Fuhrer., 2009) will also be important for the future.

Sensitivity analysis

The OAT sensitivity analysis shows variability in the importance of the different model parameters on model output with g_{max}, irradiance and VPD parameters being most important. Model estimates for POD_6 were also more sensitive than POD_0; the sensitivity analyses showed that often differences to the base case were < 10 % in terms

of POD_0. The parameters which had significant effects on the model outputs also varied between AGZs.

Uncertainties related to input variables (meteorological and O_3 concentration estimates) are not considered in this study, which are bound to be present. Engardt, (2008) reports an under/ over estimation by < 10 % while estimating O_3 concentrations in India using MATCH model.

Sensitivity analysis on the stomatal deposition model conducted for the European model parameterizations for trees (Alonso *et al.,* 2009), forests and temperate cereals (Simpson *et al.,* 2003), and for agricultural land, grass, coniferous and deciduous forests (Mészáros *et al.,* 2009) show that the uncertainties related to flux estimates are much lower than uncertainties found for AOT40, the current indicator used by EU and UNECE for O_3 control assessment (Simpson *et al.,* 2003).

5.6 Conclusion

In summary, it is acknowledged that there are uncertainties in the magnitude of estimates of the O_3 induced yield losses for Indian wheat due to uncertainties in the IN wheat O_3 flux model parameterizations. However, the evidence in Chapter 3, 4 and this Chapter shows that flux based method give a better estimate of the O_3 crops loss than the concentration based methods. The flux based method is also useful in terms of identifying the important factors such as O_3 concentration profile, crop growth period, meteorological conditions and crop physiology that determine crop sensitivity to O_3.

The model is also a useful 'tool' to help understand the factors that could affect flux and hence O_3 risk and hence can be used to assess the role that introduction of particular plant physiological or phenological traits may play in modifying plant sensitivity to O_3. As such the flux based method is more useful than the concentration based methods in providing information that could be used to improve crop biotechnology to reduce sensitivity to O_3. However, further research is necessary to improve the model performance in identifying the magnitude of O_3 damage to crops grown in SA. There is also strong evidence, from both flux and concentration based risk assessments that O_3 is

a threat to agricultural production, especially in the important IGP region.

The application of the flux based model as a tool to aid crop biotechnology is discussed further in Chapter 6. This is important since new wheat cultivars are continuously being released in India; understanding how the traits of these new cultivars may affect O_3 sensitivity will be important to help ensure continued crop productivity in key agricultural regions across SA and India.

Chapter 6 Biotechnological advancements and wheat sensitivity to O_3 in India

6.1 Introduction

India's wheat production is profoundly important within the South Asian region as well as on a global scale. Wheat, along with rice, serves as the staple food crops for the more than 1 billion people living in India (Joshi *et al.,* 2007b; World Population Prospects-UN, 2008). India produces ~12% of the global wheat production (FAOSTAT, 2011) and is the second largest consumer of wheat (Joshi *et al.,* 2007b).

The Green Revolution in the 1960s played a major role in turning India from a food grain deficient state (prior to the 1960s) to the primarily food grain self-sufficient state that it is at present and has been since the late 1990s (Larson *et al.,* 2004; Singh, 2000). A key factor for this change was the tremendous increase in India's wheat production (Aggarwal *et al.,* 2008) which rose by a factor of 6, from 12.2 million tonnes in 1965 to 80.7 million tonnes in 2009, due in part to associated increases in yield from 0.9 to 2.8 t/ha respectively (Figure 6-1; FAOSTAT). India's wheat yield was lower than that of the world average yield but it equalled the world average yield by the late 1990s (Figure 6-1). The main factors that contributed to the increase in wheat yield and production were;

(i) increase in wheat area from 13.4 in 1965 to 28 million hectares in 2009 (Figure 6-1)
(ii) improved management practices that included a substantial increase in inputs e.g., use of fertilizers, pesticides and irrigation (Chatranth *et al.*, 2006; Sankaran *et al.*, 2000).
(iii) introduction of improved high yielding, biotic or abiotic stress resistant cultivars, especially over the recent decades (Rane *et al.*, 2007).

The increase in cropping area expanded rapidly at first however, the growth in area has stagnated over the last decade due to extremely limited availability of land suitable for further cultivation (Figure 6-2). Figure 6-2 shows how this has resulted in substantially reduced growth rates in the area under wheat cultivation with subsequent reductions in growth rates of production and yield. The improvement in the management practices were more pronounced in the northern part of the IGP where there is intensive wheat

cropping (Aggarwal *et al.*, 2004). The irrigated area grew from 38% of the total wheat area pre-Green Revolution (1955-65) to more than 85% at present (1995-2005) with a concomitant decreases in area under rain-fed production (Aggarwal *et al.*, 2008; FAOSTAT, 2011; Figure 6-3). The yields in irrigated areas are higher than in the non-irrigated areas with irrigated wheat averaging 2.8 t/ha compared to rain-fed wheat averaging 1.5 t/ha (Chatranth *et al.*, 2008). Three types of wheat are grown in India, bread wheat (*Triticum aestivum*), durum wheat (*Triticum durum*) and *Triticum diococum* (Joshi *et al.*, 2007b). Bread wheat accounts for 95% of the wheat grown while durum is 4% and *Triticum diococum* is 1% (Gupta *et al.*, 2004; Mishra *et al.*, 2007).

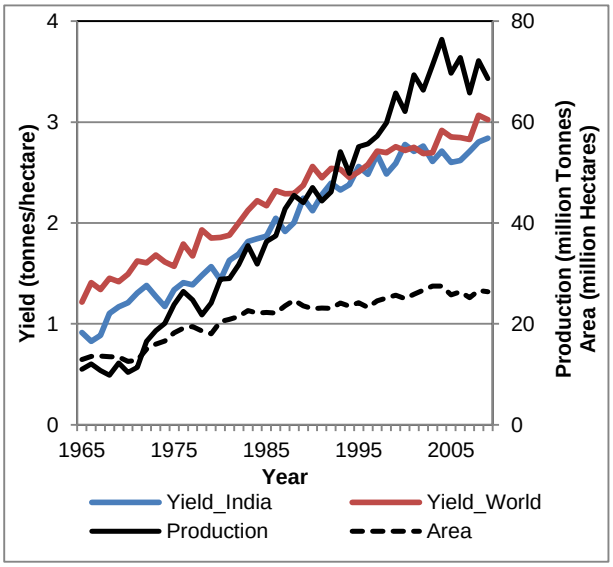

Figure 6-1: Area, yield and production statistics for wheat growing in India between 1965 to 2009. Also shown for comparison are trends in global average wheat yields for the same time period (FAOSTAT, 2011).

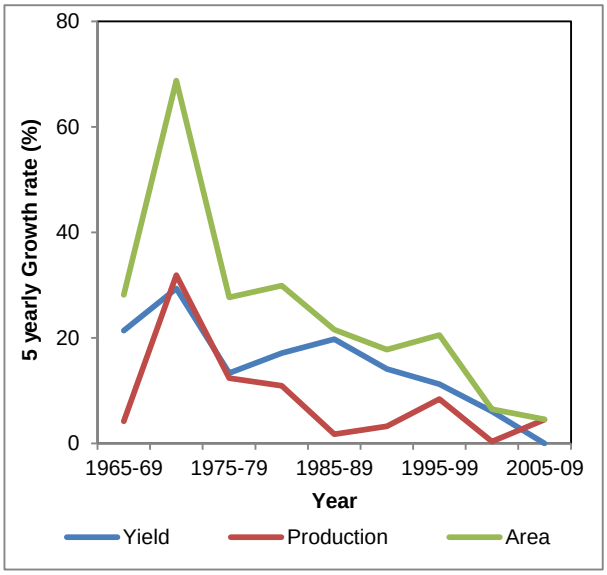

Figure 6-2: Decadal (5 yearly) growth in wheat area, yield and production in India (FAOSTAT, 2011).

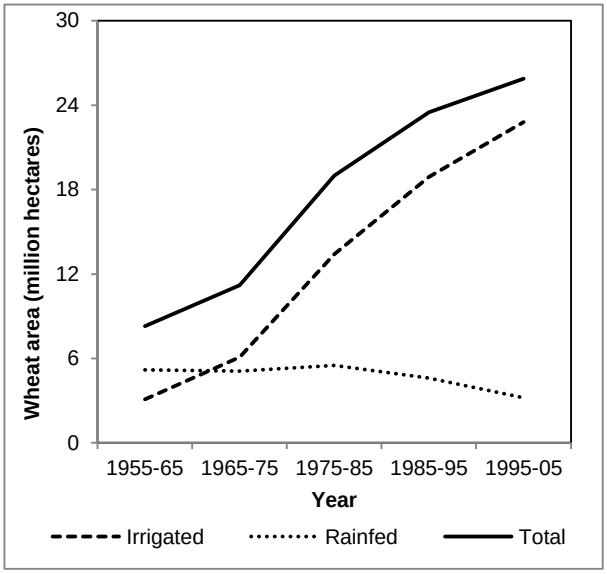

Figure 6-3: Change in area under irrigation for both rain-fed and irrigated wheat between 1955 to 2005 (Chatrath *et al.*, 2006; DACNET, 2011).

The wheat demand in India in the year 2000 was 53.3 million tonnes and the production was ~ 75 million tonnes (AGMARK; FAO). However, it is estimated that by 2020 India's wheat demand will be 87.5 million tonnes (Chatrath *et al.,* 2006). Therefore, if India is to remain food grain self-sufficient, this would imply the need for a further increase in India's wheat production in the near future, contrasting with the evidence already presented of the gradual decrease in the growth rate of yield and consequent production of wheat over the last decade (Figure 6-2). The current situation is also reflected by Indian wheat yields having recently dipped again below the world average (Figure 6-1).

At present, Indian wheat cultivars are not performing to their full potential with average yields ranging between 0.8 to 4.5 t/ha (the current average wheat yield for India is 2.7 t/ha) compared with potential yields of between 4.8 to 8.3 t/ha (Aggarwal *et al.,* 2000; Pathak *et al.,* 2003; Duxbury *et al.,* 2000; Mitra and Bhatia, 2008; DWD, 2011). An important factor for this yield gap is that many parts of the wheat cropping region in India, especially the IGP region, experience biotic (leaf and stripe rusts, smut, blight and karnal bunt; Joshi *et al.,* 2007b) and abiotic stresses (high temperature, drought/water logging, salinity, etc.; Singh, 2000; Ladha *et al.,* 2003) during the wheat growing season (Gupta and Seth, 2007). Wheat requires a cool temperature throughout the growing season with an optimum temperature of about 22°C (DWD, 2011). In many parts of the IGP, temperatures high enough to affect the yield of wheat are a common occurrence especially during the grain filling stage (Rane *et al.,* 2007). Studies have reported that in India, the cool temperature period for wheat is declining in length and there is an increasing exposure to temperature stress during the grain filling period (Rane *et al.,* 2000; Sharma *et al.,* 2002). This problem is expected to worsen in the future with the predicted increase in temperature in coming years as a result of climate change (Mitra and Bhatia, 2008). Drought is also becoming an increasingly important factor that affects wheat crops across the region (Ladha *et al.,* 2003; Rodell *et al.,* 2009). This is confounded by poor management practices and insufficient input of supplemental irrigation even though most of the wheat growing region is now under irrigation (Figure 6-3). Such supplemental irrigation may not be sustainable in the longer term particularly as in parts of the Western IGP; 60-65% of the total irrigation requirement is met by ground water (Singh, 2000).

Reversing the trend of stagnating wheat yield increases will be difficult since firstly there is no scope for further increases in the area under wheat cultivation (Bruinsma, 2009) and secondly, increases in inputs are limited due to constraints on their availability (e.g., shortage of water available for use as irrigation) (Joshi *et al.*, 2007b). Increasing in inputs is also expensive and often unlikely to lead to the practice of sustainable agricultural methods (Swaminathan, 2010). Thus, the development of new cultivars through biotechnological intervention seems to be a more realistic and sustainable option for increasing the productivity of wheat in India (Pingali, 1999; Patnaik and Khurana, 2001; Mishra *et al.*, 2007; Strickland, 2007).

Biotechnology interventions are well advanced for wheat in India with interventions targeting specific biotic and abiotic stresses that are thought to be most important in limiting wheat yields. A number of recent studies have reported an increase in O_3 sensitivity in more recent wheat cultivars in Europe (Barnes *et al.*, 1990; Velissariou *et al.*, 1992; Pleijel *et al.*, 2006b) the US (Betzelberger *et al.*, 2010) as well as in Asia (Biswas *et al.*, 2008a and b). In view of this, it is important to try to understand how key traits being introduced currently in India may affect O_3 sensitivity; such knowledge may be useful to plant breeders and could inform future breeding strategies.

With this in view, the aims of this chapter are as follows:

1. To investigate the potential application of flux based approaches as a tool capable of informing future crop biotechnology efforts
2. To perform a literature and agricultural database review identifying the traits being bred for in the new Indian wheat cultivars
3. Qualitatively assess how these traits may alter O_3 sensitivity using flux based risk assessment methods
4. Investigate whether concentration based risk assessment methods would indicate the same sensitivity of traits to O_3.

As such the overall aim of this Chapter is to investigate the traits that are being targeted for introduction to the IGP region in India and consider how these might play a role in altering O_3 sensitivity.

6.1.1 Literature and database review of biotechnology interventions for wheat in India

The FAO in its 'Statement on Biodiversity' uses the definition of biotechnology given by the Convention on Biological Diversity that defines biotechnology as "*any technological application that uses biological systems, living organisms, or derivatives thereof, to make or modify products or processes for specific use*" (CBD, 1992; FAO, 2000b). Biotechnology in a broader sense encompasses a number of tools and elements of conventional breeding techniques, bioinformatics, microbiology, molecular genetics, biochemistry, plant physiology, and molecular biology (ISAAA, 2010). In the past few decades biotechnology has tended to focus on the technological application of wheat at the molecular and cellular level to improve products and biological systems (Guilford-Blake and Stricklan, 2008). Conventional breeding is still practiced, though to a lesser extent.

The most common biotechnology breeding methods can be summarized as follows. In conventional breeding, wheat cultivars are crossed with wild relatives (e.g, *Aegilops tauschii*) that have high heritable variation for tolerance to stresses such as drought (Skovmand *et al.,* 2001, cf. Ashraf *et al.,* 2010). In marker assisted breeding (MAB), DNA markers are used to identify the quantitative trait loci (QTL) of the genes exhibiting significant effect on the expression of traits for specific stress tolerance. Genetic engineering is used to incorporate genes related to stress tolerance into crops, e.g., genetically engineering wheat plants to accumulate osmolytes such as amino acids, sugars or sugar alcohol that result in decreased osmotic potential and water deficiency to develop drought resistant wheat cultivars (Sivamani *et al.,* 2000). The new wheat cultivars in India are developed using one or a combination of these breeding methods.

An important milestone in the improvement of wheat productivity in India was the establishment of the 'All India Coordinated Wheat Improvement Project' (AICWIP) by the Indian Council of Agricultural Research (ICAR) in 1965. This project aimed to improve wheat and barley production in India (Mishra *et al.*, 2007) and is now coordinated by the Directorate of Wheat Research (DWR), Karnal, India (http://www.dwr.in/). This programme in particular, but also aided by many other national and international crop improvement programmes (e.g., Centro Internacional de Mejoramiento de Maise and Trigo -CYMMIT) has been responsible for the

improvement of wheat productivity through the introduction of high yielding and stress tolerant wheat cultivars.

Pre 1960s, most of the wheat cultivars grown in India were tall with a weak stem, were low yielding and susceptible to biotic and abiotic stresses (Borlaug, 1971; Joshi *et al.*, 2007) making them unsuitable for intensive agriculture (Smale *et al.*, 2008). Since the 1960s, most of the wheat cultivars introduced in India have been dwarf or semi dwarf cultivars with stronger stems, a greater responsiveness to enhanced inputs, higher yielding, non-lodging and with enhanced resistances to diseases. Due to these desirable traits, the dwarf and semi dwarf wheat cultivars were widely adopted by the farmers in many parts of India. This was extremely influential in increasing the yield and production of wheat in India during the Green Revolution in the 1960s (Aggarwal *et al.*, 2000), turning India into a global leader in agricultural production (Gupta and Seth, 2007). Currently semi dwarf wheat covers 90% of wheat area in India (Sankaran *et al.*, 2000).

Since 1965 more than 350 new high yielding cultivars have been introduced with traits that confer varying degrees of biotic and abiotic stress tolerant cultivars Figure 6-4; Chatrath *et al.*, 2006; Mishra *et al.*, 2007). Most of these cultivars of wheat were released through the AICWIP and new cultivars are continuously being released (Sankaran *et al.*, 2000) though the number of new cultivars released has been in decline in recent decades. Currently, about 60 different cultivars are grown by farmers across the various AGZs in India with a few prominent cultivars being those most frequently under cultivation (Nagarajan, 2005). For example, the DWD lists 34 prominent cultivars that are cultivated across India (Mishra *et al.*, 2007). These new cultivars perform to their potential only when the growing conditions are favorable for growth and development (Sankaran *et al.*, 2000).

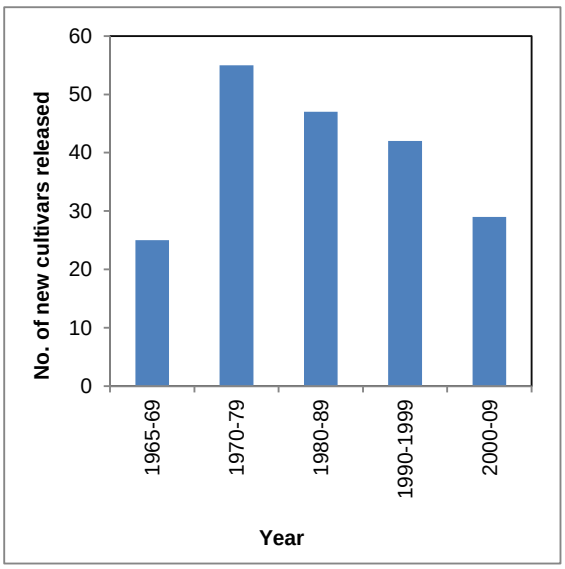

Figure 6-4: The number of new wheat cultivars released in India since 1965 (Mishra *et al.*, 2007; SeedNet, 2011; DACNET, 2011).

Most of the new wheat cultivars have been released specifically for cultivation in the IGP region (Mishra *et al.*, 2007; SeedNet, 2011). These new cultivars possess traits/ characteristics that allow improved yield under the environmental conditions that are prevalent across this region (Kalra *et al.*, 2007). For example, all the farmers in the state of Punjab and Haryana, part of the IGP which produces about 35% of India's total wheat production, continue to adopt new high yielding wheat cultivars. By contrast, the rate of adoption of new cultivars has been slow in other states (Mishra *et al.*, 2007).

In summary, over the past 4 decades biotechnological intervention has played a key role in improving the productivity of wheat in India (Mishra *et al.*, 2007), this role is expected to continue in the near future leading to improvements in the productivity of wheat through the introduction of wheat cultivars with high yield potentials, that are resistant to biotic and abiotic stresses and that are also input use efficient (Mishra *et al.*, 2007; Strickland, 2007; Pingali, 1999; Patnaik and Khurana, 2001).

6.2 New wheat varietal traits

To obtain an overview of the key traits that have provided the focus for recent biotechnological advancements in India, literature related to the improvement in Indian wheat cultivars since 1995 were collected from peer reviewed journals and also from the DWD and other national and international wheat development program reports (e.g., CYMMIT). Data was collected that described the traits that are currently being introduced as well as the growing conditions for which these traits are specifically being developed (e.g., rain-fed or irrigated, timely or late sown) were collected. A summary of these data are provided in Figure 6-5, which shows the main plant traits introduced between 1995 and 2008 and Figure 6-6 which shows how many new cultivars have been introduced for the main growing conditions under which wheat is cultivated in India over the same time period. Figure 6-5 shows that traits to improve yield under conditions of rust infestation and heat stress (either through heat tolerance or alterations to the rate of crop development) have been the most frequently introduced traits in the past decade.

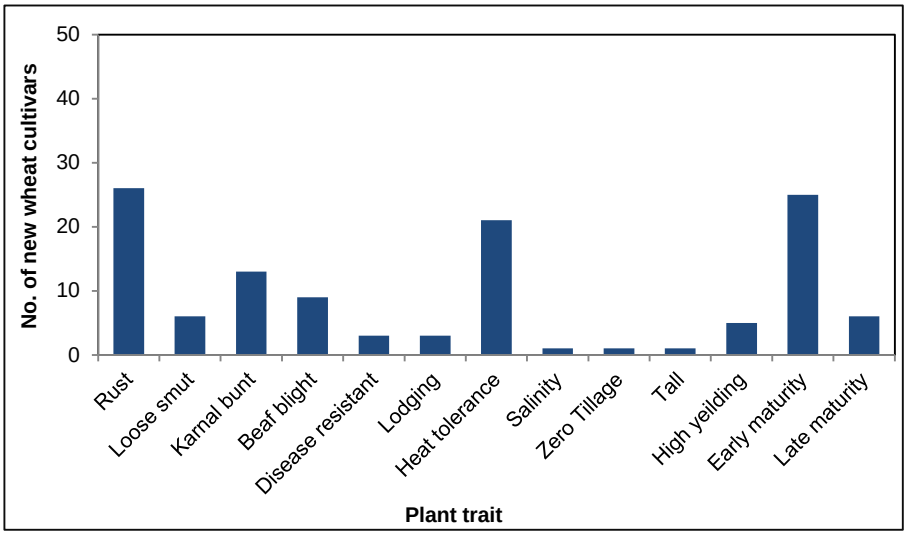

Figure 6-5: The number of wheat cultivars bred for a number of different traits that have been released between 1995 to 2008 in India (Mishra *et al.*, 2007; SeedNet, 2011; DACNET, 2011). Some cultivars possess more than one of the traits identified.

Figure 6-6 shows that the new cultivars introduced from 1995 onwards are mainly intended for use in irrigated production systems with 75% of the co-ordinated efforts on wheat development focused on irrigated wheat, of this amount 82% is focused on improvement of bread wheat (Mishra *et al.*, 2007). Most of the wheat cultivars are developed for either timely sown or late sown irrigated conditions (Rane *et al.*, 2007; Joshi *et al.*, 2007b; DWD, 2011). Timely sown wheat refers to crops sown according to the officially recommended sowing dates in India; late sown crops are sown after the recommended sowing dates. Further details of the differences in these timely and late sown cultivars are provided in section 6.3.1.2.

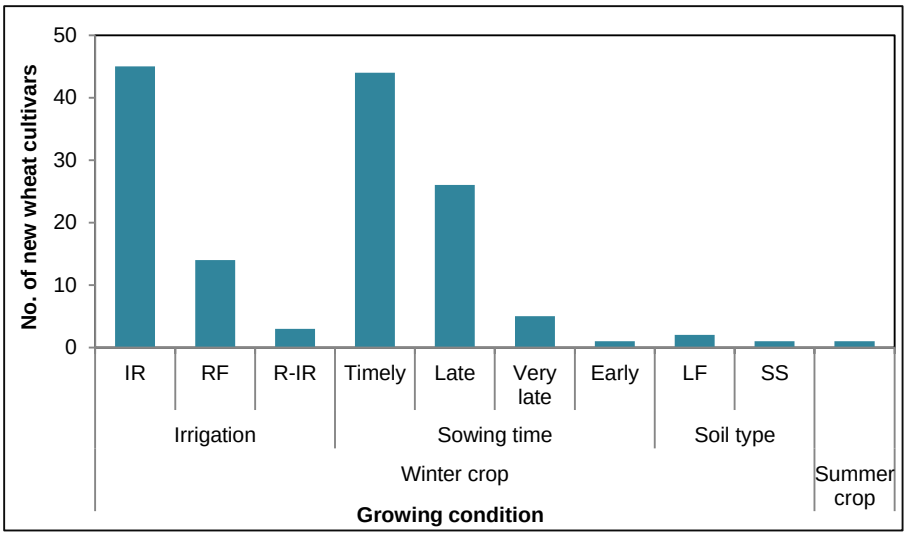

Figure 6-6: Recommended growing conditions for new wheat cultivars released from 1995 onwards in India (Mishra *et al.*, 2007; DACNET, 2011; SeedNet, 2011). Some cultivars are suited to more than one of the growing conditions. IR= irrigated; RF = rainfed; R-IR= both rainfed and irrigated.

Drought is an important stress factor affecting wheat crops in India but despite considerable effort, few drought resistant cultivars have been developed. Salinity is also an important stress in the western parts of India affecting about 4.5 million hectares under wheat cultivation in India, especially in the canal irrigated areas (Singh and Chatrath, 2001; Chatrath *et al.*, 2007), however to date efforts to breed for tolerance to salinity have not resulted in many new cultivars being released. The following section discusses the three most important traits in relation to potential O_3 sensitivity.

6.2.1 Heat tolerance and early maturity

One of the most important factors that reduces wheat yield in India is heat stress (Nagarajan, 2005). In India, current estimates show that about 13.5 million hectares of wheat under cultivation are subject to heat stress (Joshi *et al.,* 2007b; Rane *et al.,* 2007). Out of the 27 million hectares of wheat growing areas in India, about 11 million hectares are under rice-wheat cropping systems (Ladha *et al.,* 2000; Joshi *et al.,* 2007) and most parts of this region qualify as heat stressed with many areas having a mean daily temperature above 15°C even in the coolest months (Fischer and Byerlee 1991). Exposure of wheat to temperatures in excess of 35°C is known to cause reductions in yield and grain quality (Stone & Nicolas, 1994; Joshi *et al.,* 2007; Ladha *et al.,* 2003; Regmi *et al.,* 2002; Matsui *et al.,* 1997). Controlled chamber and field experiments have shown that wheat grain yield is reduced by 4-5% for every 1°C increase in mean temperature above 15°C during the grain filling period (Wardlaw and Wrigley, 1994; Chauhan *et al.,* 2005). Delays in the monsoon usually make the rice harvest occur later which in turn delays wheat sowing (Rane *et al.,* 2007; Joshi *et al.,* 2007b). This results in a shift in the wheat growing period towards the warmer part of the year and exposes wheat crops to particularly extreme rises in temperatures during grain filling, commonly referred to as terminal heat stress (Rane *et al.,* 2000; Rane and Nagarajan, 2004).

Exposure to high temperatures after anthesis increases the development of the crops and shortens the grain filling period resulting in reduced grain weight, quality and number (Yang *et al.,* 2011; Altenbach *et al.,* 2003; Hunt *et al.,* 1991; Jenner, 1991; Wheeler *et al.,* 1996). In addition to the effect on the grain filling duration and yield parameters, thermal stress also affects the physiological characteristics of the wheat crop. At higher temperature, the crop experiences higher rates of metabolism and evapo-transpiration which make the crop develop quicker (Rawson, 1988; Reynolds *et al.,* 1998, 2000). As a result there is an increased demand for growth resources such as water and nutrients (Reynolds *et al.,* 2001).

Due to the frequent delay in wheat sowing and the occurrence of terminal heat stress coupled with the projected increases in temperature under climate change (Joshi *et al.,* 2007b) and the increase in food demand in the region (Chatrath *et al.,* 2006), development of wheat cultivars that possess tolerance for heat is one of the major priorities of wheat improvement programs for the IGP region (Rane *et al.,* 2007).

In India, efforts have been made to avoid or reduce heat stress in wheat plants through management practices, increased inputs and development of heat tolerant cultivars (Mishra *et al.*, 2007). Currently, reduction of heat stress mainly relies on increased in inputs, especially irrigation (Badaruddin *et al.*, 1999). Management practices like the use of farm yard manures (FYM) and straw mulch that retain soil moisture are also useful for ameliorating heat stress (Lal, 1975; Mian *et al.*, 1985).

Biotechnology has also been targeted towards overcoming yield losses associated with terminal heat stress. A number of heat tolerant cultivars have been released in India since the 1960s. Some examples of heat tolerant wheat cultivars in India are Raj-3765, Halna, NAIW-34, NW-1014, Tepoka, WH-730, CBW-12 and HUW-234 (Mishra *et al.*, 2007; Yadav *et al.*, 2010). These cultivars possess traits that either make them tolerant to heat stress or allow the crops to avoid heat stress. Heat tolerance can be provided through inherent genetic and physiological traits such as efficient assimilate partitioning, increased number of tillers and grains/spikes, enhanced membrane thermostability, significant canopy temperature depression and an increased stay green habit (Mishra *et al.*, 2007; Joshi *et al.*, 2007d). An important trait for avoiding heat stress is early maturity (shortened growing period without yield penalty to avoid terminal heat stress), (Joshi *et al.*, 2007c; Yadav *et al.*, 2010; Reynolds *et al.*, 2001). For example, relatively higher thermal tolerance was observed in Indian wheat cultivars namely, WR-704, HD-2255 and HUW-234 that showed traits of early flowering, long grain growth and avoidance of terminal heat stress (Rane *et al.*, 2007; Rane and Chauhan, 2002a).

6.2.2 Rust resistance

Rust diseases are the most important diseases of cereals. There are three types of rust that affect wheat crops, stem (black) rust, leaf (brown) rust and stripe (yellow) rust. The most common rust is leaf rust (Navabi *et al.*, 2003; Singh *et al.*, 2004). Leaf or stripe (yellow) rust can cause up to 60% loss of yield whilst stem rust can cause up to 100 % losses (Park *et al.*, 2007; Dubin and Brenan, 2009). Rust reduces the number of leaves, root growth and yield by decreasing photosynthesis, increasing the transpiration rate, decreasing the translocation rate by moving carbohydrates to the infected area, where it is used to limit the growth of the rust pathogens (Dubin and Brenan, 2009).

Before the 1960s and the Green Revolution the wheat cultivars in India were very susceptible to diseases. India has witnessed a number of rust epidemics in the past with yield losses as high as 60-75% in some cases (Dubin and Brenan, 2009). The rust epidemics were more widespread before the Green Revolution and have been more localized since that time (Dubin and Brenan, 2009). Stripe and leaf rust are the most common type of rust in Northern and central India while in south India stem rust is more common (Dubin and Brenan, 2009). About 80% of the area under wheat cultivation in India is rust prone (Singh *et al.*, 2004). Leaf and stem rust usually occur in warm regions (10° – 35°C) while stripe rust occurs in regions with cooler (2° – 15°C) climates (Singh *et al.*, 2002).

The Indian National Wheat Rust Survey Programme has been actively monitoring wheat rusts in Indian since 1935 (Prashar *et al.*, 2008). This Programme in combination with other research has established that chemical control of rust disease is often unmanageable and expensive (Navabi *et al.*, 2003). Genetic resistance is the most economic method of reducing yield losses due to rust (Kolmer, 1999). In light of this, since the Green Revolution, efforts have focused on developing and introducing wheat cultivars resistant to different types of wheat rust. Important rust resistant cultivars are Kalyasona released in 1967, Sonalika in 1973, Sonora-64 in 1968 and PBW-343 in 1995 (Prashar *et al.*, 2008). Most cultivars remain resistant for five to six years but they eventually become susceptible to new wheat rust pathotypes (Singh *et al.*, 2002; Dubin and Brenan, 2009). As such, there is a need for the continuous release of rust resistant cultivars.

6.2.3. Drought resistance

Drought stress in wheat crops limits growth and productivity by inducing stomatal closure, reducing photosynthetic activity, increasing oxidative stress, altering cell wall elasticity and generating toxic metabolites that cause plant death (Ashraf, 2010; Ewert *et al.*, 2002; Caruso *et al.*, 2009; Khanna-Chopra and Selote, 2007; Biehler and Fock, 1996). About 50% of the wheat cropping area in the world is affected by periodic drought (Rajaram, 2001). Although more than 85% of the wheat area in India is irrigated (Figure 6-3) only one-third receives full irrigation with the remainder being

partially irrigated (i.e. receiving 1-2 irrigations over the cropping season) (Joshi *et al.*, 2007b). More than half of the total irrigation in this region comes from groundwater as a result of which there has been a decline in the ground water table in many wheat growing areas (Singh, 2000; Sinha *et al.*, 1998 cross ref. from Ladha *et al.*, 2003) and in some areas the mean depletion rate is 4.0±1.0 cm yr^{-1} (Rodell *et al.*, 2009). This suggests that in the future, there will be a further increase in drought stress and water may be a limiting factor in the production of wheat in India.

In India, efforts have been made to alleviate drought stress by improving management practices (e.g., management of irrigation, diversification / intensification of rice-wheat cropping systems), increasing inputs (e.g., irrigation and fertilizers) and by the introduction of drought tolerant cultivars (Mitra, 2007). In the past years, a considerable amount of effort has been targeted towards developing drought tolerant wheat cultivars, especially by CYMMIT through conventional breeding, marker assisted breeding (MAB) and genetic engineering but the progress to produce viable new cultivars has been slow globally as well as in India (Joshi *et al.*, 2007a; Ashraf, 2010). Very few new drought resistant wheat cultivars have been released in India over the past few years; those that have been introduced have shown little improvement in yield compared to the older drought resistant cultivars such as C-306, Sujata and NI-5439 (Mishra *et al.*, 2007). One of the reasons for the slow progress in developing drought tolerant cultivars is the low heritability of drought tolerance in wheat and the lack of effective selection strategies (Kirigwi *et al.*, 2004).

In general, the main difference between drought tolerant and susceptible wheat cultivars is the plant's water relation parameters and antioxidative defence mechanism (Ma *et al.*, 2005; Herbinger *et al.*, 2001) and these differences were also reported in drought resistant (C-306) and drought susceptible (Moti) Indian wheat cultivars (Khanna-Chopra and Selote, 2007).

6.3 Assessment of key varietal traits and their influence on F_{st}

It is evident from Section 6.2 that most effort is being put towards breeding for new wheat cultivars to reduce the impacts of heat and drought stress and to enhance rust resistance. A process based understanding of how traits influence g_{sto} could be replicated within the F_{st} model by changing key model parameterisations such that simulations could be performed to investigate whether new traits are increasing or decreasing F_{st} and hence increasing or decreasing the potential for heightened sensitivity to O_3.

Based on the current knowledge of the traits discussed in Section 6.2, only the phenological traits that influence resistance to heat stress through avoidance mechanisms can easily be incorporated into the stomatal O_3 flux model since this can be achieved by changing the sowing dates and duration of the wheat growth period. Current understanding of the processes involved in the interactions between O_3 and rust resistance is too limited to investigate these combined stresses. Although it may have been possible to investigate the effects of drought and O_3, at least from a stomatal O_3 flux point of view, the current DO_3SE model does not incorporate a soil water deficit module; this coupled with lack of data describing precipitation and irrigation scheduling events would make an investigation of this stress rather too circumspect to be useful.

The change in phenological characteristics of the new wheat cultivars can be simulated within the O_3 stomatal flux model by changing the duration and timing of the accumulation period through changes in the timing of A_{start} and A_{end}. These changes will simulate alterations both to sowing dates (mimicking timely and late sown cultivars) and the period of grain maturity (mimicking early to late maturing cultivars). These modifications will affect stomatal O_3 flux by changing the O_3 concentrations and meteorological conditions to which the wheat crops are exposed during the O_3 accumulation period with subsequent effects on the potential sensitivity of wheat to O_3.

6.3.1 Methodology

Data that describe the timing and length of the different phenological stages of the new wheat cultivars were collected to identify the likely phenological changes in the new wheat cultivars. Based on these phenological data, the wheat cultivars were grouped into different phenological types (i.e. timely or late sown each with different possible rates of maturity). The stomatal flux model was then re-parameterized to enable simulation of these phenological types, and model runs were performed to investigate the likely changes in stomatal O_3 flux. It is recognized that this method does not allow for changes in heat tolerance to be investigated since the model is only able to consider heat avoidance strategies in relation to O_3 flux, hence the analyses only provides an indication of how the potential sensitivity to O_3 of these new cultivars may be altered.

6.3.1.1 Data collection

As described in Section 6.2.1, a distinct phenological strategy that confers heat avoidance to wheat is to allow wheat to mature faster (early maturity) in both timely sown and late sown wheat cultivars. Due to the frequent occurrence of delays in the rice harvest caused by late arrival of the monsoon rains, efforts are also being made to develop wheat cultivars that are adapted for sowing late. To be able to simulate these different strategies within the stomatal O_3 flux model it is necessary to define both the likely variation in sowing date and maturing period of the new cultivars.

The different sources from which phenological data were collected are listed in Chapter 2, Table 2-2 and supplemented with other information available from peer reviewed literature (Rane *et al.,* 2007; Joshi *et al.,* 2007b; DWD, 2010a; Pal *et al.,* 2001; Tyagi *et al.,* 2003; Ladha *et al.,* 2003). These sources were used to obtain data describing i) the timing of sowing (which corresponds to the start of growing season (SGS) variable in the model) and ii) the days to maturity (days from sowing to physiological maturity of the crop) and iii) the growing conditions for which the cultivars have been bred; these data are provided for all new wheat cultivars released since 1995.

Most of the new wheat cultivars in India are released for specific AGZs. Since the

phenological characteristics of new cultivars differ by AGZs, the phenological data were collected and grouped according to the three most important AGZs (NEPZ, NWPZ and CZ).

In this Chapter, as in Chapter 4 and 5, model results are analyzed for the 3 main wheat growing AGZs. Phenological data (sowing dates and days to maturity) for 54 new wheat cultivars released between 1995 to 2008 for growing in the 3 AGZs were collected (Table 6-1). These 54 cultivars are recommended for growing under irrigated conditions. Averages of the data describing sowing and days to maturity for all cultivars in each AGZ were calculated and used to define a single representative sowing time and days required to maturity for each AGZ. The list of cultivars that were used to describe these phenological data for each AGZ is given in Table 6-1.

Out of these new cultivars, PBW-343, which was released in 1995 for the NWPZ, is the most dominant cultivar and occupies ~6 million hectares while in NEPZ the most dominant cultivar is still an old cultivar HUW 234, covering around 2–3 million hectares (Joshi *et al.*, 2007a). In CZ, another old cultivar, LOK-1 (released in the year 1982), is the dominant cultivar in central India (Joshi *et al.*, 2007b).

Table 6-1: The new wheat cultivars (released between 1995 to 2008) used to define the phenological characteristics in relation to sowing date and days to maturity. (Data source: SeedNet; DWD; NFSM; Rane and Chauhan, 2002a; Mishra *et al.*, 2007; Rane *et al.*, 2007; Joshi *et al.*, 2007a; Prashar *et al.*, 2008;).

AGZ	Phenology type	Sowing time (year day)	Days to maturity (year day)	New wheat cultivars (released between 1995 to 2008)
NEPZ	Late sown	344	105	DBW-14, Gangotri, HD-2643 (Ganga), HW-2045 (Kaushambi), LOK-45, MP-4010, NW-1014, NW-2037, NW-2036, PBW-498, Rajeshwari
	Timely sown	320	122	DBW-39, HD-2733, HP-1761, Malavshakti, HUW-468 (Malviya), PBW-443, K-8434 (Prasad), k-9107, WH-711, Raj-4120, NW-1012
NWPZ	Late sown	344	125	PBW-373, PBW-498, Raj-3765, Sonak, UP-2425, DBW-16, UP-2338
	Timely sown	320	144	PBW-34, PBW-343, PDW-233, PDW-314, HD-2678 (Shresth), WH-147, WH-711, Raj-6560
CZ	Late sown	344	108	GW-322, HI-1418, HI-1454, MP-1203, MP-4010, JW-1202, JW-1203, DL-788-2 (Vidisha), HD-2932, HD-2864
	Timely sown	320	115	HW-1085 (Bhavani), GW-1139, GW-273, Malavshakti, MP-1106, GW-366, HI-1544, Raj-6560, GW-322, JW-1142

6.3.1.2 Defining the phenological characteristics of the new Indian wheat cultivars

New wheat cultivars are either adapted for sowing at the optimum wheat sowing time (timely sown) or for sowing late (late sown). The optimum wheat sowing time in India (as explained in detail in Chapter 4, Section 4.2.2) is around the 17th of November) and for late sown is approximately the 10th of December. Wheat cultivars also have different development rates to maturity; early, medium late.

Based on the time of sowing and the time required to attain maturity, the Indian wheat cultivars have been categorized into six possible phenological types; (i) Timely sown - early maturing (TE), (ii) Timely sown - medium maturing (TM), (iii) Timely sown - late maturing (TL), (iv) Late sown - early maturing (LE), (v) Late sown - medium maturing (LM), (vi) Late sown - late maturing (LL). This default phenology represents the phenology of wheat cultivars released both before and since 1995 in India and is based on timely sown (since this is the optimum sowing time for wheat crops grown across India) and medium maturing (since this is the usual time taken to attain physiological maturity) cultivars.

In this chapter, stomatal O_3 flux model runs are performed for all these categories of wheat phenology to examine how changes in the phenological characteristics of the new wheat cultivars could potentially affect the stomatal O_3 fluxes and thus potential sensitivity of wheat to O_3.

In order to perform the stomatal O_3 uptake simulations the phenological component of the stomatal O_3 flux model has to be parameterized for each of the 6 different phenological types. As described in Chapter 4 and 5, the entire wheat growth period (from sowing to harvest), is defined according to growing degree days (GDD). The length of the O_3 accumulation period, and the timing of A_{start} and mid-anthesis within this period, is defined according to GDD. To parameterize the model for each of the 6 different phenology types requires that these different stages be defined. To achieve this it can be assumed that the sowing date refers to the SGS and A_{end} represents the time when the wheat crop reaches physiological maturity; the timing of A_{start} and mid-anthesis could either be estimated assuming i) that each of the growth stages have the same proportion of GDD associated with them as compared to the 'default phenology' or ii) that the GDD will be disproportionately divided between the different parts of the growth stage (i.e. SGS to A_{start}, A_{start} to mid-anthesis and mid-anthesis to A_{end}). Wheat phenology data exist in the literature to support both assumptions (Rajput *et al.,* 1987; Bishnoi *et al.,* 1995; Gosh and Patra, 2004; and Kichar and Niwas, 2005).

The assumption that the different growth stages can be defined by disproportionately distributed values of GDD is supported by knowledge that in the late sown cultivars, the entire wheat growing period shifts to a time when the temperature is higher (Figure 6-9) and, as mentioned earlier, this high temperature is likely to reduce the grain filling

duration (Yang *et al.,* 2011). In contrast, when the GDD is changed proportionately for the late sown cultivars, the grain-filling duration is expected to be shorter, when presented as days because of the higher temperatures towards the end of the growing period. However, in some heat tolerant late sown Indian wheat cultivars, this heat stress is avoided as the flowering starts earlier than most cultivars hence providing a longer grain filling duration (O_3 accumulation period) even if the entire growth period is relatively short (Rane and Chauhan, 2002a; Rane *et al.*, 2007). Based on the above information two possible changes in the O_3 accumulation period with respect to timings of A_{start} and mid-anthesis in the heat tolerant cultivars, especially in the late sown cultivars are expected; to allow for this, two scenarios were developed so that both these possible growth development responses could be investigated:

1. Scenario I – the thermal time (GDD) required to attain A_{start} and mid-anthesis changes proportionately with changes in GDD between SGS and A_{end}.
2. Scenario II – the thermal time (GDD) required to attain A_{start} is 20% less than that assuming a proportional distribution; as such A_{start} occurs earlier.

Figure 6-7 shows how SGS, A_{start} and A_{end} (parameters necessary for the parameterization of the f_{phen} function as described in Chapter 4) for these 6 different phenological types would compare to each other and also to the 'default phenology' that was used for the analysis in Chapter 5 which is assumed to be representative of both older and new cultivars found in all the main AGZs.

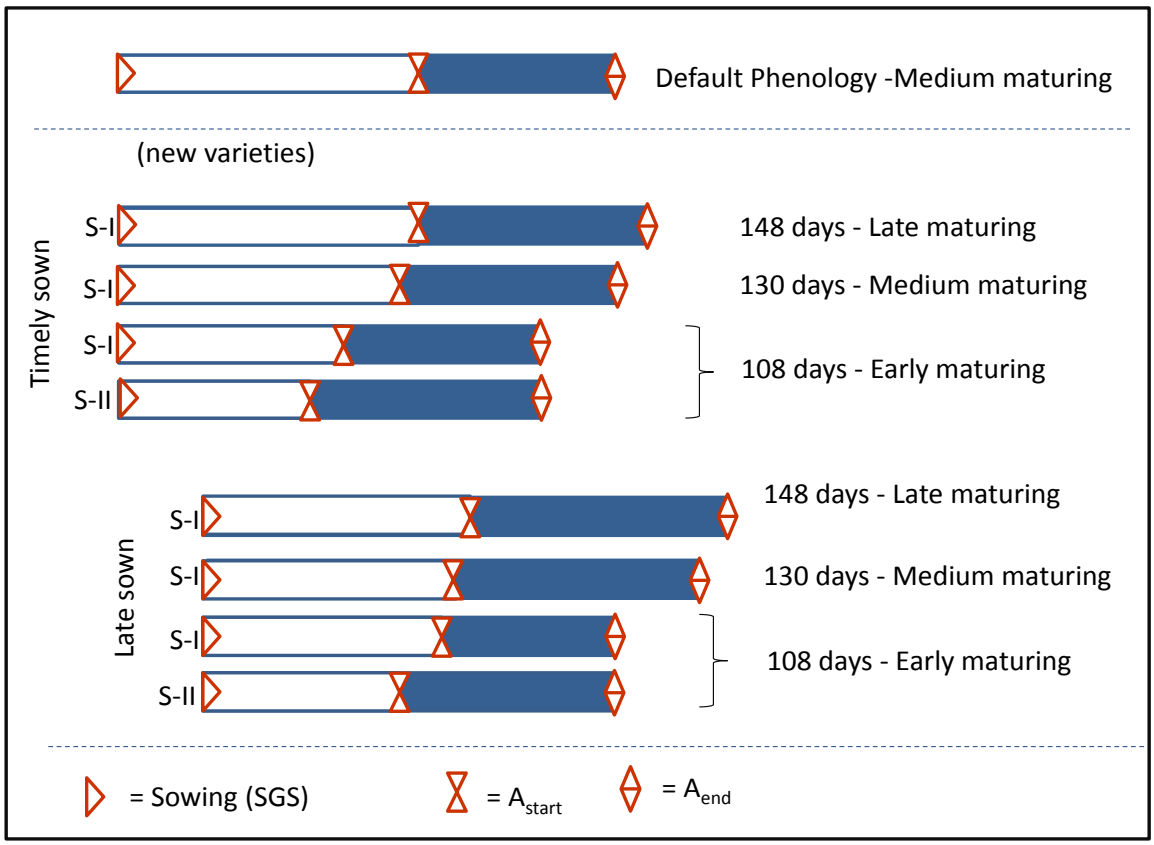

Figure 6-7: Comparison of the 6 different phenological types, including the two scenarios defined to represent new Indian wheat cultivars based on time of sowing and time to maturity. Also shown is the 'default phenology' which was used to define the Indian wheat phenology in Chapter 3 and 4. S-I refers to scenario I and S-II refers to scenario II. The days for each category were based on the early, late, and medium maturing dates given in SeedNet, DWD and NFSM.

Therefore, to parameterize the stomatal O_3 flux model for the new wheat varietes, GDD at A_{start}, A_{end}, f_{phen_e} (GDD between A_{start} and mid-anthesis) and f_{phen_f} (GDD between mid-anthesis and A_{end}) is required. GDD at these phenological stages for each wheat cultivar at each AGZ is given in Table 6-2.

Table 6-2: Parameterization for A_{start}, mid-anthesis, A_{end}, f_{phen_e} and f_{phen_f} for each of the phenology types in GDD.

Sowing time	**Maturity**		**Zone**	A_{start}	**Mid -anthesis**	A_{end}	f_{phen_e}	f_{phen_f}
Scenario I								
Timely	Early	TE	AGZ 4	597	767	1278	170	511
			AGZ 5	523	673	1121	150	449
			AGZ 6	452	581	968	129	387
			AGZ 8	697	896	1493	199	597
	Medium	TM	AGZ 4	783	1007	1679	224	672
			AGZ 5	691	889	1481	198	593
			AGZ 6	594	764	1273	170	509
			AGZ 8	899	1156	1927	257	771
	Late	TL	AGZ 4	825	1061	1768	236	707
			AGZ 5	724	931	1552	207	621
			AGZ 6	621	799	1332	178	533
			AGZ 8	928	1193	1988	265	795
Late	Early	LE	AGZ 4	658	846	1410	188	564
			AGZ 5	569	732	1219	163	488
			AGZ 6	483	621	1036	138	414
			AGZ 8	758	974	1624	217	650
	Medium	LM	AGZ 4	909	1169	1948	260	779
			AGZ 5	806	1037	1728	230	691
			AGZ 6	697	896	1493	199	597
			AGZ 8	1017	1308	2180	291	872
	Late	LL	AGZ 4	1138	1464	2440	325	976
			AGZ 5	1037	1333	2221	296	889

Table 6-2: Continued.

			AGZ 6	916	1178	1964	262	786
			AGZ 8	1261	1621	2702	360	1081
Scenario II								
Timely	Early	TE-II	AGZ 4	477	678	1278	200	601
			AGZ 5	419	594	1121	176	527
			AGZ 6	361	513	968	152	455
			AGZ 8	557	791	1493	234	702
Late	Early	LE-II	AGZ 4	526	747	1410	221	663
			AGZ 5	455	646	1219	191	573
			AGZ 6	387	549	1036	162	487
			AGZ 8	606	861	1624	254	763

6.3.1.3 Model Runs

Stomatal O_3 flux model runs were performed for Scenario I for all six phenology types described in Figure 6-7 and for Scenario II in the timely and late sown, early maturing crops only. In all, eight model runs were performed for each of the three AGZs. POD_6 and AOT40 values were calculated for the O_3 accumulation period for all eight phenological types described in Figure 6-7. The stomatal O_3 fluxes are estimated using the methods and data described in Chapter 3 (i.e. meteorology and O_3 concentration data from MATCH) and the Indian wheat parameterization described in Chapter 4; with the exception of using the SGS, A_{start}, mid-anthesis and A_{end} parameterizations specific to the different new cultivar phenology types described in Section 6.3.1.2.

6.3.2 Results

The results presented in this chapter depend upon the fact the new wheat cultivars will

have been adapted quite specifically for their respective AGZs such that the fixed days growth period can be directly translated into GDD from which crop developmental stage can be inferred. Although this may be a rather bold assumption, it is necessary to allow investigation of the potential effect of differences in developmental stage (bred to allow cultivars to cope with particular heat stress conditions) to be assessed in relation to the potential implications for sensitivity to O_3. The results presented here are not intended to necessarily reflect the actual situation for new cultivars being introduced, but rather provide an analysis of how the new cultivars could respond were particular phenological traits to be introduced.

6.3.2.1 GDD estimated growth and O_3 accumulation periods by AGZ

Figure 6-8 shows the wheat growth periods presented in terms of GDD for each of the 6 phenological types (including the two scenarios for the later maturing cultivars) for each of the three AGZs.

The growing period length in days is 108, 130 and 148 for the early, medium and late maturing cultivars for both the timely and late sown crops. Since different AGZs have different temperature climates during these fixed day growth periods different GDD values are obtained when these fixed day periods are translated into GDD by AGZ. For all AGZs growth periods with shorter fixed days always have lower GDD values; however, climate obviously affects GDD values when comparing between AGZs. For example, the hotter climate that occurs during the O_3 accumulation period in CZ (Figure 6-9) leads to higher values of GDD (between 1500 and 2600 ^{o} days) over the growth period for the phenological types; by contrast, the lower temperatures in NWP lead to lower GDD values (between 1100 and 2300 ^{o}days). For all AGZs there is also a substantial difference between the early and late sown cultivars with the range in GDD being approximately 600 ^{o}days and 1100 ^{o}days for the timely and late sown cultivars respectively. This is due to the late sown cultivars being exposed to the higher temperatures that occur in March and April (Figure 6-9) leading to more GDD being accumulated for the same fixed day duration.

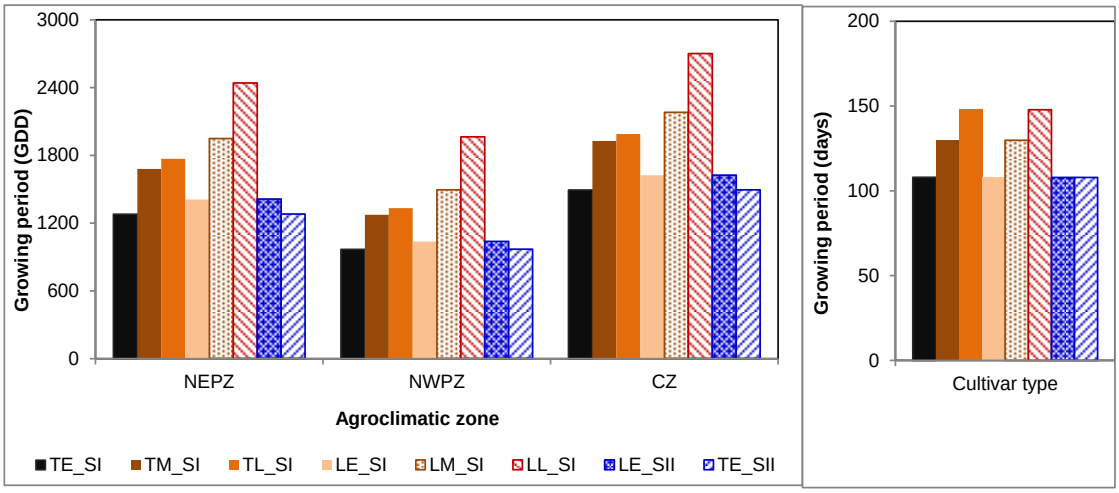

Figure 6-8: The wheat growing period in growing degree days (GDD) for the different wheat phenology types in the three main wheat AGZs in India; also shown are the growing period in fixed days from which the GDD data were inferred (SeedNet 2011; DWD, 2011, NFSM, 2011). The growing periods in fixed days are same for all the AGZ. Refer to Table 6-2 for legends.

6.3.2.2 Temperature and O_3 climate of GDD estimated growth periods

Figure 6-9 shows the maximum temperature and O_3 concentration, calculated as moving monthly averages, for the entire potential wheat growing period for the locations selected to represent the three AGZs. Also shown are the growth periods in days of each of the six phenological types along with the 'default phenology'. These growth periods can be used to delimit the temperature and O_3 climate to which each phenological type is exposed for the different climates. In broad terms, these data show that the timely sown cultivars are exposed to lower temperatures and O_3 concentrations than the late sown cultivars. They also show that, in terms of temperature, the AGZ ranking is CZ > NEPZ > NWPZ from hotter to cooler climates whilst in terms of O_3 concentration CZ has the lowest O_3 concentrations (with maximum values in mid-February reaching only 45 ppb v), followed by NEPZ with NWPZ having the highest O_3 concentrations with values during late March reaching almost 70 ppb v.

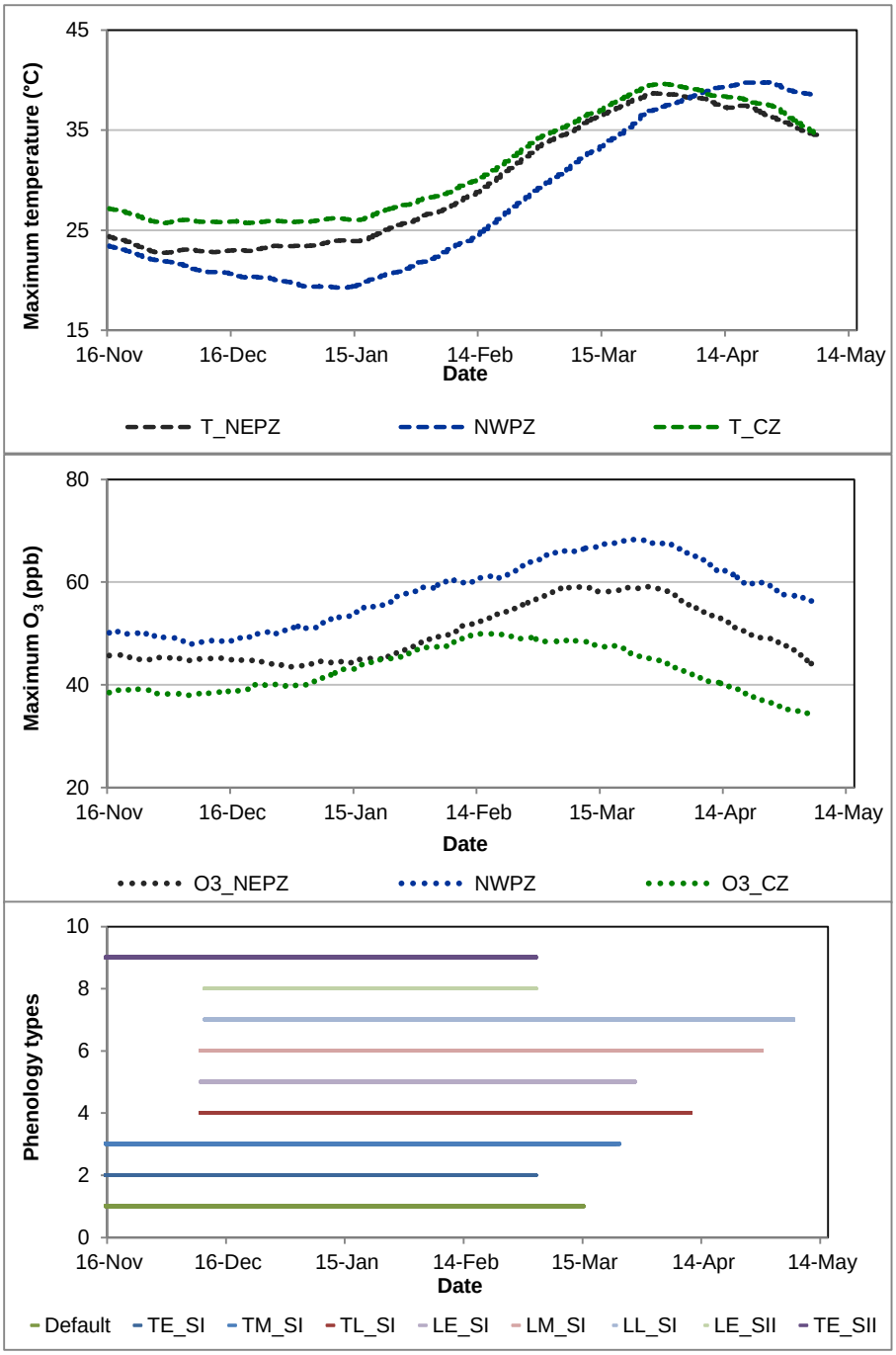

Figure 6-9: Growing period of late and timely sown cultivars plotted with moving monthly averages of maximum temperature and maximum O_3 for each AGZ. Refer to Table 6-2 for legends. O_3 and temperature data are based on hourly data from the MATCH model.

When the phenological stages in GDD are changed proportionately as compared to the 'default' phenology, the accumulation period as well as the vegetative period increases as this just represents the proportional split of a longer GDD growth period for these cultivars Figure 6-10. However, even if the GDD values for the accumulation period are higher in late sown crops, the duration (days) of accumulation period reduces. This is due to the increase in the GDD to attain A_{start} (or A_{end}), which pushes the accumulation period further toward the later part of the year when the temperatures are higher (Figure 6-9) and therefore increases the rate of accumulation of GDD and takes shorter time to accumulate the required GDD even if the GDD is more than the default GDD (Figure 6-9).

Figure 6-10 shows the different length for the two developmental stages in days for each of the phenological cultivars and AGZs. These stages are defined as the 'vegetative phase' which refers to the period between SGS and A_{start}, and the 'O_3 accumulation period' which refers to the period between A_{start}, and A_{end}.

The results show that the length of the O_3 accumulation period of the timely sown cultivars (which range between 45 and 60 days) is shorter than that of the timely sown cultivars (which range between 57 and 81 days). This is due to the lower temperatures in the early part of the growth period; because of this, the timely sown cultivars take longer to accumulate the necessary GDD to reach A_{start}, than do the late sown cultivars.

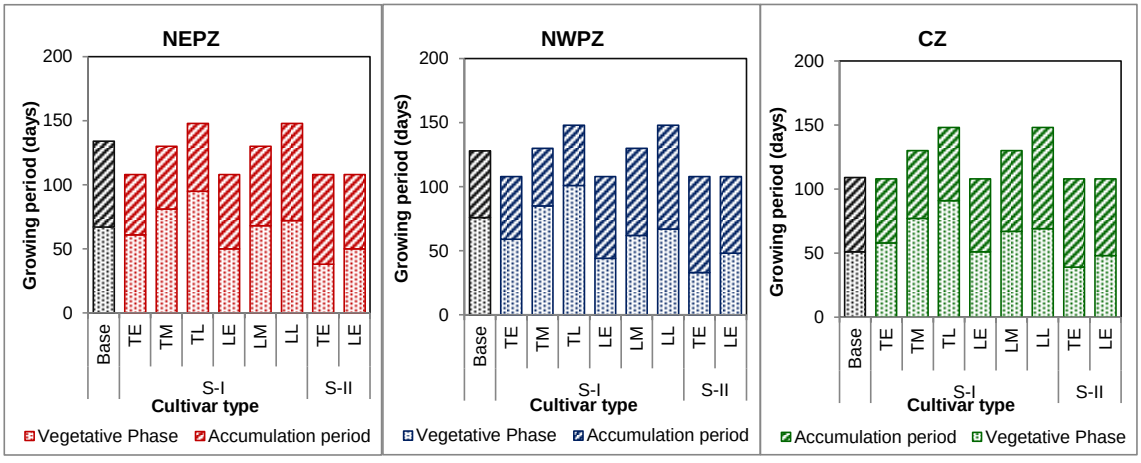

Figure 6-10: Days required to attain vegetative and accumulation (reproductive) period of old and new wheat cultivars in the three AGZ.

6.3.2.3 Stomatal O_3 flux in wheat under different scenarios

Figure 6-11 shows the stomatal O_3 flux calculated as POD_6 and the $AOT40_A$ for each of the new phenological types and each AGZ grid. The O_3 flux in the late sown cultivars is significantly reduced as compared to the O_3 flux for the 'default phenology' (= base) and this reduction is primarily observed in the late maturing cultivars.

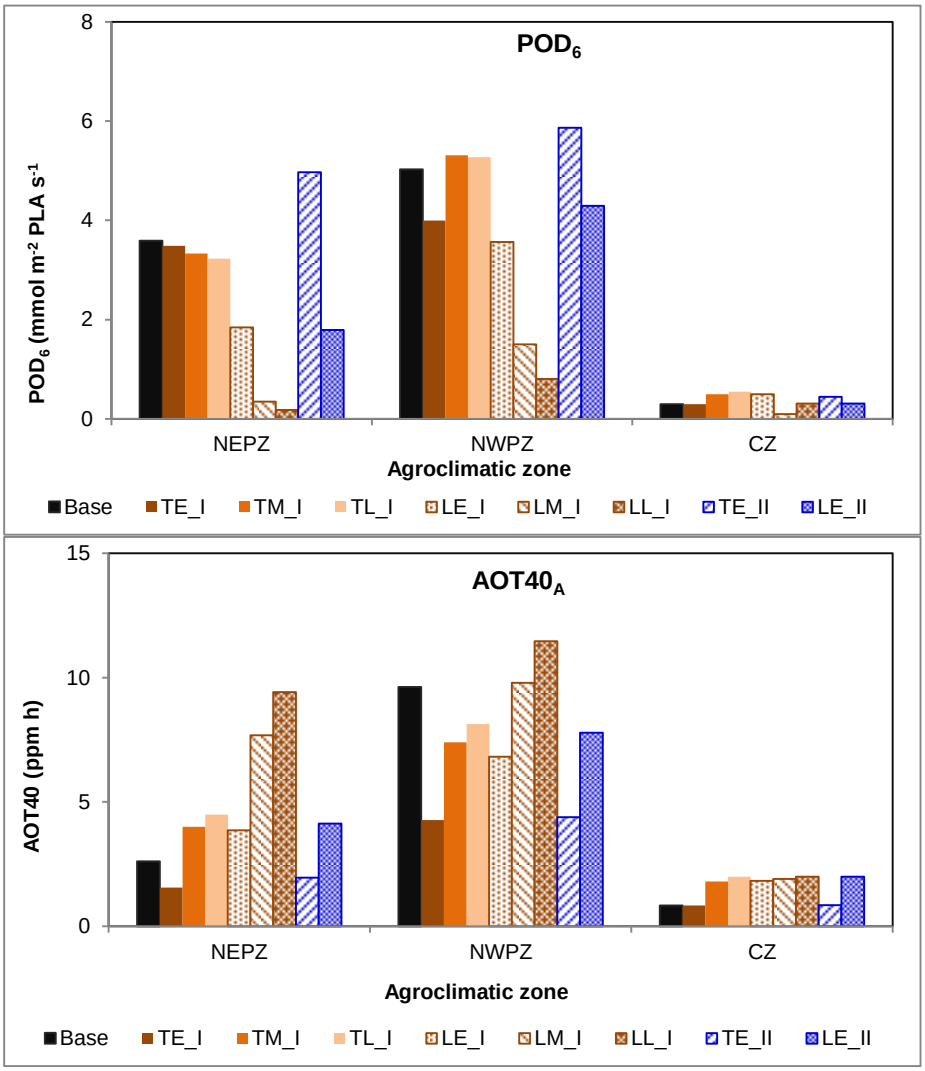

Figure 6-11: POD_6 and AOT40 values of different wheat categories for the three AGZs. "Base" represents the default phenology.

Although O_3 increases towards the end of the growing period of the late sown crops, the temperature and VPD also increases which limits g_{sto} and subsequently reduces O_3 flux. In LM_SI and LL_SI of NEPZ, POD_6 values are lower than base values by 90 and 95% respectively, and in NWPZ by 70 and 85 % respectively. On the other hand, the opposite trend is observed in $AOT40_A$ values where the values in LM_I and LL_I of NEPZ are higher than base values by a factor of 3 (Figure 6-11). In late sown crops, the shift in phenology towards the high O_3 climate - especially in NEPZ where O_3 is seasonally variable (Figure 6-9) - results in substantial increases in $AOT40_A$. In CZ the highest fluxes are observed in TM_I where the POD_6 values are less than half the base values. However, both the POD_6 and $AOT40_A$ values do not change much as compared to NEPZ and NWPZ grids.

Thus, increased duration of accumulation period and higher O_3 concentration translate into high $AOT40_A$ values but not necessarily into high O_3 fluxes as the O_3 flux depends on other flux influencing factors like temperature, light and humidity.

In Figure 6-11, the analysis was done to see the changes in fluxes of all phenological types in all three AGZs. However not all the phenological types are representative of the new cultivars in all three zones. Therefore, a further analysis was done to study which phenological types are likely to be associated with only the new cultivars in each AGZ and how this is likely to change the O_3 fluxes.

Each new wheat cultivar listed in Table 6-1 was assigned a phenology type shown in Figure 6-7 that best describes the phenology of the new cultivar. Most new cultivars released for NWPZ and NEPZ are late sown. This again is due to the rice-wheat cropping as it is in the IGP region (Figure in chapter 1). Most new cultivars released for NWPZ are late sown and have longer growing duration as compared to NEPZ. Most cultivars in CZ are timely sown (TE, TM and LE). TM and LE matures at the same time while TE matures before TM and LE.

The related POD_6 and $AOT40_A$ values of these new cultivars are given in Figure 6-12. In NEPZ and NWPZ, because of the new cultivars mostly being late sown, there is a high reduction in the O_3 fluxes even though the $AOT40_A$ values increase. On the other hand, in CZ, there are not many changes in the O_3 fluxes. This suggests that the late sown new cultivars in the NEPZ and NWPZ could potentially have lower O_3 fluxes as

compared to the timely sown cultivars while in CZ there is very little change or increase in fluxes.

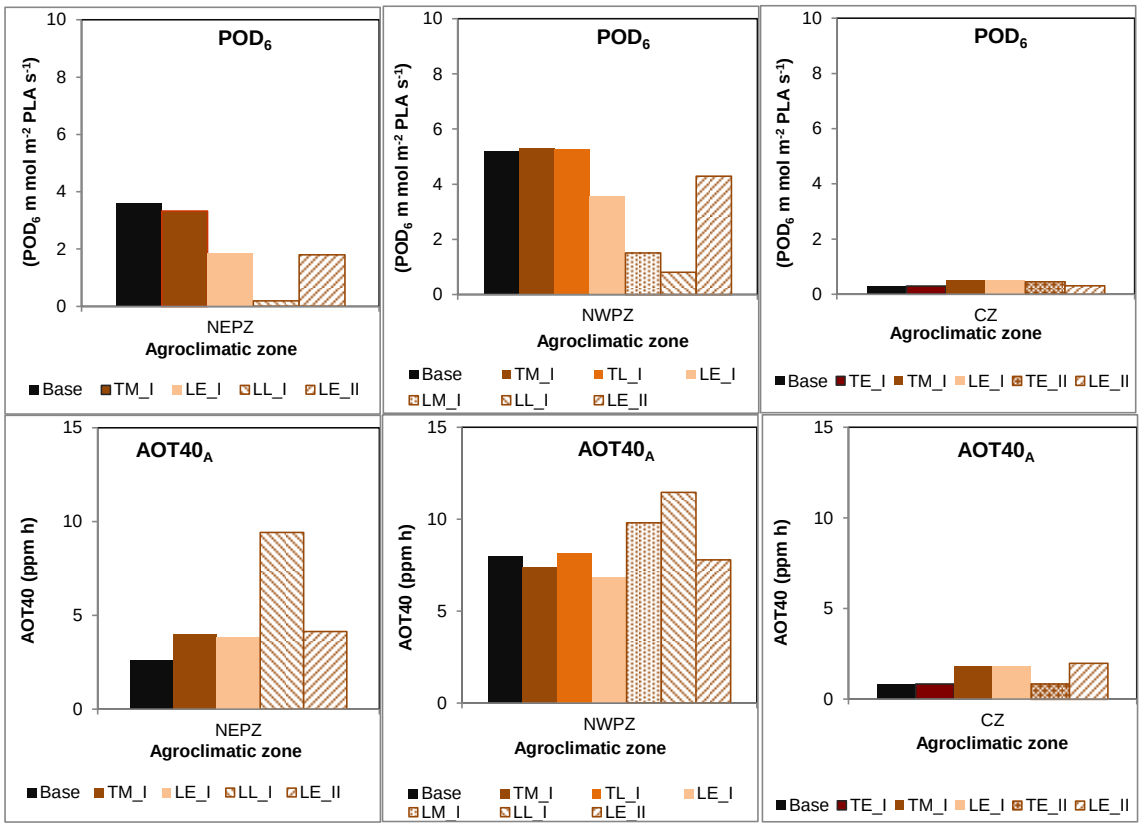

Figure 6-12: The different phenological categories of wheat cultivars in India under scenario I and II and the associated POD_6 and AOT40 values.

6.4 Discussions and conclusions

Shift of growing season

Flux modelling shows that the timing of the O_3 accumulation period is extremely important for the assessments of O_3 risk. New traits that alter the timing of this period are therefore likely to have a substantial impact on crop sensitivity to O_3, especially in AGZs which have high within-growing season variability in O_3 concentrations. Most new cultivars released for NEPZ and NWPZ are late sown cultivars. This is due to the

fact that these two zones are located in the IGP region where the rice-wheat cropping system dominates the wheat cropping area and hence harvest of rice influences the sowing of wheat. As mentioned earlier, frequent delays in the rice harvest delays wheat sowing, hence there is a need for late sown cultivars, and hence the newly developed cultivars are mostly late sown. This is also one of the reasons why a number of new wheat cultivars released are heat-tolerant. In CZ, the temperature is warmer all year through and therefore growth rate is high and GDD accumulates faster (takes less days) than in the NWPZ and NEPZ. Hence, most new cultivars released are for early maturing; the medium maturing cultivars are only used when an early sowing is possible. In Chapter 5, it was made clear that phenological timings of crops are important but at the same time the characteristics of the location's (grid's) O_3 and climates determines the importance of phenological timing. In all the three zones, the O_3 concentrations are higher towards the end of the growing season and therefore shifting of the accumulation period towards the later part of the year increases the amount of O_3 exposure and subsequently the AOT40 values. Teixeira *et al.* (2011) also showed that shifting the crop phenology changed the AOT40 values substantially by up to 25% in irrigated soybean and ~10% in wheat grown in India and suggested shifting phenology towards the period when O_3 concentrations are lower, as part of an adaption strategy to minimize O_3 impacts on crops. However, it should be noted that even though the O_3 risk may be reduced by adapting this strategy due to the decrease in O_3 fluxes, the effect will also be subject to higher temperature and VPD stress.

However, the POD_6 values from the current study showed a different story. In NEPZ and NWPZ grids, temperature and VPD also increases towards the later part of the year, this limits the O_3 flux, and hence the POD_6 values are lower when the crop phenology is shifted towards the later part of the year, whereas in CZ, the POD_6 values increased. This shows two things; (a) Phenological timing is important for O_3 risk but the importance of phenological timing is determined by both O_3 concentration and climate, (b) flux based method gives a better indication of O_3 risk than AOT40 and therefore implementing changes in phenological timings as an adaptation strategy in breeding program and policies should not be based purely on concentration-based methods. Although moving the growth period could potentially help crops adapt to O_3 as reported by Teixeira *et al.*, (2011), it is essential to also analyze the influence that meteorology as well as O_3 has on determining O_3 sensitivity.

Shifting / changing crop phenology as an adaptation strategy for crops has already been adapted in India since the 'Green Revolution' (Rane *et al.*, 2007; Kalra *et al.*, 2007; Mishra *et al.*, 2007). For example, a number of new wheat cultivars that are adapted for late sowing have been released in India specifically for the rice-wheat cropping systems, in response to the delayed wheat sowing due to delayed rice harvest (Joshi *et al.*, 2007b) or cultivars that harvest early to avoid heat stress (Rane *et al.*, 2007).

The growing period in the different phenological categories in this study has been based on the averages of growing periods of the new cultivars given in reliable databases (NFSM, SeedNet, DWD and peer reviewed literature) and therefore it is expected to be a good representation of the average growing period for each type of categories. However, there are uncertainties in defining crop growth and the O_3 accumulation period in GDD for these new cultivars. These databases do not give GDD for different phenological stages and therefore certain assumptions had to be made based on the evidence given in literature. Therefore, as mentioned earlier in Section 6.3.2, the results here are not intended to necessarily reflect the actual situation for new cultivars but just give an indication of how new cultivars would respond if particular phenological traits were to be introduced.

New cultivars may have a number of different traits in the same plant, i.e. a plant with altered phenology may also have altered gas exchange rates, which may change the O_3 flux and consequently the O_3 risk.

In relation to O_3 tolerance, some studies have reported an increase in O_3 sensitivity in more recent wheat cultivars in Europe (Barnes *et al.*, 1990; Velissariou *et al.*, 1992; Pleijel *et al.*, 2006b) as well as in Asia (Biswas *et al.*, 2008a and b). A number of theories are provided to explain this phenomenon: (i) the performance of selection trials in non-O_3 polluted regions, (ii) the selection of cultivars with enhanced g_{sto} to increase CO_2 assimilation, a trait that may also increase O_3 flux, (iii) the selection of cultivars that are dependent on, and hence trialed with, agrochemicals (fungicides, pesticides and growth regulators) which act as antioxidants and could possibly mask the O_3 effect, (iv) the selection of cultivars with improved drought, high temperature and pest and disease resistance (for example, while plant breeding, selection for drought resistant cultivars under drought conditions might reduce the harmful effect of O_3 in the field trials,

primarily due to reduced g_{sto}) (Barnes *et al.,* 1990; Velissariou *et al.,* 1992; Pleijel *et al.,* 2006b; Biswas *et al.,* 2008a and b).

As such, there is the possibility that new traits may modify, and in some cases enhance, crop sensitivity to O_3. The potential for targeted traits to alter crop sensitivity to O_3 is likely to be dependent upon the specific growing conditions for which the new cultivars are being bred and hence will be specific to particular regions.

Heat tolerance and avoidance

Exposure of wheat to O_3 affects the gas exchange parameters (Feng *et al.*, 2011), assimilate partitioning (Meyer *et al.*, 2000) and number of tillers and spikes (Sarkar and Agrawal, 2010) which are all traits important for heat tolerant wheat cultivars. O_3 can also bring forward and enhance senescence (Pleijel *et al.*, 2007) which will affect the length of the grain filling period and hence the time available for grain development. From the literature and from the previous Chapters it is evident that high temperatures (heat) are also an important factor limiting O_3 flux. Heat stress may also be important in altering the toxic effect of the absorbed O_3 dose since both heat and O_3 stress cause oxidative stress (Wahid *et al.*, 2007). The potential interactions between heat stress and O_3 flux are highlighted by the daytime temperatures often exceeding the T_{opt} for g_{sto} during the O_3 sensitive grain filling period.

The early maturity trait in the new wheat cultivars confers tolerance to heat stress through avoidance of the extreme temperatures that cause terminal heat stress. The heat tolerant wheat cultivars in India are either timely sown or late sown and most of them are early maturing. As such, investigating how stomatal O_3 flux may be influenced by potential changes in the timing of phenology and crop development of these new heat avoiding cultivars would help improve our understanding of some of the interactions between heat and O_3 stress. Data describing the phenological data of new cultivars are available from the sources summarized in Table 2-2 and can be used to simulate timely or late sowing and early maturing cultivars.

The growing period of late sown crops are pushed towards the time of the year when the temperature is high. The increase in temperature is more in the stage 3 of the accumulation period (Chapter 5, Figure 5-16) which is after anthesis. Exposure of wheat crops to high temperature at anthesis is known to increase the crop development and shorten the grain filling period (Yang *et al.,* 2011; Altenbach *et al.,* 2003; Hunt *et al.,* 1991; Jenner, 1991; Wheeler *et al.,* 1996). The shortened accumulation period will reduce the O_3 flux and thereby reduce O_3 effect. However, a reduced accumulation period (grain filling period) is also known to reduce grain weight, quality, and number (Yang *et al.,* 2011; Altenbach *et al.,* 2003; Hunt *et al.,* 1991; Jenner, 1991; Wheeler *et al.,* 1996). The gain due to reduced O_3 flux is likely to be outweighed by the reduction in yield due to a shortened grain filling period. Studies have shown that the sowing of wheat crops after the optimum sowing date in India reduces the wheat yield by more than 0.03 t/ha (DWR, 1999; Mehla *et al.,* 2000).

New high yielding cultivars adapted for sowing late are continuously being released in India (Joshi *et al.,* 2007b; Mishra *et al.,* 2007). These crops are high yielding either (i) because of the physiological characteristics which include high stomatal conductance and photosynthetic rate or (ii) they have an early onset of flowering which helps them to mature early to avoid heat stress without compromising on the yield of crop (Rane *et al.,* 2002a, 2007). Late sowing and early maturing cultivars with early flowering are similar to the wheat crop in Scenario II (LA_SII; Figure 6-7). The introduction of new high yielding cultivars with high g_{sto} or late sowing could potentially change sensitivity of the wheat crop to O_3. Studies show that modern Indian wheat cultivars are sensitive to O_3 (Sarkar and Aggrawal, 2010). Biswas *et al.* (2008a and b) reported that new wheat cultivars in Asia are more O_3 sensitive than the older cultivars which they argue was mainly due to increased uptake in O_3 from higher g_{sto} in the new cultivars and higher loss of antioxidative capacity and higher leaf dark respiration in the new cultivars as compared to the older ones in response to O_3 exposure. Similar results were also reported in European wheat cultivars that show newer European wheat cultivars to be more sensitive to O_3 than older cultivars (Barnes *et al.,* 1990; Velissariou *et al.,* 1992; Pleijel *et al.,* 2006b; Biswas *et al.,* 2008a and b).

This may suggest that in high O_3 environments, late sown crops may benefit by having reduced O_3 flux due to limitations from temperature and VPD. But the negative effects of high temperature on yield may outweigh the positive effect from reduced O_3 fluxes.

Reduced O_3 fluxes in late sown crops are likely only if there is extremely high temperature and VPD towards the end of the growing period.

Rust Tolerance

Some studies in Europe have reported the inhibition of wheat rust disease by O_3 (Tiedemann and Firsching, 2000; Dohmen, 1987) while other studies report no significant relationships between O_3 and wheat rust disease (Pfleeger *et al.,* 1999). In trees, O_3 increased rust infection by 3- to 5-fold (Plazek *et al.* 2001; Plessl *et al.* 2005; Karnosky *et al.* 2002). Given the importance of rust for India (Prashar *et al.*, 2008) and the fact that O_3 has been found to affect sensitivity to rust disease, more research is required to understand the interacting mechanisms.

Drought tolerance

In India, the drought-stressed wheat growing regions (Ladha *et al.,* 2003; Joshi *et al.,* 2007b ; Rodell *et al.,* 2009) also coincide with the regions where modelling studies have suggested that high O_3 concentrations will occur (Engardt, 2008; Roy *et al.,* 2009). Differential sensitivity of wheat crops to O_3 under drought and well watered conditions have been reported (Feng *et al.,* 2008; Wilkinson and Davies, 2010; Biswas and Jiang, 2011). Drought stress is known to influence both g_{sto} (Leuning *et al.,* 1998; Ewert *et al.,* 2002; Wilkinson and Davies, 2010) and the antioxidant mechanism in the leaves of wheat (Khanna-Chopra and Selote, 2007; Asada, 1999). Drought stress increases the absicic acid (ABA) content in the leaves which induces the stomates to close (Leuning *et al.,* 1998; Ewert *et al.,* 2002; Wilkinson and Davies, 2010), thereby reducing the flux of O_3 into the plant (Khan and Soja, 2003). However, recent studies have shown that O_3 stress increases the production of ethylene which reduces stomatal sensitivity to ABA and increases the stomatal conductance under drought stress (Wilkinson and Davies, 2010; Biswas and Jiang, 2011). Wittig *et al.* (2007) observed that exposure to O_3 (78-92 ppb) reduced g_{sto} in trees under watered conditions whereas under drought conditions it increased the g_{sto}. Biswas *et al.* (2008b) reported an 11% increase in g_{sto} of wheat crops

when exposed to O_3 concentration of about 100 ppb. Both drought and O_3 increase the production of reactive oxygen species (ROS) in wheat (Khanna-Chopra and Selote, 2007; Asada, 1999), which affects wheat physiology and subsequently yield.

Feng *et al.* (2008) reported that O_3 stress (70-75 ppb) caused a loss of >20% in yield parameters of well watered wheat crops but under drought + O_3 stress, the yield losses were reduced by <15%. Similarly, Khan and Soja (2003) reported 35-39% reductions in yield of well watered (75% of soil water capacity) wheat when exposed to an AOT40 of 25-37 ppmh, but no reductions in drought stressed (25% s.w.c.) wheat. Both the studies attributed the reduced O_3 effect in drought stressed wheat mainly to the reduction in O_3 uptake due to reduced g_{sto} under drought stress.

Most of the studies to determine wheat responses to O_3 and drought stress have investigated growth and yield (Khan and Soja, 2003; Soja *et al,* 1996). More studies need to be carried out to understand the interactive effect of O_3 and drought stress on wheat's antioxidative defence system and physiology, namely, photosynthesis and stomatal conductance (Biswas and Jiang, 2011). However, from available evidence on wheat's response to drought and O_3 stress, it is likely that breeding for drought tolerance will have an impact on the O_3 sensitivity of wheat.

The analysis in this Chapter has focused on the O_3 uptake component of O_3 damage and not the O_3 toxicity; different cultivars will also have different sensitivities to O_3 dose that are not a result of modified flux.

The traits being bred for may well enhance O_3 fluxes whilst at the same time protecting plants for the target stress and that flux based methods allow an assessment of at least the O_3 uptake component of O_3 damage and hence the F_{st} model could be viewed as a tool for investigating potential trait combinations that could improve the development of O_3 resistance in crop breeding programmes.

This also highlights the importance of having a more biologically significant method of O_3 risk assessment that calculates O_3 fluxes into crops rather than concentration based methods.

6.5 Limitations

1. Changes in physiological factors like stomatal conductance, photosynthetic rate, water use efficiency, etc., are expected to occur in the new cultivars (Rane *et al.*, 2002a, 2007; Fischer *et al.*, 1998). These changes will influence O_3 sensitivity of wheat and also the response of wheat to O_3 exposure and it is important to factor in all these changes in order to have a more robust estimation of O_3 flux to the new wheat cultivars. However, detailed information on these physiological factors in the new wheat cultivars are not available as per our current knowledge and therefore in this chapter a more conservative analysis only by changing the phenological data, in terms of growing period, is used to model stomatal O_3 flux.

2. Data pertaining to sowing date and growing period of the new cultivars were obtained for each of the new cultivars. However, for the model runs, data on A_{start} and mid anthesis were not available. Therefore, in the model runs, proportionality between GDD and different growth periods was assumed to study the relative changes in O_3 fluxes in the new cultivars due to variation in phenology. In reality, the changes in these phenological stages are not always proportional as it will depend on the plant physiology and genetic factors in addition to the meteorological conditions.

Chapter 7 Discussions and conclusions

7.1 Summary of key findings of the research

This study was done to assess the impact of O_3 on staple crops grown in SA and to identify suitable risk assessment methods for improving crop biotechnology in the region. A number of different O_3 risk assessment methods were used to assess the extent and magnitude of O_3 risk to rice, wheat, potato and soybean crops grown in SA (Chapter 2). This study has shown that there are substantial yield losses due to O_3 exposure on staple crops grown in SA and that the important crop growing areas, especially the northern parts of SA, are at high risk from O_3. This suggests a threat to food security in the region. In India, the highest wheat yield losses were observed in the IGP region which is the most important wheat growing area producing ~80 % of India's total wheat output (DWD, 2011). This region is high in O_3 precursors due to higher prevalence of anthropogenic activities (Ghude *et al.,* 2007, 2008; Roy *et al.,* 2009). The main emission sources in this region are biomass burning for domestic cooking, coal-based thermal power plants, vehicles, coal and fuel based industries and fossil fuel extraction (coal mining, crude oil production, natural gas production, etc.), (Beig *et al.,* 2008; Ghude *et al.,* 2008; Lal *et al.,* 2008; Sahu *et al.,* 2008). In addition to the high precursors, the high O_3 concentrations in this region are also due to the atmospheric conditions (e.g., temperature) being favourable for O_3 formation (Beig *et al.,* 2006; Beig and Ali, 2006; Lal *et al.,* 2008; Roy *et al.,* 2008, 2009).

This study has also shown that the geographical location as well as cropping pattern is important in determining the crop sensitivity to O_3. There were substantial differences in O_3 impact estimates between the different O_3 risk assessment methods. Although soybean is more sensitive to O_3 than wheat crop, the soybean cropping area has relatively lower O_3 concentration as compared to the wheat cropping areas and during the soybean growing season the O_3 concentrations are relatively lower as compared to that of the wheat growing season. Due to this, the O_3 induced yield losses in SA for soybean (0.1 to 4 %) are less than that of wheat (0.6 – 10.5 %).

The yield loss estimates made for wheat for India using both the concentration- as well as flux-based indices are presented in Table 7-1. These estimates show high variability (0.6 – 16 %) dependent upon which O_3 exposure index was used for the assessment but

predicted yield losses are substantial at the higher end of the estimated range. Yield loss estimates using POD_6 values are 39 % higher than that of AOT40 estimates for wheat grown in India. Resulting production losses vary from 0.5 to 14.6 million tonnes (Table 7-1). Translated to economic losses values range between 0.07 – 2.2 billion US$ for the cropping year 1999 – 2000. Such economic losses would offset the country's growth in GDP by 0.2 – 4.8 %.

Table 7-1: Summary of the relative yield losses (in %) for wheat grown in India estimated using different O_3 exposure metrics and comparison with estimates from other global study.

References	**AOT40**	**M7**	**W126**	**SUM06**	**POD_6**
Current study	11.5	0.6	4.2	2.4	16
Van Dingenen *et al.*, 2009	28	13	-	-	-
Avnery *et al.*, 2011a	30	9	-	-	-

Other global O_3 risk assessments studies (Van Dingenen *et al.*, 2009; Avnery *et al.*, 2011a) have also shown that O_3 is a potential threat to crops grown in SA and India. Using AOT40 and M7 O_3 exposure indices, Van Dingenen *et al.* (2009) and Avnery *et al.* (2011) reported that yield losses for wheat in India were about 13-28 % and 9-30 % respectively while this thesis study found yield losses were generally lower ranging between 0.6-13 % using AOT40 and M7 indices (Table 7-1). The O_3 induced yield loss estimates in Chapter 2 and 5 are within the range of the yield loss estimates reported in field experiments (Table 2-8) while the Van Dingenen *et al.* (2009) and Avnery *et al.* (2011a) are likely to be over estimating the O_3 impact. The differences in concentration-based yield loss estimates, as highlighted in Chapter 2, were likely due to the use of different photo-chemistry models to estimate O_3 concentration fields as well as the spatial and temporal resolution of input data and model resolution. The finer resolution of modelling performed in this SA study will provide a more realistic estimate of the local variation and subsequent interaction between O_3 precursor emissions, O_3 photo-chemistry, O_3 exposure to crops and crop distribution resulting in

an improved estimate of O_3 risk when using essentially the same risk assessment methods.

This thesis study has shown differences in the spatial pattern of risk between the flux- and concentration- based indices (see Chapter 5) which are consistent with similar European assessments (Simpson *et al.,* 2007). Even when comparing yield loss estimates performed using only concentration based indices there were differences between the cumulative (e.g., AOT40) and seasonal average (M7 / M12) indices; again these findings were consistent with global risk assessment studies (Van Dingenen *et al.*, 2009; Avnery *et al.*, 2011. However, the evidence in Chapter 3, 4 and 5 shows that the flux based methods give a better estimate of O_3 risk than concentration-based indices and that the flux-based estimates of yield losses were within the range of the data from field experiments. As such, flux-based risk assessment methods can be used to estimate O_3 risk to agriculture across the region so that appropriate policy response can be implemented to alleviate impacts). Yield losses estimated using flux based indices were higher at 16 %; this is consistent with studies conducted in Europe which also showed that flux based indices gave higher yield losses compared to AOT40 (Simpson *et al.*, 2007).

This study has also shown that stomatal conductance (in terms of g_{max}), crop phenology, geographical location of the crop and meteorological conditions such as, temperature, VPD and light are the main factors that influence the crop sensitivity to O_3 on crops grown in India. It can therefore be concluded that O_3 risk is determined by interactions between O_3 concentrations, crop growth period and physiology and prevailing meteorological conditions. For example, Chapter 5 clearly showed that it was not only high O_3 concentrations that determined O_3 risk but also the occurrence of more moderate environmental conditions that allowed greater g_{sto} and hence O_3 uptake. Therefore, as climate changes, the conditions may become less optimum for g_{sto} (with higher VPDs and higher temperatures) such that even though O_3 concentrations may increase, O_3 uptake may reduce. An important determinant of how these co-variations play out and what it might mean for O_3 uptake is likely to be what happens to the timing of the crop growth period. This again highlights the fact that flux-based approach represents a better and more relevant quantification of O_3 effects on crop yield.

New crop cultivars with improved yield and having traits for tolerance to biotic and abiotic stresses, especially for important crops like wheat, are continuously being introduced in India. The evidence in Chapter 6 suggests that the crop phenological (e.g., sowing and maturity timings) and physiological (e.g., g_{sto}) traits that are being bred for in new Indian wheat cultivars might change O_3 fluxes and hence the O_3 sensitivity of the crop whilst at the same time protecting the crops from the target stress and therefore it is important to factor in O_3 sensitivity while breeding crops in the future. The results in Chapter 6 shows the importance of flux based O_3 risk assessment methods while developing adaptation to O_3 strategies and that flux based method can be used as a tool for investigating potential trait combinations that could improve the development of O_3 resistance in crop breeding programs. In Chapter 6, the flux-based O_3 risk assessment models were used to assess the influence of change in new traits that alter the phenological timings of the wheat crops on O_3 sensitivity. The results indicate that shift in phenological timings leads to large changes in the F_{st} values. In addition to the changes in phenological triats, new crop cultivars are likely to have altered gas exchange rates which will change the O_3 flux and consequently the O_3 risk.

Global risk assessment studies have also projected yield losses for 2030 (Avnery *et al*., 2011b and Van Dingenen *et al*., 2009). These projected yield losses are listed in Table 7-2. Anvery *et al*. (2011b) estimated very high O_3 induced yield losses of between 12-48 % and 10-37 % for wheat for the year 2030 under IPCC (2007) A2 and B1 scenarios respectively for India. These A2 and B1 scenarios represent the upper and lower boundary trajectories, respectively for O_3 precursor emission (Anvery *et al*., 2011b). Under these two scenarios, the highest yield losses in 2030 are projected to be in Bangladesh with losses of 26-80 % and 15-65 % for A2 and B1 scenarios respectively. Van Dingenen *et al*. (2009) estimated that yield losses in India would increase by 11 % by 2030 as compared to 2000 under a current legislation scenario (CLE) which assumes full implementation of CLE by 2030. However, this CLE scenario did not include the introduction of EURO-3 standards for four-wheeled vehicles in India which are likely to substantially reduce traffic emissions after 2010 and hence the projected O_3 concentrations may be overestimates (HTAP, 2010).

Table 7-2: RYLs for the year 2030 under different scenarios estimated by global risk assessment studies using AOT40 and M7 metrics for wheat in India. CLE = Current legislation in place at year 2001 and assumes full implementation by 2030; A2 and B1 are IPCC scenarios (see text for further details). *average of M7 and AOT40 estimates.

References	**Scenario**	**AOT40**	**M7**
Van Dingenen *et al.*, 2009	CLE	+41% *	
Avnery *et al.*, 2011b	A2	48	12
	B1	37	10

Based on these projected RYL estimates (Table 7-2) it is clear that a range of different emission scenarios all have a tendency to project increases in future surface O_3 concentrations for SA and India, at least in the near term. These are largely due to increased emissions from the transport and power generation sectors (Dentener *et al.*, 2006; Royal Society, 2008) that are projected to occur even with the implementation of CLE that has introduced in efforts to improve air quality across the region. Modelling studies have projected that SA could become one of the most O_3 polluted regions in the world by the 2030s to 2050s (Dentener *et al.*, 2006; Prather *et al.*, 2001). The recent HTAP (2010) analysis is useful for highlighting the likely range in projected O_3 concentrations according to four different scenarios developed for IPCC (2013). These Representative Concentration Pathway (RCP) scenarios represent very different views of how the world may look out to 2100, with RCP 2.6 showing the effects of strong mitigation and RCP 8.5 the impacts of 'business as usual' in which we continue to use fossil fuels with no mitigation (HTAP, 2010). Importantly for SA, Figure 7-1 shows that even under the most optimistic emission scenario, the O_3 concentration will not decrease but is expected to remain constant. By contrast, in all of the other global regions (North America, Europe and East Asia) the more optimistic scenarios look likely to provide a decrease in surface O_3 concentrations. However, it is important to note that these scenarios were targeted towards CO_2 and greenhouse gas emissions reductions and therefore are not specifically targeted towards O_3 control. Ultimately, the projected increases in surface O_3 in SA suggest that the threat posed by O_3 on

agricultural crops in this region will not improve, and actually looks set to worsen, out to at least 2050.

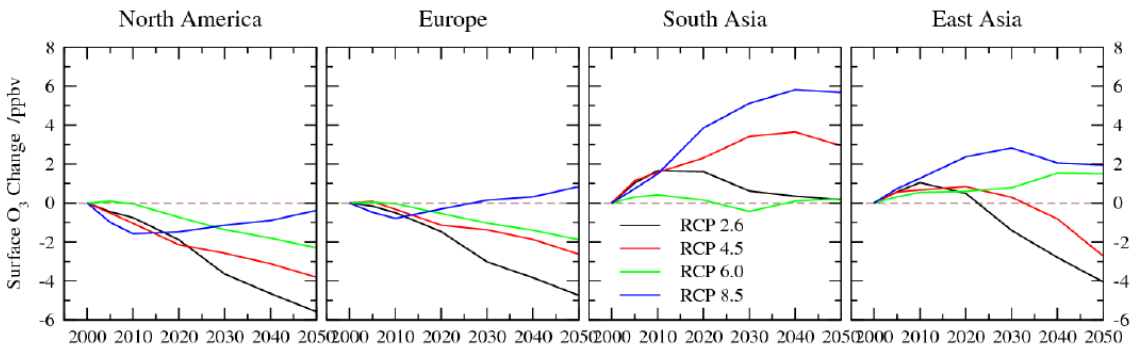

Figure 7-1: Mean surface O_3 changes over North America, Europe, South Asia and East Asia based on different RCP (representative concentration pathways) scenarios constructed for IPCC-AR5 (HTAP, 2010).

As such, the flux-based method offer greater opportunities to develop future O_3 risk assessment approaches, especially when it is considered that future conditions will change not only in terms of increased O_3 concentrations but also climate (IPCC, 2007). The opportunities for developing flux based risk assessments are considered in more detail in the next section which also addresses the current limitations to the study performed within this thesis.

7.2 Limitations of the current study

7.2.1 O_3 concentrations

The MATCH modelled O_3 data used in this thesis study shows good agreement with both seasonal and diurnal patterns found in the published literature; even though these data are rather limited in extent and hence their ability to represent conditions across SA and India (Engardt, 2008). For this region, limited O_3 monitoring data from rural areas makes it difficult to validate the photochemical model outputs and hampers model improvements. There is an urgent need for observed O_3 data, especially in rural areas to evaluate and improve models that predict O_3 in the region (Engardt, 2008, Roy *et al.*, 2009). This requires a good network of monitoring studies in rural areas across the

region and perhaps especially in the important crop growing regions.

The O_3 monitoring network of the Indian Meteorological Department (IMD; http://www.imd.gov.in) in collaboration with the World Meteorological Organization (WMO) and Central Pollution Control Board (CPCB; http://www.cpcb.nic.in/air/new/continus.pdf) continuously measures surface O_3 concentration but only at 6 locations across India; 3 of these locations are in Delhi and all are located at urban sites. The only standardized monitoring network for O_3 concentrations in rural/remote sites is that hosted by the Malé Declaration (http://www.rrcap.unep.org/male/). However, this network has only 7 sites across the entire SA and, most importantly, only monitors using passive diffusion tube samplers. As such, continuous hourly or even daily O_3 concentrations are unavailable. There are also O_3 data collected from rural areas by academics working in isolation; however, the lack of standardization of monitoring procedures used in these rather *ad hoc* monitoring initiatives makes it difficult to compare O_3 concentrations between sites and hence trust these data enough to be sure they provide suitable evaluation data.

For flux based risk assessments, O_3 data from rural areas where agricultural crops are grown are required to ensure a true indication of the O_3 concentrations where agricultural crops are grown can be provided by photochemical models (Ramanathan *et al.*, 2008). In addition to O_3 monitoring networks, improvement of emission inventories using Indian emission inventories are also important (Roy *et al.*, 2007, 2009).

7.2.2 Experimental data describing O_3 induced yield losses

A big limitation in this current study is lack of large-scale co-ordinated experimental studies in SA to i) provide data to develop SA specific ER functions and ii) to validate the model estimates of crop yield losses. This study has made use of O_3 risk assessment methods developed for North America and Europe. There will be uncertainties associated with cultivar differences in sensitivity to O_3 and use of ER functions developed for different geographic regions. To a certain extent, the flux-based approach can incorporate some of the factors that might alter O_3 sensitivity between different global regions due to variable meteorology and crop physiology. However, certainty in

the flux-based results is limited, particularly in relation to the parameterization of the g_{sto} component of the flux model due to a lack of data describing SA crop physiology. Also, flux-based yield loss estimates rely on flux-response relationships developed for European conditions with no guarantee that the detoxification capacity of wheat grown in SA would be similar (Heath *et al.*, 2009).

A co-ordinated pan SA experimental study, similar to the NCLAN and EOTC studies conducted in North America and Europe, to assess the impacts of O_3 on crops would help develop SA dose-response relationships. If similar studies could be performed in SA, with experiments being designed specifically to provide data to help develop flux-based risk assessment methods, substantial gains could be made in our knowledge of O_3 impacts across the region.

In the future such experimental data could perhaps be more efficiently and readily obtained through collaboration of O_3 effects researchers with organizations that are already working on crop improvement programs in the region. Currently in SA, and especially in India, there is a good network of agricultural research under different national and international organizations (ICAR, IARI, ICRISAT, CGIAR; IRRI) and programmes (AICWP). There are also a number of long running Long Term Experiments (LTEs) especially in the rice wheat cropping systems in the IGP (Timsina and Connor, 2001; Ladha *et al.*, 2003; Pathak *et al.*, 2003; Tirol-Padre and Ladha, 2006). These organizations have experimental study sites with well-established crop management practices, crop growing facilities (many going on for more than 30 years) that could provide useful study locations for future O_3 effects related research.

7.2.3 Multiple stresses

Crops grown across SA are subjected to a number of stresses, both physical (drought, salinity, other pollutants etc.) and biological (diseases such as rusts, blights, etc.). Important stresses to wheat grown in India such as temperature, drought, salinity and rusts are likely to interact with O_3 affecting crop growth and yield (see Chapter 6). Some studies have shown changes in sensitivity of wheat to rust due to O_3 exposure (Dohment, 1987; Tiedmann and Frisching, 2000) while others have reported changes in

sensitivity to O_3 under drought stress (Feng *et al.*, 2008; Biswas and Jiang, 2011; Wilkinson and Davies, 2010) through changes in g_{sto} either due to changes in crop water potential or increased production of ABA (Ewert *et al.*, 2002; Wilkinson and Davies, 2010). Studies on the effects of SO_2, NO_2 and O_3 on wheat crops grown in India have also showed that all the 3 pollutants either in combination or individually, can reduce yield (Agrawal *et al.*, 2003). More studies are required to improve the understanding of these interactions.

The flux-based study conducted in this thesis assumed that wheat crops received plentiful irrigation and hence that there was no soil water deficit and hence limitation to O_3 flux through water stressed induced g_{sto} closure. In reality, only ~ 85 % of wheat growing area is irrigated; and only two thirds of the irrigated area receives full irrigation. If soil water restrictions were allowed in the study, the differences in the spatial patterns of risk defined by AOT40 and flux would likely to have been even greater, especially in the hot dry parts of SA. This is because, soil water stress will restrict the stomatal flux of O_3 in warm and dry weather which usually also is when higher O_3 concentrations and hence high AOT40 values would normally be experienced (Simpson *et al.*, 2007). Future applications of the flux-based approach would ideally implement the new DO_3SE soil moisture model (Bueker *et al.*, submitted) though this should first be evaluated for wheat growing under water stress conditions in SA. Also, the application of such a model requires spatial data describing the presence and absence of irrigation and irrigation management procedures which is not easy to obtain.

Many of the multiple stresses identified above are likely to increase in the future due to projected increases in climate change (IPCC, 2007). Climate change and air pollution (in particular O_3) have been recognized, especially in the past two decades, as increasingly important factors that could be affecting wheat yield and crops in general across SA and especially in the IGP (Karla *et al.*, 2007; Pathak *et al.*, 2003b; Debaje *et al.*, 2010; Avnery *et al.*, 2011). To truly understand the interactions between these different stresses would likely require a modelling approach, based on robust experimental data, to assess the interactions and trade-offs in crop response to stress. For example, the implications of reduced g_{sto} in protecting against O_3, reducing water loss but at the same time reducing CO_2 uptake and subsequent photosynthetic assimilation. The combination of crop growth models and O_3 deposition models to study the co-variation in O_3 exposure and influence of crop management practices

(irrigation schemes, nutrient availability, spatial and temporal scale of cropping, increase CO_2, etc…) on aspects such as water use efficiency could provide a useful modelling tool by which these interactions and trade-offs could be investigated further.

Such a tool could also help direct efforts in biotechnology through the identification of particular plant traits, suitable for particular AGZ conditions that might afford benefits in terms of yield. Given that more than 350 wheat cultivars have been released for growing in India since 1965 and that recent studies suggest more recently released cultivars have a higher sensitivity to O_3 (Biswas *et al.,* 2008) such a tool would seem to be timely for development.

7.2.4 Food security

This study, along with the other global risk assessment studies, has shown substantial economic losses in India due to O_3 induced crop production losses. However these are based on a simple economic model where the production losses are directly converted into equivalent economic losses. In reality, changes in the supply and demand of wheat will in turn affect the price of wheat depending on the price elasticity; ideally this would be considered for a more realistic economic loss assessment (Adams *et al.,* 1989). Economic models that incorporate changes in supply and demand patterns and changes in trade of the commodity due to changes in production due to O_3 have been used to study O_3 effects on agriculture in the US (Adams *et al.,* 1989) as well as in Europe (van der Erden *et al.,* 1988). Since there are huge differences in crop production and crop price within the region, the economic impact due to O_3 crop losses is expected to vary between the regions, and also between consumers and producers (Figure 7-2) with implications for food security.

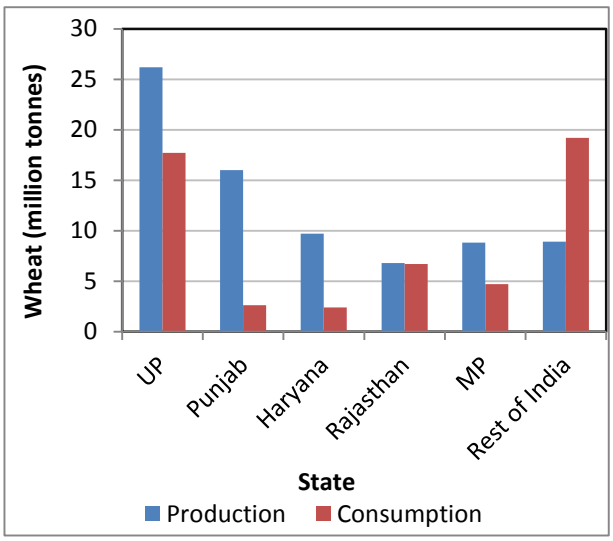

Figure 7-2: Wheat production and consumption statistics for five major wheat producing states and rest of India for the year 2000. Data source: (i) Production-DWD (2010), (ii) Consumption – NSS (2007); Jha *et al.*, (2007); DWD (2010); FCI (2011).

This can be highlighted by considering the 5 key Indian states that produce ~88 % of India's total wheat production (Figure 7-2). Most of these states (Haryana, Punjab, MP and UP) produce more wheat than is consumed and therefore are important exporters of wheat to other states. The results from this thesis study showed consistently that the IGP region, where Haryana, Punjab and UP are located, suffer the maximum risk of O_3 induced crop losses. Since these states supply a substantial share of India's wheat demand, changes in production in these states will influence the supply and demand pattern of wheat, not only in these states, but also in the rest of India. Since India's food grain economy is one of the worlds largest (primarily based on wheat and rice) any changes in grain production and economy could even have significant implications for global markets of these commodities (Jha *et al.*, 2007).

In addition, O_3 risk to crop productivity in the region may hamper any food production improvement programmes targeted towards meeting increased food demand resulting from increasing population and economic development (with associated increased personal incomes and purchasing power).

7.3 Policy response to O_3 in SA

Although uncertainties in the models and limitations in observed data have made it difficult to model the exact extent and magnitude of O_3 concentration and risk to crops in SA, it is evident from all the studies that surface O_3 is a problem at present and that in the future it is going to increase primarily due to increases in O_3 precursor emissions (Dentener *et al.,* 2006; Ramanathan *et al.,* 2008; HTAP, 2010). Global model projections under different policy scenarios show that there will be high O_3 precursor emissions in SA (HTAP, 2010) and that even with the implementation of current legislations there will be further increases in O_3 impacts on crops in SA (Van Dingenen *et al.,* 2009).

This highlights the importance of developing policy to either mitigate against further increases in O_3 precursor emissions or adapt to O_3 impacts. Policies to mitigate increasing O_3 levels would benefit from a target below which O_3 concentrations could be deemed relatively safe in terms of agricultural impacts. In Europe and North America, such targets are usually termed Air Quality Guidelines (AQGs). Table 7-3 lists the O_3 AQGs that have been established in different parts of the world; the primary standards are for human health while the secondary standards are for vegetation. Once established these AQGs can be used to identify emission control options and monitor progress to implementation of air quality management policy.

Table 7-3: List of O_3 air quality standards in different parts of the world.

Country/ Region	References	Primary standard	Secondary standard
		Level (Averaging time)	**Level (Averaging time)**
Global	World health Organization (WHO)	50ppb (8-hour)	
Regional			
EU	EU directive on Ambient air and clean air for Europe[1]	60 ppb not to be exceeded for more than 25 days per year averaged over 3 years (8 hours)	
National			
US	US-EPA, 2008	75 ppb (8-hour)	Same as Primary
UK	UK-Air Quality Standards Regulations, 2010	90ppb (8-hour)	AOT40 18000 $\mu g/m^3$ (May to July averaged over 5 years)
India	AQS, 2009	50ppb (8-hour)	
India	AQS, 2009	90ppb (1-hour)	
Pakistan	Pakistan-EPA,	90ppb (1-hour)	

Currently, the only region with O_3 AQGs for vegetation is the European region. In the rest of the world including North America, O_3 standards have only been established to protect human health. In India and Pakistan there are O_3 standards for human health which have the same value as the WHO air quality guidelines for human health (50 ppb, 8 hours average), (Central Pollution Control Board (CPCB), Government of India and

National Environmental Quality Standards, Pakistan). In addition to this, India also has a 1 hour O_3 standard of ~90 ppb. Given the results from the study presented in this thesis it might seem timely that an AQS for vegetation, and particularly arable crops, be introduced in India since it is unlikely that the existing AQG for human health, which is enforced only in urban areas, will protect against O_3 induced damage to crops.

There are also opportunities to adapt agricultural practices to reduce the risk of O_3 induced yield losses. For example, the Royal Society (2008) has highlighted the urgency of integrating O_3 tolerance into national crop breeding and selection programmes, and into biotechnology research programmes. There is good potential for O_3 resistance to be bred into new crop cultivars given the range of cultivar sensitivity to O_3 that already exists (Biswas *et al.,* 2009). However, O_3 first needs to be recognized by the crop breeding community as a potential threat to yield improvements. The results from the application of the flux based model described in Chapter 6 also highlighted the importance of understanding how crop traits, O_3 concentrations and prevailing environmental conditions combine to influence O_3 risk and that concentration based risk assessments were not fit for purpose to develop agricultural management adaptation options. Again this highlights the importance of further developing a flux approach for biotechnological advancement in India.

Due to the transboundary nature of O_3 (i.e., that O_3 and its precursor gases can be transported to different political regions from emission sources), international agreements are essential to try to tackle the O_3 problem. UNEP's Malé Declaration on control and prevention of air pollution and its likely transboundary effects for SA was signed in 1998 by the South Asian countries to address the issue of the fast growing problems of pollution across the region. The Malé Declaration could provide an important overseeing intergovernmental body to push for the further development of scientific evidence demonstrating the threat that O_3 poses to agricultural productivity across the region and to identify appropriate mitigation and adaptation policies that will alleviate future O_3 impacts. Such policies also require improved communication between the different stake holders such as scientist, policymakers and the society at large (Chakraborty and Newton, 2011). This will help in getting the right kind of scientific information for policy development, development of relevant policies for mitigating O_3 impacts on crops and incorporating other issues such as climate change and food security to identify policy interventions that can benefit multiple issues.

Definitions

Symbol	Definition	Units
A_{end}	End of F_{st} accumulation period, equivalent to end of grain filling period or physiological maturity	^{o}C days
AOT40	Accumulated O_3 above a threshold of 40 ppb, accumulated over 3 months of crop growing season	ppm h
$AOT40_A$	Accumulated O_3 above a threshold of 40 ppb, accumulated over the O_3 flux accumulation period	ppm h
A_{start}	Start of F_{st} accumulation period, equivalent to ear emergence	^{o}C days
F_{st}	Stomatal O_3 flux	nmol O_3 m^{-2} PLA s^{-1}
GDD	Growing degree days	^{o}C days
g_{sto}	Stomatal conductance of O_3	mmol O_3 m^{-2} PLA s^{-1}
I_{diff}	Diffuse sunlight	W m^{-2}
I_{dir}	Direct sunlight	W m^{-2}
LAI	(Projected) Leaf area index	m^2 m^{-2}
M7	Seasonal 7 hours mean daytime O_3 concentrations	ppb v
M12	Seasonal 12 hours mean daytime O_3 concentrations	ppb v
PAR	Photosynthetically active radiation	W m^{-2}
PODy	Phyto-toxic O_3 dose over a threshold y	mmol O_3 m^{-2} PLA
$pPAR_{total}$	Potential PAR	W m^{-2}
R_a	Aerodynamic resistance	m s^{-1}
R_b	Boundary layer resistance to O_3	m s^{-1}

r_{ext}	External plant surface resistance (leaf-level)	m s^{-1}
R_{inc}	In canopy resistance	m s^{-1}
R_{soil}	Soil resistance to O_3	m s^{-1}
SUM06	Sum of hourly O_3 concentrations when the O_3 concentrations are ≥60 ppb v during a 3 month period of the crop growing season	ppm h
T_{air}	2 m air temperature	^{o}C
VPD	Vapour pressure deficit of air	kPa
W126	sum of hourly average O_3 concentrations that have been weighted according to a sigmoid function based on a hypothetical vegetation response	ppm h
y	Detoxification threshold	nmol O_3 m^{-2} PLA s^{-1}

Glossary

AICWIP	All India Coordinated Wheat Improvement Project
CGIAR	Consultative Group on International Agricultural Research
CZ	Central zone
DO_3SE	Deposition of O_3 for stomatal exchange
DRR	Directorate of Rice Research, Government of India
DWD	Directorate of Wheat Development, Government of India
DWR	Directorate of Wheat Research, Government of India
ECMWF	European Centre for Medium-Range Weather Forecasts
EDGAR 3.2	Emissions Database for Global Atmospheric Research
EDU	Ethylene diurea, an O_3 specific chemical protectant experimental tool
EOTCP	European Open Top Chamber Program
ER	Exposure response functions
GIS	Geographical Information System
IARI	Indian Agricultural Research Institute
ICAR	Indian Council of Agricultural Research
ICRISAT	International Crops Research Institute for the Semi-Arid Tropics
IRRI	International Rice Research Institute
LRTAP	Long Range Transboundary Air Pollution
LTE	Long Term Experiments
M7	7 hour daytime mean
MATCH	Multi-scale Atmospheric Transport and Chemistry photochemical model
MOZART-2	Model for O_3 and Related Chemical Tracers version 2.0

NCLAN	National Crop Loss Assessment Network
NEPZ	North-Eastern Plains zone
NHZ	Northern Hill zone
NOAA	National Oceanic and Atmospheric Administration
NOx	nitrogen oxides
NSFM	National Food Security Mission, India
NWPZ	North-Western Plains zone
PZ	Peninsular zone
SZ	Southern Hill zone
TM5	Tracer Model 5
UNECE	United nations Economic Commission for Europe
UNECE LRTAP Convention	United Nations Economic Commission Convention on Long-range Transboundary Air Pollution
VOC	Volatile organic compounds

References

Aben, J.M.M., Janssen-Jurkovicova, M., Adema, E.H., 1990. Effects of low level ozone exposure under ambient conditions on photosynthesis and stomatal control of *Vicia faba* L., Plant Cell Environ 13, 463-469.

Abrol, I.P., 1999. Sustaining rice-wheat system productivity in the Indo-Gangetic plains: water management-related issues, Agricultural Water Management 40, 31-35.

Acevedo, E., Silva, P., Silva, H., 2002. Wheat growth and physiology. In BREAD Curtis, B.C., Rajaram S. and Macpherson, H. G. (Eds). WHEAT: Improvement and Production. FAO Plant Production and Protection Series No. 30, FAO, Rome. http://www.fao.org/DOCREP/006/Y4011E/y4011e06.htm.

Adams, R.M., Glyer, J.D., Johnson, S.L., McCarl, B.A., 1989. A reassessment of the economic effects of ozone on United States agriculture. Journal of the Air Pollution Control Association 39 (7), 960-968.

Aggarwal, P.K., Hebbar, K.B., Venugopalan, M.V., Rani, S., Bala, A, Biswal, A., Wani, S.P., 2008. Quantification of Yield Gaps in Rain-fed Rice, Wheat, Cotton and Mustard in India. Global Theme on Agroecosystems Report no. 43. Patancheru 502 324, Andhra Pradesh, India: International Crops Research Institute for the Semi-Arid Tropics. 36 pages.

Aggarwal, P.K., Joshi, P.K., Ingram, JS.I., Gupta, R.K., 2004. Adapting food systems of the Indo-Gangetic plains to global environmental change: key information needs to improve policy formulation, Environmental Science and Policy 7, 487-498.

Aggarwal, P.K., Mall, R.K., 2002. Climate change and rice yields in diverse agro-environments of India. II, Effect of uncertainties in scenarios and crop models on impact assessment, Climate Change, 52, 331-343.

Aggarwal, P.K., Sinha, S.K., 1984. Differences in water relations and physiological characteristics in leaves of wheat associated with leaf position on the plant, Plant physiology 74, 1041-1045.

Aggarwal, P.K., Talukdar, K.K., Mall, R.K., 2000. Potential yields of rice-wheat system in the Indo-gangetic plains of India. Rice-wheat Consortium Paper Series 10, New Delhi, India: Rice-wheat Consortium for the Indo-Gangetic Plains, pp. 16.

AGMARK, Post harvest Profile of wheat, Agricultural marketing information network, Ministry of Agriculture, India.

Agrawal, M., 2003. Air pollution and vegetation in India. In: Emberson, L., Ashmore, M., Murray, F. (Eds.), Air Pollution Impacts on Crops and Forests: A Global Assessment. Imperial College Press, London, pp. 165-187.

Agrawal, M., Singh, B., Rajput, M., Marshall, F., Bell, J.N.B. 2003. Effect of air pollution on peri-urban agriculture: A case study, Environmental Pollution 126, 323-329.

Agrawal, M.K., Panda, S.N., Panigrahi, B, 2004. Modeling water balance parameters

for rain-fed rice, Journal of Irrigation Drainage Engineering 130, 129–139

Agrawal, S.B., Singh, A., Rathore, D., 2005. Role of ethylene-diurea (EDU) in assessing impact of ozone on *Vigna radiata* L. plants in a suburban area of Allahabad (India), Chemosphere 61(2), 218-228.

Agri info Agricultural meteorology [Report]. - India: http://www.agriinfo.in/?page=topicandsuperid=1andtopicid=394, last accessed in May 2011.

Ahammed, Y.N., Reddy, R R., Gopal, K.R., Narasimhulu, K., Basha, D.B., Siva, L., Reddy, S., Rao, T.V.R., 2006. Seasonal variation of the surface ozone and its precursor gases during 2001–2003, measured at Anantapur (14.628 N), a semi-arid site in India, Atmospheric Research 80 (25) 151–164.

Ainsworth, E.A., 2008. Rice production in a changing climate: a meta-analysis of responses to elevated carbon dioxide and elevated ozone concentration, Global Change Biology 14, 1642-1650.

Allen, R.G., Pereira, L.S., Raes, D., Smith, M., 1998. Crop evapotranspiration - Guidelines for computing crop water requirements - FAO Irrigation and drainage paper 56. FAO, Rome.

Altenbach, S.B., DuPont, F.M., Kothari, K.M., Chan, R., Johnson, E.L., Lieu, D., 2003. Temperature, water and fertilizer influence the timing of key events during grain development in US spring wheat, Journal of Cereal Science 37, 9-20.

Altimir, N., Kolari, P., Tuovinen, J-P., Vesala, T, Back, J, Suni, T., Kulmala, M., Hari, P., 2006. Foliage surface ozone deposition: a role for surface moisture, Biogeosciences Discussions 2, 1739-1793.

Ambasht, N.K., Agrawal, M., 2003. Effects of enhanced UV-B radiation and tropospheric ozone on physiological and biochemical characteristics of field grown wheat, Biologia Plantarum 47, 625-628.

Asada, K., 1999. The water-water cycle in chloroplasts: scavenging of active oxygen and dissipation of excess photons, Annual Review of Plant Physiology and Plant Molecular Biology 50, 601–639.

Ashmore, M.R., 2005. Assessing the future global impacts of ozone on vegetation, Plant, Cell and Environment 28, 949–964.

Ashraf, M., Ashraf, M., Ali, Q., 2010. Response of two genetically diverse wheat cultivars to salt stress at different growth stages: leaf lipid peroxidation and phenolic contents, Pakistan Journal of Botany 42(1), 559-565.

Ashraf, M., 2010. Inducing drought tolerance in plants: Recent advances, Biotechnology Advances 28, 169-183.

Ashraf, M., Bashir, A., 2003. Relationship of photosynthetic capacity at the vegetative stage and during grain development with grain yield of two hexaploid wheat (*Triticum aestivum* L.) cultivars differing in yield, European Journal of Agronomy 19, 277-287.

Ashraf, M., Parveen, N., 2002. Photosynthetic parameters at the vegetative stage and during grain development of two hexaploid wheat cultivars differing in salt tolerance, Biologia Plantarum 45 (3), 401-407.

Assmann, S.M., Shimazaki, K-L., 1999. The multisensory guard cell, stomatal responses to blue light and abscisic acid, Plant Physiology 119, 809–816.

Aunan, K., Berntsen, T.K., Seip, H.M., 2000. Surface ozone in China and its possible impact on agricultural crop yields, AMBIO: A Journal of the Human Environment 29, 294–301.

Avnery, S., Mauzerall, D.L., Liu, J., Horowitz, L., 2011a. Global crop yield reductions due to surface ozone exposure: 1. Year 2000 crop production losses and economic damage, Atmospheric Environment 45(13), 2284-2296.

Avnery, S., Mauzerall, D.L., Liu, J., Horowitz, L., 2011b. Global crop yield reductions due to surface ozone exposure: 2. Year 2030 potential crop production losses and economic damage under two scenarios of O3 pollution, Atmospheric Environment 45(13), 2297-2309.

Badarinath, K.V.S., Kharol, S.K., Chand, T.R.K., Latha, K.M., 2011. Characterization of aerosol optical depth, aerosol mass concentration, UV irradiance and black carbon aerosols over Indo-Gangetic plains, India, during fog period, Meteorology Atmospheric Physics 111, 65–73.

Badaruddin, M., Reynolds, M.P., Ageeb, O.A..A., 1999. Wheat management in warm environments. Effect of organic and inorganic fertilizer, irrigation frequency and mulching, Agronomy Journal 91, 975-983.

Baier, M., Kandlbinder, A., Golldack, D. and Dietz, K.-J. 2005, Oxidative stress and ozone: perception, signalling and response, Plant, Cell and Environment 28, 1012–1020.

Bambawale, O.M., 1986. Evidence of ozone injury to a crop plant in India, Atmospheric Environment 20 (7), 1501-1503.

Bambawale, O.M., 1989. Control of ozone injury on potato, Indian Phytopathology 42, 509-513.

Barnes, J.D., Davison, A.W., Booth, T.A., 1988. Ozone Accelerates Structural Degradation of Epicuticular Wax on Norway Spruce Needles, New Pytologist 110, 309-318.

Barnes, J.D., Velissariou, D., Davison, A.E., Holevas, C.D., 1990: Comparative ozone sensitivity of old and modern Greek cultivars of spring wheat, New Phytologist 116, 707-714.

Bassin, S., Pierluigi Calanca, Tamas Weidinger, Giacomo Gerosa, Jurg Fuhrer, 2004. Modeling seasonal ozone fluxes to grassland and wheat: model improvement, testing, and application, Atmospheric Environment 38 (15), 2349-2359.

Beig, G., Ali, K., 2006. Behavior of boundary layer ozone and its precursors over a great alluvial plain of the world: Indo-Gangetic Plains, Geophysical Research Letters, 33.

Beig, G., Ghude, S.D., Polade, S.D., Tyagi, B., 2008 Threshold exceedances and cumulative ozone exposure indices at tropical suburban site, Geophysical Research Letters, 35.

Beig, G., Gunthe, S., Jadhav, D.B., 2007. Simultaneous measurements of ozone and its precursors on a diurnal scale at a semi urban, Indian Journal of Atmospheric Chemistry 57, 239–253.

Bender, J., Weigel, H.-J., 2011. Changes in atmospheric chemistry and crop health: A review, Agronomy for Sustainable Development 31, 81-89.

Bermejo, V., Gimeno, B.S., Sanz, J., de la Torre, D., Gil, J.M., 2003. Assessment of the ozone sensitivity of 22 native plant species from Mediterranean annual pastures based on visible injury, Atmospheric Environment 37 (33), 4667-4677.

Betzelberger, A.M., Gillespie, K.M., McGrath, J.M., Koester, R.P., Nelson, R.L. and Ainsworth, E.A. 2010. Effects of chronic elevated ozone concentration on antioxidant capacity, photosynthesis and seed yield of 10 soybean cultivars, Plant, Cell and Environment 33, 1569-1581.

Bhandari, A.L., Ladha, J.K., Pathak, H., Dawe, D., Gupta, R.K., 2002. Trends of yield and soil nutrient status in a long-term rice- wheat experiment in Indo-Gangetic Plains of India, Soil Science Society of America Journal 66, 162–170.

Biehler, K., Fock, H., 1996. Evidence for the Contribution of the Mehler-Peroxidase Reaction in Dissipating Excess Electrons in Drought-Stressed Wheat, Plant Physiology 112, 265-272.

Bishnoi, O.P., Singh, S., Niwas, R., 1995. Effect of temperature on phonological development of wheat (*Triticum aestivum*), Indian journal of agricultural sciences 65(3), 211-214.

Biswas, D.K., Jiang, G.M., 2011. Differential drought-induced modulation of ozone tolerance in winter wheat species, Journal of Experimental Botany 62 (12), 4153-4162.

Biswas, D.K., Xu, H., Li, Y.G., Liu, M.Z., Chen, Y.H., Sun, J.Z., Jiang, G.M., 2008a. Assessing the genetic relatedness of higher ozone sensitivity of modern wheat to its wild and cultivated progenitors/ relatives, Journal of Experimental Botany 59 (4), 951-963.

Biswas, D.K., Xu, H., Li, Y.G., Sun, J.Z., Wang, X. Z., Han, X.G., Jiang, G.M., 2008b. Genotypic differences in leaf biochemical, physiological and growth responses to ozone in 20 winter wheat cultivars released over the past 60 years, Global Change Biology 14 (1), 1365-2486.

Black, V.J., Black, C.R., Roberts, J.A., Stewart, C.A., 2000. Impact of ozone on the reproductive development of plant, Tansley Review No. 115, New Phytologist 147, 421–447.

Boni, G., Castelli, F., Entekhabi, D., 2001. Sampling Strategies and Assimilation of Ground Temperature for the Estimation of Surface Energy Balance Components, IEEE Transactions on Geoscience and Remote Sensing 39(1), 165-172.

Booker F.L., Miller J.E., Fiscus E.L., Pursley W.A., Stefanski L.A., 2005. Comparative responses of container- versus ground-grown soybean to elevated CO_2 and O_3, Crop Science 45, 883–895.

Borlaug, N.E., 1971. The green revolution: for bread and peace, Bulletin of the Atomic Scientists 27 (6), 6.

Breierova, L., Choudhari, M., 1996. An Introduction to Sensitivity Analysis. MIT System Dynamics in Education Project, Massachusetts Institute of Technology, 47.

Breuer, L. Klaus Eckhardt, Hans-Georg Frede, 2003. Plant parameter values for models in temperate climates, Ecological Modelling, 169 (2-3), 237-293.

Bruinsma, J., 2009. The Resource Outlook to 2050, By how much do land, water use and crop yields need to increase by 2050? in Expert Meeting on "How to Feed the World in 2050" 2009: FAO, Rome.

Büker, P. *et al*., 2011: DO3SE modelling of soil moisture to determine ozone flux to European forest trees. Submitted

Bunce, J.A., 2000. Responses of stomatal conductance to light, humidity and temperature in winter wheat and barley grown at three concentrations of carbon dioxide in the field, Global Change Biology 6, 371-382.

Caird, M.A., Richards, J.A., Donovan, L.A., 2007. Nighttime stomatal conductance and transpiration in C3 and C4 plants, Plant Physiology 143, 4-10.

Calatayud A., Barreno E., 2000. Foliar spraying with zineb increases fruit productivity and alleviates oxidative stress in two tomato cultivars, Photosynthetica 38, 149–154.

Calatayud A., Barreno E., 2001. Cholorophyll a fluorescence, antioxidant enzymes and lipid peroxidation in tomato in response to ozone and benomyl, Environmental Pollution 115, 283–289.

Calatayud, A., Barreno, E., 2004. Response to ozone in two lettuce varieties on chlorophyll a fluorescence, photosynthetic pigments and lipid peroxidation, Plant Physiology and Biochemistry 42, 549-555.

Campbell, G.S., Norman, J.M., 1998. An introduction to environmental biophysics. 2nd edition. Springer-Verlag, New York.

Campolongo, F., Cariboni, J., Saltelli, A. 2007. An effective screening design for sensitivity analysis of large models, Environmental modelling and software 22, 1509-1518.

Cape, J.N., Hamilton, R., Heal, M.R., 2009. Reactive uptake ofozone at simulated leaf surfaces: Implications for 'non–stomatal'ozone flux, Atmospheric Environment 43, 1116–1123.

Cariboni, J, Gatelli, D, Liska, R, Saltelli, A., 2007. The role of sensitivity analysis in ecological modelling, Ecological Modelling 203, 167–182.

Carmichael, G.R., Ferm, M., *et al.*, 2003. Measurements of sulphur dioxide, ozone and

ammonia concentrations in Asia, Africa, and South America using passive samplers, Atmospheric Environment 37, 1293–1308.

Carmichael, G.R., Sakurai, T., Streets, D., *et al.,* 2007. MICS-Asia II: The model intercomparison study for Asia Phase II methodology and overview of findings, Atmospheric Environment 42 (15), 3468-3490.

Caruso, G., Cavaliere, C., Foglia, P., Gubbiotti, R., Samperi, R, Lagana, A, 2009. Analysis of drought responsive proteins in wheat (*Triticum durum*) by 2D-PAGE and MALDI-TOF mass spectrometry, Plant Science 177 (6), 570-576.

CBD, 1992. Text on the Convention on Biological Diversity, Article 2. Use of Terms. http://www.cbd.int/convention/text/.

CGIAR, 2009. http://research.cip.cgiar.org/confluence/display/wpa/Bangladesh last accessed on 16th Sept 2009.

Chambers, J.L., Hinckley, T.M., Cox, G.S., Metcalf, C.L., Aslin R.G., 1985. Boundary-line analysis and models of leaf conductance for 4 oak-hickory forest species, Forest Science 31, 437–450.

Chameides, W.L., *et al.,* 1999. Is ozone pollution affecting crop yields in China?, Geophysical Research Letters 26, 867-870.

Chand, D., Lal, S., 2004. Variations in ozone at a high altitude station in India: transport at local and regional scales, Geophysical Research 6, 10–12.

Chand, D., Lal, S., 2000. High ozone at rural sites in India, Atmospheric Chemistry and Physics Discussion 4, 3359–3380.

Chand, R., Prasanna, P.A.L., Singh, A., 2011. Farm Size and Productivity: Understanding the Strengths of Smallholders and Improving Their Livelihoods, Economic and Political Weekly Supplement 116 (26 & 27), 5-11.

Chapin III, F.S., Matson, P.,A., Mooney, H.A., 2002. Principles of terrestrial ecosystem ecology, Springer-Verlag New York, Inc.

Chatranth, R., Mishra, B., Shoran J., 2008. Yield potential survey – India. In: Reynolds, M.P., Pietragalla, J., Braun, H.J., (Eds.), International Symposium on wheat Yield Potential: Challenges to International Wheat Breeding. Mexico, D.F. CYMMIT.

Chatrath, R., Mishra, B., Joshi, A.K., Ortiz-Ferrara, G., 2006. Challenges to wheat production in South Asia, In: Reynolds, M.P., Godinez, D., (Eds.), Extended abstracts of the international symposium on wheat yield potential "Challenges to International Wheat Breeding", Cd. Obregon, Mexico. CIMMYT, Mexico, D.F., p 6.

Chatrath, R., Mishra, B., Ortiz Ferrara, G., Singh, S.K., Joshi, A.K., 2007. Challenges to wheat production in South Asia, Euphytica 157, 447-456.

Chauhan, S., Khandelwal, R.S., Prabhu, K.V., Sinha, S.K. Khanna-Chopra, R., 2005. Evaluation of Usefulness of Daily Mean Temperature Studies on Impact of Climate Change, Journal of Agronomy and Crop Science 191, 88–94.

Collatz, G.J., Ball, J.T., Grivet, C., Berry, J.A., 1991. Physiological and environmental regulation of stomatal conductance, photosynthesis and transpiration: a model that includes a laminar boundary layer, Agricultural and Forest Meteorology 54, 107-136.

Cooley, D.R., Manning, W.J., 1987. The impact of ozone on assimilate partitioning in plants: a review, Environmental Pollution 47, 95–113.

Cornic, G., Ghashghaie, J, 1991. Effect of temperature on net CO2 assimilation and photosystem II quantum yield of electron transfer of French bean (*Phaseolus vulgaris* L.) leaves during drought stress, Planta 185, 255–260.

Coyle, M.. Nemitz, E., Storeton-West, R., Fowler, D., Cape, J.N., 2009. Measurements of ozone deposition to a potato canopy, Agricultural and Forest Meteorology 149, 655–666.

Cure, J.D., Acock, B., 1986. Crop responses to carbondioxide doubling: a literature survey, Agricultural and Forest Meteorology 38, 127-145.

Curtis, B.C., 2002. Wheat in the world. In BREAD Curtis, B.C., Rajaram S. and Macpherson, H. G. (Eds). WHEAT: Improvement and Production. FAO Plant Production and Protection Series No. 30, FAO, Rome. http://www.fao.org/DOCREP/006/Y4011E/y4011e06.htm.

CWC, 2006. Central Water Commission, India Water and Related Statistics [Book]. - New Delhi : Central Water Commission, India, 2006.

DACNET, 2011. http://dacnet.nic.in/dwd/wheat_prod1/allndiaarea_prod.htm and http://dacnet.nic.in/apy/crop_fryr_toyr.aspx (Last accessed in May 2011)

Dai, Z., Edwards, G.E., Ku, M.S.B.,1992. Control of photosynthesis and stomatal conductance in Ricinus communis by leaf-to-air vapour pressure deficit, Plant Physiology 99, 1426–1434.

Danielsson, H., Pihl Karlsson, G., Karlsson, P.E., Pleijel, H., 2003. Ozone uptake modelling and flux–response relationships- an assessment of ozone-induced yield loss in spring wheat, Atmospheric Environment 37, 475–485.

Dann, M.S., Pell, E.J. 1989. Decline of activity and quantity of ribulose bisphohphate carboxylase oxygenase and net photosynthesis in ozone-treated potato foliage, Plant Physiology 91, 427-432.

Dawe, D., Dobermann, A., Moya, P., Abdulrachman, S., Lal, P., Li, S.Y., Lin, B., Panaullah, G., Sariam, O., Singh, Y., Swarup, A., Tan, P.S., Zhen, Q.X., 2000. How widespread are yield declines in long-term rice experiments in Asia?, Field Crops Research 66, 175–193.

De Temmerman L., Wolf, J., Colls, J., Bindi, M., Fangmeier, A.. Finnan, J., Ojanperä, K., Pleijel, H., 2002. Effect of climatic conditions on tuber yield (*Solanum tuberosum* L.) in the European 'CHIP' experiments, European Journal of Agronomy 17 (4), 243-255.

Debaje, S.B., Kakade, A.D, 2009. Surface ozone variability over western Maharashtra, India, Journal of Hazardous Materials 161, 686–700

Debaje, S.B., Jeyakumar, S.J., Ganesan, K., Jadhava, D.B., Seetaramayya, P., 2003. Surface ozone measurements at tropical rural coastal station Tranquebar, India, Atmospheric Environment 37(35), 4911-4916.

Debaje, S.B., Kakade, A.D., 2006. Weekend Ozone Effect over Rural and Urban Site in India, Aerosol and Air Quality Research 6(3), 322-333.

Debaje, S.B., Kakade, A.D., Jeyakumar, S.J., 2010. Air pollution effect of O3 on crop yield in rural India, Journal of Hazardous Materials 183, 773-779.

Della Torre, G., Ferranti, F., Lupattelli, M., Pocceschi, N., Figoli, A., Nali, C., Lorenzini, G., 1998. Effects of ozone on morpho-anatomy and physiology of Hedera helix L, Chemosphere 36, 651–656.

Dentener, F., Stevenson, D., Ellingsen, K., Van Noije, T., Schultz, M., et al., 2006. The global atmospheric environment for the next generation, Environmental Science and Technology 40, 3586-3594.

Dentener, F., Van Dingenen, R., 2007. Atmospheric Dispersion calculations in GAINS: fine particulate matter and surface ozone. JRC European commission, GAINS Delhi http://www.iiasa.ac.at/rains/gains_asia/data/Meeting3/7_Frank%20Dentener.pdf.

Deosthali, V., 1999. Assessment of impact of urbanization on climate: an application of bio-climatic index, Atmospheric Environment 33, 4125–4133.

Dermody, O., Long, S.P., McConnaughay, K., DeLucia, E.H., 2008. How do elevated CO2 and O3 affect the interception and utilization of radiation by a soybean canopy?, Global Change Biology 14, 556-564.

Dias, A.S., Lidon, F.C., 2009. Evaluation of grain filling rate and duration in bread and durum wheat, under heat stress after anthesis, Journal of Agronomy and Crop Science 195, 137–147.

Dohmen, G.P., 1987. Secondary effects of air pollution: ozone decreases brown rust disease potential in wheat, Environmental Pollution 43, 189–194.

Dorjee, K., Broca, S., Pingali, P., 2003. Diversification in South Asian agriculture: Trends and constraints. FAO, Rome, ESA Working Paper No. 03-15, Agriculture and Development Division.

Drake, B.G., Gonzàlez-Meler, M.A., Long, S.P., 1997. More efficient plants: a consequence of rising atmospheric CO2?, Annual Review of Plant Physiology and Plant Molecular Biology 48, 609–639.

DRR, 2011. Directorate of Rice Research, Indian Council of Agricultural Research, Ministry of Agriculture, Government of India, http://www.drricar.org/

Dubin, H.J., Brennan, J.P., 2009. Combating Stem and Leaf Rust of Wheat. Historical Perspective, Impacts, and Lessons Learned. IFPRI Discussion Paper 00910. International Food Policy Research Institute.

Duxbury, J.M., Abrol, I.P., Gupta, R.K., Bronson, K.F., 2000, Analysis of long-term soil fertility experiments with rice-wheat rotations in South Asia. In: Abrol, I.P.,

Bronson, K.F., Duxbury, J.M., Gupta, R.K. (Eds.), Long-term Soil Fertility Experiments with Rice–Wheat Rotations in South Asia. Rice–Wheat Consortium Paper Series No. 6. Rice–Wheat Consortium for the Indo-Gangetic Plains, New Delhi, India, pp. 7–22.

DWD, 2010. Directorate of Wheat Development, Ministry of Agriculture, Government of India, http://dacnet.nic.in/dwd/, last accessed on May 2011.

DWR, 2011. Directorate of wheat Research, Government of India, http://www.dwr.in/ last accessed on May 2011.

Emberson L.D., Ashmore M.R., Murray F., *et al.* 2001. Impacts of air pollutants on vegetation in developing countries. Water Air and Soil Pollution 130, 107–118.

Emberson, L., Büker, P., Ashmore, M.R., 2007. Assessing the risk caused by ground level ozone to European forest trees: a case study in pine, beech and oak across different climate regions. Environmental Pollution 147, 454–466.

Emberson, L.D., Ashmore M.R., Cambridge, H.M., Simpson, D., Tuiovonen, J.P., 2000. Modelling stomatal ozone flux across Europe, Environmental Pollution 109, 403-413.

Emberson, L.D., Ashmore, M.R., Cambridge, H.M., 1998. Development of Methodologies for Mapping Level II Critical Levels of Ozone (DETR Report No. EPG 1/3/82). Imperial College, London.

Emberson, L.D., Büker, P., Ashmore, M.R., Mills,G., Jackson, L.S., Agrawal, M., Atikuzzaman, M.D., Cinderby, S., Engardt, M., Jamir, C., Kobayashi, K., Oanh, N.T.K., Quadir, Q.F., Wahid, A., 2009. A comparison of North American and Asian exposure–response data for ozone effects on crop yields, Atmospheric Environment 43 (12), 1945-1953.

Emberson, L.D., Simpson, D., Tuovinen, J.P., Ashmore, M.R., Cambridge, H.M., 2000b. Towards a model of ozone deposition and stomatal ozone uptake over Europe [Journal] // Norwegian Meteorological Institute, Oslo. EMEP MSC-W Note 6/2000. p.57.

Engardt, M., 2008. Modelling of near-surface ozone over South Asia, Journal of Atmospheric Chemistry 59, 61–80.

Erenstein, O., 2011. Cropping systems and crop residue management in the Trans-Gangetic Plains: Issues and challenges for conservation agriculture from village surveys, Agricultural Systems, 104 (1), 54–62.

Evans, L.T., Dunstone, R.L., 1970. Some physiological aspects of evolution in wheat, Australian Journal of Biological Science 23, 725-741.

Ewert, F., Rodriguez, D., Jamieson, P., Semenov, M.A., Mitchell, et al., 2002. Effects of elevated CO_2 and drought on wheat: testing crop simulation models for different experimental and climatic conditions, Agriculture, Ecosystems and Environment 93, 249-266. London, London

FAO, 1995. World agriculture: Towards 2010 or AT-2010.

FAO, 1996. Synthesis report of regional documents: Africa Asia and Pacific, FAO, Rome (Italy).

FAO, 1996b. Rome Declaration on World Food Security: World Food Summit. Rome, 13 November 1996, FAO.

FAO, 1998. Crop Evapotranspiration – Guidelines for computing crop water requirements. Irrigation and Drainage paper 56. FAO, Rome.

FAO, 2000a. Tropical Storms, Typhoons and Monsoon Floods seriously jeopardise food prospects and supplies in Asia and bring misery to millions, FAO/GIEWS Special Alert No. 312:. Food and Agriculture Organization of the United Nations http://www.reliefweb.int/rw/rwb.nsf/AllDocsByUNID/f0ae79df517bfedf8525696200505146

FAO, 2000b. FAO Statement on Biotechnology. http://www.fao.org/biotech/stat.asp.

FAO, 2006. The State of Food and Agriculture in Asia and the Pacific. Rome, Italy.

FAO, 2006a. Undernourishment around the world; Counting the hungry: trends in the developing world and countries in transition. The State of Food Insecurity in the World, FAO.

FAO, 2007. Sustainable Bioenergy: A Framework for Decision Makers. UN-Energy Report.

FAO, 2007b. Environment and Agriculture. Committee on Agriculture 20th session, Rome, 25 - 28 April 2007, FAO ftp://ftp.fao.org/docrep/fao/meeting/011/j9289e.pdf.

FAO, 2008. High-Level Conference on World Food Security: the Challenges of Climate Change and Bioenergy, FAO, Rome.

FAOSTAT, 2011. Food and Agricultural Organization of the United Nations. Available at: http://faostat.fao.org/site/567/default.aspx#ancor/ (last accessed April, 2011).

Fares, S., McKay, M., Holzinger, R., Goldstein, A.H., 2010. Ozone fluxes in a Pinus ponderosa ecosystem are dominated by non-stomatal processes: Evidence from long-term continuous measurements, Agricultural and Forest Meteorology 150, 420–431.

Fares, S., Park, J.H., Ormeno, E., Gentner, D.R., McKay, M., Loreto, F., Karlik, J., Goldstein, A.H., 2010b. Ozone uptake by citrus trees exposed to a range of ozone concentrations, Atmospheric Environment, 44, 3404–3412.

FAS-USDA, 2005.
http://www.fas.usda.gov/pecad/highlights/2005/07/in_soybean/in_soy200507.htm

FCI, 2011. Food Corporation of India, http://fciweb.nic.in/ (last accessed, August 2011)

Felzer, B., Reilly, J., Melillo, J , *et al.,* 2005. Future effects of ozone on carbon sequestration and climate change policy using a global biogeochemical model, Climatic Change 73, 345–373.

Felzer, B.S., Cronin, T., Reilly, J.M., Melillo, J.M., Wang, X., 2007. Impacts of ozone on trees and crops, Comptes rendus Geoscience 339, 784-798.

Feng, Z., Kobayashi, K., 2009. Assessing the impacts of current and future

concentrations of surface ozone on crop yield with meta-analysis, Atmospheric Environment 43, 1510–1519.

Feng, Z., Pang, J., Kobayashi, K., Zhu J, Ort, D.R., 2011. Differential responses in two varieties of winter wheat to elevated ozone concentration under fully open-air field conditions. Global Change Biology, 17, 580–591.

Feng, Z., Pang, J., Nouchi, I., Kobayashi, K., Yamakawa, T., Zhu, J., 2010. Apoplastic ascorbate contributes to the differential ozone sensitivity in two varieties of winter wheat under fully open-air field conditions, Environmental Pollution 158, 3539–3545.

Feng, Z., Kobayashi, K. Ainsworth, E.A., 2008. Impact of elevated ozone concentration on growth, physiology, and yield of wheat (*Triticum aestivum* L.): a meta-analysis, Global Change Biology 14, 2696–2708.

Feng, Z., Kobayashi, K., 2009. Assessing the impacts of current and future concentrations of surface ozone on crop yield with meta-analyses. Atmospheric Environment 43, 1510-1519.

Feng, Z.W., Jin, M.H., Zhang, F.Z. and Huang, Y.Z., 2003. Effects of ground-level ozone (O_3) pollution on the yields of rice and winter wheat in the Yangtze River Delta. Journal of Environmental Science (China) 15, 360–362.

Ferreira, M.I., Katerji, N., 1992. Is stomatal conductance in a tomato crop controlled by soil or atmosphere?, Oecologia 92, 104-107.

Finlayson-Pitts, B., James, N., Pitts, Jr., 1993. Volatile organic compounds: ozone formation, alternative fuels and toxics, Chemistry and Industry 18, 796-800.

Finnan, J.M., Donnelly, A., Burke, J.I., Jones, M.B., 2002. The effects of elevated concentrations of carbon dioxide and ozone on potato (*Solanum tuberosum* L.) yield, Agriculture, ecosystems and environment 88, 11-22.

Finnan, J.M., Jones, M.B., Burke, J.I., 1996. A time–concentration study on the effects of ozone on spring wheat (*Triticum aestivum* L.) 1: effects on yield, Agriculture, Ecosystems and Environment 57, 159–167.

Fischer, R.A., Byerlee, D.B., 1991. Trends of wheat production in the warmer areas: major issues and economic considerations. In: Wheat for the Non-traditional Warm Areas. Proc. of Conf., Iguazu, Brazil, 29 Jul.–3 Aug. 1990. CIMMYT, Mexico, DF. pp 3–27.

Fischer, G., Frohberg, K., Parry, M.L., Rosenzweig, C., 1996. The potential effects of climate change on world food production and security. In: Bazzaz F. and Sombroek W. (Eds.) Global climate change and agricultural production. Direct and indirect effects of changing hydrological, pedological and plant physiological processes. FAO, UN and John Wiley and Sons.

Fischer, R.A., Rees, D., Sayre, K.D., Lu, Z.-M., Condon, A.G., Larque-Saavedra, A. 1998. Wheat yield progress associated with higher stomatal conductance and photosynthetic rate, and cooler canopies. Crop Sci. 38 (6): 1467-1475.

Fiscus E.L., Booker F.L., Burkey K.O., 2005. Crop responses to ozone: uptake, modes

of action, carbon assimilation and partitioning. Plant, Cell and Environment 28, 997–1011.

Fisher, R.A., Byerlee, D.R., 1991. Trends of wheat production in the warmer areas: major issues and economic considerations. In: Saunders, D. A. (Ed.), Wheat for Non-Traditional, Warm Areas. pp. 3-27. CIMMYT, Lisboa, Mexico.

Fluckiger, W., Braun, S., Hiltbrunner, E., 2002. Effects of air pollutants on Biotic Stress, In: Bell, J.N.B., M., Treshow, (Eds.) Air pollution and Plant life. John Wiley and Sons Ltd. pp. 389.

Fowler, D., Cape, J.N., Leith, I.D., Paterson, I.S., Kinnaird, J.W., Nicholson, I.A., 1982. Rainfall acidity in northern Britain, Nature, London 297, 383-386.

Fowler, D., Flechard, C., Cape, J.N., Storeton-West, R.L., Coyle, M., 2001. Measurements of ozone deposition to vegetation quantifying the flux, the stomatal and non-stomatal components, Water Air and Soil Pollution 130, 63-74.

Fowler, D., Flechard, C., Skiba, U., Coyle, M., Cape, J.N., 1998. The atmospheric budget of oxidised nitrogen and its role in ozone formation and deposition, New Phytologist 139, 11-23.

Fowler, D., Pilegaard, K., Sutton, M.A., Ambus, P., Raivonen, M., *et al.*, 2009. Atmospheric composition change: ecosystems-atmosphere interactions, Atmospheric Environment 43, 5193–5267.

Frei, M., Pariasca, Tanaka, J., Wissuwa, M., 2008. Genotypic variation in tolerance to elevated ozone in rice: dissection of distinct genetic factors linked to tolerance mechanisms, Journal of Experimental Botany 59 (13), 3741–3752.

Fuhrer, J., 1997. Ozone sensitivity of managed pasture. In: Cheremisinoff PN (Ed.) Ecological advances and environmental impact assessment, advances in environmental control technology series. Gulf, Houston, pp. 681-706.

Fuhrer, J., Booker, F., 2003, 'Ecological issues related to ozone: agricultural issues', Environment International 29, 141-154.

Fuhrer, J., 2009. Ozone risk for crops and pastures in present and future climates, Naturwissenschaften 96, 173-194.

Fuhrer, J., Grandjean G., Tschannen W., Shariat-Madari, H., 1992. The response of spring wheat (*Triticum aestivum* L.) to ozone at higher elevations. II Changes in yield, yield components and grain quality in response to ozone flux, New Phytologist 121, 211–219.

Fuhrer, J., Skarby, L., Ashmore, M.R., 1997. Critical levels for ozone effects on vegetation in Europe, Environmental Pollution 97 (1–2), 91–106.

Fumagalli, I., Gimeno, B., Velissariou, D., de Temmerman, L., Mills, G., 2001. Evidence of ozone-induced adverse effects on crops in the Mediterranean region. Atmospheric Environment 35, 2583–2587.

GADM, 2008. Global Administrative Area Database, http://www.gadm.org/ (last

accessed in March 2008).

Gandhi, V.P., Zhou, Z-Y., Mullen, J., 2004. India's wheat economy: Will demand be a constraint or supply? Economic and Political Weekly, 4737-4746.

García, M.A., Sánchez, M.L., Pe´rez, I.A., de Torr, B., 2005. Ground level ozone concentrations at a rural location in northern Spain, Science of the Total Environment 348, 135– 150.

Garg, A., Shukla, P.R., Kapshe, M., 2006. The sectoral trends of multigas emissions inventory of India, Atmospheric Environment 40, 4608-4620.

Gelang, J., Pleijel, H., Sild, E., Danielsson, H., Younis, S., Sellden, G., 2000. Rate and duration of grain filling in relation to flag leaf senescence and grain yield in spring wheat (Triticum aestivum) exposed to different concentrations of ozone, Physiologia Plantarum 110, 366-375.

Gelang, J., Pleijel, H., Sild, E., Danielsson, H., Younis, S., Selldén, G., 2000. Rate and duration of grain filling in relation to flag leaf senescence and grain yield in spring wheat (*Triticum aestivum*) exposed to different concentrations of ozone, Physiologia plantarum 110, 366-375.

Gerosa, G., Marzuoli, R., Desotgiu, R., Bussotti, F., Ballarin-Denti, A., 2009. Validation of the stomatal flux approach for the assessment of ozone visible injury in young forest trees. Results from the TOP (transboundary ozone pollution) experiment at Curno, Italy, Environmental Pollution 157, 1497–1505.

Gerosa, G., Cieslik, S., Ballarin-Denti, A., 2003. Micrometeorological determination of time-integrated stomatal fluxes over wheat, Atmospheric Environment 37, 777–788.

Ghildiyal, M.C., Rafique, S., Sharma-Natu, P., 2001. Photosynthetic acclimation to elevated CO_2 in relation to leaf saccharide constituents in wheat and sunflower, Photosynthetica 39(3), 447-452.

Ghimiray, M., Wangdi, K., Chhetri, G.B., Bockel, L., Punjabi, M., 2007, Rice Commodity Chain Analysis, Ministry of Agriculture, Bhutan, http://www.moa.gov.bt/moa/downloads/downloadFiles/MoADownload7ek1905rn.pdf

Ghude, S.D., Jain, S.L., Arya, B.C., Beig, G., Ahammed, Y.N., Kumar, A., et al , 2008. Ozone in ambient air at a tropical megacity, delhi: Characteristics, trends and cumulative ozone exposure indices, Journal of Atmospheric Chemistry 60, 237-252.

Ghude, S.D., Beig, G., Polade, S., 2007. Tropospheric ozone and precursor gases over Indian subcontinent observed from the space, International symposium on Aerosol-Chemistry-Climate Interaction, PRL Ahmedabad, 20–22 November 2007, 205–206, 2007.

Ghude, S.D., Fadnavis, S., Beig, G., Polade, S.D., Van der, A..R.J., 2008. Detection of surface emission hot spots, trends and seasonal cycle from satellite-retrieved NO2 over India, J. Geophysical Research, 113.

Ghude, S.D., Jain, S.L., Arya, B.C., Kulkarni, P.S., Kumar, A., Ahmed, N., 2006. Temporal and Spatial Variability Of Surface Ozone At Delhi and Antarctica,

International Journal of Climatology 26, 2227–2242.

Ghude, S.D., Van der A,R.J., Beig, G., Fadnavis, S., Polade, S.D., 2009. Satellite derived trends in NO2 over the major global hotspot regions during the past decade and their inter-comparison, Environmental Pollution 157(6), 1873–1878.

Gimeno, B.S., Bermejo, V., Reinert, R.A., Zheng, Y., Barnes, J.D., 1999. Adverse effects of ambient ozone watermelon yield and physiology at a rural site in Eastern Spain. New Phytologist 144, 245–260.

GOI, 2007. Agricultural statistics at a glance 2007. Government of India, http://eands.dacnet.nic.in/At_Glance_2007.htm

Gosh, M., Patra, B.K., 2004. Effects of sowing date on heat units and yield of wheat varieties at Raghunatpur. Indian Agriculture 48 (1and2), 137-139.

Goumenaki, E, Fernandez, I.G., Papanikolaou, A., Papadopoulou, D., Askianakis, C., Kouvarakis, G., Barnes, J., 2007. Derivation of ozone flux-yield relationships for lettuce: A key horticultural crop, Environmental Pollution 146 (3), 699-706.

Goumenaki, E, Taybi, T., Borland, A., Barnes, J., 2010. Mechanisms underlying the impacts of ozone on photosynthetic performance, Environmental and Experimental Botany 69 (3), 259-266.

Grantz, D.A., Yang, S., 2000. Ozone impacts on allometry and root hydraulic conductance are not mediated by source limitation nor developmental age, Journal of Experimental Botany 51, 919-927.

Grantz, D.A., Zhang, X., Carlson, T., 1999. Observations and model simulations link stomatal inhibition to impaired hydraulic conductance following ozone exposure in cotton, Plant, Cell and Environment 22, 1201-1210.

Grennfelt, P., 2004. New Directions: Recent research findings may change ozone control policies, Atmospheric Environment 38, 2215–2216.

Grunhage, L., Jager, H-J., 2003. From critical levels to critical loads for ozone: a discussion of a new experimental and modelling approach for establishing flux-response relationships for agricultural crops and native plant species, Environmental Pollution 125 (1), 99-110.

Grünhage, L., Haenel, H.-D., Jäger, H.J., 2000. The exchange of ozone between vegetation and atmosphere: micrometeorological measurement techniques and models, Environmental Pollution 109, 373–392.

Grunhage, L., Jager, H.-J., Haenel, H.-D., Hanewald, K., Krupa, S., 1997. PLATIN (Plant-ATmosphere INteraction) II: Co-occurrence of high ambient ozone concentrations and factors limiting plant absorbed dose, Environmental Pollution 98 (1), 51-60.

Gruters, U., Fangmeier, A, Jager, H.J., 1995. Modelling stomatal responses of spring wheat (Triticum aestivum L. cv. Turbo) to ozone at different levels of water supply, Environmental Pollution 87, 141-149.

Guenther, A., Hewitt, C.N., Erickson, D., Fall, R., Geron, C., *et al.*, 1995. A global model of natural volatile organic compound emissions, Journal of Geophysical Research 100, 8873–8892.

Guidi, L., Degl'Innocenti, E., Soldatini, G.F., 2002. Assimilation of CO_2, enzyme activation and photosynthetic electron transport in bean leaves, as effected by high light and ozone, New Phytologist 156, 377-388.

Guilford-Blake, R., Stricklan, D., 2008. Guide to Biotechnology. Biotechnology Industry Organisation (BIO), Washington, DC. http://www.bio.org/speeches/pubs/er/BiotechGuide2008.pdf.

Gupta, P.K., Sahai, S., Singh, N., Dixit, C.K., Singh, D.P., Sharma, C., Tiwari, M.K., Gupta, R.K. Garg, S.C., 2004. Residue burning in rice-wheat cropping system: causes and implications, Current Science 87, 1713–1717.

Gupta, R., Seth, A., 2007. A review of resource conserving technologies for sustainable management of the rice-wheat cropping systems of the Indo-Gangetic plains (IGP), Crop Protection 26, 436-447.

Gupta, R.K., 2004. Quality of Indian wheat and infrastructure for analysis. In: Joshi AK, Chand R, Arun B, Singh G (Ed.s) A compendium of the training program (26–30 December, 2003) on wheat improvement in eastern and warmer regions of India: Conventional and non-conventional approaches. NATP project, (ICAR), BHU, Varanasi, India.

Hamby, D.M., 1994. A review of techniques for parameter sensitivity analysis of Environmental models, Environmental monitoring and Assessment 32,135-154.

Harmens, H., Mills, G., Emberson, L.D., Ashmore, M.R., 2007. Implications of climate change for the stomatal flux of ozone, Environmental Pollution 146 (3), 763 – 770.

Hassan, I.A., 2006. Physiology and biochemical response of potato (*Solanum tuberosum* L. cv. Kara) to O3 and antioxidant chemicals: possible roles of antioxidant enzymes, Annals of Applied Biology 148, 197–206.

Heagle, A.S., 1989. Ozone and crop yield, Annual Review of Phytopathology 27, 397-423.

Heagle, A.S., Flagler, R.B., Patterson, R.P., Lesser, V.M., Shafer, S.R., Heck, W.W., 1987. Injury and yield response of soybean to chronic doses of ozone and soil moisture deficit. Crop Science 27, 1016-1024.

Heagle, A.S., Lesser, V.M., Rawlings, J.O., Heck, W.W., Philbeck, R.B., 1986. Response of soybeans to chronic doses of ozone applied as constant or proportional additions to ambient air. Phytopathology 76(1): 51-56.

Heagle, A.S., Miller, J.E., Pursley, W.A., 2000. Growth and yield responses of winter wheat to mixtures of ozone and carbon dioxide, Crop Science 40, 1656-1664.

Heagle, A.S., Miller, J.E., Sherrill, D.E., Rawlings, J.O., 1993. Effects of ozone and carbon dioxide mixtures on 2 clones of white clover. New Phytol. 123, 751–762.

Heath RL , 2008 Modification of the biochemical pathways of plants induced by ozone: what are the varied routes to change? Environ Pollution 155:453–463.

Heath, R.L., Lefohn, A.S., Musselman, R.C., 2009. Temporal processes that contribute to nonlinearity in vegetation responses to ozone exposure and dose, Atmospheric Environment 43, 2919–2928.

Heck, W.W., Adams, R.A., Cure, W.W., Heagle, A.S., Heggestad, H.E., Kohut, R.J., Kress, L.W., Rawlings, J.O., Taylor, O.C., 1983. A reassessment of crop loss from ozone. Environ. Sci. Technol. 17(12): 573A-581A.

Heck, W.W., Taylor, O.C., Tingey, D.T., 1988. Assessment of Crop Loss from Air Pollutants. In: Proceedings of the International Conference. Elsevier Applied Science, Raleigh, North Carolina, USA, London.

Heggestad, H.E., Anderson, E.L., Gish, T.J., Lee, E.H., 1988. Effects of ozone and soil water deficit on roots and shoots of field-grown soybeans. Environmental pollution 50: 259-278.

Herbinger, K., Tausz, M., Wonisch, A., Soja, G., Sorger, A., Grill, D., 2002. Complex interactive effects of drought and ozone stress on the antioxidant defence systems of two wheat cultivars, Plant Physiology and Biochemistry 40 (6-8), 691-696.

Herbinger, K., Tausz, M., Wonisch, A., Soja, G., Sorger, A., Grill, D., (2002). Complex interactive effects of drought and ozone stress on the antioxidant defence systems of two wheat cultivars. Plant Physiology and Biochemistry 40, 691–696.

Hobbs, P., Morris, M., 1996. Meeting South Asia's Future Food Requirements from Rice-Wheat Cropping Systems: Priority Issues Facing Researchers in the Post-Green Revolution Era. NRG Paper 96-01. Mexico, D.F.: CIMMYT.

Hogg, A., Uddling, J., Ellsworth, D., Carroll, M.A., Pressley, S., Lamb, B., Vogel, C., 2007. Stomatal and non-stomatal fluxes of ozone to a northern mixed hardwood forest. Tellus, 59B, 514–525.

Hogsett, W.E., Tingey, D.T., Lee, E.H., 1987. Ozone exposure indices: Concepts for development and evaluation of their use. In: Heck, W.W., Taylor, O.C., Tingey, D.T., (Eds.), *Assessment of crop loss from air pollutants. Proceedings of an international conference*. NCLAN- US EPA. Elsevier publications, pp 107-138.

Holland, M., Kinghorn, S., Emberson, L., Cinderby, S., Ashmore, M., Mills, G., Harmens, H, 2006. Development of a framework for probabilistic assessment of the economic losses caused by ozone damage to crops in Europe. Part of the UNECE International Cooperative Programme on Vegetation. Contract Report EPG 1/3/205. CEH Project No: C02309NEW. pp. 49

Holland, M., Mills, G., Hayes, F., Buse, A., Emberson, L., Cambridge, H., Cinderby, S., Terry, A., Ashmore, M., 2002. Economic Assessment of Crop Yield Losses from Ozone Exposure, Centre for Ecology and Hydrology http://www.airquality.co.uk/archive/reports/cat10/final_ozone_econ_report_ver2.pdf.

Hollaway, M.J., Arnold, S.R., Challinor, A.J., Emberson, L.D., 2011. Intercontinental trans-boundary contributions to ozone-induced crop yield losses in the Northern

Hemisphere, Biogeosciences Discussions 8, 8645–8691.

Honor, S.J., Webb, A.A.R., Mansfield, T.A., 1995. The response of stomata to abscisic acid and temperature are interrelated. Proceedings of Royal Society of London B: Biological Sciences 259, 301–306.

Horowitz, *et al.*, 2003. A global simulation of tropospheric ozone and related tracers: description and evaluation of MOZART, version 2, Journal of Geophysical Research 108, 4784.

HTAP, 2010. Hemispheric transport of air pollution 2010. Part A: Ozone and particulate matter. Air pollution studies No. 17, United Nations Commission for Europe, Geneva.

Hundal, S.S., Singh, R., Dhaliwal, L.K., 1997. Agroclimatic indices for predicting phenology of wheat (*Triticum aestivum*) in Punjab, Indian Journal of Agricultural Sciences 67 (6), 265- 268.

Hunt, L.A., van der, P.G., Pararajasingham, S., 1991. Post-anthesis temperature effects on duration and rate of grain filling in some winter and spring wheat, Canadian Journal of Plant Science 71, 609-617.

Hurkman, W.J., Vensel, W.H., Tanaka, C.K., Whitehand, L., Altenbach, S.B., 2009. Effect of high temperature on albumin and globulin accumulation in the endosperm proteome of the developing wheat grain, Journal of Cereal Science 49 (1), 12-23.

Idso, K.E., Idso, S.B., 1994. Plant responses to atmospheric CO_2 enrichment in the face of environmental constraints: a review of the past 10 years' research. 69, 153-203.

IEO, 2006. International Energy Outlook for 2006, http://www.eia.doe.gov.

IFPRI, 2001. Sustainable food security for all by 2020. September 4-6, Bonn, Germany. pp1-2.

IFPRI, 2010. Achieving rice self-sufficiency in Bhutan: Long-term projections. 'Agricultural and food policy research and capacity strengthening' project report, http://www.ifpri.org/sites/default/files/publications/bhutannote02.pdf

Ilan, N., Moran, N., Schwartz, A., 1995. The role of potassium channels in the temperature control of stomatal aperture, Plant Physiology 108, 1161–1170.

IPCC, 2007. Climate Change 2007: Synthesis Report. Contribution of Working Groups I, II and III to the Fourth Assessment Report of the Intergovernmental Panel on Climate Change Core Writing Team, Pachauri, R.K, Reisinger, A., (Eds.). IPCC, Geneva, Switzerland, pp.104.

ISAAA., 2010. Agricultural Biotechnology (A Lot More than Just GM Crops). International Service for the Acquisation of agri-biotech applications. Manila, Phillipines. http://www.isaaa.org/.

Ishii, S., Bell, J.N.B., Marshall, F.M., 2007. Phytotoxic risk assessment of ambient air pollution on agricultural crops in Selangor State, Malaysia, Environmental Pollution 150, 267-279.

Iyngararasan, M., A. Jayaraman, M. Lawrance, T. Nakajima, T. Oki, *et al.,* 2008. Atmospheric Brown Clouds: Regional Assessment Report with Focus on Asia. UNEP, Kenya.

Jackson, R.D., Reginato, R.J., Idso, S.B., 1977. Wheat canopy temperature: A practical tool for evaluating water requirements, Water resources Research 13, 651-656.

Jäger, H.J., Unsworth, M., De Temmermann, L., Mathy, P., 1992. (Eds.), Effects of Air Pollution on Agricultural Crops in Europe – Results of the European Open-Top Chamber Project, Commission of the European Communities, Brussels Air Pollution Research Report 46.

Jain, D., 2005. Modeling the performance of greenhouse with packed bed thermal storage on crop drying application, Journal of Food Engineering 71 (2), 170-178.

Jain, N.K., Maurya, D.P., Singh, H.P., 1971. Effects of time and method of applying nitrogen to dwarf wheat, Expl Agriculture 7, 21-26.

Jain, S.L., B.C. Arya, Kumar, A., Ghude, S.D., Kulkarni, P.S., 2005. Observational Study of Surface Ozone at New Delhi, India, International Journal of Remote Sensing 21 (16), 3515-3526.

Jarvis, P.G., 1976. The interpretations of the variation in leaf water potential and stomatal conductance found in canopies in the field. Philos. Trans. R. Soc. London. Ser. B 273, 593–610

Jarvis, P.G., 1980. Stomatal response to water stress in conifers. In, Turner and Kramer (Eds.) Adaptation of plants to water and high temperature stress. John Wiley and Sons, New York. pp. 111.

Jarvis, P.G., Morison, J.I.L., 1981. The control of transpiration and photosynthesis by the stomata. In. Jarvis P.G., Mansfield, T.A., (Eds.) Stomatal Physiology. Cambridge University Press, Cambridge. pp. 247-279.

Jenner, C.F., 1991. Effects of exposure of wheat ears to high temperature on dry matter accumulation and carbohydrate metabolism in the grain of two cultivars. I. Immediate responses, Australian Journal of Plant Physiology 18, 165-77.

Jha, S., Srinivisan, P.V., Landes, M., 2007. Indian wheat and rice sector policies and the implications of reform. Economic Research Report, US Department of Agriculture, Economic Research Service, No 41.

Jones, H. G., 1994. Plants and Microclimate. Cambridge: Cambridge University Press

Jonson, J.E., Sundet, J.K., Tarrasón, L., 2001. Model calculations of present and future levels of ozone and ozone precursors with a global and a regional model, Atmospheric Environment 35 (1), 525-537.

Joshi, A.K., Chand, R., Arun, B., Singh, R.P., 2007a. Breeding crops for reduced tillage management in the intensive rice-wheat systems of South Asia, Euphytica 153, 135-151.

Joshi, A.K., Kumari, M., Singh, V.P., Reddy, C.M., Kumar, S., Rane, J., Chand, R.,

2007d. Stay green trait: variation, inheritance and its association with spot blotch resistance in spring wheat (*Triticum aestivum* L.), Euphytica 153, 59–71.

Joshi, A.K., Mishra, B., Chatranth, R., Ortiz-Ferrara, Singh, R.P., 2007b. Wheat improvement in India: Present status, emerging challenges and future prospects, Euphytica 157, 431-446.

Joshi, A.K., Ortiz-Ferrara, G., Crossa, J., Singh, G., Sharma, R.C., Chand, R., Parsad, R., 2007c. Combining superior agronomic performance and terminal heat tolerance with resistance to spot blotch (*Bipolaris sorokiniana*) of wheat in the warm humid Gangetic Plains of South Asia, Field Crops Research 103 (1), 53-61.

Kalra, N., Chakraborty, D., Kumar, P.R., Jolly, M., Sharma, P.K., 2007. An approach to bridging yield gaps, combining response to water and other resource inputs for wheat in northern Indian, using research trials and farmers' fields data. Agricultural Water Management, 93, 54-64.

Kalra, N., Chakraborty, D., Sharma, A., Rai, H.K., Jolly, M., Chander, S., Kumar, R.K., Bhadraray, S., Barman, D., Mittal, R.B., Lal, M., Segha, M., 2008. Effect of increasing temperature on yield of some winter crops in North West India, Current Science 94 (1): 82-88.

Kant, S., Pahuja, S.S., Pannu, R.K., 2004. Effect of seed priming on growth and phenology of wheat under late-sown conditions. Tropical science 44: 9-15.

Karlsson, P.E., Braun, S., Broadmeadow, M., Elvira, S., Emberson, L., Gimeno, B.S., Le Thiec, D., Novak, K., Oksanen, E., Schaub, M., Uddling, J., Wilkinson, M., 2007a. Risk assessments for forest trees: the performance of the ozone flux versus the AOT concepts, Environment Pollution 146: 608–616.

Karlsson, P.E., Tang, L., Sundberg, J., Chen, D., Lindskog, A., Pleijel, H., 2007b. Increasing risk for negative ozone impacts on vegetation in northern Sweden, Environmental Pollution 150: 96-106.

Karnosky, D.F., Percy, K.E., Xiang, B., Callan, B., Noormets, A., *et al.*, 2002. Interacting elevated CO_2 and tropospheric O_3 predisposes aspen (Populus tremuloides Michx.) to infection by rust (*Melampsora medusae* f. sp. tremuloidae). Global Change Biology 8, 329–38.

Katerji, N., Van Hoorn, J. W., Hamdy, A., Mastrorilli, M., Mon-Karzel, E., 1997. Osmotic adjustment of sugar beets in response to soil salinity and its influence on stomatal conductance, growth and yield, Agricultural Water Management 34, 57–69.

Kats, G., Dawson, P.J., Bytnerowicz, A., Wolf, J.W., Thompson, C.R., Olszyk, D.M., 1985. Effects of ozone or sulphur dioxide on growth and yield of rice, Agriculture, Ecosystems and Environment 14, 103-117.

Khan, S., Soja, G., 2003. Yield responses of wheat to ozone exposure as modified by drought-induced differences in ozone uptake, Water Air Soil Pollution 147, 299–315.

Khanna-Chopra, R., Selote, D.S., 2007. Acclimation to drought stress generates oxidative stress tolerance in drought-resistant than -susceptible wheat cultivar under field conditions, Environmental and Experimental Botany 60 (2), 276-283.

Kharel, K., Amgain, LP., 2010. Assessing impact of ambient ozone on growth and yield of crop at Rampur, Chitwan, The Journal of Agriculture and Environment 11, 39-45.

Khemani, L.T., Momin, G.A., Rao, P.S.P., Vijayakumar, R., Safai, P.D., 1995. Study of surface ozone behavior at urban and forested sites in India, Atmospheric Environment 29, 2021–2024.

Kichar, M.L., Niwas, R., 2005. Impact of sowing environment on growing days, phenology, growth and yield of wheat. Haryana Journal of Agronomy 21(2), 122-124.

Kichar, M.L., Niwas, R., 2007. Thermal effect on growth and yield of wheat under different sowing environments and planting systems, Indian Journal of Agricultural Research 41(2), 92-96.

Kiehl, J.T., *et al.*, 1998. The National Center for Atmospheric Research Community Climate Model: CCM3, Journal of Climate 11, 1131–1149.

Kirigwi, F.M., van Ginkel, M., Trethowan, R., Sears, R.G., Rajaram, S., Paulsen, G.M., 2004. Evaluation of selection strategies for wheat adaptation across water regimes, Euphytica 135 (3), 361-371.

Kley, D., Kleinmann, M., Sanderman, H., Krupa, S., 1999. Photochemical oxidants: state of the science, Environmental Pollution 100, 19–42.

Kobayashi, K., Okada, M., Nouchi, I., 1995. Effects of ozone on dry matter partitioning and yield of Japanese cultivars of rice (*Oryza sativa* L.), Agriculture, Ecosystems and Environment 53, 109-122.

Köllner, B., Krause, G.H.M., 2000. Changes in carbohydrates, leaf pigments and yield in potatoes induced by different ozone exposure regimes. Agriculture, Ecosystems and Environment 78, 149-158.

Kolmer, J.A., 1996. Genetics of resistance to wheat leaf rust, Annual Review of Phytopathology 34, 435-455.

Kolmer, J.A., 1999. Physiologic specialization of Puccinia triticina in Canada in 1997. Plant Dis. 83, 194–97.

Korner, C.H., Scheel, J.A., Bauer, H., 1979. Maximum leaf diffusive conductance in vascular plants, Photosynthetica 13(1), 45-82.

Krupa, S., 2003. Atmosphere and agriculture in the new millennium, Environmental Pollution 126, 293-300.

Krupa, S.V., Nosal, M., Legge, A.H., 1998. A numerical analysis of the combined open-top chamber data from the USA and Europe on ambient ozone and negative crop responses. Environmental Pollution 101, 157-160.

Kumar, A., Tripathi, R.P., 1991. Characterisation and quantification of water stress in wheat by soil-induced plant components, Journal of Agronomy and Crop Science 167, 196-200.

Kumar, A., Turner, N.C., Singh, D.P., Singh, P., Barr, M., 1999. Diurnal and seasonal

patterns of water potential, photosunthesis, evapotranspiration and water use efficiency of clusterbean, Photosynthetica 37(4), 601-607.

Kumar, N., Kumar, S., Ahuja, P.S., 2005. Photosynthetic characteristics of Hordeum, *Triticum, Rumex*, and Trifolium species at contrasting altitudes, Photosynthetica 43 (2), 195-201.

Kumar, R., Naja, M., Venkataramani, S., Wild, O., 2010. Variations in surface ozone at Nainital: A high-altitude site in the central Himalayas, Journal of Geophysical Research 115.

Lacasse, N.L., Treshow, M., 1976. Diagnosing vegetation injury caused by air pollution, US Environmental Protection Agency Handbook.

Ladha, J.K., Dawe, D., Pathak, H., Padre, A.T., Yadav, R.L., Singh, B., *et al*., 2003. How extensive are yield declines in long-term rice–wheat experiments in Asia?, Field Crops Research 81, 159–180.

Ladha, J.K., Fischer, K.S., Hossain, M., Hobbs, P.R., Hardy, B., 2000. Improving the productivity and sustainability of rice-wheat systems of the Indo-Gangetic planins: A synthesis of NARS-IRRI partnership research, International Rice Research Institute (IRRI) Discussion Paper No. 40.

Laisk, A., Kull, O., Moldau, H., 1989. Ozone concentration in leaf intercellular air spaces is close to zero, Plant Physiology 90, 1163-1167.

Lal, R., 1975. Role of mulching techniques in tropical soil and water management. International Institute of Tropical Agriculture, Technical Bulletin, 1.

Lal, S., Naja, M., Subbaraya, B.H., 2000. Seasonal variations in surface ozone and its precursors over an urban site in India, Atmospheric Environment 34, 2713-2724.

Lamboni, M., Makowski, D., Lehuger, S., Gabrielle, B., Monod, H., 2009. Multivariate global sensitivity analysis for dynamic crop models, Field Crops Research. 113 (3), 312-320.

Lange, O.L., Losch, R., Schulze, E.-D., Kappen, L. 1971. Responses of stomata to changes in humidity, Planta 100, 76-86.

Larson, D.W., Jones, E., Pannu, R.S., Sheokand, R.S., 2004. Instability in Indian agriculture--a challenge to the Green Revolution Technology, Food Policy 29 (3), 257-273.

Laurila, T., Jonson, J.E., Langner, J., Sundet, J., Tuovinen, J.-P., Bergström, R., Foltescu, V., Tarvainen, V., Isaksen, I.S.A.., 2004. Ozone exposure scenarios in the Nordic countries during the 21st century. EMEP/MSCW Technical Report 2/2004. Norwegian Meteorological Institute, Oslo. pp. 41.

Lawson, T., Craigon, J., Black, C.R., Colls, J.J., Tulloch, A.-M., Landon, G., 2001. Effects of elevated carbon dioxide and ozone on the growth and yield potatoes (*Solanum tuberosum*) grown in open-top chambers, Environmental Pollution 111, 479-491.

Lee, E.H., Tingey, D.T., Hogsett, W.E., 1988. Evaluation of ozone exposure indexes in exposure-response modelling, Environmental Pollution 53, 43-62.

Lefohn, A.S., Lawrence, J.A., Kohut, R.J., 1988. A comparison of indices that describe the relationship between exposure to ozone and reduction in the yield of agricultural crops, Atmospheric Environment 22, 1229-1240.

Lefohn, A.S., Runeckles, V.C., 1987. Establishing a standard to protect vegetation - ozone exposure/dose considerations, Atmospheric Environment 21, 561-568.

Leitao, L., Bethenod, O., Biolley, J.-P., 2007. The Impact of Ozone on Juvenile Maize (Zea mays L.) Plant Photosynthesis: Effects on Vegetative Biomass, Pigmentation, and Carboxylases (PEPc and Rubisco), Plant Biology 9, 478–488.

Lesser, V.M., Rawlins, J.O., Spruill, S.E., Somerville, M.C., 1990. Ozone effects on agricultural crops: Statistical methodologies and estimated dose-response relationships, Crop Science 30, 148–155.

Leuning, R., Dunin, F.X., Wang, Y.-P., 1998. A two-leaf models for canopy conductance, photosynthesis and partitioning of available energy II. Comparison with measurements, Agricultural and Forest Meteorology 91, 113–125.

Li, X., Waddington, S.R., Dixon, J., Joshi, A.K., de Vicente, M.C., 2011. The relative importance of drought and other water-related constraints for major food crops in South Asian farming systems, Food Security 3, 19-33.

Lohani, B.N., 2007. Clouds over Asia's future, Development and Cooperation 48(3): 106-107.

Long, S.P., Ainsworth, E.A., Leaky, A.D.B., Morgan, P.B., 2005. Global food insecurity. Treatment of major food crops with elevated carbon dioxide or ozone under large-scale fully open-air conditions suggests recent models may have overestimated future yields, Philosophical Transactions of the Royal Society B-Biological Sciences 360, 2011-2020

Long, S.P., Ainsworth, E.A., Leakey, A.D., Nösberger, J., Ort, D.R., 2006. Food for thought: lower-than-expected crop yield stimulation with rising CO2 concentrations, Science 312(5782), 1918-1921.

Long, S.P., Ainsworth, E.A., Leakey, A.D., Morgan, P.B., 2005. Global food insecurity: treatment of major food crops with elevated carbon dioxide or ozone under largescale fully open-air conditions suggests recent models may have overestimated future yields, Philosophical Transactions of the Royal Society B 360, 2011-2020

Long, S.P., Naidu, S.L., 2002. Effects of oxidants at the biochemical, cell and physiological levels, Treshow, M., Editor, Air Pollution and Plants, John Wiley, London, UK, pp. 69–88.

LRTAP Convention , 2004. Manual on Methodologies and Criteria for Modelling and Mapping Critical Loads and Levels and Air Pollution Effects, Risks and Trends. Chapter 3: Mapping Critial Levels for Vegetation.

LRTAP Convention , 2010. Manual on Methodologies and Criteria for Modelling and

Mapping Critical Loads and Levels and Air Pollution Effects, Risks and Trends. Chapter 3: Mapping Critial Levels for Vegetation, http://icpvegetation.ceh.ac.uk/manuals/mapping_manual.html.

Lu, Z.M., Percy, R.G., Qualset, C.O., Zeiger, E., 1998. Stomatal conductance predicts yields in irrigated Pima cotton and bread wheat grown at high temperatures, Journal of Experimental Botany 49, 453–460.

Ma, R., Zhang, M., Li, B., Du, G., Wang, J., Chen, J., 2005. The effects of exogenous Ca2+ on endogenous polyamine levels and drought-resistant traits of spring wheat grown under arid conditions, Journal of Arid Environments 63 (1), 177-190.

Maggs, R., Ashmore, M.R., 1998. Growth and yield responses of Pakistan rice (*Oryza sativa* L.) cultivars to O_3 and NO_2, Environmental pollution 103, 159-170.

Mall, R.K., Singh, R., Gupta, A., Srinivasan, G., Rathore, L.S., 2006. Impact of climate change on Indian agriculture: A review, Climatic Change 78, 445-478.

Marino, S., Hogue, I.B., Ray, C.J., Kirschner, D.E., 2008. A Methodology For Performing Global Uncertainty And Sensitivity Analysis In Systems Biology, Journal of Theoritical Biology 254 (1), 178-196.

Massman, W.J., 2004. Toward an ozone standard to protect vegetation based on effective dose: a review of deposition resistance and a possible metric, Atmospheric Environment 38, 2323–2337.

Matsui, T., Namuco, O.S., Ziska, L.H., Horie, T., 1997. Effect of high temperature and CO_2 concentration on spikelet sterility in indica rice, Field crops research 51, 213-219.

Matyssek, R., Bytnerowicz, A, Karlsson, P.-E., Paoletti, E., Sanz, M., Schaub, M., Wieser, G., 2007. Promoting the O3 flux concept for European forest trees, Environmental Pollution 146, 587-607.

Matyssek, R., Sandermann, H., Wieser, G., Booker, F., Cieslik, S., Musselman, R., 2008. The challenge of making ozone risk assessment for forest trees more mechanistic. Environmental Pollution 156, 567e582.

Mauzeral, D.L., Logan, J.A., Jacob, D.J., Anderson, B.E., Blake, D.R., Bradshaw, J.D., Sachse, G.W., Singh, H.B., Talbot, R.W., 1998. Photochemistry in biomass burning plumes and implications for tropospheric ozone over the tropical south Atlantic, Journal of Geophysical Research 103, 8401-8423.

Mauzerall, D.L., Wang, X., 2001. Protecting agricultural crops from the effects of Tropospheric ozone exposure: Reconciling Science and standard setting in the United States, Europe and Asia, Annual review of Energy and Environment.26, 237-268.

McAinsh, M.R., Evans, N.H., Montogomery, L.T., North, K.A, 2002. Calcium signalling in stomatal responses to pollutants, New Phytologist 153, 441-447.

McKee, I.F., Bullimore, J.F., Long, S.P., 1997. Will elevated CO_2 concentrations protect the yield of wheat from O_3 damage? Plant, Cell & Environment 20, 77–84.

McKee, I.F., Long, S.P., 2001. Plant growth regulators control ozone damage to wheat

yield. New Phytologist 152, 41–51.

McKee, I.F., Farage, P.K., Long, S.P., 1995. The interactive effects of elevated CO2 and O3 concentration on photosynthesis in spring wheat, Photosynthesis Research 45, 111–119.

McKee, I.F., Mulholland, B.J., Craigon, J., Black, C.R., Long, S.P., 2000. Elevated concentrations of atmospheric CO_2 protect against and compensate for O_3 damage to photosynthetic tissues of field-grown wheat, New Phytologist 146, 427-435.

McMaster, G.S., Wilhelm, W.W., 1997. Growing degree-days: one equation, two interpretations, Agricultural and Forest Meteorology 87, 291-300.

McMaster, G.S., White, J.W., Hunt, L.A., Jamieson, P.D., Dhillon, S.S., Ortiz-Monasterio, J.I., 2008. Simulating the Influence of Vernalization, Photoperiod and Optimum Temperature on Wheat Developmental Rates, Annals of Botany 102, 561–569.

Mehla, R.S., Verma, J.K., Gupta, R.K., Hobbs, P.R., 2000, Stagnation in the Productivity of Wheat in the Indo-Gangetic Plains: Zero-till-seed-cum-fertilizer Drill as an Integrated Solution, Rice-Wheat Consortium Paper Series 8, Rice-Wheat Consortium for the Indo-Gangetic Plains, CIMMYT, Delhi, India.

Meyer, B. Køllner, J., Willenbrink, G.H.M., Krause, 2000. Effects of different ozone exposure regimes on photosynthesis, assimilates and thousand grain weight in spring wheat, Agriculture, Ecosystems and Environment 78 (1), 49–55.

Mian, M.I.A., Rouf, M.A., Rashid, M.A., Mazid, M.A., Eaqub., M., 1985. Residual effects of triple super phosphate (TSP) and farmyard manure (FYM) under renewed application of urea on the yield of crops and some chemical properties of soil, Bangladesh Journal of Agricultural Science 10(2), 99-109.

Miller, J.E., Pursley, W.A., Heagle, A.S., 1994. Atmospheric pollutants and trace gases. Effects of ethylenediurea on snap bean at a range of ozone concentrations, Journal of Environmental Quality 23, 1082-1089.

Miller, P.R., 1983. Ozone effects in the San Bernardino National Forest. In: Air pollution and the productivity of the forest. In Eds. Davis, D.D., Miller, A.A., Dochinger, L., Walton, I., League of America, 161-97.

Mills, G., Buse, A., Gimeno, B., Bermejo, V., Holland, M., Emberson, L., Pleijel, H., 2007. A synthesis of AOT40-based response functions and critical levels for ozone for agricultural and horticultural crops, Atmospheric Environment 41, 2630–2643.

Mills, G., Hayes, F., Simpson, D., Emberson, L., Norris, D., Harmens, H., Büker, P., 2010. Evidence of widespread effects of ozone on crops and (semi-)natural vegetation in Europe 1990–2006) in relation to AOT40– and flux-based risk maps, Global Change Biology 17, 592–613.

Mills, G., Pleijel, H., Braun, S., Buker, P., Bermejo, V., Calvo, E., *et al.,* 2011. New stomatal flux-based critical levels for ozone effects on vegetation. Atmospheric Environment, 45 (28). 5064-5068.

Milne, A.E., Wheeler, H.C., Lark, R.M., 2006a. On testing biological data set for the presence of a boundary, Annals of Applied Biology 149, 213-222.

Milne, A.E., Ferguson, R.B., Lark, R.M., 2006b. Estimating a boundary line model for a biological response by maximum likelihood, Annals of Applied Biology 149, 223-234.

Mishra, B., Chatranth, R., Mohan, D., Saharan, M.S., Tyagi, B.S., 2007. Perspective plan: Vision 2025, Directorate of Wheat Research, Karnal, India.

Mishra, B., Shoran, J., Chatranth, R., Sharma, A.K., Gupta, R.K., Sharma, R.K., Singh, R., Rane, J., Kumar, A., 2005. Cost effective and sustainable wheat production technologies, Technical Bulletin No.8, Directorate of wheat Research, Karnal, India.

Mitchell, J.F.B., Johns, T.C., Gregory, J.M., Tett, F.B. 1995. Climate response to increasing levels of greenhouse gases and sulphate aerosols, Nature 376, 501-504.

Mitra, R., Bhatia, C.R., 2008. Bioenergetic cost of heat tolerance in wheat crop, Current Science 94(8), 1049-1052.

Mitra, A.P., 2006. ABC and India. DELHI, ABC Meeting, 13 Feb 2006.

Mittal, M.L., 2006. Modelling air pollution in the Indian region. A report on surface ozone concentrations. www.osc.edu/research/pcrm.

Mittal, M.L., Hess, P.G., Jain, S.L., Arya, B.C., Sharma, C., 2007. Surface ozone in the Indian region, Atmospheric Environment 41, 6572-6584.

Mittal, S., 2008. Demand- Supply trends and projections of food in India. Working paper No. 209. Indian council for research on international economic relations.

Mittler, R., Blumwald, E., 2010. Genetic engineering for modern agriculture: challenges and perspectives, Annual Review of Plant Biology 61, 1–20.

Mohanty, S., Peterson, W., 2001. "Will India Be Able to Feed Itself?" Paper Presented at the annual meeting of Southem Agricultural Economics Association.

Morgan, P.B., Bernacchi, C.J., Ort, D.R., Long, S.P., 2004. An in vivo analysis of the effect of season-long open-air elevation of ozone to anticipated 2050 levels on photosynthesis in soybean, Plant Physiology 135, 2348-2357.

Morgan, P.B., Mies, T.A., Bollero, G.A., *et al.*, 2006. Season-long elevation of ozone concentration to projected 2050 levels under fully open-air conditions substantially decreases the growth and production of soybean. New Phytologist 170, 333–343.

Morgan, P.B., Ainsworth, E.A., Long, S.P., 2003. How does elevated ozone impact soybean? A meta-analysis of photosynthesis, growth and yield, Plant, Cell and Environment 26, 1317–1328.

Morris, M.S. 1991. Factorial sampling plans for preliminary computational experiments. Technometrics, 33, 161-174.

Mouida, *et al.*, 2011. http://www.ijcsi.org/papers/IJCSI-8-3-1-369-377.pdf

Mudd, J.B., 1996. Resistance mechanisms in plants against air pollution. In: Yunus, M.,

Iqbal, M., (Eds). Plant Response to Air Pollution. John Willy and Sons, Chinchester, England.

Mulchi, C., Rudorff, B., Lee, E., Rowland, R., Pausch, R., 1995. Morphological responses among crop species to full-season exposures to enhanced concentrations of atmospheric CO_2 and O_3, Water, air and soil pollution 85, 1379-1386.

Mulholland, B.J., Craigon, J., Black, C.R., Colls, J.J., Atherton, J.G.A., Landon, G., 1997a. Effects of elevated CO_2 and O_3 on the growth and yield of spring wheat (*Triticum aestivum* L.), Journal of Experimental Botany 48, 113-22.

Mulholland, B.J., Craigon J., Black, C.R., Colls, J.J., Atherton, J., Landon, G., 1997b. Impact of elevated atmospheric CO2 and O3 on gas exchange and chlorophyll content in spring wheat (Triticum aestivum L.), Journal of Experimental Botany 48, 1853-1863.

Munns, R., Tester, M., 2008. Mechanisms of salinity tolerance, Annual Review of Plant Biology 59, 651–681.

Musselman, R.C., A.S., Lefohn, 2007. The use of critical levels for determining plant response to ozone in Europe and in North America. Short Communication. Proceedings: Impacts of Air Pollution and Climate Change on Forest Ecosystems, The Scientific World Journal 7(S1), 15–21.

Musselman, R.C., Massman, W.J., 1998. Ozone flux to vegetation and its relationship to plant response and ambient air quality standards, Atmospheric Environment 33, 65–73.

Musselman, R.C., Lefohn, A.S., Massman,W.J., Heath, R.L., 2006. A critical review and analysis of the use of exposure- and flux-based ozone indices for predicting vegetation effects, Atmospheric Environment 40, 1869-1888.

NAAQS, 2009. National Ambient Air Quality Standards, India, http://cpcb.nic.in/National_Ambient_Air_Quality_Standards.php.

Nagarajan, S., 2005. Can India produce enough wheat even by 2020, Current Science 89, 1467–1471.

Nair, P.R., Chand, D., Lal, S., Modh, K.S., Naja, M., Parameswaran, K., Ravindran, S., Venkataramani, S., 2002. Temporal variations in surface ozone at Thumba (8.6°N, 77°E)—a tropical coastal site in India, Atmospheric Environment 36, 603–610.

Naja, M., Lal, S., 2002. Surface ozone and precursor gases at Gadanki (13.5°N, 79.2°E), a tropical rural site in India, Journal of Geophysical Research 107 (D14).

Navabi, A., Singh, R.P., Tewari, J.P., Briggs, K.G., 2003. Genetic Analysis of Adult-Plant Resistance to Leaf Rust in Five Spring Wheat Genotypes, Plant Disease 87 (12), 1522-1529.

NEGTAP, 2001. National Expert Group on Transboundary Air Pollution. Transboundary Air Pollution: Acidification, Eutrophication and Ground-Level Ozone in the UK. Department for Environment, Food and Rural Affairs, UK.

Newton, A.C., Johnson S.N., Gregory, P.J., 2011. Implications of climate change for diseases, crop yields and food security, Euphytica 179 (1), 3-18.

NFSM, 2011. National Food Security Mission, Ministry of Agriculture, India http://nfsm.gov.in/, last accessed in April 2011.

NOAA, 2009. http://www.ncdc.noaa.gov/oa/mpp/freedata.html (last accessed November 2009)

NSS, 2007. National Sample Survey, India. http://mospi.nic.in. (last accessed May 2010)

Nussbaum, S., Geissmann, M., Fuhrer, J., 1995. Ozone exposure-response relationships for mixtures of perennial ryegrass and white clover depend on ozone exposure patterns, Atmospheric Environment 29, 989-995.

Nussbaum, S., Remund, J., Rihm, B., Mieglitz, K., Gurtz, J., Fuhrer, J., 2003. High-resolution spatial analysis of stomatal ozone uptake in arable crops and pastures, Environment International 29, 385-392.

Olivier, J.G.J., Bloos, J.P.J., Berdowski, J.J.M., Visschedijk, A.J.H., Bouwman, A.F., 1999. A 1990. global emission inventory of anthropogenic sources of carbon monoxide on 1x1 developed in the framework of EDGAR/GEIA, Chemosphere: Global Change Science, 1, 1–17.

Olivier, J.G.J., *et al.*, 1996. Description of EDGAR Version 2.0: A Set of Global Emission Inventories of Greenhouse Gases and Ozone Depleting Substances for All Anthropogenic and Most Natural Sources on a Per Country Basis and on a 1 x 1 Degree Grid, RIVM Rep. 771060 002/TNO-MEP Rep. R96/119. National Institute for Public Health and the Environment, Bilthoven, Netherlands.

Olivier, J.G.J., Peters, J. A. H. W., Bakker, J., Berdowski, J. J. M., Visschedijk, A. J. H., Bloos, J.P.J., 2002. Applications of EDGAR: emission database for global atmospheric research, Report no.: 410.200.051. RIVM, The Netherlands.

Pääkkönen, E., Holopainen, T., Kärenlampi, L., 1995. Effects of ozone on birch (*Betula pendula* Roth) clones, Water Air and Soil Pollution 85, 1331–1336.

Pakistan Gov. http://www.pakistan.gov.pk/divisions/ContentListing.jsp?DivID=10andcPath=91_96

Pakistan-EPA, 2008. National Environmental Quality Standards for Ambient Air, Government of Pakistan, http://www.environment.gov.pk/act-rules/NEQS%20for%20Ambient%20Air.pdf

Pal, S.K., Verma, U.N., Singh, M.K., Upasani, R.R., Thakur, R., 2001. Growth and yield of late sown wheat (*Triticum aestivum*) under different irrigation schemes, Indian journal of Agricultural Science 71(10), 664-667.

Pang, J., Kobayashi, K., Zhu, J.G., 2009. Yield and photosynthetic characteristics of flag leaves in Chinese rice (*Oryza sativa* L.) varieties subjected to free-air release of ozone, Agriculture, Ecosystems and Environment 132, 203–211.

Paoletti, E., De Marco, A., Racalbuto, S., 2007b. Why Should We Calculate Complex Indices of Ozone Exposure? Results from Mediterranean Background Sites, Environmental Monitoring and Assessment 128, 19–30.

Paoletti, E., Grulke, N.E., 2010. Ozone exposure and stomatal sluggishness in different plant physiognomic classes, Environmental Pollution 158 (8), 2664-2671.

Paoletti, E., Manning, W.J., 2007. Toward a biologically significant and usable standard for ozone that will also protect plants, Environmental Pollution 150, 85-95.

Paoletti, E., Nali, C., Lorenzini, G., 2007a. Early Responses to Acute Ozone Exposure in Two Fagus Sylvatica Clones Differing in Xeromorphic Adaptations: Photosynthetic and Stomatal Processes, Membrane and Epicuticular Characteristics, Environmental Monitoring and Assessment 128 (1-3), 93-108.

Pararajasingham, S., Hunt, L.A., 1991. Wheat Spike Temperature in Relation to Base Temperature for Grain Filling Duration, Canadian Journal of Plant Science 71, 63-69.

Park, R.F., Bariana, H.S., Wellings, C.R., 2007. Special Issue: Global Landscapes in Cereal Rust Control, Australian Journal of Agricultural Research 58 (6), 469-469.

Pathak, H., Aggarwal, P.K., Roetter, R., Kalra, N., Bandyopadhaya, S.K., Prasad, S., Van Keulen, H., 2003a. Modelling the quantitative evaluation of soil nutrient supply, nutrient use efficiency, and fertilizer requirements of wheat in India, Nutural Cycle of Agroecosystems 65, 105–113.

Pathak, H., Ladha, J.K., Aggarwal, P.K., Peng, S., Das, S., Singh, Y., Singh, B., Kamra, S.K., Mishra, B., Satri, A.S.R.A.S., Aggarwal, H.P., Das, D.K., Gupta, R.K., 2003b. Trends of climatic potential and on-farm yields of rice and wheat in the Indo-Gangetic plains, Field Crops Research 80, 223–234.

Patnaik, D., Khurana, P, 2001. Wheat biotechnology: A mini review, Journal of Biotechnology. 4(2), 74-102

Peel, M.C., Finlayson, B.L., McMahon, T.A. , 2007. Updated world map of the Köppen-Geiger climate classification, Hydrology and Earth system sciences 11, 1633-1644.

Pell, E.J., Schlagnhaufer, C.D., Arteca, R.N., 1997. Ozone-induced oxidative stress : Mechanisms of action and reaction, Physiologia Plantarum 100, 264-273.

Pell, E.J., Sinn, J.P, Brendley, B.W., Samuelson, L., Vinten-Johansen, C., Tien, M., Skillman, J., 1999. Differential response of four tree species to ozone-induced acceleration of foliar senescence, Plant Cell and Environment 22, 779–790.

Pell, E.J., Pearson, N.S., Vinten-Johansen, C., 1988. Qualitative and quantitative effects of ozone and/or sulfur dioxide on field-grown potato plants, Environmental pollution 53, 171-186.

Peltonen-Sainio, P., Forsman, K., Poutala, T., 1997. Crop management e€ ects on pre- and post-anthesis changes in leaf area index and leaf area duration and their contribution to grain yield, Journal of Agronomy and Crop Science 179, 47-61.

Percy, K.E., Awmack, C.S., Lindroth, R.L., Kubiske, M.E., Kopper, B.J., Isebrands, J.G., *et al.* 2002. Altered performance of forest pests under atmospheres enriched by CO_2 and O_3, Nature 420, 403–407.

Percy, K.E., Jensen, K.F., McQuattie, C.J., 1992. Effects of ozone and acidic fog on red spruce needle epicuticular wax production, chemical composition, cuticular membrane ultrastructure and needle wettability, New Phytologist 122, 71–80.

Pfleeger, T.G., da Luz, M.A., Mundt, C.C., 1999. Lack of a synergistic interaction between ozone and wheat leaf rust in wheat swards, Environmental and Experimental Botany 41 (3), 195-207.

Phadnis, M.J., Levy II, H., Moxim, W.J., 2002. On the evolution of pollution from south and Southeast Asia during the winter-spring monsoon, Journal of Geophysical Research, 107(D24), 4790.

Piikki, K., De Temmerman, L., Högy, P. and Pleijel, H., 2008. The open-top chamber impact on vapour pressure deficit and its consequences for stomatal ozone uptake. Atmospheric Environment 42, 6513–6522.

Piikki, K., De Temmerman, L., Ojanpera, K., Danielsson, H., Pleijel, H., 2008. The grain quality of spring wheat (*Triticum aestivum* L.) in relation to elevated ozone uptake and carbon dioxide exposure, European Journal of Agronomy 28, 245–254.

Pingali, P.L., 1999. Global Wheat Research in a Changing World: Challenges and Achievements. In: CIMMYT 1998-99 World Wheat Facts and Trends. Mexico, D.F.: CIMMYT.

Pingali, P.L., Rosegrant, M.W., 1998. Supplying Wheat for Asia's Increasingly Westernized Diets. American Journal of Agricultural Economics 80 (5), 954-959.

Pinstrup-Andersen, P. 2001. The future world food situation and the role of plant diseases. The Plant Health Instructor. DOI: 10.1094/PHI-I-2001-0425-01. http://www.apsnet.org/Education/feature/FoodSecurity/

Plazek, A., Hura, K., Rapacz, H., Zur, I., 2001. The influence of ozone fumigation on metabolic efficiency and plant resistance to fungal pathogens, Journal of Applied Botany 75, 8–13.

Pleijel H., Danielsson H., Ojanpera K., Temmerman L. De, Hogy P., Badiani M., Karlsson P. E., 2004. Relationships between ozone exposure and yield loss in European wheat and potato--a comparison of concentration- and flux-based exposure indices, Atmospheric Environment. 38, 2259-2269.

Pleijel H., Danielsson, H., Emberson, L., Ashmore, M.R., Mills., G., 2007. Ozone risk assessment for agricultural crops in Europe: Further development of stomatal flux and flux-response relationships for European wheat and potato, Atmospheric Environment 41, 3022-3040.

Pleijel, H., Berglen Eriksen, A., Danielsson, H., Bondesson, N., Sellden, G., 2006b. Differential ozone sensitivity in an old and a modern Swedish wheat cultivar--grain yield and quality, leaf chlorophyll and stomatal conductance, Environmental and Experimental Botany. 56 (1), 63-71.

Pleijel, H., Danielsson, H., Gelang, J., Sild, E., SelldeÂn, G., 1998. Growth stage dependence of the grain yield response to ozone in spring wheat (*Triticum aestivum* L.), Agriculture Ecosystems and Environment 70, 61-68.

Pleijel, H., Danielsson, H., Pihl Karlsson, G., Gelang, J., Karlsson, P.E., Sellden, G., 2000. An ozone flux–response relationship for wheat, Environmental Pollution 109, 453–462

Pleijel, H., Danielsson, H., Vandermeiren, K., Blum, C., Colls, J., Ojanperä, K., 2002. Stomatal conductance and ozone exposure in relation to potato tuber yield – results from the European CHIP programme, European Journal of Agronomy 17, 303-317.

Pleijel, H., OjanperaÈ , K., Danielsson, H., Sild, E., Gelang, J., Wallin, G., Skarby, L., Sellden, G., 1997. Effects of ozone on leaf senescence in spring wheat Ð possible consequences for grain yield, Phyton (Austria) 37, 227-232.

Plessl, M., Heller, W., Payer, H.D., Elstner, E.F., Habermeyer, J., Heiser, I., 2005. Growth parameters and resistance against *Drechslera teres* of spring barley (*Hordeum vulgare* L. cv. Scarlett) grown at elevated ozone and carbon dioxide concentrations, Plant Biology 7, 694–705.

PORG, UK Photochemical Oxidants Review Group (Ed.), 1998. Ozone in the United Kingdom, Fourth Report of the Photochemical Oxidants Review Group. 1st ed. The Department of the Environment Transport and the Regions, Edinburgh.

Porter, J.R., Gawith, M., 1999. Temperatures and the growth and development of wheat: a review, European Journal of Agronomy 10 (1), 23-36.

Prashar, M., S.C., Bhardwaj, S.K., Jain, Y.P., Sharma, B., Mishra, 2008. Perspective on wheat rusts in India. In Eds. Rudi Appels, Russell Eastwood, Evans Lagudah, Peter Langridge, Michael Mackay, Lynne McIntyre, Peter Sharp. Proceedings of the 11th International Wheat Genetics Symposium 2008. Sydney University Press, Sydney, Australia, 3, 812-814.

Prashar, M., Bhardwaj, S.C., Jain, S.K., Datta, D., 2007. Pathotypic evolution in Puccinia striiformis in India during 1995–2004, Australian Journal of Agricultural Research 58 (6), 602-604.

Prather, M., Ehhalt, D., Dentener, F., Derwent, R., Dlugokencky, E., Holland, E., Isaksen, I., Katima, J., Kirchhoff, V., Matson, P., Midgley, P., Wang, M., 2001. Atmospheric chemistry and greenhouse gases. In: Houghton, J.T., Ding, Y., Griggs, D.J., Noguer, M., van der Linder, P.J., Dai, X., Maskell, K., Johnson, C.A., eds. Climate change 2001: the scientific basis. Contribution of Working Group I to the Third Assessment Report of the Intergovernmental Panel on Climate Change. Cambridge, UK/New York, NY, USA: Cambridge University Press, 239–287.

Pulikesi, M., Baskaralingam, P., Elango, D., Rayudu, V.N., Ramamurthi, V., Sivanesan, S., 2006. Air quality monitoring in Chennai, India, in the summer of 2005. Journal of Hazard Mater 136, 589–596.

Purcell, L.C., 2003. Comparison of thermal units derived from daily and hourly temperatures, Crop Science 43, 1874–1879.

Rai, R., Agrawal, M., 2008. Evaluation of physiological and biochemical responses of two rice (*Oryza sativa* L.) cultivars to ambient air pollution using open top chambers at a rural site in India, Science of the Total Environment 407, 679-691.

Rai, R., Agrawal, M., Agrawal, S.B., 2007. Assessment of yield losses in tropical wheat using open top chambers, Atmospheric Environment 41, 9543-9554.

Rai, R., Agrawal, M., Agrawal, S.B., 2010. Threat to food security under current levels of ground level ozone: A case study for Indian cultivars of rice, Atmospheric Environment 44, 4272-4282.

Rajaram, S., 2001. Prospects and promise of wheat breeding in the 21s t century, Euphytica 119, 3-15.

Rajput, M., Agrawal, M., 2005. Biomonitoring of air pollution in a seasonally dry tropical suburban area using wheat transplants, Environmental Monitoring and Assessment 101, 39–53.

Rajput, M., Agrawal, M., 2004. Physiological and yield responses of pea plants to ambient air pollution, Indian Journal of Plant Physiology 9(1), 9-14.

Rajput, R.P., Deshmukh, M.R., Paradkar, V.K., 1987. Accumulated heat units and phenology relationships in wheat as influenced by planting dates under late sown conditions, Journal of Agronomy and Crop Science 159 (5), 345-348.

Ramanathan, V., Agrawal, M., Akimoto, H., Aufhammer, M., Devotta, S., Emberson, L., Hasnain, S.I., *et al.*, 2008. Atmospherix Brown Clouds: Regional Assessment Report with Focus on Asia. Published by the United Nations Environment Programme, Nairobi, Kenya.

Rane, J., Nagarajan, S., 2004. High temperature index for field evaluation of heat tolerance in wheat varieties, Agricultural Systems 79 (2), 243-255.

Rane, J., Chauhan, H., 2002a. Rate of grain growth inadvanced wheat (Triticum aestivum L.) accessions under late sown environment, Indian Journal of Agricultural Science, 72, 581–585.

Rane, J., Pannu, R.K., Sohu V.K., Sani, R.S., Mishra, B., Shoran, J., Crossa, J., Vargas, M., Joshi, A.K., 2007. Performance of yield and stability of advanced wheat genotypes under heat-stress environments of the Indo-Gangetic plains, Crop Science 47, 1561-1573.

Rane, J., Shoran, J., Nagarajan, S., 2000. Heat stress environments and impact on wheat productivity in India: Guestimate of losses, Indian Wheat News Letters 6(1), 5–6.

Ranieri, A., Castagna, A., Padu, E., Moldau, H., Rahi, M., Soldatini, G.F., 1999. The decay of O3 through direct reaction with cell wall ascorbate is not sufficient to explain the different degrees of O3-sensitivity in two poplar clones, Journal of Plant Physiology 154, 250–255.

Ranieri, A., D'Urso, G., Nali, C., Lorenzini, G., Soldatini, G.F., 1996. Ozone stimulates apoplastic antioxidant systems in pumpkin leaves, Physiologia Plantarum 97, 381–387.

Ranieri, A., Petacco, F., Castagna, A., Soldatini, G.F., 2000. Redox state and peroxidase system in sunflower plants exposed to ozone, Plant Science 159, 159–167.

Ranieri, A. Castagna, A., Soldatini, G.F., 2000. Differential stimulation of ascorbate

peroxidase isoforms by ozone exposure in sunflower plants, Journal of Plant Physiology 156, 266–271.

Rao, M.V., Lee, H.I., Davis, K.R., 2002. Ozone-induced ethylene production is dependent on salicylic acid, and both salicylic acid and ethylene act in concert to regulate ozone-induced cell death, The Plant Journal 32, 447–456.

Rawson, H.M., Richards, R.A., Munns, R., 1988. An examination of selection criteria for salt-tolerance in wheat, barley and triticale genotypes, Australian Journal of Agricultural Research 39, 759–772.

Regmi, A.P., Ladha, J.K., Pathak, H., Pasuquin, E., Bueno, C., Dawe, D., Hobbs, P., Joshy, D., Maskey, S.L., Pandey, S.P., 2002. Analyses of yield and soil fertility trends in a 20-year rice-rice-wheat experiment in Nepal, Soil Science Society of America Journal 66, 857-867.

Reynolds, M.P., Nagarajan, S., Razzaque, M.A., Ageeb, O.A.A., 2001. Heat Tolerance. In Reynolds, M.P., J.I. Ortiz-Monasterio, and A. McNab (Eds.). Application of Physiology in Wheat Breeding. Chapter 10. Mexico, D.F., CIMMYT.

Reynolds, M.P., Singh, R.P., Ibrahim, A., Ageeb, O.A., Larqué-Saavedra, A., Quick, J.S., 1998. Evaluating physiological traits to compliment empirical selection for wheat in warm environments, Euphytica 100, 85-94.

Reynolds, M.P., van Ginkel, M., Ribaut, J.-M., 2000. Avenues for genetic modification of radiation use efficiency in wheat, Journal of Experimental Botany 51, 459–473.

Robertson, L., Langner, J., Engardt, M., 1999. An Eulerian limited-area atmospheric transport model. Journal of Applied Meteorology 38, 190–210.

Rodell, M., *et al.*, 2009. Satellite-based estimates of groundwater depletion in India, Nature 460, 999–1002.

Roemer, M., Beekmann, M., Bergström, R., Boersen, G., Feldmann, H., *et al.*, 2003 Ozone trends according to ten dispersion models. EUROTRAC- 2 Special Report, ISS Munich.

Roetter, R.P., Van Keulen, H., 2007. Science for Agriculture and Rural Development in Low-income Countries. Springer, Netherlands, pp 27-56.

Rosegrant, M.W., Cline, S.A., 2003. Global food security: Challenges and Policies, Science 302, 1917-1919.

Roy, S., Beig, G., Jacob, D., 2008. Seasonal distribution of ozone and its precursors over the tropical Indian region using regional chemistry-transport model, Journal of Geophysical Research, 113.

Roy, S., Beig, G., Ghude, S., 2009. Exposure-plant response of ambient ozone over the tropical Indian region, Atmospheric Chemistry and Physics Discussions 9(1), 4141-4157.

Royal Society, 2008 Ground-level ozone in the 21st century: future trends, impacts and policy implications, The Royal Society, UK

Runeckles, V.C., Chevone, B.I., 1992. Crop responses to ozone. In: Lefohn, A.S., (Eds.) Surface Leve1 Ozone Exposures and Their Effects on Vegetation. CRC Press, Boca Raton, FL, pp. 185-266.

Saharan, M.R., Singh, R. 1984. Flag leaf stomatal frequency and conductance in relation to photosynthesis, RuBP Carboxylase and grain yield of field grown wheat genotypes, Indian Journal of Plant Physiology 27 (3), 223-231.

Sahu, S.K., Beig, G., Sharma, C., 2008. Decadal growth of black carbon emissions in India, Geophysical Research Letters, 35.

Saitanis, C.J., 2003. Background ozone monitoring and phytodetection in the greater rural area of Corinth –Greece, Chemosphere, 51, 913–923.

Saltelli, A., Ratto, M., Tarantola, S., Campolongo, F., 2006. Sensitivity analysis practices: Strategies for model-based inference, Reliability Engineering and System Safety 91, 1109-1125.

Samuel, S.R., Deshmukh, P.S., Sairam, R.K., Kushwaha, S.R., 2000. Influence of Benzaladenine on yield and yield components in wheat genotypes under normal and late planting conditions, Indian Journal of Plant Physiology 5(3), 240-243.

Sandhu, I.S., Sharma, A.R., Sur, H.S., 1999. Yield performance and heat unit requirement of wheat (*Triticum aestivum*) variety as affected by sowing dates under rainfed conditions, Indian Journal of Agricultural Sciences 69 (3), 175-179.

Sankaran, V.M., Aggarwal, P.K., Sinha, S.K., 2000. Improvement in wheat yields in northern India since 1965: measured and simulated trends, Field Crops Research 66 (2), 141–149.

Sarkar, A., Agrawal, S.B., 2010a. Elevated ozone and two modern wheat cultivars: An assessment of dose dependent sensitivity with respect to growth, reproductive and yield parameters. Environmental and Experimental Botany. 69 (3): 328-337.

Sarkar, A., Agrawal, S.B., 2010b. Identification of ozone stress in Indian rice through foliar injury and differential protein profile, Environmental Monitoring Assessment 161(1-4), 205-215.

Sarkar, A., Agrawal, S.B., 2010. Elevated ozone and two modern wheat cultivars: An assessment of dose dependent sensitivity with respect to growth, reproductive and yield parameters, Environmental and Experimental Botany 69, 328–337.

Sarkar, A., Rakwal, R., Agrawal, S.B., Shibato, J., Ogawa, Y., Yoshida, Y., *et al.* , 2010. Investigating the impact of elevated levels of ozone on tropical wheat using integrated phenotypical, physiological, biochemical, and proteomics approaches, Journal of Proteome Research 9, 4565-4584. .

Satsangi, G.S., Lakhani, A., Kulshrestha, P.R., Taneja, A., 2004. Seasonal and Diurnal variation of surface ozone and a preliminary analysis of exceedance of its critical levels at a semi arid site in India, Journal of Atmospheric Chemistry, 47, 271 - 286.

Sawada, H., Kohno, Y., 2009. Differential ozone sensitivity of rice cultivars as indicated by visible injury and grain yield, Plant Biology 11 (Suppl. 1), 70–75.

Sawhney, V, Singh, D.P., 2002. Effect of chemical desiccation at the post-anthesis stage on some physiological and biochemical changes in the flag leaf of contrasting wheat genotypes, Field Crops Research 77 (1), 1-6.

Sayre, K.D., 2002. Management of irrigated wheat. In BREAD Curtis, B.C., Rajaram S. Macpherson, H.G. (Eds). WHEAT: Improvement and Production. FAO Plant Production and Protection Series No. 30, FAO, Rome. http://www.fao.org/DOCREP/006/Y4011E/y4011e06.htm.

Scott, G.J., Rosegrant, M.W., Ringler, C., 2000. Roots and Tubers for the 21st Century Trends, Projections, and Policy Options. International Food Policy Research Institute 2033 K Street, N.W., Washington, D.C. 20006-1002 U.S.A.

SeedNet, 2011, National initiative for information on quality seeds, Government of India, http://seednet.gov.in/, last accessed May 2011.

Sharma, N., Gupta, N.K., Gupta, S., Hasegawa, H., 2005. Effect of NaCl salinity on photosynthetic rate, transpiration rate, and oxidative stress tolerance in contrasting wheat genotypes, Photosynthetica 43(4), 609-613.

Sharma, S.N., Bhatnagar, V.K., Mann, M.S., Shekhawat, U.S., Sain, R.S., 2002. Maximization of wheat yields with a unique variety in warmer areas, Wheat information series 95, 11–16.

Sharma, S.N., Bohra, J.S., Singh, P.K., Srivastava, R.K., 2002. Effect of tillage and mechanization on production potential of rice (*Oryza sativa*)-wheat (*Triticum aestivum*) cropping system, Indian Journal of Agronomy 47 (3), 305-310.

Shi, G., Yang, L, Wang, Y., *et al.*, 2009. Impact of elevated ozone concentration on yield of four Chinese rice cultivars under fully open-air field conditions, Agriculture, Ecosystems and Environment 131, 178–184.

Shirke, P.A., Pathre, U.V., 2004. Influence of leaf-to-air vapour pressure deficit (VPD) on the biochemistry and physiology of photosynthesis in *Prosopis juliflora*, Journal of Experimental Botany 55 (405), 2111-2120.

Simmons, S.R., Oelke, E.A., Anderson, P.M., 1995 Growth and Development - Guide for Spring Wheat. http://www.extension.umn.edu/distribution/cropsystems/DC2547.html.

Simpson, D, Tuovinen, J.P, Emberson, LD., Ashmore, M.R., 2003b. Characteristics of an ozone deposition module, Water Air and Soil Pollution: Focus 1, 253-262.

Simpson, D., 2002. Modelling of ozone and secondary organic aerosol across Europe: Results from the EMEP models. NATO Science Series - Series IV - Earth and Environmentals Sciences [1568-1238], 16, 51 -56.

Simpson, D., Andersson-Sköld, Y., Jenkin, M.E., 1993. Updating the chemical scheme for the EMEP MSC-W oxidant model: current status. EMEP MSC-W Note 2/93.

Simpson, D., Ashmore, M. R., Emberson, L., Tuovinen, J.P., 2007. A comparison of two different approaches for mapping potential ozone damage to vegetation. Amodel study, Environmental Pollution 146**,** 715-725.

Simpson, D., Fagerli, H., Jonson, J., Tsyro, S., Wind, P., Tuovinen, J.-P., 2003a. The EMEP Unified Eulerian Model. Model Description. EMEP MSC-W Report 1/2003. The Norwegian Meteorological Institute, Oslo, Norway.

Simpson, D., Tuovinen, J.P, Emberson, L.D., Ashmore, M.R., 2003c. Characteristics of ozone deposition module II: Sensitivity analysis. Water Air and Soil Pollution, 143, 123-137.

Singh, A., Agrawal, S.B., Rathore, D., 2005. Amelioration of Indian urban air pollution phytotoxicity in Beta vulgaris L. by modifying NPK nutrients. Environmental Pollution 134: 385–395.

Singh, A., Sarin, S.M., Shanmugam, P., Sharma, N., Attri, A.K., Jain, V.K., 1997. Ozone distribution in the urban environment of Delhi during winter months. Atmospheric Environment 31(20), 3421-3427.

Singh, K.N., Chatrath, R., 2001. Salinity tolerance. In: Reynolds MP, Ortiz-Monasterio JI, McNab A (Eds) Application of hysiology in wheat breeding. CIMMYT, Mexico, DF, pp 101–110.

Singh, P., Agrawal, M., Agrawal, S.B., 2009. Evaluation of physiological, growth and yield responses of a tropical oil crop (*Brassica campestris* L. var. Kranti) under ambient ozone pollution at varying NPK levels, Environmental Pollution 157, 871–880.

Singh, R.B., 2000. Environmental consequences of agricultural development: a case study from the Green Revolution state of Haryana, India, Agriculture, Ecosystems and Environment 82 (1-3), 97-103.

Singh, R.P., Huerta-Espino, J., Roelfs, A.P., 2002. The wheat rusts. In Eds. Curtis, B.C., Rajaram, S., Macpherson, H.G., BREAD WHEAT: Improvement and Production. FAO Plant Production and Protection Series No. 30.

Singh, R.P., William, H.M., Huerta-Espino, J., Rosewarne, G., 2004. Wheat Rust in Asia: Meeting the Challenges with Old and New Technologies. In Eds. Fischer, T., *et.al.,* 2004. New directions for a diverse planet: Proceedings for the 4th International Crop Science Congress, Brisbane, Australia.

Singh, S., Agrawal, S.B., 2010. Impact of tropospheric ozone on wheat (*Triticum aestivum* L.) in the eastern Gangetic plains of India as assessed by ethylenediurea (EDU) application during different developmental stages, Agriculture, Ecosystems and Environment 138, 214–221.

Singh, S., Agrawal, S.B., Singh, P., Agrawal, M., 2010. Screening three cultivars of *Vigna mungo* L. against ozone by application of ethylenediurea (EDU). Ecotoxicological and Environmental Safety 73: 1765-1775.

Singh, S., Agrawal, S.B., Agrawal, M., 2009. Differential protection of ethylenediurea (EDU) against ambient ozone for five cultivars of tropical wheat. Environmental Pollution 157: 2359–2367.

Singh, S., Agrawal, S.B., 2009. Use of ethylene diurea (EDU) in assessing the impact of ozone on growth and productivity of five cultivars of Indian wheat (*Triticum aestivum* L.), Environmental Monitoring and Assessment 159, 125-41.

Singh, S., Kaur, D., Agrawal, S.B., Agrawal, M., 2010. Responses of two cultivars of Trifolium repens L. to ethylene diurea in relation to ambient ozone. Journal of Environmental Science (China) 22, 1096-103.

Singh, B., Datta, P.S., 2010. Effect of low dose gamma irradiation on plant and grain nutrition of wheat, Radiation Physics and Chemistry 79, 819–825.

Singh, M., Bishnoi, O.P., Yadav, S.K., Singh, B. 1993 A study of seasonal changes in Leaf water potential, stomatal resistance and canopy temperature of wheat (*Triticum aestivum* L.) under different soil moisture regimes, Indian Journal of Plant Physiology 26 (3), 197-199.

Singh, P., Wolkewitz, H., Kumar, R., 1987. Comparative performance of different crop production functions for wheat (*Triticum aestivum* L.). Irrigation Science 8(4), 273-290.

Singh, S., Agrawal M., 2010. Impact of tropospheric ozone on wheat (*Triticum aestivum* L.) in the eastern Gangetic plains of India as assessed by ethylenediurea (EDU) application during different developmental stages, Agriculture, Ecosystems and Environment 138, 214–221.

Singh, S., Agrawal, S.B., Agrawal, M., 2009. Differential protection of ethylenediurea (EDU) against ambient ozone for five cultivars of tropical wheat Environmental Pollution xxx: 1–9

Singh, T., Singh, H. 1989. Leaf water potential and stomatal conductance of wheat (*Triticum aestivum* L.) as effected by water stress, Indian Journal of Plant Physiology 32 (3), 278-280.

Sinha, S.K., Singh, G.B., Rai, M., 1998. Decline in crop productivity in Haryana and Punjab: myth or reality? Indian Council of Agricultural Research, New Delhi, India, 89 pp.

Sivamani, E., Bahieldin, A., Wraith, J.M., Al-Niemi, T., Dyer, W.E., Ho, T.-H. D., Qu, R., 2000: Improved biomass productivity and water use efficiency under water deficit conditions in transgenic wheat constitutively expressing the barley *HVA*1 gene, Plant science 155, 1-9.

Skovmand, B., Reynolds, M.P., Delacy, I.H., 2001. Mining wheat germplasm collections for yield-enhancing traits, Euphytica 119, 25–32.

Smale, M., Singh, J., Di Falco, S., Zambrano, P., 2008, Wheat breeding, productivity and slow variety change: evidence from the Punjab of India after the Green Revolution, Australian Journal of Agricultural and Resource Economics 52, 419–432

Soja G., Barnes J.D., Posch M., Vandermeiren K., Pleijel H., Mills G., 2000. Phenological weighting of ozone exposures in the calculation of critical levels for wheat, bean and plantain, Environmental Pollution 109, 517-524.

Soja, G., 1996. Growth stage as a modifier of ozone response in winter wheat. In: Knoacher, M., Schneider, J., Soja, G. (Eds.), Exceedance of Critical Loads and Levels. Conference Papers Vol. 15. Federal Environment Agency, Vienna, Austria, pp. 155-163

Soja, G., Khan, S., Bolhàr-Nordenkampf, H.R., 1996. Drought Stress as a Modifier of Ozone Response in Wheat, in: Kärenlampi, L., Skärby, L. (eds), Critical Levels for Ozone in Europe: Testing and Finalizing the Concepts. UN-ECE Workshop Report, University of Kuopio, Department of Ecol. and Environ. Sci., Finland, pp. 308–313.

Solberg, S., Bergström, R., Langner, J., Laurila, T., Lindskog, A., 2005 Changes in Nordic surface ozone episodes due to European emission reductions in the 1990s, Atmospheric Environment 39, 179–192.

Sombroek, W.G., Gommes, R., 1996. The climate change - Agriculture conundrum. In: Bazzaz F. and Sombroek W. (Eds.) Global climate change and agricultural production. Direct and indirect effects of changing hydrological, pedological and plant physiological processes. FAO, UN and John Wiley and Sons.

Srivastava, A.C., Khanna, Y.P., Meena, R.C., Pal, M., Sengupta, U.K., 2002. Diurnal changes in photosynthesis, sugars, and nitrogen of wheat and mungbean grown under elevated CO_2 concentration, Photosynthetica 40(2), 221-225.

Stevenson, D.S., Dentener, F.J., Schultz, M.G., Ellingsen, K., van Noije, T.P.C., *et al.*, 2006. Multimodel ensemble simulations of present-day and near-future tropospheric ozone. Journal of Geophysical Research, 111.

Stone, P.J., Nicolas, M.E., 1994. Wheat varieties vary widely in their responses of grain yield and quality to short periods of post-anthesis heat stress, Australian Journal of Plant Physiology 21, 887–900.

Stone, P.J., Nicolas, M.E., 1995a. Comparison of sudden heat stress with gradual exposure to high temperature during grain-filling on two wheat varieties differing in heat tolerance. I. Grain growth. Australian Journal of Plant Physiology 22, 935–944.

Stone, P.J., Nicolas, M.E., 1995b. A survey of the effects of high temperature during grain-filling on yield and quality of 75 wheat cultivars. Australian Journal of Agricultural Research 46 (3), 475–492.

Streets, D.G., Bond, T.C., , G.R., Fernandes, S.D., Fu, Q., He, D., Klimont, Z., Nelson, S.M., Tsai, N.Y., Wang, M.Q., Woo, J.-H., Yarber, K.F., 2003. An inventory of gaseous and primary aerosol emissions in Asia in the year 2000, Journal of Geophysical Research 108, 8809.

Strickland, D., 2007. The Guide to Biotechnology. Biotechnology Industry Organization (BIO). Washington, DC. www.bio.org.

Stull, R. M.: 1989, An Introduction to Boundary Layer Meteorology. Kluwer, Dordrecht.

Swaminathan, M.S., 2010. Achieving food security in times of crisis, New Biotechnology 27 (5), 453-460.

Syri, S., Amann, M., Schopp, W. and Heyes, C. 2001 Estimating long-term population exposure to ozone in urban areas of Europe, Environmental Pollution, 113, 59-69.

Tarrasón, L., Thunis, P., Vignati, E., White, L., Wind, P., 2007. Evaluation of long-term ozone simulations from seven regional air quality models and their ensemble, Atmospheric Environment 41 (10), 2083-2097.

Tarrasón, L., Benedictow, A., Fagerli, H., Jonson, J.E., Klein, H., *et al.*, 2005. Transboundary acidification, eutrophication and ground level ozone in Europe in 2003. EMEP Status Report 1/2005, Norwegian Meteorological Institute.

Teixeira, A., Fischer, G., van Velthuizen, H., van Dingenen, R., Dentener, F., Mills, G., Walter, C., Ewert, F., 2011. Limited potential of crop management for mitigating surface ozone impacts on global food supply, Atmospheric Environment 45, 2569-2576.

Tenhunen, J.D., Lange, O.L., Gebel, J., Beyschlag, W. and Weber, J.A. 1984 Changes in photosynthetic capacity, carboxylation efficiency, and CO_2 compensation point associated with midday stomatal closure and midday depression of net CO_2 exchange of leaves of Quercus suber, Planta 162, 193-203.

Tiedemann, A.V., Firsching, K.H., 2000. Interactive effects of elevated ozone and carbon dioxide on growth and yield of leaf rust-infected versus non-infected wheat, Environmental Pollution 108 (3), 357-363.

Tilmes, S., Brandt, J., Flatøy, F., Bergström, R., Flemming, J., Langner, J., Christensen, J.H., Frohn, L.M., Hov, Jacobsen, I., Reimer, E., Stern, R., Zimmermann, J., 2002. Comparison of five Eulerian air pollution forecasting systems for the summer of 1999 using the German Ozone monitoring data, Journal of Atmosphere and Chemosphere 42, 91–121.

Timsina, J., Connor, D.J., 2001. Productivity and management of rice-wheat cropping systems: issues and challenges, Field Crops Research 69, 93-132.

Tirol-Padre, A., Ladha, J.K., 2006 Integrating rice and wheat productivity trends using the SAS mixed-procedure and meta-analysis, Field Crops Research 95, 75–88.

Tiwari, S., Agrawal, M., Manning, W.J., 2005. Assessing the impact of ambient ozone on growth and productivity of two cultivars of wheat in India using three rates of application of ethylenediurea (EDU). Environmental Pollution 138, 153-160.

Tiwari, S., Agrawal, M., 2009. Protection of palak (*Beta vulgaris* L. var All green) plants from ozone injury by ethylenediurea (EDU): roles of biochemical and physiological variations in alleviating the adverse impacts, Chemosphere 75, 1492-1499.

Tiwari, S., Agrawal, M., 2010. Effectiveness of different EDU concentrations in ameliorating ozone stress in carrot plants, Ecotoxicology and Environmental Safety 73, 1018-1027.

Tiwari, S., Agrawal, M., Marshall, F., 2006. Evaluation of ambient air pollution impact on carrot plants at a sub urban site using open top chambers, Environmental Monitoring and Assessment 119, 15–30.

Tiwari, S., Rai, R., Agrawal, M., 2008. Annual and seasonal variations in tropospheric ozone concentrations around Varanasi, International Journal of Remote Sensing 29, 4499-4514.

Tripathi, R., Sarkar, A., Pandey, Rai, S., Agrawal, S.B., 2011. Supplemental ultraviolet-B and ozone: impact on antioxidants, proteome and genome of linseed (*Linum usitatissimum* L. cv. Padmini), Plant Biology 13, 93–104.

Tuovinen, J.-P., Ashmore, M., Emberson, L., Simpson, D., 2004. Testing and improving the EMEP ozone deposition module, Atmospheric Environment 38, 2373-2385.

Tuovinen, J.-P., Emberson, L., Simpson, D., 2009. Modelling ozone fluxes to forests for risk assessment: status and prospects, Annals of Forest Science 66, 401.

Tuzet, A., Perrier, A., Loubet, B., Cellier, P., 2011. Modelling ozone deposition fluxes: The relative roles of deposition and detoxification processes, Agricultural and Forest Meteorology 151 (4), 480-492.

Tyagi, P.K., Pannu, R.K., Sharma, K.D., Chaudary, B.D., Singh, D.P., 2003. Performance of wheat genotypes under late sown field conditions, Haryana Journal of Agronomy 19 (1), 123-125.

U.S.-EPA, 1996. Air Quality Criteria for Ozone and Related Photochemical Oxidants. United States Environmental Protection Agency, pp. 1-1e1-33.

U.S.-EPA, 2008. Ozone Air Quality Standards, http://www.epa.gov/glo/standards.html.

U.S.-EPA. 2006. Air Quality Criteria for Ozone and Related Photochemical Oxidants (2006 Final). U.S. Environmental Protection Agency, Washington, DC, EPA/600/R-05/004aF-cF.

Uddling, J., Gunthardt-Goerg, M.S., Matyssek, R., Oksanen, E., Pleijel, H., Selldéna, G., Karlssonf, P.E., 2004. Biomass reduction of juvenile birch is more strongly related to stomatal uptake of ozone than to indices based on external exposure, Atmospheric Environment 38, 4709–4719.

UK-Air Quality Standards Regulations, 2010. Environmental protection, The Air Quality Standards Regulations 2010, No. 1001, http://www.legislation.gov.uk/uksi/2010/1001/pdfs/uksi_20101001_en.pdf.

Umali-Deininger, D.L., Deininger, K.W., 2001. Towards greater food security for India's poor: balancing government intervention and private competition, Agricultural Economics 25, 321–335.

UNCTS, 2011. United Nations Commodity Trade Statistics Database, http://comtrade.un.org/db/default.aspx, (last accessed August 2011).

UNPP, 2009. World Population Prospects: The 2008 Revision. Population Division of the Department of Economic and Social Affairs of the United Nations Secretariat. http://esa.un.org/unpp.

Unsworth, M.H., Geissler, P., 1992. Results and achievements of the European Open Top Chamber Network. In: Jäger, H.J., Unsworth, M., De Temmerman, Mathy, P. (Eds.), Effects of Air Pollution on Agricultural Crops in Europe Air Pollution Research Report 46.

Uprety, D.C., Sirohi, G.S., 1987a. Comparative study on the effect of water stress on the photosynthesis and water relations of Triticale, Rye and Wheat, Journal of Agronomy and Crop Science 159, 349-355.

Uprety, D.C., and Sirohi, G.S. 1987b. Diurnal changes on photosynthesis in triticale, rye

and wheat, Current Science 56, 1292-1294.

USDA, 1994. Major world crop areas and climatic profiles. In: Agricultural Handbook No. 664. World Agricultural Outlook Board, U.S. Department of Agriculture Available at: http://www.usda.gov/oce/ weather/pubs/Other/MWCACP/MajorWorldCropAreas.pdf.

Van der Zijpp, A.J., 1999. Animal food production: the perspective of human consumption, production, trade and disease control, Livestock Production Science 59(2-3), 199-206.

Van Dingenen, R., Dentener, F.J., Raes, F., Krol, M.C., Emberson, L., Cofala, J., 2009. The global impact of ozone on agricultural crop yields under current and future air quality legislation, Atmospheric Environment 43(3), 604-618.

Van Erden, L.J., van der, Tonneijck, A.E.G., Wijnands, J.H.M., 1988. Crop loss due to air pollution in The Netherlands, Environmental Pollution 53 (1-4), 365-376.

Varshney, C.K., Rout, C., 1998. Ethylene diurea (EDU) protection against ozone injury in tomato plants at Delhi, Bulletin of Environmental Contamination and Toxicology 61, 188-193.

Varshney, C.K., Padhy, P.K., 1999. Estimation of total volatile organic compounds (TVOC) emissions from anthropogenic sources in India, Journal of Industrial Ecology 2, 93–105.

Velissariou, D., 1999. In: Toxic effects and losses of commercial value of lettuce and other vegetables, due to photochemical air pollution in agricultural areas of Attica Greece. Critical Levels for Ozone Level II. Environmental Documentation No. 115 (Eds. Fuhrer J, Achermann B), pp. 253–256. Swiss Agency for the Environment, Forests and Landscape, Bern, Switzerland.

Velissariou, D., Barnes, J.D., Davison, A.W., 1992. Has inadvertent selection by plant breeders affected the O_3 sensitivity of modern Greek cultivars of spring wheat?, Agriculture, Ecosystems and Environment 28, 79-89.

Verma, S., Venkataraman, C., Boucher, O., 2011. Attribution of aerosol radiative forcing over India during the winter monsoon to emissions from source categories and geographical regions, Atmospheric Environment 45, 4398-4407.

Vingarzan, R., 2004. A review of surface ozone background levels and trends. Atmospheric Environment 38, 3431-3442.

Vorne, V., Ojanperä, K., De Temmerman, L., Bindi, M., Högy, P., Jones, M.H., Lawson, T., Persson, K., 2001. Effects of elevated carbon dioxide and ozone on potato tuber quality in the European multiple-site experiment ‘CHIP-project’, European Journal of Agronomy 17, 369–381.

Wahid, A., 2003. Air Pollution impacts on vegetation in Pakistan, In Eds. Emberson, L., Ashmore, M., Murray, F., Air Pollution Impacts on crops and Forests: A Global Assessment, Air Pollution Reviews, Volume 4, Imperial College Press, pp189.

Wahid, A., 2006. Influence of atmospheric pollutants on agriculture in developing

countries: a case study with three new wheat varieties in Pakistan, Science of the Total Environment 371, 304–313.

Wahid, A., Ahmad, S.S., Butt, Z.A., Ahmad, M., 2011. Exploring the hidden threat of gaseous pollutants using rice (*Oryza sativa* L.) plants in Pakistan, Pakistan Journal of Botany 43(1), 365-382.

Wahid, A., Gelani, S., Ashraf, M., Foolad, M.R., 2007. Heat tolerance in plants: An overview, Environmental and Experimental Botany 61, 199–223.

Wang, X., Mauzerall, D.L., 2004. Characterizing distributions of surface ozone and its impact on grain production in China, Japan and South Korea: 1990 and 2020, Atmospheric Environment 38, 4383–4402.

Wang, Z., Fu, J., He, M., Tian, Q., Cao, H., 1997. Effects of source/sink manipulation on net photosynthetic rate and photosynthate partitioning during grain rolling in winter wheat, Biologia Plantarum 39, 379-385.

Wardlaw, I.F., Wrigley, C.W., 1994. Heat tolerance in temperate cereals: an overview, Australian Journal of Plant Physiology 21, 695-703.

Webb, R.A., 1972. Use of the boundary line in the analysis of biological data, Journal of Horticultural Science 47, 309–319.

Weber, P., Rennenberg, H., 1996. Dependency of nitrogen dioxide (NO_2) fluxes to wheat (*Triticum aestivum* L.) leaves from NO_2 concentration, light intensity, temperature and relative humidity determined from controlled dynamic chamber experiments, Atmospheric Environment 30 (17), 3001-3009.

Weiss, A., Norman, J.M., 1984. Partitioning solar radiation into direct and diffuse, visible and near-infrared components, Agricultural and Forest Meteorology 34, 205-213.

Wesely, M.L., 1989. Parameterization of surface resistance to gaseous dry deposition in regional-scale numerical models, Atmospheric Environment 23, 1293-1304.

Westenbarger, D.A., Frisvold, G.B., 1995. Air pollution and farm-level crop yields: an empirical analysis of corn and soybeans, Agricultural and Resource Economics Review 24 (2), 156–165.

Wheeler, R., Hong, T.D., Ellis, R.H., Batts, G.R., Morison, J.I.L., Hadley, P., 1996. The duration and rate of grain growth, and harvest index, of wheat (*Triticum aestivum* L.) in response to temperature and CO_2, Journal of Experimental Botany 47(5), 623-630.

Wilkinson, S., Clephan, A.L., Davies, W.J., 2001. Rapid low temperature-induced stomatal closure occurs in cold-tolerant *Commelina communis* leaves but not in cold-sensitive tobacco leaves, via a mechanism that involves apoplastic calcium but not abscisic acid, Plant Physiology 126, 1566–1578.

Wilkinson, S., Davies, W.J., 2010. Drought, ozone, ABA and ethylene: new insights from cell to plant to community, Plant, Cell and Environment 33, 510–525.

Wittig, V.E., Ainsworth, E.A., Long, S.P., 2007. To what extent do current and

projected increases in surface ozone affect photosynthesis and stomatal conductance of trees? A meta-analytic review of the last three decades of experiments, Plant, Cell and Environment 30, 1150–1162.

WMO, 2008. Measurement of ozone, Chapter 16, In: Guide to Meteorological Instruments and Methods of Observation, WMO Publication No. 8, World meteorological Organisation, pp. 1.16-1.

World Bank, 2011. http://data.worldbank.org/indicator/SL.AGR.EMPL.ZS (last accessed August 2011).

World Population Prospects-UN, 2008. World Population Prospects: The 2008 Revision. Population Division of the Department of Economic and Social Affairs of the United Nations Secretariat, http://esa.un.org/unpp.

Yadav, R., Singh, S.S., Singh, G.P., Prabhu, K.V., 2010. Wheat Production in India: Technologies to Face Future Challenges, Journal of Agricultural Science 2 (2), 164-173.

Yadav, R.L., 1998. Factor productivity trends in a rice-wheat cropping system under long-term use of chemical fertilizers, Experimental Agruiculture 34, 1-18.

Yadav, R.L., Prasad, K., Dwivedi, B.S., Tomar, R.K. and Singh, A.K. 2000. Cropping systems. In Singh, G.B., Sharma, B.R., (eds.), Fifty years of natural resource management research, pp. 411–446. New Delhi, Indian Council of Agricultural Research.

Yamaji, K., Ohara, T., Akimoto, H., 2004. Regional-specific emission inventory for NH_3, N_2O, and CH_4 via animal farming in South, Southeast, and East Asia, Atmospheric Environment 38, 7111–7121.

Yang, F., Jørgensen, A.D., Li, H., Søndergaard, I., Finnie, C., Svensson, B., Jiang, D., Wollenweber, B., Jacobsen, S., 2011. Implications of high-temperature events and water deficits on protein profiles in wheat (*Triticum aestivum* L. cv. Vinjett) grain, Proteomics 11, 1684–1695.

Younglove, T., McCool, P.M., Musselman, R.C., Kahl, M.E., 1994. Growth-stage dependent crop yield response to ozone exposure, Environmental Pollution 86, 287-295.

Zhang, L., Vet, R., Brook, J.R., Legge, A.H., 2006. factors effecting stomatal uptake of ozone by canopies and a comparison betweendose and exposure, Science of Total Environment 370, 117-132.